

PUBLICATION OF THE NETHERLANDS GEODETIC COMMISSION

PROCEEDINGS
OF THE
INTERNATIONAL SYMPOSIUM
ON
ELECTROMAGNETIC DISTANCE MEASUREMENT
AND
THE INFLUENCE OF ATMOSPHERIC REFRACTION,

HELD UNDER THE AUSPICES OF THE INTERNATIONAL ASSOCIATION
OF GEODESY
AT
WAGENINGEN, THE NETHERLANDS, MAY 23-28, 1977

edited by
P. Richardus

1978

Rijkscommissie voor Geodesie, Thijsseweg 11, Delft, The Netherlands

"ISBN" 90 - 6132 - 028 - 3

P R E F A C E

The Netherlands Geodetic Commission has pleasure in presenting herewith the proceedings of the "International Symposium on Electromagnetic Distance Measurement and the Influence of Atmospheric Refraction", held at Wageningen, May 23 - 28, 1977. The initiative to this symposium was taken by Dr.Ir. P. Richardus who immediately after the previous symposium in Stockholm suggested to hold the next meeting in The Netherlands, offering at the same time to act as convener and as editor of the proceedings of this symposium. His efforts in making a success of it are gratefully acknowledged. We also wish to express our thanks to the members of the organizing committee and the scientific advisers for their assistance and contributions to this symposium. Thanks are likewise due to the Agriculture University for their financial support, to the International Agriculture Centre for providing the accommodation, help with the organization and printing of the proceedings and last but not least to the Department of Surveying and Photogrammetry of the Agriculture University for the excellent arrangements.

The President of the
Netherlands Geodetic Commission,

Prof.Ir. G.J. Bruins



CONTENTS

	page
Preface	
Organizing Committee	I
Programme	II
Opening speeches	III
Keynote address	IV
Minutes of the meeting of SSG 1:42	328
Minutes of the workshop meeting	336
List of participants	340 - 347

PRESENTED PAPERS

Bradsell, R.H. <i>A simple calibrator for the mekometer EDM instrument</i>	1 - 6
Froome, K.D., Bradsell, R.H. <i>Long-term stability of an NPL mekometer III wavelength standard</i>	7 - 16
Meier-Hirmer, B. <i>Mekometer ME 3000 - theoretical aspects, frequency calibration, field tests -</i>	21 - 39
Herrewegen van den, M. <i>Testing electro-optical distances on an interferometric base-line</i>	41 - 55
Allan, A.L. <i>The plane mirror in electro-optical distance measurement</i>	56 - 62
Stenström, J. <i>A new laser distance meter with range up to 40 km - Aga geodimeter 600 -</i>	64 - 73
Parm, T. <i>High precision traverse of Finland and the utilization of it</i>	76 - 79
Witte, B.U. <i>Precise measurement of vertical distances using electro-optical rangefinders</i>	81 - 91
Zeeman, F.W. <i>A laser system for ranging to satellites</i>	92 - 100
Tengström, E. <i>Some absolute tests of the results of IDM-measurements in the field with a description of formulas used in the tests</i>	101 - 124

CONTENTS	PAGE
Maier, U. <i>Die erfassung der repräsentativen temperatur bei laser-streckenmessungen über den Rheingraben</i>	127 - 132
Atia, K.A. <i>Strength of trilateration networks observed in pairs</i>	133 - 140
Huggett, G.R., Slater, L.E. <i>Recent advances in multiwavelength distance measurement</i>	141 - 152
Huggett, G.R., Slater, L.E., Pavlis, G. <i>Precision leveling with a two-fluid tiltmeter</i>	153 - 155
Williams, D.C. <i>First field tests of an angular dual wavelength instrument</i>	163 - 170
Felletschin, V. <i>Möglichkeiten der genauigkeitssteigerung in der EDM mit licht- und mikrowellen</i>	171 - 184
Hradelik, L. <i>Determination of crustal movements by three-dimensional triangulation</i>	185 - 190
Stellingwerff Beintema, S. <i>The use of radiofrequencies for electronic positioning systems and the application in Sercel's Syledis</i>	193 - 202
Hopfield, H.S. <i>Tropospheric correction of electromagnetic ranging signals to a satellite: study of parameters</i>	205 - 213
Kahmen, H. <i>Some considerations on the stochastic behaviour of the angles of refraction and of the refraction indices, concerning laser- and microwave distance measurements</i>	216 - 228
Bruckner, R. <i>Scintillationmeasurements of a laserbeam</i>	230 - 243
Brunner, F.K. <i>Experimental determination of the co-efficients of refraction from heat flux measurements</i>	245 - 255
Mendel, W. <i>A refraction model for electro-optical range finding in the mountains</i>	261 - 274
Glissmann, T. <i>A co-incidence method for refraction eliminating angle measurement</i>	276 - 286
Munck de, J.C. <i>Applying the movement smoothness of a vehicle to determine the position of transponders</i>	290 - 301

CONTENTS

PAGE

Brunner, F.K., Fraser, C.S. <i>An atmospheric turbulent transfer model for EDM reduction</i>	304 - 315
Rinner, K. <i>Meteorological correction of laser and microwave disatances</i>	318 - 321
Richardus, P. Masée, R.H. <i>An experiment with a high precision method of alignment</i>	323 - 327
Meeting of SSG 1.42	328 - 335
Minutes of the workshop meeting	336 - 338
Resolutions	339
List of participants	340 - 347

Organizing Committee

- Chairman** - Ir. G.A. van Wely
Wageningen, The Netherlands
- Convenor** - Dr. P. Richardus
Wageningen, The Netherlands
- Administrative Secretary/Treasurer** - Ing. H.E. van Dissel
Wageningen, The Netherlands
- Members** - Dr. Ir. L. Aardoom
Delft, The Netherlands
Ir. J.E. Alberda
Delft, The Netherlands
Ir. J.C. de Munck
Delft, The Netherlands
- Scientific Advisors** - Prof. P.L. Beatslé
Brussels, Belgium
Dr. B. Chovitz
Rockville, U.S.A.
Prof. M. Odianicki-Poczobutt
Krakow, Poland
Prof. Dr. Ing. K. Rinner
Graz, Austria
Prof. Dr. E Tengström
Uppsala, Sweden

PROGRAMME

- Sunday, May 22
19.00 - 22.00 hrs. Arrival of participants
Registration
- Monday, May 23
09.00 - 11.00 hrs. Registration
11.00 - 12.30 hrs. Opening of the Symposium by:
- Prof. Dr. Ir. J.P.H. van der Want, Rector Magnificus
Agricultural University, Wageningen. (Represented by
Dr. R. Maris, Secretary of the Board of the University);
Prof. Ir. G.J. Bruins, President of the Netherlands
Geodetic Commission;
M. Louis, Secretary-General of the International
Association of Geodesy;
Prof. Dr. E. Tengström, Chairman of S.S.G. 1:42 of the
I.A.G. (keynote address).
- 14.00 - 17.00 hrs. Chairman: K. Poder
- 1) R.H. Bradsell - Teddington, U.K.
A simple calibrator for the mekometer EDM instrument
 - 2) K.D. Froome/R.H. Bradsell - Teddington, U.K.
Long term stability of an NPL III wavelength standard
 - 3) B. Meier-Hirmer - Karlsruhe, F.R. of Germany
Mekometer ME 3000, theoretical aspects, frequency
calibration, field tests
- Tea -
- 4) M. v.d. Herrewegen - Belgium
Testing electro optical distances on an interferometric
baseline
 - 5) A.L. Allen - London, U.K. (presented by D. Proctor)
The plane mirror in electro-optical distance measurement
 - 6) J.T. Stenström - Eschborn, F.R. of Germany
A new laser distance meter with range up to 40 km
- 18.00 hrs. Departure by coach to the Krölller-Müller Museum in the
National Park Hoge Veluwe, followed by a reception offered
by the Ministry of Agriculture and Fisheries
- Tuesday, May 24 Chairman: L. Hradilek
- 7) T.V.J. Parm - Helsinki, Finland
High precision traverse of Finland and the utilisation
of it
 - 8) B.V. Witte - Bonn, F.R. of Germany
Precise measurement of vertical distances using optical
rangefinders
 - 9) F.W. Zeeman - Apeldoorn, The Netherlands
A laser system for ranging to satellites
- Coffee -

Tuesday, May 24
(cont'd)

- 10) E. Tengström - Uppsåla, Sweden
Some absolute tests of the results of the EDM
terrestrial field measurements in Uppsåla, with a
description of the formulas used in the tests
- 11) U. Maier - Karlsruhe, F.R. of Germany
Distance measurements over the Rhine Valley
- 12) K.A. Atia - Egypt (U.K.)
Strength of trilateration network observed in pairs

14.00 - 17.30 hrs.

Chairman: E. Tengström

- 13) G.R. Huggett - Seattle, U.S.A.
Recent advances in multi wavelength distance
measurement
 - 14) D.C. Williams - Teddington, U.K.
First field tests of an angular dual wavelength
instrument
 - 15) V. Felletschin - Karlsruhe, F.R. of Germany
Possibilities for raising the accuracy of light
and microwave measurements
- Tea -
- 16) L. Hradilek - Prague, Czechoslovakia
Determination of crustal movements by three
dimensional triangulation
 - 17) S. Stellingwerff-Beintema - Voorhout, The Netherlands
The use of radio-frequencies of electronic positioning
systems and the application in Sercel's Syledis

Wednesday, May 25
09.00 - 12.00 hrs.

Chairman: J.C. de Munck

- 18) H.S. Hopfield - Laurel, U.S.A.
Tropospheric correction of electromagnetic ranging
signals to a satellite: study of parameters
- Coffee -
- 19) H. Kahmen - Karlsruhe, F.R. of Germany
Some considerations on the stochastic behaviour of
the angles of refraction and of the refraction index,
concerning laser- and microwave distance measurements
 - 20) R. Bruckner - Hannover, F.R. of Germany
Scintillation measurements of a laser-beam

13.00 hrs.

Departure by coach from the IAC
Excursion to Lelystad, Ketelhaven, Urk
Reception and dinner at Ketelhaven

Thursday, May 26
09.00 - 12.30 hrs.

Chairman: H. Kahmen

- 21) F.K. Brunner - Kensington, Australia
Experimental determination of the co-efficients of
refraction from heat flux measurements
- 22) W. Mendel - Graz, Austria
Refraktions Modell für Entfernungsmesser mit Licht-
wellen in Gebirge

Thursday, May 26
(cont'd)

23) T. Glissman - Hannover, F.R. of Germany
A coincidence method for refraction eliminating
angle measurement

- Coffee -

24) J. de Munck - Delft, The Netherlands
Intersection of transponders by distance measure-
ment from a smoothly moving vehicle

25) F.K. Brunner/C.S. Fraser - Kensington, Australia
An atmospheric turbulent transfer model for EDM
reduction

14.00 - 15.30 hrs.

Chairman: M.R. Richards

26) K. Rinner - Graz, Austria

Diskussion von Laser-dauermessungen im Testnetz
Graz

- Tea -

15.30 hrs.

Meeting S.S.G. 1:42

19.00 hrs.

Symposium Dinner

Friday, May 27

09.00 - 12.30 hrs.

Workshop

14.00 - 15.30 hrs.

Resolutions and closing ceremony

Dr. R. Maris, Secretary of the Board of the Agricultural University

Mr. Chairman, Ladies and Gentlemen, it is a great honour for me to open this Symposium of the International Association of Geodesy. On behalf of the Board of the Agricultural University, I may extend a hearty welcome to all of you in the city of Wageningen. To be honest, we are not at the moment in the city of Wageningen. We are just outside it.

As you may know, many Dutch towns are surrounded by canals for purposes of defense in old times.

Famous are the canals of our capital Amsterdam. Wageningen too possesses its canal. If during a break in this conference you look through the window downstairs, and if you do not mind to take a very small walk through the garden of this beautiful centre, you will reach after a few meters the boundary of our city, the city canal. Only one building of the University of Agriculture is situated inside the original town. The other buildings of our University, about 50, are outside.

Why, you may ask, has the Agricultural University been founded here in Wageningen? The town does not even have a railway station.

Well, the reason is quite simple. Just here in Wageningen one can find three different types of soil, which is very important for an Agricultural School. In the first place riverclay from the river Rhine in the south; in the second place the low peat lands in the north of our city; in the third place the sandy soils of the Veluwe in the east, where we will have a reception this evening.

Nowadays the Agricultural University had broadened its scope. In fact agriculture is not its only subject, but the interrelationship between man, soil, plants and animals is; in general the interrelationship between man and his environment. Our University counts about 70 departments, one of which being the Department of Surveying and Photogrammetry. This Department, the Department of Mr. van Wely and Mr. Richardus, conducts courses in engineering surveying, photogrammetry, photo-interpretation and also remote sensing for senior students of various other departments.

A long tradition of research exists within the department. For many years research has been conducted in optical methods of distance measurements and the influence of atmospheric refraction, until the methods of electro-magnetic distance measurement came into practical daily use. They became subject to special study. For this reason we are proud of being your host at the International Symposium of Electro-magnetic Distance Measurement.

Your papers and your discussions will be of highest scientific importance. Surely you will enjoy the personal contacts too and I wish you all a very useful and very pleasant conference.

Prof. Ir. G.J. Bruins, President of the Netherlands Geodetic Commission

Mr. Chairman, Mijnheer de Secretaris van de Landbouwhogeschool, Monsieur le Secrétaire Général de l'Association Internationale de Géodésie, Ladies and Gentlemen,

On behalf of The Netherlands Geodetic Commission I bid you a cordial welcome to this Symposium.

I am glad, the Organising Committee - or perhaps I may say the convenor - Dr. Richardus - has chosen Wageningen and the Agricultural University for this meeting.

The mere name of Wageningen and of this University is very well known in Dutch surveying and geodetic circles. Especially our older Dutch colleagues will remember that nearly 60 years ago - in 1919 - it was at this University that for the first time the education in surveying in Holland was brought at an academic level.

A 4-year course started at that time. Many surveyors and geodesists received their certificate here.

In the following years the head of the new surveying department, Prof. Dieperink, spent the little time that he had left for research on his special field of interest: "the optical distance measurement".

When, in 1935, the education for surveyor was transferred to the Technological University at Delft, the Department of Surveying at the University here got the task to provide lectures in surveying for agricultural and forestry students. Prof. Kruidhof, who was at that time entrusted with the lectures, again had "the optical distance measurement" as his special field of research.

So, on historical backgrounds, this town, this University and this Department of Surveying is a good choice for this Symposium.

But times have changed. The results of physical research during the first decades of this century followed by the research in electronic technology have changed the instruments and methods of distance measurement accordingly. Not only the visible light, but many other parts of the range of wave-lengths (or frequencies) are used for the instruments and methods dealt with during this Symposium. Characteristics of these instruments - in combination with their internal errors - and the properties of the raypath - in combination with the external errors - the latter mainly due to meteorological conditions - will be discussed by you at a most advanced level - which I can only follow as an onlooker, not as a specialist.

But perhaps one remark may be of interest to some of you.

It regards the meteorological conditions. For some years a mast of 200 meters of the Royal Netherlands Meteorological Institute measures day and night the meteorological data at each multiple of twenty meters height, the knowledge of which is very important for the atmospheric refraction, a subject of this Symposium.

Mr. Chairman, Ladies and Gentlemen,

The Netherlands Geodetic Commission wishes you a very good Symposium.

May your efforts be fruitful in every respect and give the results you are hoping for.

Mr. M. Louis, Secretary General of the International Association of Geodesy

Monsieur le Secrétaire du Centre International d'Agriculture,
Monsieur le Président du Comité National néerlandais de
Géodésie et Géophysique,

Monsieur le Président du Comité d'organisation,

Mesdames,

Mes chers Collègues,

Au nom de l'Association International de Géodésie je tiens à remercier chaleureusement Monsieur le Recteur de l'Université d'Agriculture et Monsieur le Secrétaire-Général qui nous accueillent si aimablement dans cette charmante cité calme et pourtant si industrielle.

Je remercie la Commission géodésique néerlandaise qui nous a invités et le Comité d'organisation du Symposium qui s'est dépensé sans compter pour que nos travaux se déroulent dans les meilleures conditions. Avec de tels atouts ce "Symposium international sur la mesure électromagnétique de distance et l'influence de la réfraction atmosphérique" ne peut être qu'un succès.

Comme dans une pièce de théâtre, le rideau se lève, le décor est planté, rien n'y manque, les acteurs peuvent venir en scène Ils vont tenir leur rôle, ils vont nous dire combien les méthodes devenues si précieuses de mesure électromagnétique de distance ont encore progressé depuis la dernière conférence internationale, comment les instruments se sont perfectionnés grâce à une collaboration fructueuse entre les constructeurs et les utilisateurs, comment l'on peut, à présent, aborder et résoudre le problème lié à la si capricieuse météorologie. Puissent ces acteurs être clairs et convaincants, mais aussi ouverts au dialogue avec tous les collègues ici présents. Car là est bien l'intérêt de tout symposium. C'est le lieu privilégié de rencontre entre ceux qui cherchent, ceux qui trouvent parfois, ceux qui subissent des échecs mais ne se découragent pas Ainsi tous mettent en commun pendant plusieurs jours leurs expériences et leurs réflexions. Lorsque le rideau retombera sur notre scène de théâtre nous repartirons avec de nouvelles connaissances, de nouvelles certitudes, et aussi de nouvelles voies de recherche.

Ainsi progresse la Science, des étapes où chacun est confronté seul avec la réalité et les difficultés, puis des rencontres où tout se discute, tout s'explique et s'éclaire

Merci encore à ceux qui, par leur générosité et leur hospitalité si chaleureuse, vont nous permettre d'avoir, pendant ces quelques jours de franches et amicales discussions qui font vivre et progresser la connaissance.

Prof. E. Tengström, Chairman of the S.S.G. 1:42 of the I.A.G.

Dear Dr Maris, dear foremen, colleagues, ladies and gentlemen,

I feel greatly honoured through the fact, that I myself and my study group 1.42 of IAG have been given the opportunity to play a role at this important symposium.

The theory of electromagnetic wave propagation in a planet's atmosphere, which includes also its ionosphere, is of great importance for a correct interpretation from geometrical and physical observations of received wave signals, travelling through this atmosphere. Using geodetic observations with new techniques for the Earth-Moon system, and for the whole planetary system, it is now-a-days possible to study the geometry and the gravitational fields of all bodies in our solar system, eliminating errors of wave propagation with great accuracy.

In interpreting our observation data, the propagational behaviour of signals of various frequencies, which we receive at our Earth-bound sites, is very essential. The knowledge of the distribution in space of the index of refraction in various spectral regions, used for our information, is certainly necessary, if we should be able to draw correct conclusions from the received signals.

For observations in the Earth's atmosphere, this could be done in three ways:

Pro primo: From the knowledge of the atmospheric conditions, given to us by meteorological and ionospheric observations along the line of the propagated wave-signal, and made simultaneously with the geodetic measurements.

Pro secundo: From adjustment of geometrical figures with refractive parameters originally unknown but obtained in the LS-solution.

Pro tertio: Elimination of atmospherical effects by dispersion

methods. Multi-wave method.

These three aspects of studying refractional (wave propagation) problems for geodesy and planetary geometry and physics are all here in Wageningen of great importance and will be presented with papers from various members of my study group.

I am happy to say, that more than one third of this group (1.42) is here, and will try to impose on you their points of view.

As to my own opinion, the multi-wave method will represent a guide-line for the future in our work to obtain a correct geodetic interpretation of propagated signals, which means eliminating all atmospherical effects of no interest to us. On the other hand could the eliminated atmospheric integrals, in the form they are given to us, improve the knowledge of the wave propagation in the atmosphere observed, and thus also improve our knowledge of the composition and behaviour of our atmosphere.

Two frequency techniques are already used with success to eliminate refractional effects in various geodetic measurements, e.g. ionospheric effects in Doppler, recently also in VLBI (Very Long Baseline Interferometry), and dry atmospherical effects in angle- and electromagnetic distance measurements. For higher ionospheric correction terms and ev. for humid atmosphere we would need more than two frequencies, suitably chosen in the electromagnetic spectrum. Or we have to trust simultaneous observations of other kind.

Depending on the duration of our measurements, longer or shorter periods of refractional changes have significance. It is the duty of our group to try to analyse the amplitudes and phases in various parts of the refractional oscillatory spectrum. Dense determinations of refraction at small time-intervals, using multiple wave methods, should be done, and spectral analysis of the results be made, so that the behaviour of the atmosphere and ionosphere will be better understood. Using lasers in optical geodetic measurements for eliminating the influence of refraction, it is possible to make

such studies, because very short exposure times are often sufficient to obtain good measurable interference patterns.

Of course, the various multi-wave methods should be absolutely tested before we can reach a full conviction in them. Methods for such tests ought to be elaborated for various types of geodetic and astronomic measurements. This is also a task for the group.

The variations we observe in our corrections is partly due to real external physical causes in the medium of the propagated signal, partly to instrumental causes. In this connection it should be emphasized, that the word noise must be used with care. In fact, nothing is stochastic, every elongation in our timeseries has its cause and should be explained. The word noise contrary to the word signal is only an excuse for our lack of knowledge of the causes. Perhaps we may say, that noise is that part of the variations, which for the moment is impossible to study by spectral analysis. That is, no peaks in their spectral density can be detected. The only thing we can do is then to try to improve our instruments and observational techniques, so that the noise level is sufficiently low compared to errors accepted for the physical interpretation.

We in the SSG 1.42, which I represent here, are dealing with results from various types of instruments, and are of course, interested in a honest and realistic information of their - clearly defined - noise level, and in eventual improvements for eliminating systematic errors in them. This is a task for the constructors of our instruments which naturally also includes spectral analysis of various errors of observations, done with them, as we e.g. did with our theodolite scales once, but in a more rude way, applying Least Squares on our Fourier series.

Would it not be of interest to create a study group in IAG, dealing with such instrumental questions? This group could intimately collaborate with SSG 1.42 and other study groups, and such a cooperation would probably intensify the manufacturerers' and inventors' efforts to improve their in-

struments for the benefit of the users.

Studies of the wave propagation in the atmosphere and ionosphere by means of such instruments with low noise level and negligible systematic errors, is also the task of our study group. Characteristic parameters of the atmosphere, such as density, temperature, wind velocity components etc. can be statistically investigated from records of them. Regarded as stationary or generally nonstationary random functions, correlation functions might be constructed, from which the spectral density can be derived. In the nonstationary case the mean value changes with time, but we can describe the process by the difference $F(t) = f(t+\tau) - f(t)$, where $\tau = t_2 - t_1$ is not too large. Slow changes in $f(t)$ do not affect F_τ , so F_τ can be regarded as approximately stationary. This derived random function with stationary first increments defines the s.c. structure function, from which the correlation function and then the spectral density might be found. For further theory see e.g. Tatarski. [1]

I would be very interested if it could be decided, that various problems of spectral analysis of the physical components, determining the n-map as a function of time and thus also the wave propagation in various spectral regions could be touched during the workshop on Friday. In any case, plans for intensive studies in the future, with the basic theories of Tatarski and the contribution from Blackband 1962 [2] could then be planned in my group during this symposium.

The spectral analysis concept is certainly, today replacing LS-methods in our attempts to find physical laws behind the statistical behaviour of our observations.

Quite as a study of the total refractive variations and its physical components in aforementioned way must deepen our knowledge of all types of electromagnetic wave propagation in various media, the investigation of the whole geodynamical spectrum has become essential nowadays. Long period variations, Earth Tides, Free Oscillations, very short periods recorded from seismic waves, are only spectral parts of it, but investigations of all these parts are necessary for a total

understanding of the Earth's response to various external and internal forces and consequently also for finding out the Earth's internal physical properties.

I am closing this short review of the pertinent work on EDM and refraction and my recommendations for the intensification of this work by telling you that I am proud to be able to devote my time to such an important study group as 1.42, the activities of which are of very great importance for geodesy.

Many problems of wave propagation and refraction (e.g. parallactic refraction and shimmer) remain. Study groups of our kind with repeated meetings between the assemblies, and with well defined goals and programmes are - and will always be - essential for the scientific activity of our association. IAG is one of the oldest international communities. We should thank God that we belong to this association, being still one of the best working research communities in the world, not least because of its study group activities. To destroy the SSG-system would be to help IAG to die. But, of course, and I think Mr Louis agrees with me, their work must be made as efficient and up to date as possible in all respects, so that it does not lose its original meaning, always to create fresh blood to our beloved association.

We have here today my friend Mr Knud Poder present, who was before Grenoble president of the EDM study group, which was cancelled there. Unfortunately this group was not replaced by another one in the area of instrumental errors of EDM measurements, which was suggested. I hope, that a new group might be created during the forthcoming assembly in Australia, especially dealing with instrumental problems. And I hope, that Mr Poder will accept to conduct it. I would be happy, if this happens, and I hope I'll live as long to be able to start the cooperation personally with him and his group-members.

It is quite natural, that Knud takes the chairmanship for our sessions today between 14.00 and 17.00, which contain paper presentations of great interest to a presumptive SSG

of the kind I just mentioned.

Knud Poder has, fortunately, agreed to take this responsibility, and I ask him to stand up before us to receive an applause for his decision and also not least for all previous contributions of his to this area of the IAG research.

References:

- [1] Tatarski, V.I.: Wave Propagation in a Turbulent Medium.
(Translated from the Russian by R.A. Silverman), Dover Publ., New York 1967.

- [2] Blackband, W.T. (ed.): Propagation of Radio Waves at Frequencies Below 300 kc/s.
(Proceedings of the Seventh meeting of the AGARD Ionospheric Research Committee, Munich 1962), Pergamon Press 1964.

Introduction by Dr. K. Poder, Chairman.

Dear Colleagues,

The subject we are going to deal with this afternoon, is more or less the "machinery" in Electro-magnetic distance measurements. When you consider the evolution of the EDM instrumentation, then in the beginning we had only the geodimeter, with which it was possible to cover a range of 20 km; there were rumours, however, of people who measured distances of 45 km. But it turned out in the beginning that the aim of measuring first order sights directly was very hard to achieve in general visibility conditions, and my personal opinion at the time was that it was going to have the same fate as the invar wires, which originally were envisaged to be used for measuring first order sights directly, but turned out in most cases just to be used for base lines of some few km. Some (few) nations have used longer lines, but the average invar baselines were 12 km. I felt that electro-optical instrumentation could not achieve the goal of observing first order sights. Later, the machinery gave this possibility, there were lasers and better optics and there were microwave instruments so that the direct termination of the first order sights became possible. The situation was then that the refraction was more or less a dominant problem, the instrumental errors were not very significant as a matter of fact. If the instrument had a reasonable stable frequency, then it would produce a reasonable length standard; it was actually difficult to make a crystal oscillator that bad, that one obtained a badly determined frequency. And so, what we focused on was more or less the refraction. Then, let us say, not according to the wish of the geodesists, but more or less possibly to satisfy the wishes of the ordinary landsurveyors and cadastral surveyors, there were short range instruments; they often applied infrared light, and in general had a very good resolution, and were intended to measure short ranges. They of course were clearly not of interest to geodesy, that was at least my assumption.

Later we found out that there could possibly come a lot of advantage to geodesy in measuring short lines; They would have the advantage that the requirement to meteorology as to the refractive index of air, the model would be much simpler, because one only had to cover the short range in which one were propagating the signal. This meant that the chances of determining the refractive index with a good approximation just from simple determining measurements was much better.

This raised the question of instrumental errors. Because obviously, if you instead of measuring a 40 km line with may be a systematic index correction of, let's say some millimeters or half a centimeter, one could subdivide this line in 20 sections of 2 km each, then of course the index of the instrument became very important. So the instrumental requirements were actually much higher than those for first order sights. And I think we are going to see a lot of scale determinations in the fundamental networks, coming from many short lines, in addition to the triangulation.

So I see we should be thankful for the work that has been done, and encourage other research on this subject.

This is my introduction to the discussion on the "machinery" and I hope that you know this is a friendly community here and all contributions are welcome. I also hope we can have good discussions on the subjects presented here.

The first speaker this afternoon is dr. Bradsell, who is nearly one of the old timers in EDM. I visited Dr. Bradsell around 1960, when the mekometer was some electronic component on a piece of pliewood. He demonstrated how it had a tremendous amount of light, and that was the time where we had all the trouble with the weak light of the early model one geodimeter. That was my first meeting with Dr. Bradsell; it has been nice to see him at all time, and I think you all will enjoy what he has to say.

A SIMPLE CALIBRATOR FOR THE MEKOMETER EDM INSTRUMENT

R.H. Bradsell, Division of Quantum Metrology, National Physical Laboratory,
Teddington, Middlesex, United Kingdom

Abstract

A system is described which will allow a Mekometer EDM instrument to be calibrated by the user who wishes to achieve the greatest possible accuracy. The operating frequency is compared with an off-air standard to an accuracy of better than one part per million. The calibrator was developed for use with the NPL prototype Mekometer III, results on the long-term stability being given by Froome and Bradsell (1977); however it is fully applicable to the Kern ME 3000.

Introduction

Many EDM instruments require only a simple frequency measurement by way of calibration since their optical or microwave carrier wave is continuously modulated. To appreciate the system used to calibrate the Mekometer it is first necessary to understand the way in which its optical carrier wave is modulated. The instrument produces a burst of modulation (approx 500 MHz) with a duration of 40 μ s and a frequency of $(f_m + \Delta f)$ ten milliseconds later a second burst with a frequency of $(f_m - \Delta f)$; this process is repeated continuously. What we require to measure is the modulating frequency f_m . It can be seen that this modulating frequency is itself frequency modulated at 100 Hz with an excursion in the order of 100 kHz.

The Method

In essence this is very simple. A stable but tunable oscillator is adjusted to produce a continuous wave signal at frequency f_m and this is mixed with the modulation signal available from the test socket on the ME 3000 and the

resulting heterodyne beat is displayed on an oscilloscope set so that it triggers on each modulation burst and displays 40 μ s approximately full screen. When the VFO is set to exactly fm the oscilloscope will show a beat of Δf on each time base sweep and these will be exactly superimposed. A variation of the VFO frequency of as little as one part per million shows a clear difference between the alternate beat signal patterns when superimposed on a cathode ray tube. The repetition rate of 100 Hz ensures that there is no flicker.

The Equipment

This is based as far as possible on commercially available instruments and the general layout is shown in the block diagram. The only items which were especially produced were the crystal controlled VFO and the frequency multiplier and these will be described in detail later.

The VFO produces a signal at about 15.6 MHz which has very good short term stability and can be fine tuned. This signal is multiplied by thirty-two to bring it up to fm, at about 500 MHz, here a double balanced mixer is used to generate the beat which is then displayed on the oscilloscope. This oscilloscope does not have to have great frequency response since the beat it sees has a frequency less than 100 kHz, it is only required to have good triggering and adequate trace brightness to view a 40 μ s duration beat at 100 Hz repetition rate. The normal amplitude of the beat signal is of the order of 100 mV peak to peak.

To compute the Mekometer modulating frequency it is only necessary to measure the VFO frequency of about 15.6 MHz with a counter giving 1 Hz resolution and multiply the result by thirty-two. It is necessary that the frequency counter used should have the facility of connecting an external clock, normally 1 or 10 MHz, since most counters will not have an internal crystal oscillator of sufficient accuracy. The clock frequency is most conveniently provided by an off-air standard and in our case used the 200 kHz transmission from Droitwich whose carrier when used to phase-lock a quartz crystal oscillator has more than adequate accuracy. Off-air standard receivers are readily available commercially.

VFO and Multiplier

The variable frequency oscillator is quartz crystal controlled and is of the Clapp variety. The oscillator is tuned, over the limited range required to calibrate a Mekometer, by varactor so as to give smooth noiseless tuning. Excellent short term stability is achieved with no drift after a tuning adjustment has been made. The oscillator is buffered by a FET source follower stage so that the frequency counter can be connected without frequency pulling. As can be seen from the circuit diagram the AT-cut quartz crystal oscillates in the fundamental mode, however the second harmonic at 31.2 MHz is picked off by a tuned circuit in the transistor collector where it is successively multiplied by four stages of single transistor doublers until the frequency reaches 500 MHz, here an amplifier is used to clean up the signal and raise the level to about 20 mW. To prevent any tendency to frequency-pull the double balanced mixer is buffered by a 20 dB, 50 ohm attenuator pad. The VFO/multiplier is built into a small compartmented box which can include the 20 dB pad and mixer.

In the NPL prototype calibrator the above unit together with the counter and off-air standard were incorporated into a single carrying case and battery operated. The only external unit was the oscilloscope, thus the unit lent itself to field use.

The Calculation

The design of the Mekometer ME 3000 is such that it has an internal wavelength (not frequency) standard which compensates for the changing refractive index of the air by altering the modulation frequency of the instrument so as to maintain a constant wavelength of in fact 600 mm. It is clear that to calibrate a Mekometer it is necessary to compute the modulation frequency it should give under the prevailing atmospheric conditions and to compare this with the actual measured value. From a knowledge of air temperature and pressure the prevailing refractive

index can be calculated and the following formula gives the modulation frequency f_m in MHz from the temperature T in K and pressure P in mmHg:

$$f_m = \frac{499.654\ 177}{1 + 0.000\ 111(P/T)} \text{ MHz.}$$

In Conclusion

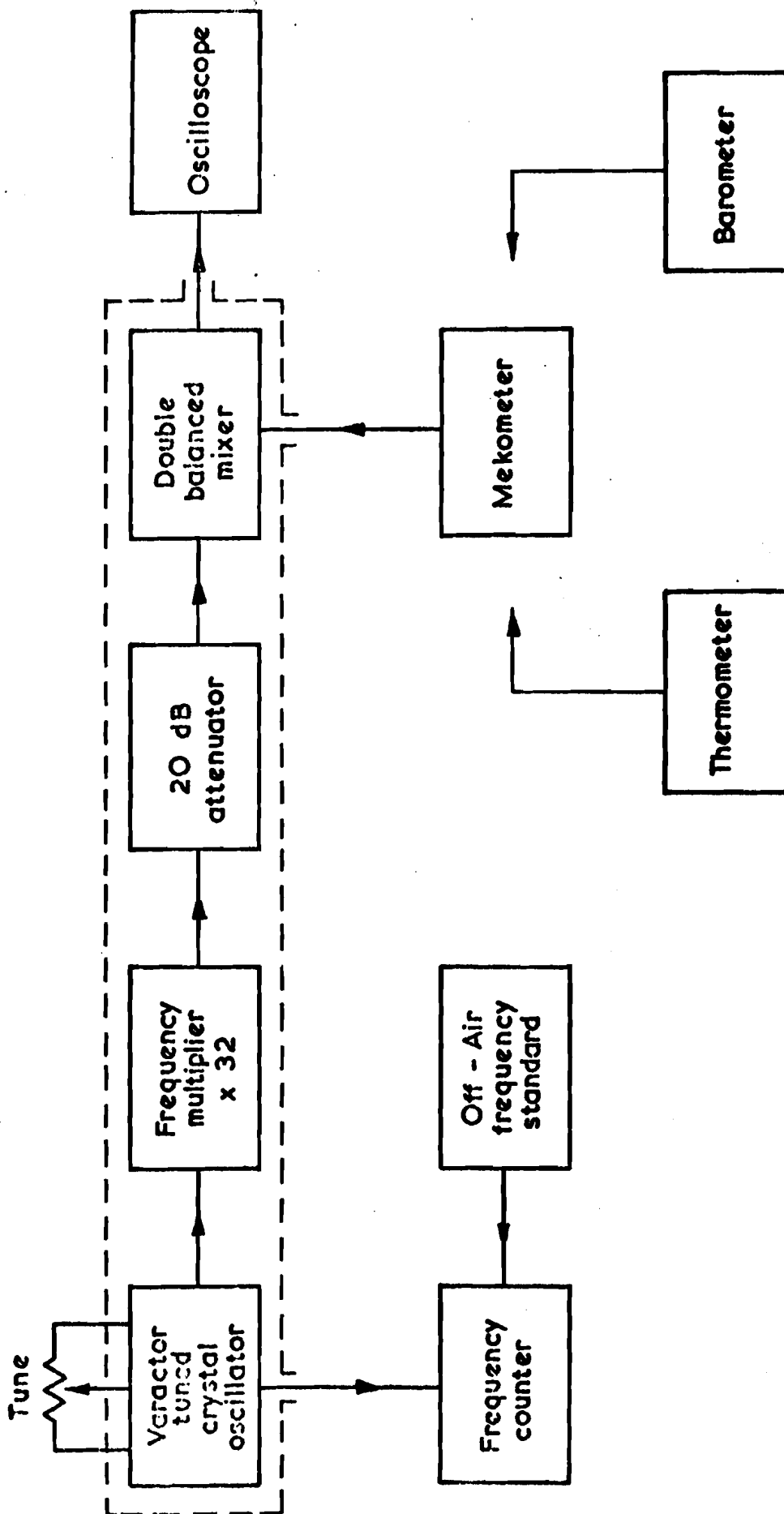
The calibrator described has been in operation over a considerable period and has been found to be quick and simple to use. At first sight it might seem that the necessity of having an oscilloscope might be a disadvantage, however in practice it much increases the versatility of the device since considerable diagnostic information is available from the oscilloscope trace. For instance the degree of frequency modulation, modulation pulse length, frequency stability during the pulse, Q factor of the wavelength standard may all be monitored in addition to a frequency measurement of accuracy in excess of one part in a million.

Acknowledgement

I am indebted to Dr K D Froome the originator of the Mekometer for much encouragement and many useful discussions.

References

- Froome, K D and Bradsell, R H (1961) J Sci Instrum Vol 38 pp 458-462
Froome, K D and Bradsell, R H (1966) J Sci Instrum Vol 43 pp 129-133
Bradsell, R H (1966) Electronic Eng Vol 38 pp 281-287
Froome, K D (1971) Survey Rev Vol 21 pp 98-112
Bradsell, R H (1971) Survey Rev Vol 21 pp 112-118
Bradsell, R H (1972) Alta Frequenza Vol 41 pp 759-770
Meier-Hirmer, B (1975) Allgemeine Vermessungs-Nachrichten Vol 82 pp 41-59
Meier-Hirmer, B (1975) Allgemeine Vermessungs-Nachrichten Vol 82 pp 373-387
Froome, K D and Bradsell, R H (1977) Survey Rev, to be published



MEKOMETER CALIBRATOR

LONG-TERM STABILITY OF AN NPL MEKOMETER III WAVELENGTH STANDARD

K.D. Froome and R.H. Bradsell, Division of Quantum Metrology, National Physical Laboratory, Teddington, Middlesex, United Kingdom

Abstract

One of the unusual features of the Mekometer is the use of a small microwave cavity resonator, constructed of fused quartz, to control the wavelength of the polarization modulation on the light beam used for distance measurement. A brief history of the evolution of this standard is given, followed by details of the performance of the NPL Metric Mekometer III extending over a period in excess of six years.

1. Introduction

The Mekometer began its life as a laboratory demonstration of the feasibility of using polarization modulation of a light ray for short-range electromagnetic distance measurement (EDM) (Froome and Bradsell 1961, 1963). In fact, the modulation frequency of this experimental Mk I was very high, namely 9 GHz and corresponded to a modulation wavelength of only 3.3 cm, the object of the research at this time being to study new methods for the calibration of invar tapes of up to 50 m in length.

However, it occurred to us that a more beneficial line to pursue would be to produce a short-range EDM system which could replace the tape (inexpensive to purchase; very expensive to use) for distance measurement in the range of up to say, one mile or 1.5 km. Today short range EDM is universally accepted, but at the time of Mekometer I the suggestion appeared very revolutionary and, undoubtedly, it was this factor which delayed the production of Mekometer II which did not appear until 1966 (Froome and Bradsell 1966).

The aim behind Mekometer II was stated as follows: "Mekometer II has been designed as a prototype instrument to investigate the measurement of lengths up to about 5000 ft (1.5 km) in the simplest possible manner. The potential users for such an instrument would be builders, engineers, and those surveyors interested in town and property measurement. For those purposes it is highly desirable that the required distance should be obtained directly without any calculations, calibrations or the customary atmospheric refractive index observations. Also, the accuracy should be better than 1 in 10^5 in order to satisfy engineering requirements and the sensitivity should be at least 1 mm". It should be recalled, here, that in 1966 EDM - in the form of the optical Geodimeter and microwave Tellurometer - was well-established for the measurement of long ranges to an accuracy of some centimetres, but there was still no short-range system.

The modulation frequency employed was approximately 500 MHz, corresponding to a modulation half-wavelength of 1 ft. (The Metric Mekometers are now based on 30 cm). The atmospheric refractivity compensation, to the aimed-for accuracy, was obtained by the use of invar cavity resonators to control the modulation wavelength in place of the customary crystal frequency standards which, of course, require the measurement of atmospheric temperature and pressure in order to calculate, from a knowledge of the velocity of light in vacuo, the actual measuring wavelength at the prevailing ambient conditions.

The decision to use such resonators was carefully considered and evolved from early work by one of us (KDF) on the precision measurement of the refractive index of air and its principal constituent at microwave frequencies and his personal association with Dr L. Essen (Essen and Froome 1951, Essen 1953, Froome 1955). Dr Essen, already

well-known for his use of cavity resonators for two determinations of the velocity of light, actually used the large 9 GHz invar cavity resonator of his 1953 refractivity measurements for the basis of a proposed new aether drift experiment (Essen 1954) which was later performed (Essen 1955) with a null result to a much higher accuracy than the celebrated Michelson-Morley optical experiment. Used in Essen's experiment to control the frequency of a microwave oscillator, a frequency stability at least as good as 1 in 10^9 per hour was attained.

Mekometer II, although large and heavy, did, at the invitation of some civil engineers, make some useful field measurements, the personal and technical benefits from these encounters being extremely encouraging.

Mekometer III ('Imperial!'), which overcame the size, weight and other shortcomings of Mk II, went ahead very rapidly and was first demonstrated at the Commonwealth Survey Officers Conference in August 1967. It achieved a genuine sub-millimetre resolution of ± 0.1 mm and an estimated accuracy of ± 3 parts per million (p.p.m.) of the measured distance to a maximum range of 3 km. In September 1967, at the invitation of a Swiss firm of consulting engineers, it began, with dam deformation studies, an extensive period of field tests. It is interesting to recall here that throughout our many contacts with potential users no consumer resistance was encountered; all welcomed the Mekometer concept.

The Metric Mekometer, essentially very similar to the Imperial model, began measuring early in 1970 and we have a record of the wavelength standard's history from May of that year. This wavelength standard, as with the commercial Mekometer, is a silver-plated fused

quartz, microwave cavity resonator operating at nine times the light-beam modulation frequency of approximately 500 MHz. The standard is filled with dry air, as shown by the dark-blue condition of its associated silica-gel desiccant, but allowed to acquire the ambient pressure and temperature as far as is practicable. It is well-known that a cavity resonator is often more correctly referred to as a 'wavemeter' because the wavelength of the oscillations in it is only related to the physical dimensions of the cavity.

2. Experimental

The theory of Mekometer III has been described (Froome 1971, so only a summary of the action of the wavelength standard is required here. If the refractive index of the air in the standard cavity was identical with that along the optical path and the cavity operating under the average ambient conditions, then the compensation could be made to be perfect, but for the following reasons this is not so in practice: the very high refractive index of water vapour at microwave frequencies, not so at optical frequencies, requires that the air in the standard be dry; the microwave refractivity of dry air is approximately 20 p.p.m. lower than the corresponding group refractive index for an optical wavelength of 0.48 μm , the effective operating wavelength of the Mekometer xenon flash light source and detector system. This figure of 20 p.p.m. is about one-fifteenth of the total optical refractivity effect at one standard atmosphere, but this does not imply an error of that magnitude because the microwave cavity resonator can be adjusted to produce exactly the correct optical modulation wavelength at a standard atmosphere condition. But if the Mekometer is used under extreme conditions, for example in a tunnel pressurized at two

atmospheres, then in this case, a correction of 20 p.p.m. would have to be applied to the measured distance. This correction is small compared to the 300 p.p.m. which would be the comparable correction for EDM based on a frequency standard. A smaller correction to the Mekometer readings arises if it is used at high altitudes (Froome and Bradsell 1966). The standard cavity is placed within the instrument and encouraged to acquire ambient temperature by thermally insulating it from the instrument case and circulating air around it by means of a small fan. A small leak into the standard, or connection to water-vapour proof bellows accommodates atmospheric pressure fluctuations. The compensation is thus achieved only at one end of the line to be measured, but normally for short lines this is adequate, and can be somewhat improved, if necessary, by measuring the atmospheric temperature along the line and applying the appropriate correction of 1 p.p.m. per $^{\circ}\text{C}$ mean difference from the standard cavity temperature. Pressure equalisation presents no problems and neither does the level of atmospheric water vapour at optical wavelengths.

But occasionally in practice we have encountered extremely good, stable, atmospheric conditions which have enabled a resolution of a few parts in ten million to be achieved. If it is desired to measure length to this accuracy, on-site determinations of pressure, temperature, and modulation frequency do then become necessary and the latter can be conveniently achieved by means of the calibrator used to obtain the results presented herein and which is described in the accompanying paper by R.H. Bradsell (1977).

Fig. 1 (Froome 1971) shows the mounting of the quartz quarter-wave standard cavity resonator in its surrounding copper container. The quartz resonator is constructed by grinding from a rod of the solid

material, the interior surfaces being silver-plated by firing-on at 650 °C a silver paste mixture supplied by Johnson Matthey Ltd. Coupling of microwave energy into and out from the cavity is achieved by means of very small wire loops through small holes, 1.5 mm in diameter, in the base of the standard. The diameter of the quartz item is approximately 20 mm, the height of the central quarter-wave resonant stub is 13 mm, the overall height of the quartz being 30 mm. Thus, the heart of Mekometer III is conveniently small, the resonant frequency being around 4500 MHz and nine times the polarization modulation frequency on the transmitted light beam - when producing the standard modulation wavelength of 60 cm.

The effect of the silver plating is to increase somewhat the basic thermal expansion of fused quartz above its normal value of 0.4 p.p.m. per °C and the mounting of the cavity within the copper container is arranged to compensate for this unwanted expansion effect (Froome 1971). Recently, G. Russell of the NPL has successfully applied an alternative plating process which has less effect on the residual thermal expansion than the silver paste process and is very reproducible in its characteristics: the cavity is first chemically cleaned and a continuous film of copper, about 0.4 µm thick is deposited by a chemical reduction method. This film is then silver plated in a cyanide silver bath, the current and time being controlled to give a final thickness of 5 µm. This is a thinner and more uniform coat than that achieved with the paste material, yet is electrically equivalent or even superior giving rise to cavity Q-factors approaching 4000.

Fig. 2 shows a plot of the results obtained since May 1970 when the quartz cavity currently in use in the NPL Metric Mekometer III was first installed. The measurements plotted represent frequency

deviations from the nominal value appropriate to the ambient conditions, expressed in parts per million. Each point has been obtained from laboratory measurements of the modulation frequency by the method to be described, together with simultaneous measurements of standard cavity temperature and the external air pressure. From such atmospheric observations it is possible to calculate what the resonant frequency should be and to express the actual difference from this nominal value in parts per million. The actual temperatures ranged from 7.0 °C to 37.0 °C, pressures from 739.5 to 771.8 mmHg. In its early days the cavity was re-set several times (by means of the trimming adjustment shown in Fig. 1) to a frequency as close as possible to the calculated nominal value. These adjustments, arising from minor damage to the instrument during field trials took place in December 1970, October 1971 and June 1972. The cause of the last mentioned damage is interesting: severe electrical discharges encountered at the rim of Mt Etna's volcanic cone, following its eruption earlier that year, caused a microwave diode to fail! There have been no breakdowns or adjustments since this date, the quartz cavity itself having survived intact up to the present time from May 1970.

It is seen that of the sixty results shown, only seven lie outside a limit of ± 2 p.p.m. from the overall mean. This mean value is 0.4 p.p.m. above the nominal axis, thus indicating we had a slight tendency to set the cavity resonant frequency this amount high when adjusting it. There is no evidence of systematic or secular shift during the recorded period of 6½ years.

References

- Bradsell, R.H., 1977, Survey Rev., to be published.
- Essen, L., 1953, Proc. Phys. Soc., B66, 189.
- Essen, L., 1954, Nature, 173, 734.
- Essen, L., 1955, Nature, 175, 793.
- Essen, L. and Froome, K.D., 1951, Proc. Phys. Soc., B64, 662.
- Froome, K.D., 1955, Proc. Phys. Soc., B68, 833.
- Froome, K.D., 1971, Survey Rev., 21, 98.
- Froome, K.D. and Bradsell, R.H., 1961, J. Sci Instrum., 38, 458.
- Froome, K.D. and Bradsell, R.H., 1963, Brit. Pat. 919368 (Appl date:
Sept 22, 1960).
- Froome, K.D. and Bradsell, R.H., 1966, J. Sci. Instrum., 43, 129.

Figure captions

- Figure 1. Microwave wavelength standard.
- Figure 2. Results obtained since May 1970.

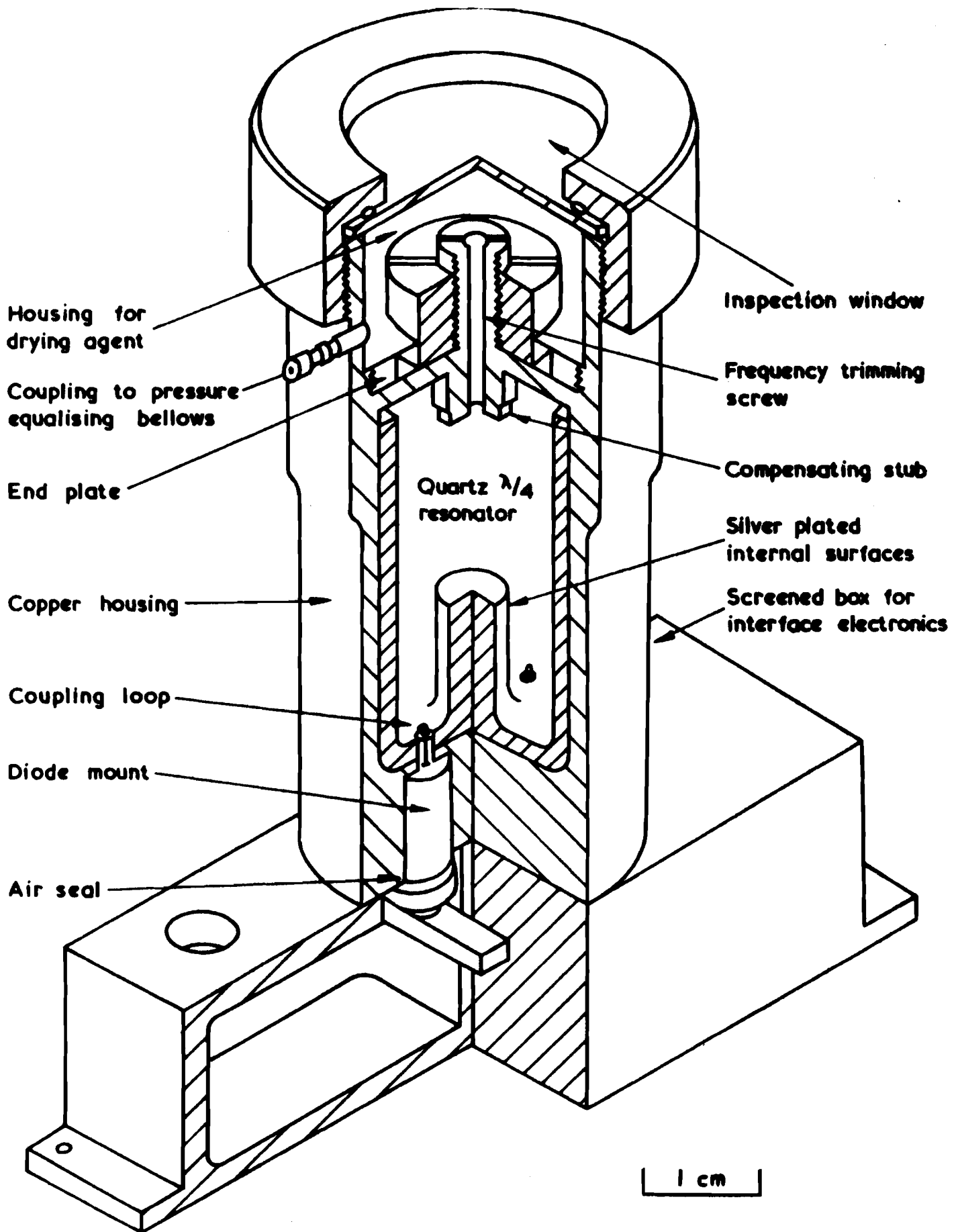


Fig.1 MICROWAVE WAVELENGTH STANDARD

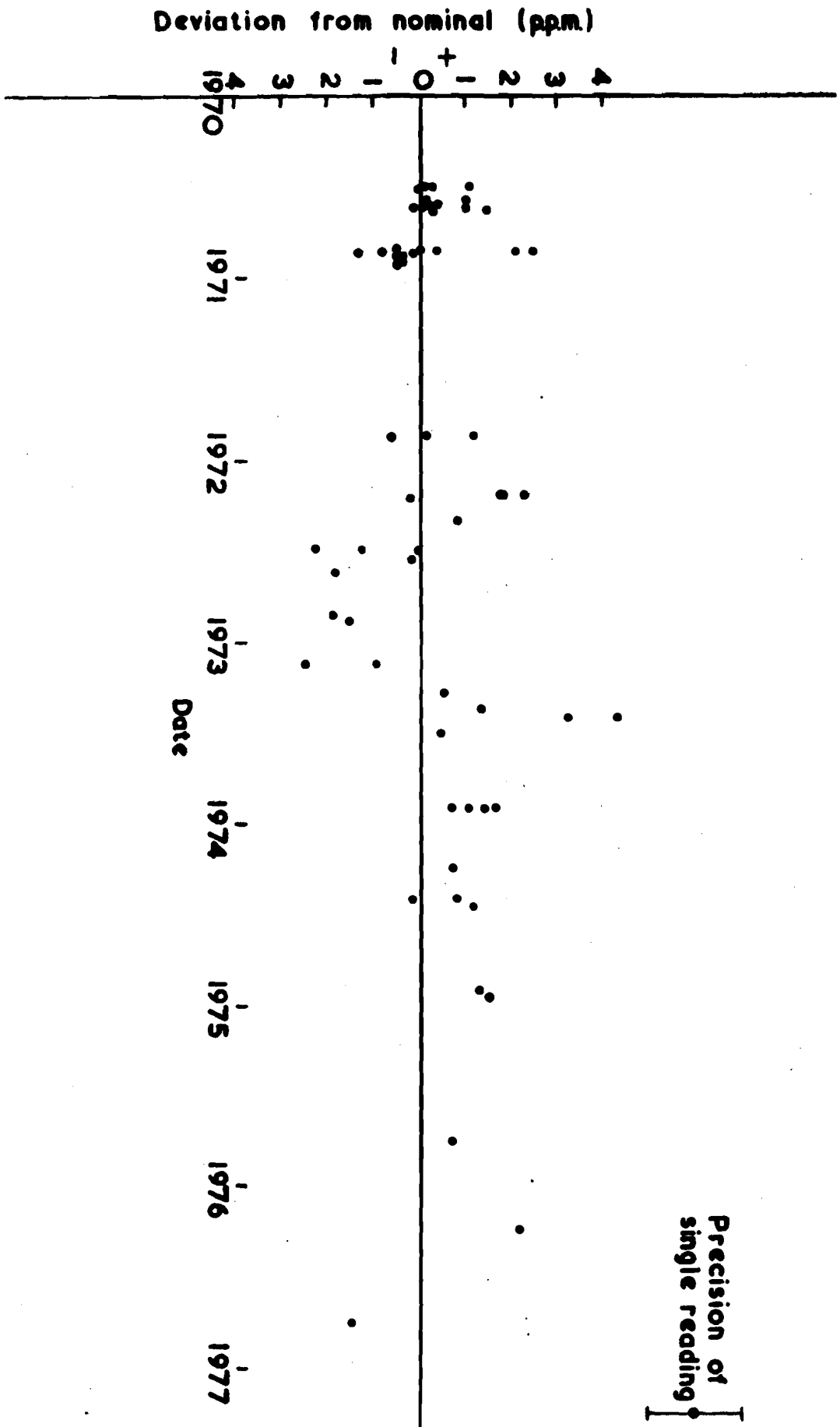


FIG 2 RESULTS OBTAINED SINCE MAY 1970

Discussion (papers 1 and 2)

Q. If you would redesign the mekometer would you use a quartz crystal in order to obtain a better accuracy ?

A. The accuracy of the cavity resonator was equal to the quartz crystal, but it had the additional advantage that it was not a frequency standard, it was a wave-length standard, and in fact it was a wave-length we wished to generate to measure distance. So if we could eliminate the necessity certainly on short ranges for having to measure temperature and pressure and applying a correction, we had a feature that was very attractive to people who were going to use the instrument, and this was the reason for doing this. Admittedly to produce such a wave-length standard is both expensive and difficult and having produced it one in fact has to adjust it, so that it tracks the characteristics of the changes of the refractive index. It is not an easy thing to do and certainly to do this commercially is reasonably expensive and I think this is probably answering your question why the instruments cost is very high.

But again I am right in saying that for short distances it is the most accurate instrument and in this world one has to pay for accuracy.

Q. But would you use a quartz crystal now ?

A. When I could answer this, I think, if I was going to start again I would indeed use a quartz crystal, but I would achieve the refractive index compensation by using two colours. So what I'm saying is the next stage of instruments what we would yet to see were in fact to use a frequency standard and would use one, two or more radiations of different wave-lengths. We should hear from dr. Huggett about this no doubt.

Q. Are you at present conducting research and trying to design an instrument that applies different wavelengths ?

A. Certainly, at the NPL- we have been doing research into a two-colour instrument and for various political and financial reasons, which I shall not go into, our progress has been rather slow, in fact for a while the work was abandoned. The economic situation required that we withdrew some of the areas of research. Now dr. Froome is embarking again upon the two-colour instruments.

Work is going back onto this again. But there has been perhaps an almost two-years gap, when we have done very little for purely financial reasons.

We feel that certainly there are two areas in EDM, which are very useful.

One is the two-colour method for very long distances, where it is impractical to fly aeroplanes and trying to measure the refractive index. So here is an area, where two-colours is extremely valuable.

The other at very long distances is to consider the system of the tellurometer which is a transponder with a micro-wave device and to try to apply this to an optical instrument- in other words - to produce an optical transponder, which is operating in two-colours and this is I think going to the third generation and then it has all desirable features with a very long range, because we would not be working on an inverse fourth power law, we are working on an inverse square law and so it would have a lot more return radiation by not using a passive target. Also we have been able to evaluate the refractive index by using two-colours, but we await laser-technology. Certainly the blue lasers are very difficult and one has many problems, and I think that eventually there will be- and I think dr. Huggett is going to tell us very soon - a practical two-colour instrument, which I certainly believe is the next state we will go to.

Q. The accuracy of the mekometer was quoted as $0,2 \text{ mm} \pm 3 \text{ ppm}$
Are these components not out of proportion when compared to one another ?

A. This is for the mekometer that's right.
The reason that I quoted three parts in a million is because the mekometer system samples the air at the instrument only. That is the problem. If you measure the refractive index along the path, you can in fact achieve better accuracy.

Q. About frequency-range, modulation from about 9 mega-herz to about 500 MHz. Did you use a 500 MHz for better adjusting or better dealing with the refractive index or refractive problems or is there another reason ?

A. There was a practical reason, that we started off in the micro-wave region, where the half-wave length was in fact $1\frac{1}{2}$ cm.
So in a long distance you had the problem resolving how many $1\frac{1}{2}$ cm there were in the distance. So that you had a great difficulty in finding your

order of incidents of the pieces you had to head up and certainly, when you had changed the refractive index, you had scintillation: it made it very difficult to find this order of interference. So we found from experience that about 30 cm half-wave length was practical over a range of about three kilometers, where one could positively find the order of interference. You could still use a mechanical phase-measuring device, which is very accurate and contain it within the shell of the instrument. If you have 10 meters then a 10 meter folded light inside is not very practical. So this gave you a practical compromise. And I think this is probably the answer to your question.

Q. You are talking about long ranges, where you of course are dealing with refraction problems and so on. One has seen in the last years the development of the for instance Hewlett Packet laser interferometer , where you can measure very accurately over relatively short ranges. However, you loose sometimes your fringes. If you would design an instrument for- and I think there might be a need in industry- for ranges- let's say - upto 15 meters, would you go to the higher frequencies in modulation, let's say, in 9 giga-herz, that you are talking about ?

A. Yes, this is a good point. That if you have something like a fringe counter, you have to have a physical connection between the adistant point and the instrument, something like a small railway-line on what you can move a corner cube very accurately and you have to count fringes. I agree that this is a difficult thing and I think there probably is a market for a phase-measuring device, where you can get an absolute measurement of a distance without physical contact. I agree with you certainly there one goes to a higher frequency and this is the very reason that we did this on our initial experiment, where we thought we were designing an instrument to measure to calibrate surveyors tapes, where the maximum length was 50 meters. Yes, that is right, we worked with the micro-wave frequency. We achieved sensitivities of about 0,2 mm and I think one could do better than that in fact. So, I agree if there is a market. For instance the mekometer would measure 10 meters to about 0,1 mm. (with care)
But I agree with you that if you want better than this one should go to a higher modulation frequency.

Q. May I please continue my question ? This modulator of 9 giga-herz, were they commercial or did you build something yourself ?

A. As a matter of fact we built them ourselves. It was a 9-giga-herz cavity-resonator, which was totally filled with KDP-crystal. It did not produce a high modulation index, it was only something like 2 or 3 percent, where-as in the mekometer-using a pulse system, which is basically high-power we produce almost the theoretical limit of modulation. And this makes phase-measurement much more easy. When working on low level, we are very troubled with polarisation effects in the optics and such sort of thing.

Remark: I would like to tell the legend, which said that when Bergstrand designed the first geodimeter it was to improve the measurement of the velocity of light, not to measure distance. Being a geodesist he also turned the situation around.

Q. I should like to say something about the cavity resonator. You have the equation, expressing the distance as a multiple of the wavelength. It actually implies a model, where the refractive index is constant along the path. This is the model imitation of the mekometer. If you have a two coloured instrument, then the model imitation becomes troublesome, not because of the constancy of the refractive index, but rather the gradient of the refractive index. This is one of the limitations of two coloured instruments namely that you have different colours. We put the weakness of the model far away, so therefore of course two coloured instruments will actually be a continuation for long ranges on a compensation principle. The high modulation frequency-as a part of your technical problems, let's call them passive(?ed) frequencies - is the guarantee for the high resolution, and it is of course quite immaterial whether you use a cavity-resonator or a quartz resonator. It is a very clever system. The limitation of the early geodimeters was that one could not use a Kerr-cell for the modulation for more than 10 MHz. Later one has improved, but again, if one has a modulating principle with 500 MHz, then almost any other system will of course get the high resolution.

I hope you are going into the two colour system.

A. We are very interested in what is coming out and we have very good faith in succesful results.

MEKOMETER ME 3000 - THEORETICAL ASPECTS, FREQUENCY CALIBRATION, FIELD TESTS -
Birgit Meier-Hirmer, Geodätisches Institut der Universität Karlsruhe, Federal
Republic of Germany

Abstract:

The Mekometer ME 3000 is a high-resolution EDM instrument incorporating an automatic correction for atmospheric refractive index. Distances up to some hundred metres can be measured with an accuracy of a few tenths of a millimetre.

This high precision can only be achieved however, if the typical corrections of the measuring system are well known. Mathematical models for the light-microwave correction and for a supplementary meteorological correction are discussed.

By testing the instrument it is shown how effects of acclimatization, heating up effects and the temperature dependence of the wave length standard can be taken into account, if necessary.

The efficiency of the Mekometer is demonstrated in three practical examples.

1. Basic Principles

The Mekometer ME 3000, a short range EDM instrument, is being manufactured since 1974 by the Kern Company in Aarau, Switzerland, in cooperation with Com-Rad Ltd. in Slough, Great Britain. Compared with already existing EDM devices it differs in two characteristic features: high precision and automatic correction for atmospheric refractive index. The principle of the Mekometer is based on K.D. FROOME [1], who introduced in 1965 a prototype Mekometer II at the International Symposium on EDM in Oxford [2, 3]. The development from the prototypes [4-8] to a commercially available instrument lasted nearly ten years. The high accuracy, to a few tenths of a millimetre, is achieved through the short modulation wavelength as well as the very simple optical-mechanical phase measuring system, which works by a variable light-path.

The automatic correction of the atmospheric refractive index is attained by using a wave length standard (microwave cavity resonator) instead of a frequency standard which is used in other EDM instruments. Although an understanding of the operation principles is not of fundamental importance to an average user, it is of interest. In order to better understand the report which follows we will now briefly outline the most important of these principles. Those wishing for a more complete description of the ME 3000 are referred to the papers [9, 10].

Figure 1 shows a block diagram of the Mekometer ME 3000. The modulation wavelength of the ME 3000 is determined by reference to the resonance of a small microwave cavity resonator (standard cavity) operating at nine times the modulation frequency of the basic measuring unit. The modulation frequencies are generated in a second microwave resonator (modulation cavity). Before comparison with the frequency f_s of the standard cavity the modulation frequencies f_1, f_2, f_3, f_4, f_5 are either multiplied by nine or ten and then mixed with the outputs $f_{q_1}, f_{q_2}, f_{q_3}$ of quartz oscillators. Only three side-band oscillators are required to produce five modulation frequencies, necessary for a length measurement within the range of three kilometres. The following system is used:

$9 f_1 - f_{q_1} = f_s$	$4\ 495.594 - 22.478 = 4\ 473.116\ \text{MHz}$
$10 f_2 - f_{q_1} = f_s$	$4\ 495.594 - 22.478 = 4\ 473.116\ \text{MHz}$
$9 f_3 + f_{q_1} = f_s$	$4\ 450.638 + 22.478 = 4\ 473.116\ \text{MHz}$
$9 f_4 - f_{q_2} = f_s$	$4\ 491.098 - 17.982 = 4\ 473.116\ \text{MHz}$
$9 f_5 - f_{q_3} = f_s$	$4\ 495.144 - 22.028 = 4\ 473.116\ \text{MHz}$

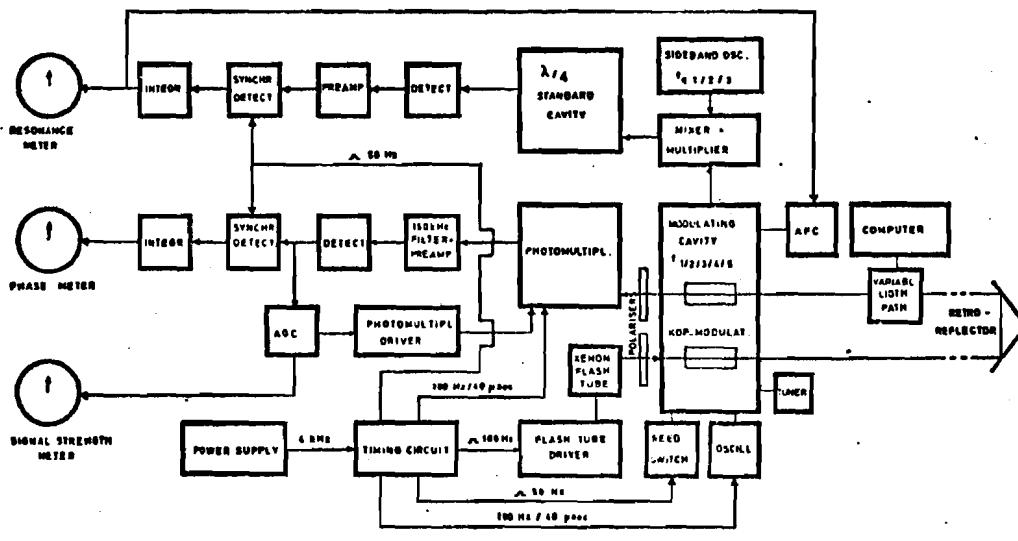


Fig. 1 Block diagram of the Mekometer ME 3000

The side-band oscillators do not have to be of high stability since their frequencies are only 0.5 % of the 4.5 GHz standard frequency. Starting a phase measurement one has to set the modulating cavity by a tuner to produce the fundamental wavelength. A light beam emerging from a Xenon flash tube ($0.485 \mu\text{m}$) is modulated by this frequency by KDP crystals arranged within the modulation cavity. The resonance frequency of the standard cavity determines substantially the unit of length measurement. The value of this frequency (4.5 GHz) is essentially given by the dimensions of the standard cavity and the atmosphere inside the resonator.

The standard cavity is filled with dry air. By ventilation it attains atmospheric temperature and through a small hole the pressure is adjusted. If the dimensions of the cavity are independent of temperature and pressure, the measuring wavelength stays constant. Changes in the atmospheric refractive index causes changes in the resonance frequency of the standard cavity, in accordance with the formula of ESSEN and

FROOME. For a measurement with microwaves the standard cavity would automatically correct for the influence of the atmospheric refractive index, but this is not so for measurements done with the Mekometer using light radiation for carrier wave. Refractive index changes for light follow the formula of BARRELL and SEARS. It is possible however, to achieve the exact correction required for a distinct "standard atmosphere". For deviations from this standard atmosphere the measured results have to be corrected. The corrections stay small, if the standard cavity is kept dry, because the influence of humidity on the refractive index of microwaves is two orders of magnitude larger than for light. Therefore a drying agent (Silicagel) inside the standard cavity housing provides for dry air.

A full mathematical treatment of the correction problem is presented in [9].

The velocity of light waves c_L is given by

$$c_L = \frac{c_0}{n_L} = l_0 \cdot f_0 \quad (1)$$

c_0 = velocity of light in vacuum
 n_L = refractive index for light waves
 f_0 = modulation frequency
 l_0 = wavelength

For an automatic correction of the atmospheric refractive index the wavelength

$$l_0 = \frac{c_0}{n_L \cdot f_0} \quad (2)$$

must be constant.

This condition is fulfilled by tuning the measuring frequency to the reference frequency of the standard cavity. As already mentioned this works exactly for microwave radiation but not for light. If we let \bar{f} be the measuring frequency, λ the appertaining wavelength, n_M the refractive index for microwaves, n_{MS} and n_{ML} the refractive indexes of the standard atmosphere, \bar{f} may be written:

$$\bar{f} = \frac{c_0}{n_M \cdot \lambda} = \frac{c_0}{n_L \cdot \lambda} \left(\frac{n_L \cdot n_{MS}}{n_M \cdot n_{LS}} \right) = \frac{c_0}{n_L \cdot \lambda_0} \left(\frac{n_L \cdot n_{MS}}{n_M \cdot n_{LS}} \right) \quad (3)$$

This equation contains all the important relationships. For the wavelength standard one has

$$\lambda_0 = \lambda \cdot \frac{n_{MS}}{n_{LS}} \quad (4)$$

Thus we get for the standard atmosphere $f = f_0$, otherwise the bracket deviates from one and consequently \bar{f} differs slightly from f_0

$$\bar{f} = f_0 \left(\frac{n_L \cdot n_{MS}}{n_M \cdot n_{LS}} \right) \quad (5)$$

According to BARRELL and SEARS we obtain for the lightwave used in the Mekometer

$$(n_L - 1) \cdot 10^7 = \frac{3096.06}{1 + \alpha t} \cdot \frac{p}{760} - \frac{0.55}{1 + \alpha t} \cdot e \quad (6)$$

and according to ESSEN and FROOME for microwaves

$$(n_M - 1) \cdot 10^7 = \frac{2879.35}{1 + \alpha t} \cdot \frac{p}{760} - \frac{0.63}{1 + \alpha t} \left(1 - \frac{105.35}{1 + \alpha t} \right) \cdot e \quad (7)$$

Because of the drying agent, which provides for dry air inside the standard cavity, we can put $e = 0$ in the microwave formula (7). For light waves we can take an average value of $e = 10$ Torr, because the influence of humidity on the refractive index of light is small.

For the selected standard atmosphere $t_S = 20^{\circ}\text{C}$ and $p_S = 760$ Torr we obtain $(n_{LS} - 1) \cdot 10^7 = 2879.73$ and $(n_{MS} - 1) \cdot 10^7 = 2682.91$. With these values we can calculate a relative frequency correction - identical with a relative length correction - directly from formula (3) due to the difference in refractive index between light and microwaves. By an expansion we get a simple relation

$$\frac{\Delta S}{S} = \frac{f_0 - \bar{f}}{\bar{f}} = \left(201.9 - \frac{216.7}{1 + \alpha t} \cdot \frac{p}{760} \right) \cdot 10^{-7} \quad (8)$$

and in the vicinity of the standard atmosphere we can simplify further

$$\frac{\Delta S}{S} = \frac{f_0 - \bar{f}}{\bar{f}} = [0.69 (t - t_S) - 0.27 (p - p_S)] \cdot 10^{-7} \quad (9)$$

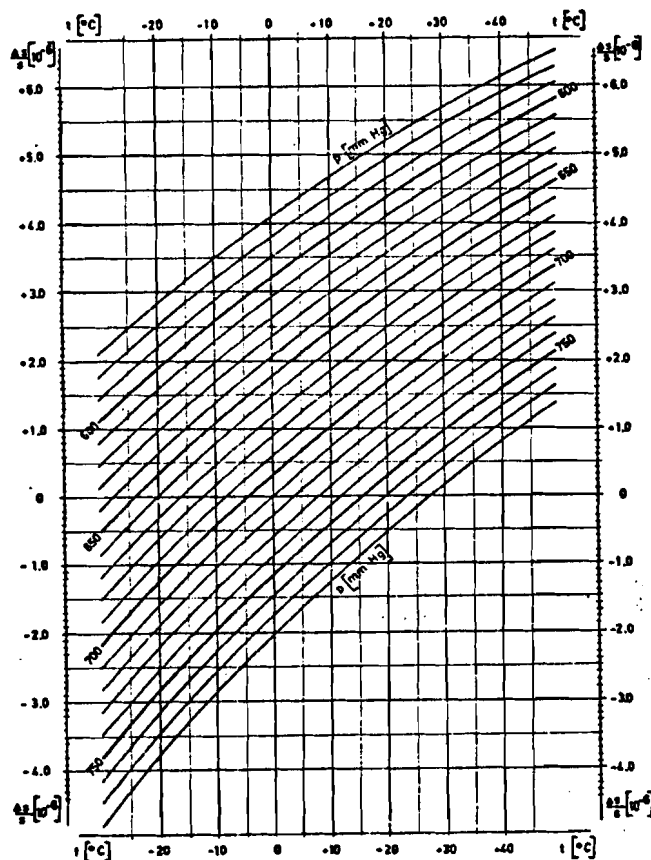


Fig. 2 Relative length correction due to the difference in refractive index between light and microwaves

Figure 2 shows a graph calculated from the correction formula (8). Formula (9) allows an estimate of the order of magnitude of the relative length correction. We see that for a $(t-t_s)$ of about 15°C and for a $(p-p_s)$ of about 40 Torr, a correction of $1 \cdot 10^{-6}$ results.

At this stage we must emphasize, that compensating for the influence of the atmospheric refractive index is only correct for the immediate surroundings of the Mekometer station. For the case of inhomogenous atmospheric conditions along the light path one has to measure, perhaps at several points, the temperature and pressure, and calculate the average values t_r and p_r . According to the formula of BARRELL and SEARS, we get an additional meteorological correction, dependent on the difference between the values t_r and p_r and those of t and p at the Mekometer station. Thus we get for this additional meteorological correction

$$\frac{\Delta S}{S} = \left[\frac{11.3}{(1+\alpha t)^2} \cdot \frac{p}{760} (t_r - t) - \frac{4.1}{1+\alpha t} (p_r - p) \right] \cdot 10^{-7} \quad (10)$$

or simplified, if we calculate the coefficients for the standard atmosphere

$$\frac{\Delta S}{S} = [9.8 (t_r - t) - 3.8 (p_r - p)] \cdot 10^{-7} \quad (11)$$

Figure 3 shows a graph for the additional meteorological correction.

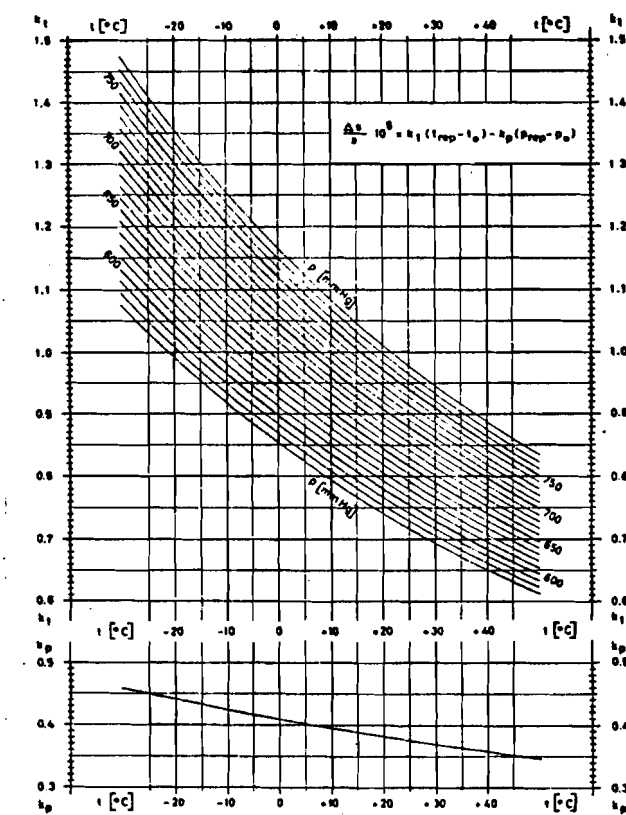


Fig. 3 Relative length correction due to several meteorological measuring stations

An important fact for precision measurements with the Mekometer is the performance of the wave length standard. The standard cavity can be tested by frequency calibrations. The calibration frequency for the standard atmosphere is given by

$$f = \frac{c_0}{n_{MS} \cdot l} = \frac{c_0}{n_{LS} \cdot l_0} \quad (12)$$

With $l_0 = 60$ cm (effective 30 cm) we get $f = 499.5104$ MHz. For deviations from the standard atmosphere, equation (3) must be used, which can be written in the following form

$$\bar{f} = \frac{c_0}{n_{MS} \cdot l} \left(\frac{n_{MS}}{n_M} \right) = f \left(\frac{n_{MS}}{n_M} \right) \quad (13)$$

By expansion one obtains

$$\bar{f} - f = f \left(2682.9 - \frac{2879.4}{1 + \alpha t} \frac{p}{760} \right) \cdot 10^{-7} \quad (14)$$

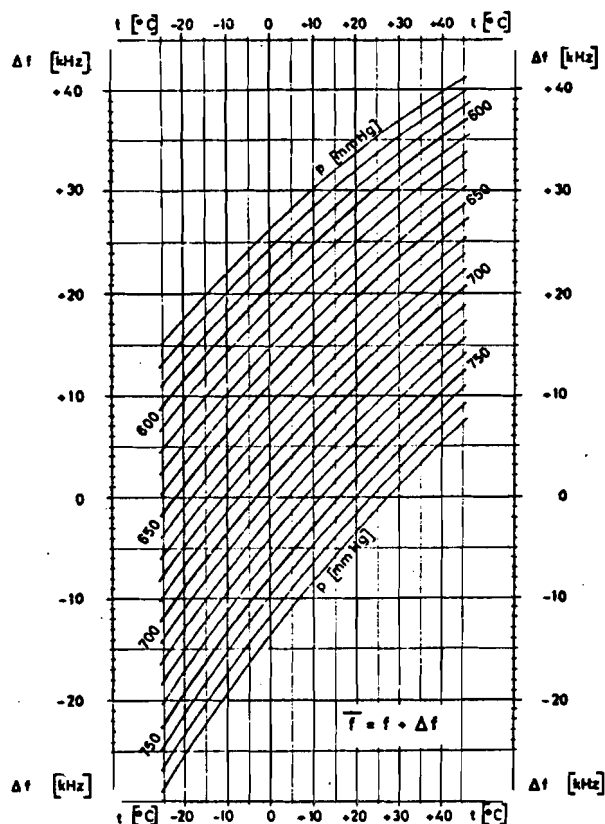


Fig. 4 Calibration frequency as a function of pressure and temperature

or simplified in the vicinity of the standard atmosphere

$$\Delta f = \bar{f} - f = f [9.2 (t-t_S) - 3.5 (p-p_S)] \cdot 10^{-7} \quad . \quad (15)$$

Figure 4 shows the dependence of the calibration frequency on pressure and temperature.

2. Tests for the Automatic Correction of the Influence of the Atmospheric Refractive Index

The standard cavity plays an important role in determining the absolute accuracy of the results and therefore extensive frequency calibrations are necessary. However the frequency measurement is not comparable to other EDM devices. The mode of modulation and the high frequency require special equipment for frequency calibration. At the "Geodätisches Institut der Universität Karlsruhe" we constructed such an equipment and tested thoroughly several Mekometers. The results of the investigations on our instrument are given in detail in [10]. In this paper we review only the most important results. The tests refer mainly to the behaviour of the standard cavity under different atmospheric conditions. For the simulation of temperature and pressure we used a temperature controlled room and a pressure chamber.

The results of the pressure test can be taken first. They showed, that the pressure equalising works well, even though the small hole at the standard cavity was closed with a plastic cap to prevent humidity entering. Figure 5 shows the measured values of the pressure test of the standard cavity.

Temperature tests on the standard cavity should indicate the performance of the wave length standard. During the preliminary length measurements, we observed slight systematic effects at the beginning of every measuring period. We presumed there to be a correlation between these effects and the behaviour of the standard cavity. During the frequency calibration we measured therefore not only the room temperature but also the cavity temperature.

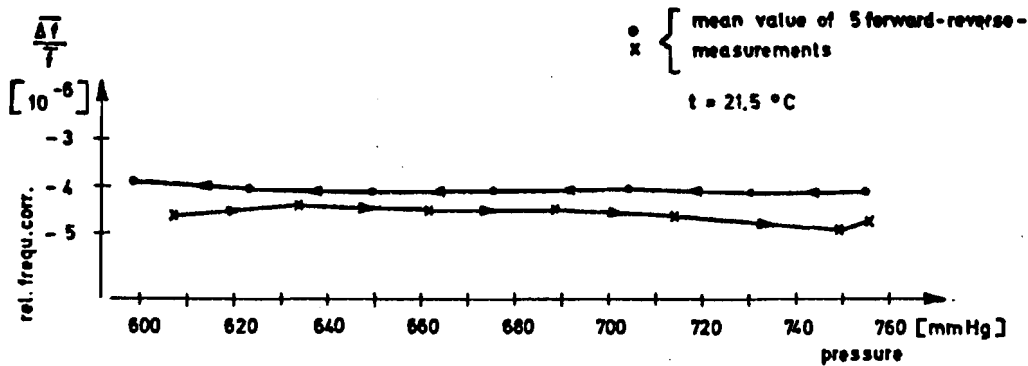


Fig. 5 Pressure test of the standard cavity

We started the calibrations by determining the so called "acclimatisation process". For this we cooled the Mekometer down to 2°C and measured the acclimatisation process when it was placed at a room temperature of 19°C . This was done by simultaneously measuring the frequency and temperature of the standard cavity. We then repeated this process with the starting temperature of 36°C . Figure 6 indicates, that the frequency needs almost two hours to get stable within $1 \cdot 10^{-6}$ for the chosen temperature difference of 17°C , i.e. about 6 minutes per degree temperature difference. To avoid long delays in the field, before one can actually start a precise measurement, the Mekometer should be exposed to atmospheric temperature as early as possible.

Figure 7 shows another temperature effect and the related frequency effect of the standard cavity. The temperature of the standard cavity rose about 1.8°C during the first two hours after switching on, although the instrument was acclimatized and the ventilation was working well. This temperature difference is related to a frequency change of $2 \cdot 10^{-6}$. Without ventilation these values become after 2 hours, 4°C and $5 \cdot 10^{-6}$. Therefore one has to provide good ventilation and to wait for about 1 hour until the frequency gets stable. To get reasonable data for the temperature dependence of the standard cavity we measured this heating up effect at every temperature point.

Figure 8 shows the temperature dependence of the wave length standard determined using the frequency at the end of the heating up period. The standard cavity is not independent of temperature and therefore the automatic correction of atmospheric refractive index is not fully

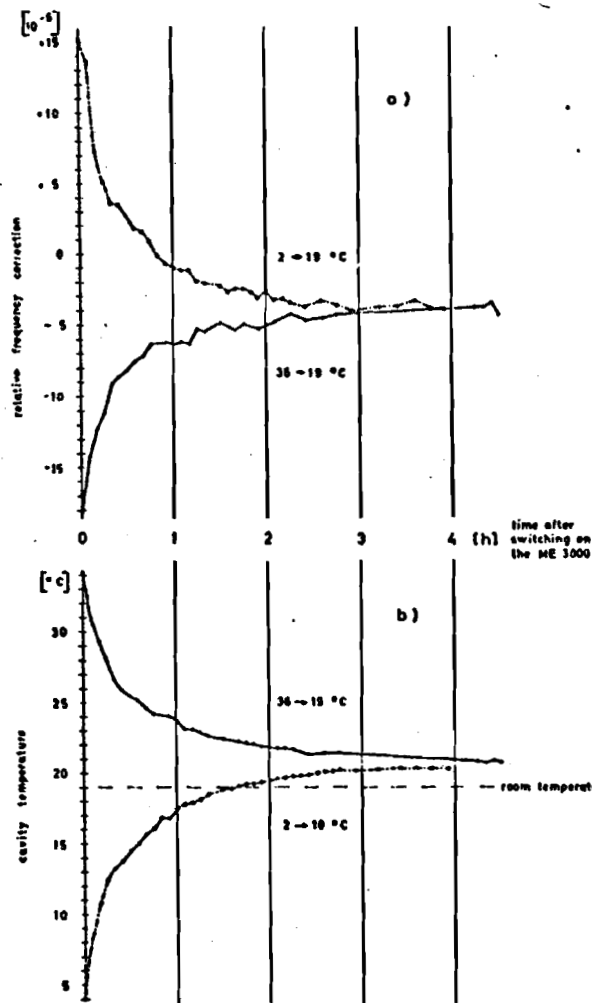


Fig. 6 Acclimatisation process
 a) Relative frequency correction
 b) Cavity temperature

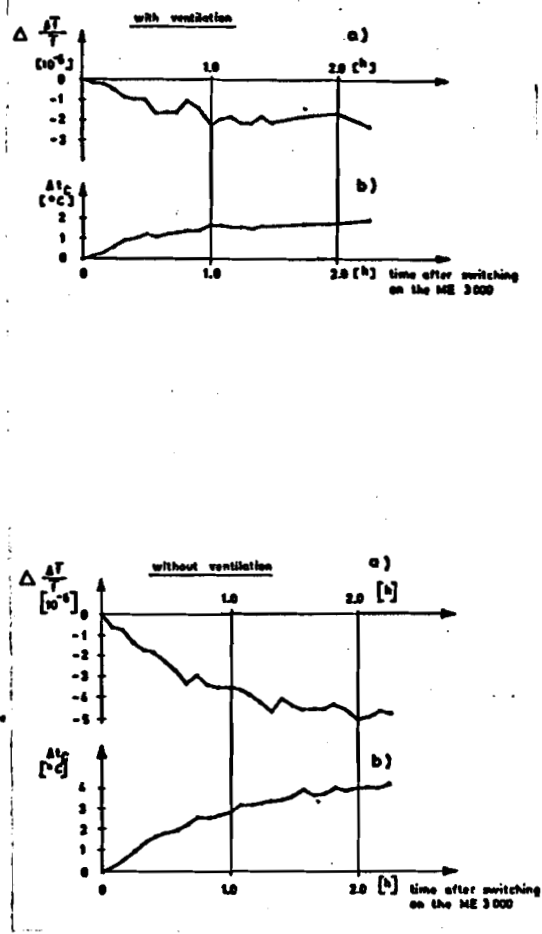


Fig. 7 Heating up process
 a) Relative frequency correction
 b) Cavity temperature

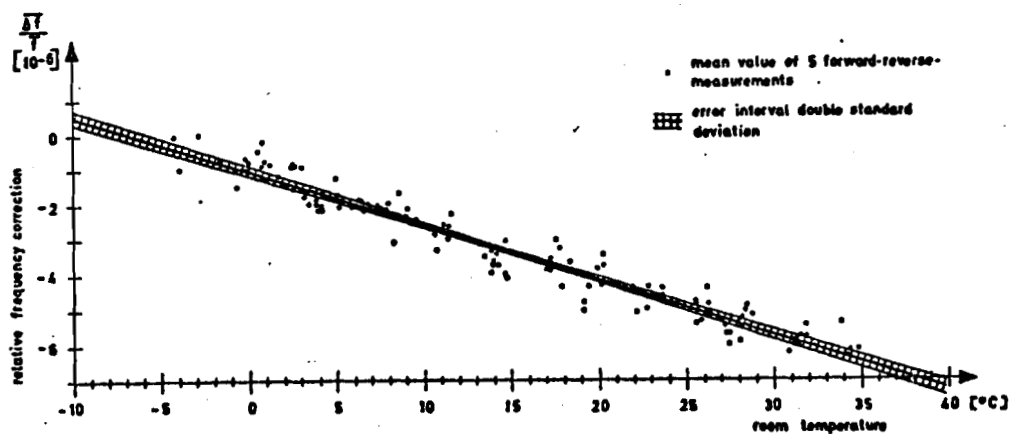


Fig. 8 Temperature dependence of the standard cavity

achieved. In the case of our Mekometer we get a linear dependence and this error can be corrected by a suitable frequency correction. A "least squares" fit gives a relative frequency correction of

$$\frac{\overline{\Delta f}}{f} = [- (1.02 \pm 0.06) - (0.156 \pm 0.003)t] \cdot 10^{-6} \quad (16)$$

We took data from -6°C to $+36^{\circ}\text{C}$ in steps of 3°C and measured also the heating up effect of the standard cavity at every temperature. It was possible, therefore, to make a "least squares" fit for the whole data set. The heating up effect was independent of temperature and had an exponential time dependence. We used the following mathematical model for the fit.

$$F(t,z) = \frac{\overline{\Delta f}}{f} = a + bt + c \cdot e^{-z/d} \quad (17)$$

a, b, c and d are constants, t and z are the variables for temperature and time. For $z \rightarrow \infty$ we again get the linear calibration function

$$F(t) = a + bt \quad (18)$$

corresponding to equation (16). The total heating up effect is given by

$$F(t,\infty) - F(t,0) = -c \quad (19)$$

The result of this combined "least squares" fit was

$$\frac{\overline{\Delta f}}{f} = [-(1.00 \pm 0.04) - (0.163 \pm 0.001)t + (2.34 \pm 0.07) \cdot e^{-z/(0.74 \pm 0.05)}] \cdot 10^{-6} \quad (20)$$

With this complete calibration function, it is possible in principle to correct length measurements made with an acclimatized Mekometer immediately after switching on. We have to insert t in $^{\circ}\text{C}$ and z in hours. In the same way we also did a "least squares" fit for the standard cavity temperature. We could show, that the change of the wave length standard during the heating up period of the Mekometer can be completely explained by the temperature rise of the standard cavity.

All the frequency measurements were done in the range "10 - 500 m", because the high precision of the Mekometer is only useful in this range. On the long term stability of the standard cavity we can make no statement at the moment, but current frequency controls at our instrument indicate a reasonable stability.

Considering this theoretical aspects and the results of the frequency calibration, it is seen that the resulting corrections can considerably exceed the precision of the instrument and thus can generally not be neglected.

3. Field Tests

Three practical examples should demonstrate the efficiency of the Mekometer ME 3000.

3.1 Dam Movements at the Linach Reservoir

Within the framework of surveying exercises we introduced the Mekometer to students. To make these exercises realistic, we tried to measure a possible temperature induced movement of the Linach reservoir dam during a day with the Mekometer as well as with angle measurements (Wild T 3). Figure 9 shows a location plan and the results of a typical observation day with sunshine and a temperature rise of 6°C from morning till noon. We recognize two features:

- the higher accuracy of the Mekometer measurements in comparison to the angle measurements. With a linear "least squares" fit we obtain a standard error of ± 0.15 mm for the observations;
- the result of the angle measurements from pillar V is in good agreement with the Mekometer result, whereas the angle measurements from pillar III show a strong deviation. Obviously effects of lateral refraction show a dam movement, which is infact not present. Pillar III is situated on a slope with sunshine, whereas pillar V is in shadow.

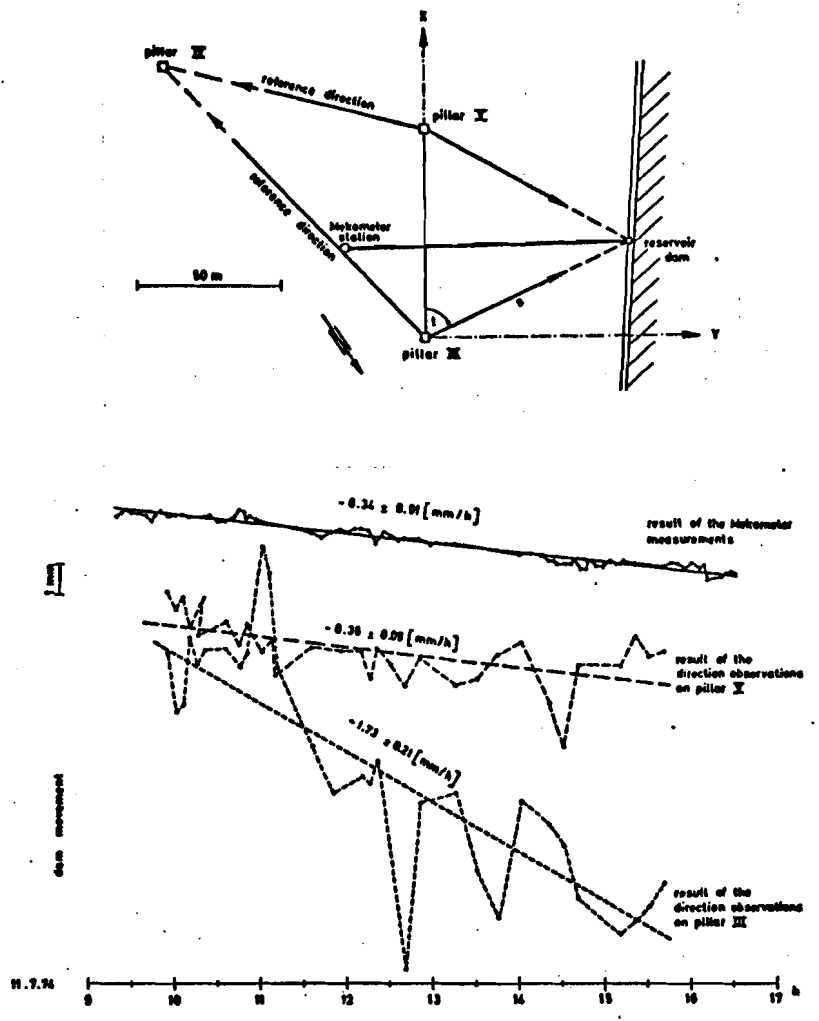


Fig. 9 Determination of dam movements at Linach reservoir

3.2 Deformation Measurements at the Hornberg Reservoir

The Hornberg reservoir, situated in the south of the Black Forest, was built by the "Schluchseewerk AG" and serves as a water reservoir for energy storage. In cooperation with the "Landesvermessungsamt Baden-Württemberg" we made angle and Mekometer measurements on the reservoir. The network consists of 12 double walled pillars sitting on the rim of the reservoir and of five pillars for reference some distance from the reservoir. Until now the network has been independently measured four times and has been on each occasion freely adjusted by a linear network as well as by a combined linear-angle network. The following table shows the accuracies resulting from the adjustments.

linear network combined linear- angular network angular network	(1)	mean observation error before adjustment		average standard error of distance after adjustment	average standard error of position
	(2)	distances	directions		
	(3)	[mm]	[cc]	[mm]	[mm]
initial measure- ment 9/74	(1)	± 0.36		± 0.25	± 0.31
	(2)	± 0.69	± 4.0	± 0.37	± 0.40
first current measurement before filling 9/75	(1)	± 1.04		± 0.48	± 0.59
	(2)	± 1.22	± 3.2	± 0.42	± 0.44
second current measurement after partly filling 10/75	(1)	± 0.56		± 0.36	± 0.43
	(2)	± 0.74	± 3.3	± 0.37	± 0.40
third current measurement after complete filling 6/76	(1)	± 0.47		± 0.30	± 0.36
	(2)	± 0.43	± 3.0	± 0.24	± 0.27
	(3)		± 3.5		± 1.02

Accuracies resulting from adjustments of Hornberg reservoir network

The number of redundant observations was about 45 in the linear network and 120 in the combined network. Although the measured lengths lie between 100 and 500 m and the centering was done by a Kern centering device over thread bolts with a marked centre, we obtained a rather high accuracy for the length measurement. The average standard errors for position lie, with only one exception, below 0.5 mm. The reduced accuracy of the measurements in September 1975 is mainly caused by unfavourable meteorological conditions, which not only increased the error in determining the atmospheric refractive index but also influenced the centering accuracy. A comparison of the linear adjustment with the combined linear-angular adjustment shows, that the angle measurement did not decisively influence the accuracy already obtained in the length measurement. On the other hand the length measurement can essentially increase the accuracy of an angle measurement as is noted in the last line of the table, which shows the errors of the angular adjustment. By the length measurement we could diminish the average standard error for position from ± 1.02 mm to ± 0.27 mm. Thus the question arises, whether in this network one can abandon angular measurements, which are much more troublesome than length measurements. Figure 10 shows the horizontal movements between the measurements from October 1975 and June 1976. Both adjustments are practically identical.

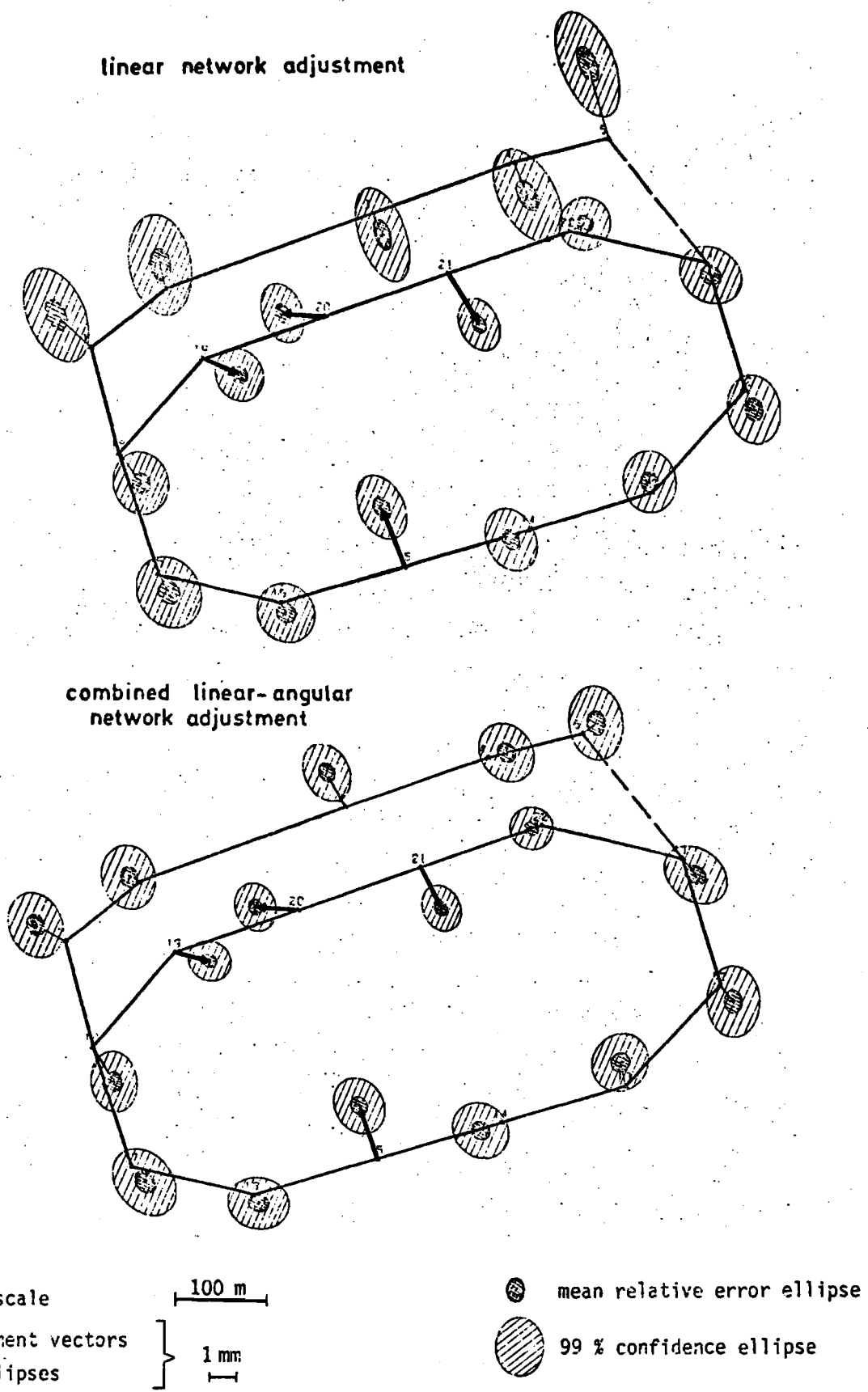


Fig. 10 Hornberg reservoir - Horizontal movements computed from coordinate differences (free network adjustments) between October 1975 and June 1976

3.3 Control Measurements at a Railway Bridge

Another interesting example, which demonstrates the power of the Mekometer is a trigonometrical study of a railway bridge over the Gauchach gorge. Additionally we can show that new configurations of networks are possible with precision measurements in connection with adequate angle measurements. Within this gorge it was impossible to establish a trigonometric network because of topographical reasons. It was already difficult to find safe stations for plummeting from the bridge. Therefore we chose the network from figure 11 for control measurement.

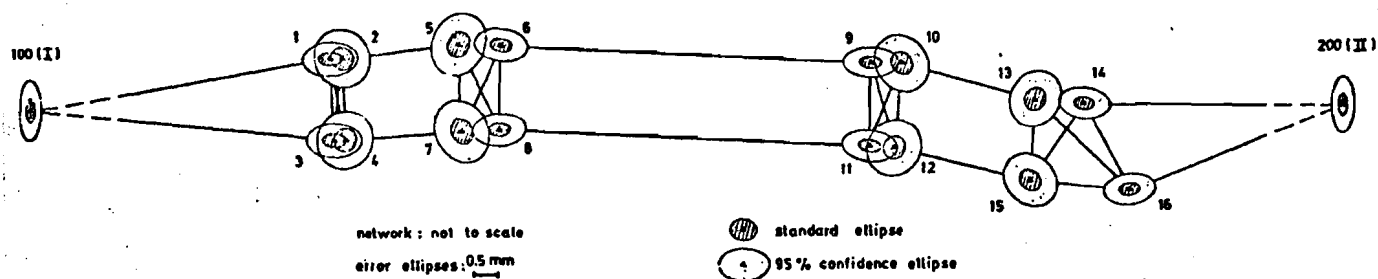


Fig. 11 Trigonometric network of Gauchach Bridge with error ellipses of the initial measurement

Pillars I and II are reference points, grappled in rock, and are not effected by possible movements in the bridge region according to the opinion of geological experts. The distance between the pillars is about 400 m. On the top of piers there are solid squares of sandstone, which served as ideal carrier for the Kern ball centering device. For mutual reference on each pier we connected together four points into a point group. The observation scheme provided for a length measurement from pillar I and II to all points on the bridge with the Mekometer and for an angle measurement with the DKM 2. Moreover we measured on each side of the bridge the angle of refraction from point group to point group for a mutual stabilisation. Additionally the distances within the point groups have been measured by a 10 m invar tape to one or two tenths of a millimetre - comparable to the accuracy of the Mekometer length measurements. Up to the present we have made three independent measurements. In the following table we compare the results of the error adjustments of the network. The results speak for themselves, considering, that the coordinate differences between the adjustments of the initial measurement and the first current measurement did

not exceed 0.4 mm, i.e. they lie within the range of the average error of position. We conclude therefore that not only are there no significant position shifts between the measurements, but also we confirmed the reproducibility of a position accuracy to some tenths of a millimetre.

period of measurement	mean observation error before adjustment		average standard error of distance after adjustment	average standard error of position
	distances	directions		
	[mm]	[cc]		
initial measurement in the beginning of May '76	± 0.39	± 1.9	± 0.24	± 0.28
first current measurement at the end of May '76	± 0.42	± 2.1	± 0.26	± 0.31
second current measurement after blasting August '76	± 0.36	± 1.8	± 0.22	± 0.26

Accuracies resulting from adjustments of the Gauchach Bridge network

4. Conclusions

To take advantage of the high precision of the ME 3000 and to obtain accuracies of some tenths of a millimetre, one has in our experience to consider a series of important points:

- restriction to the measuring range "10 - 500 m" and an accurate determination of the additive constant (zero correction). In the range "500 - 3000 m" we have only limited experiences. The sensitivity is less good, the frequency correction has in addition to be determined and moreover errors due to meteorological influences can exceed the accuracy of the instrument. In this range accuracies better than one millimetre are hardly achievable;
- one has to measure principally in the "forward" and "reverse" mode to eliminate zero drifts from the electronic part of the instrument;
- one has to regard all corrections, which reach an order of magnitude of a tenth of a millimetre. The heights measured have to be adequately precise;

- the centering accuracy has to be one tenth of a millimetre or better. Therefore pillars should be used and if possible they must be double walled to prevent effects from sun radiation. An accuracy better than one millimetre is hardly ever achievable with the use of tripods. The optical plummets of the instrument and of the reflector are not precise enough in our experience. Even by lateral centering one has to expect movements of the tripods during a measurement;
- finally we recommend a frequency calibration before and after a precise measurement or, if one has no adequate equipment, to test the instrument with a base for calibration. Furthermore the air in the standard cavity must be absolutely dry. One should check the dark blue colour of the drying agent before starting a measurement and exchange it if necessary.

References:

- [1] FROOME, K.D.
BRADSELL, R.H. Distance measurement by means of a light ray modulated at a microwave frequency. J.Sci.Instr. (1961), Vol. 38 pp. 458 - 462.
- [2] CONNELL, D.V.
ARMSTRONG, J.A. N.P.L. Hilger Mekometer. Manuskript, Intern. Symp. f. EDM in Oxford, Sept. 1965.
- [3] FROOME, K.D.
BRADSELL, R.H. Distance measurement by means of a modulated light beam yet independent of the speed of light. Manuskript, Intern. Symp. f. EDM in Oxford, Sept. 1965.
- [4] FROOME, K.D.
BRADSELL, R.H. A new method for the measurement of distances upon to 5000 ft by means of a modulated light beam. J.Sci.Instr. (1966), Vol. 43, pp. 129 - 133.
- [5] BRADSELL, R.H. The electronic principles of the Mekometer II. Electronic Engineering, May 1966, pp. 282 - 287.
- [6] FROOME, K.D.
BRADSELL, R.H. N.P.L. Mekometer III. AVN 4/1968.
- [7] FROOME, K.D. EDM with sub-millimetre resolution. Survey Review, July 1971, Nr. 161.
- [8] BRADSELL, R.H. The electronic principles of the Mekometer III. Survey Review, July 1971, Nr. 161.
- [9] MEIER-HIRMER, B. Präzisionsstreckenmessung mit dem Mekometer ME 3000. AVN 2/1975.
- [10] MEIER-HIRMER, B. Frequenzuntersuchungen am Mekometer ME 3000. AVN 11/1975.

Discussion (paper 3)

Q. I understand that in the triangulation, and trilateration carried out for this type of measurement, the accuracy has been indicated by standard ellipses. Are these the standard ellipses of the coordinates or are they the standard ellipses of the differences of the coordinates which give the actual displacements of the dam. If the former case prevails, it will give quite a different picture of the accuracy.

A. They are the standard ellipses of the differences.

Q. You stated or rather derive some operation rules or principles or instructions, issues; for instance, that the instrument should be acclimatised and in a reasonable state of temperature before the start of the measurement. Have they been applied to your measurements ?

A. Sure.

Remark: I would also add one comment to whether one should measure distance or angles while doing deformation-measurements. The idea is of course in general to detect the active spots or regions in the higher order network.

Thereafter it is a matter of putting the instruments on positions where you can actually display the maximum effect on what happened. I mean that, if you are questioning by the measurement of distances, then it is a matter of putting the instrument in this distance where you expect the largest deformation. Of course it requires an expensive general network to find these spots. Obviously some positions of observation would be more clear in telling what happened. We assume as you have disclosed in what direction a point moves, that then you don't have need of a network; All you have to do is to measure the displacement in its main direction.

TESTING ELECTRO-OPTICAL DISTANCES ON AN INTERFEROMETRIC BASE-LINE

M. van den Herrewegen, IGN, Brussels, Belgium

1. Description of the measurements.

1.1. Introduction.

The fundamental distance equation for most actual E.D.M.-equipment can be written as follows :

$$D = N \frac{C_0}{2fn} + \frac{\Phi}{2\pi} \cdot \frac{C_0}{2fn} + k$$

where :

- D : the measured distance
- n : the refractive index
- C₀ : the velocity of light in vacuo
- f : the modulation frequency
- Φ : the phase shift between the outgoing and returning light
- N : an unknown number of half wavelengths
- k : zero or additive constant.

The precision of an instrument i.e. the agreement of a series of measurements with one another, depends on the stability of the frequency f and the accuracy of the phase measurement. Whereas the accuracy of a measured distance, i.e. its closeness to the true value, is characterised by many more parameters such as :

- centering errors
- cyclic errors
- pointing errors
- an incorrect assumption of the refractive index
- the accuracy with which the zero or additive constant has been determined
- the strength of the reflected signal.

It was our aim to analyse the accuracy of a Tellurometer MA 100 and a CD 6 instrument with regard to their cyclic errors and the accuracy of the additive constants k.

1.2. The interferometric base-line.

The tests were executed at the interferometric base-line of the "Departement de Génie civil et Connaissance des matériaux" of the FACULTE POLYTECHNIQUE de Mons (Belgium). This base line is situated in a cellar and has a length of 55 m. On one side the HP laser measuring system is positioned, on the other side the instrument to be tested. For the determination of the additive constant, it is necessary to perform absolute measurements, while for the analysis of the cyclic error, the technique of differential measurements is preferable. The centering plate which supports the instrument is fixed permanently on the rail. As for the centering plate of the reflector, it can be put anywhere along the rail and is provided with a micrometer. So it is possible to realize accurately any wished distance on the base-line.

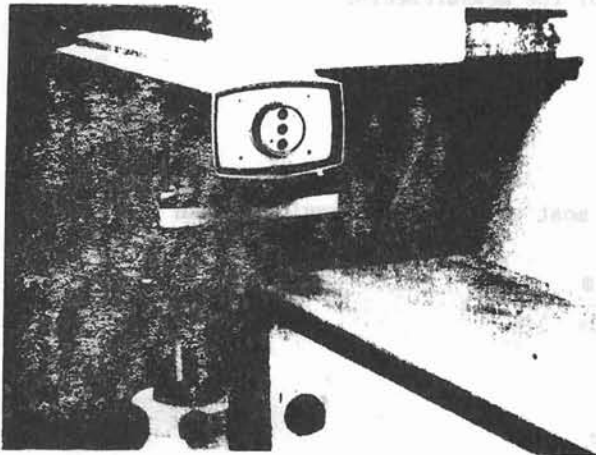


Fig 1 - The HP-laser positioned on one side of the base-line

The measuring carriage supports two reflectors (one for the interferometer, the other for the instrument) and a microscope. Both WILD GDF 4 and KERN tribrachs can be used with the centering plates. To avoid the reduction of slope distances to the horizontal, the reflector on the carriage and the socle can be put on the same heights as the instrument.

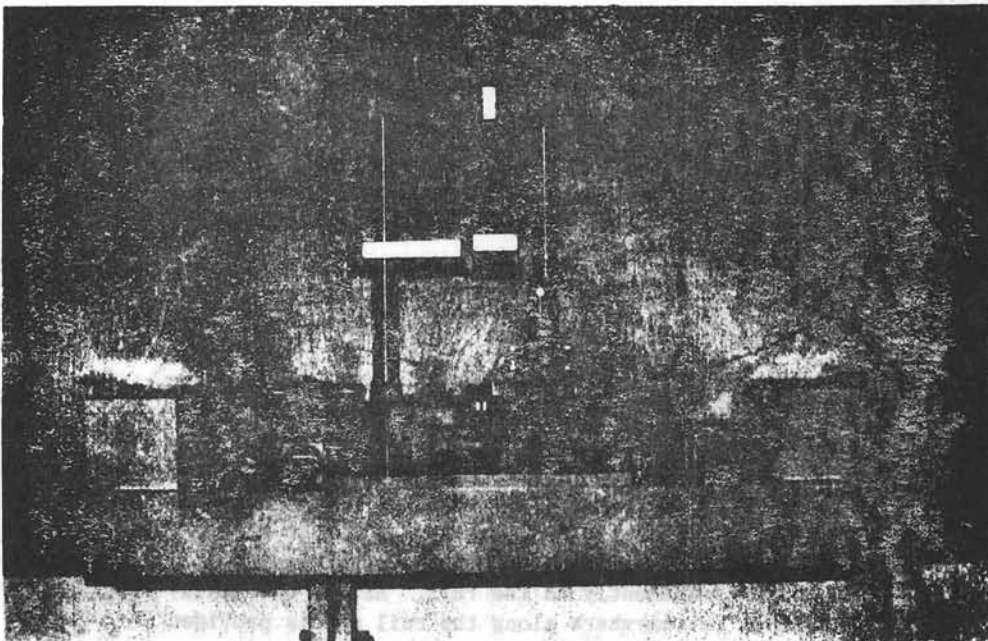


Fig 2 - The measuring carriage with reflectors and microscope

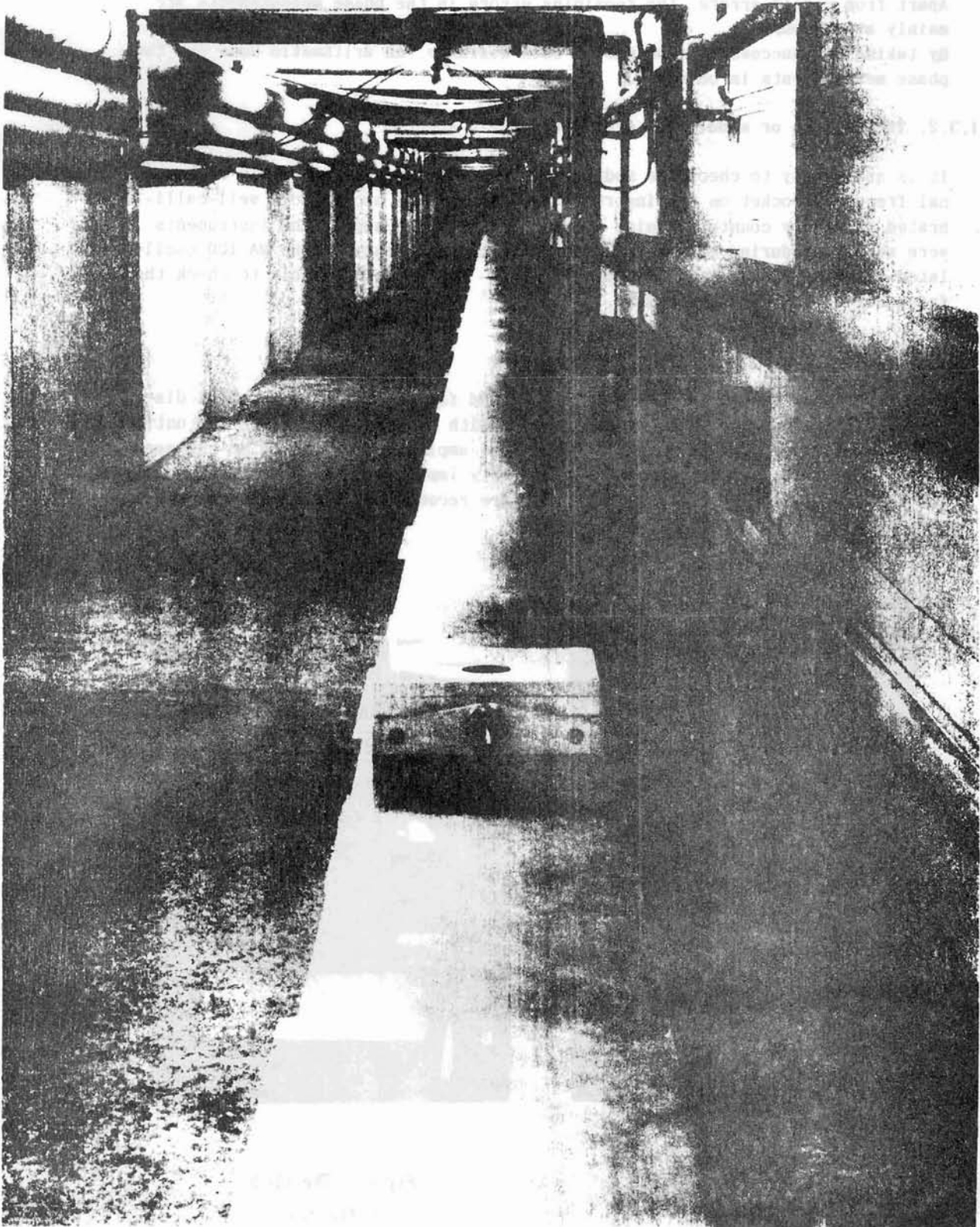


Fig 3 - General view on the base line.

1.3. Sources of error.

1.3.1. Phase measurements.

Apart from cyclic errors, the remaining errors in the phase measurements are mainly at random.

By taking ten successive readings of each distance, an arithmetic mean for the phase measurements is obtained.

1.3.2. The pattern or modulation frequency (scale error).

It is quite easy to check the modulation frequency provided there is an external frequency socket on the instrument and if one has access to a well-calibrated frequency counter. Using a regulated DC power supply the instruments were warmed up during one hour. Afterwards the frequency of the MA 100 oscillated a few cycles around its nominal value. It was not possible to check the frequency of the CD 6-instrument.

1.3.3. Strength of the reflected signal.

The diaphragm of the MA 100 is not very suited for measurements on short distances. Therefore the reflector was masked with a symmetrical diaphragm until the internal and external signal had the same amplitude. By doing so the sensibility in pointing the beam was considerably improved.

For the CD 6 instrument, the normal procedure recommended by the constructor was used,

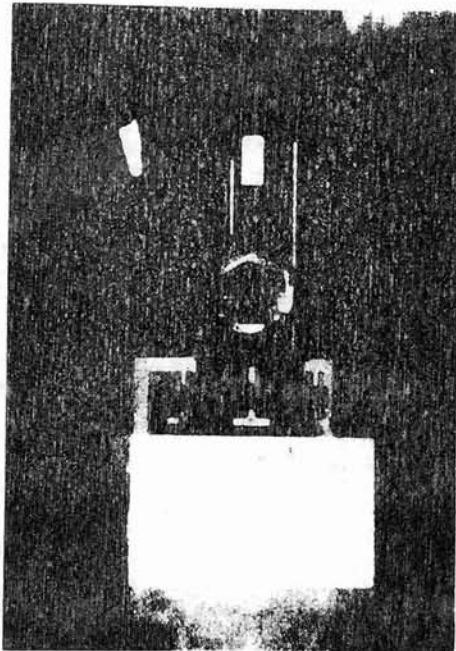


*Fig 4 - The MA 100
reflector*

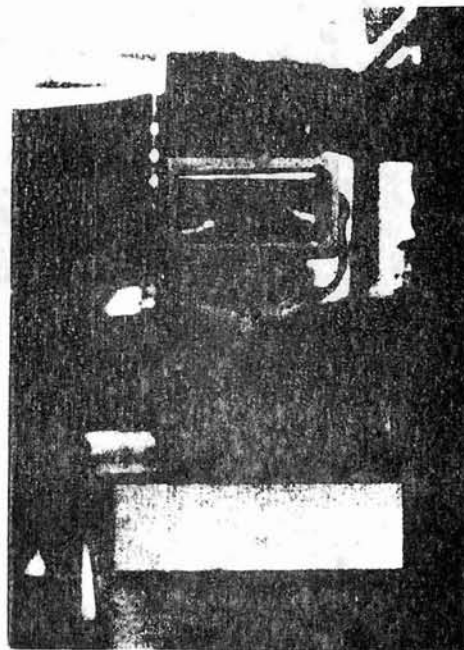


*Fig 5 - The CD 6
reflector*

1.3.4. Pointing errors.

The reflector samples only a portion of the radiated energy. As there are small time delays between different portions of the radiated energy (due to time delays on the surface of the emitted diode) the additive constant will depend in some extent on the exact alignment of the instrument relative to the reflector. To get an idea about the significance of this kind of errors, different pointings were performed for each measurement.

1.3.5. Refractive index.

The atmospheric conditions in the cellar are quite stable and did not change significantly during the tests. The MA 100 and the CD 6 were tested on different days. Each time we found a refractive index of $n = 1,000273$. This value matches remarkably with the assumed refractive index $n = 1,000274$ of both instruments. Consequently the meteorological corrections were neglected.

The interferometric distances are compensated automatically for the variations of the meteorological conditions.

1.3.6. Centering errors.

The centering errors could only have interfered in the determination of the additive constant. The tube in which the spherical centering system of the Wild GDF 4 tribrach is housed was constructed with extreme care. When measuring with the interferometer, this tube will facilitate the pointing with the microscope. Indeed, this pointing has been done at the endpoints of a diameter parallel with the axis of the rail. So the center of the tube, which will act as a reference point for the instrument (or the reflector), is defined by the average of both readings at the ends of its diameter. Once the tribrach has been put in place, and carefully levelled, any excentricity between the center of the tube and the detection point of the instrument is attributable to the additive constant. The same condition is valid for the reflector.

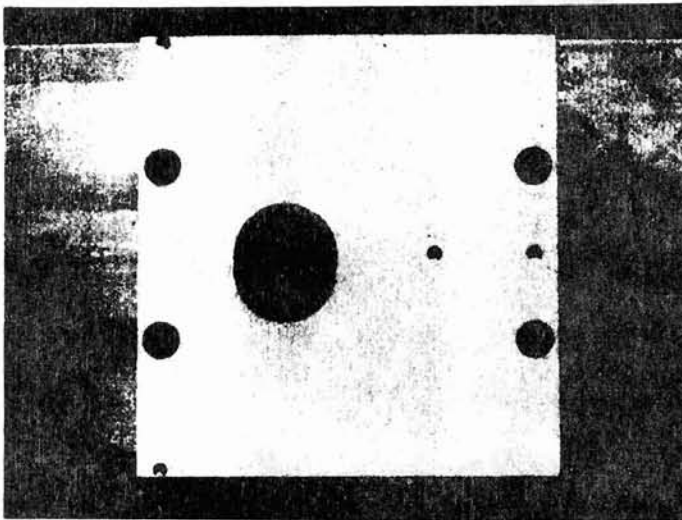


*Fig 6 - The centering plate
for the reflector*

2. The determination of the additive constant.

2.1. Execution of the measurements.

One should avoid to determine the additive constant just for one well-known distance, especially if its length is only about 50 meters. In fact this correction is not constant for all distances.

$$k = D_t - D_m$$

with D_t : the actual or true distance

D_m : the measured distance

The determination of k may be affected by cyclic and pointing errors. Therefore k has been determined at an integral number of half wavelengths of the modulation frequency.

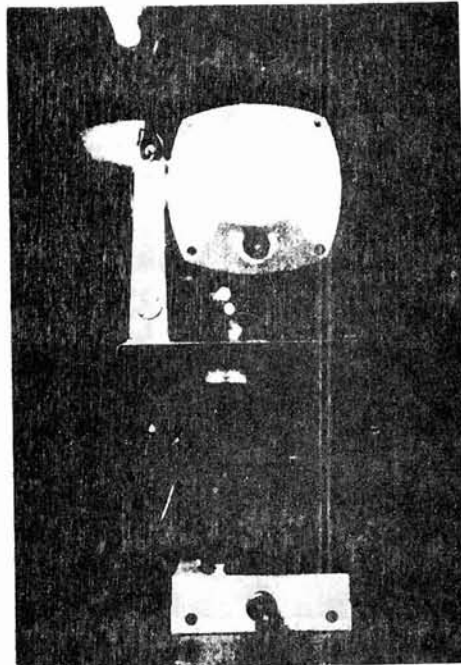
The true distances resulting from the measurements with the interferometer were :

For the MA 100-test : $D_t = 51999,9868$ mm

For the CD 6-test : $D_t = 50000,0085$ mm.

During the tests, the variations on the laser display of these values were about ± 1 μm .

Afterwards the reflector and the instrument were fixed on their respective centering plates at the same height above the rail. Using the signal monitor meter the MA 100 was aligned respective to the reflector. Because of the mask on the reflector, this pointing became very sensitive.



For the CD 6-instrument the recommended procedure for the orientation of the instrument was used. Each measurement is the result of ten successive phase readings ($i = 1 \dots q$). Ten different measurements were performed ($j = 1 \dots p$). The results for the MA 100 are given in Table 1 and for the CD 6 in Table 2. Note that :

$$\bar{x}_i = \frac{1}{q} \sum_{i=1}^q x_i$$

$$\hat{\sigma}_i^2 = \frac{\sum_{i=1}^q (\bar{x}_i - x_i)^2}{q - 1}$$

Table 1 - MA 100 Results

The approximate distance was : $D_m = 52,06$ m. The units used in this table are millimeters. Each value is the mean of a forward and reverse reading.

$\begin{matrix} p \\ \backslash \\ q \end{matrix}$	1	2	3	4	5	6	7	8	9	10
1	62,30	61,95	62,00	61,95	61,65	61,35	61,05	63,05	60,00	62,10
2	62,45	62,05	62,25	62,15	61,75	60,90	61,15	63,10	59,75	61,85
3	62,20	61,50	61,75	61,60	61,60	61,00	61,30	63,25	60,50	61,90
4	62,35	61,90	61,50	62,35	61,45	61,20	61,20	63,15	59,75	61,50
5	62,25	61,95	62,20	62,05	61,80	61,15	61,20	63,40	60,10	61,80
6	62,50	62,15	61,95	61,75	61,75	61,45	61,20	63,45	59,75	61,85
7	62,25	62,05	61,65	62,05	61,80	61,20	61,40	63,30	59,80	61,80
8	62,25	61,60	61,55	62,20	61,90	60,75	61,45	62,90	60,15	62,05
9	62,25	61,85	61,75	62,10	61,20	61,40	61,25	63,25	59,85	61,65
10	62,10	61,75	61,85	62,25	61,40	60,75	61,20	62,90	60,20	62,10
\bar{x}_i	62,29	61,87	61,84	62,04	61,63	61,12	61,24	63,17	59,99	61,86
$\hat{\sigma}_i$	0,12	0,21	0,26	0,23	0,22	0,26	0,12	0,19	0,25	0,19

Table 1



Fig 8

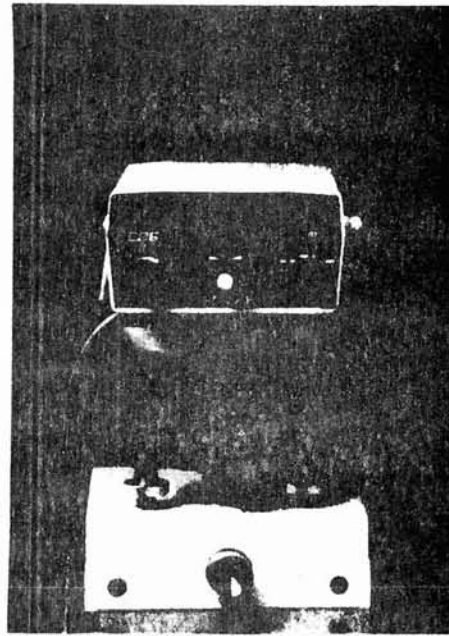


Fig 9

The CD 6 - instrument

Table 2 - CD 6 Results

The approximate distance D_m was about 50 m. In this table only the cm and mm readings are presented (units are centimeters).

$\begin{matrix} p \\ q \end{matrix}$	1	2	3	4	5	6	7	8	9	10
1	0.2	0.7	0.4	0.3	0.4	0.5	0.2	0.3	0.3	0.4
2	0.1	0.4	0.4	0.1	0.3	0.2	0.5	0.5	0.3	0.4
3	0.3	0.4	0.3	0.3	0.6	0.1	0.3	0.3	0.3	0.4
4	0.5	0.4	0.5	0.1	0.4	0.2	0.3	0.4	0.4	0.4
5	0.4	0.5	0.5	0.5	0.3	0.6	0.2	0.3	0.4	0.4
6	0.6	0.3	0.5	0.4	0.4	0.1	0.2	0.3	0.4	0.5
7	0.5	0.4	0.3	0.4	0.2	0.4	0.2	0.8	0.2	0.6
8	0.5	0.3	0.4	0.4	0.6	0.6	0.2	0.1	0.5	0.7
9	0.4	0.4	0.5	0.4	0.5	0.2	0.2	0.4	0.6	0.4
10	0.3	0.4	0.5	0.5	0.5	0.3	0.2	0.9	0.3	0.5
\bar{x}_i	0.38	0.42	0.43	0.34	0.42	0.32	0.25	0.43	0.37	0.47
$\hat{\sigma}_i$	0.15	0.11	0.08	0.14	0.13	0.19	0.10	0.25	0.12	0.11

Table 2

2.2. Analysis of the measurements.

2.2.1. Basic assumptions.

We can reasonably suppose that the q phase readings x_i of each measurement are independant and follow a normal distribution. We will prove now that the p measurements have the same variance.

To test the null-hypothesis :

$$H_0 : \hat{\sigma}_1^2 = \hat{\sigma}_2^2 = \dots = \hat{\sigma}_p^2$$

we will use a BARTLETT's test. This test is principally based on the variance ratio test (F-test) but it has the advantage of testing different variances simultaneously. A practical formula for computing χ_{obs}^2 is :

$$\chi_{obs}^2 = \frac{2,3026 \left\{ (N-p) \log \hat{\sigma}^2 - \sum_{i=1}^p [(q-1) \log \hat{\sigma}_i^2] \right\}}{1 + \frac{1}{3(p-1)} \left[\frac{p}{q-1} - \frac{1}{N-p} \right]}$$

with :

p : number of measurements

q : number of phase lectures in each measurement

$N = pq$

$$\hat{\sigma}^2 = \frac{1}{p} \sum_{i=1}^p \hat{\sigma}_i^2$$

The null-hypothesis is rejected if :

$$\chi_{obs}^2 \geq \chi_{1-\alpha}^2$$

With $p-1$ degrees of freedom and at a risk level α of 5 %

$$\chi_{0,95}^2 = 16,9$$

After computing we found

$$\text{For the MA 100-test : } \chi_{obs}^2 = 9,8$$

$$\text{For the CD 6-test : } \chi_{obs}^2 = 19,0$$

For the MA 100-test we see that the null-hypothesis, i.e. the equality of the p variances $\hat{\sigma}_i^2$, is accepted. In the case of the CD 6-test our null-hypothesis is rejected.

From Table 2 we can see that the rejecting of the null-hypothesis is due to the 8th measurement ($\hat{\sigma}_8 = 0,25$).

If we do the computations over and neglect this measurement, we find that :

$$\chi_{0,95}^2 = 15,5$$

$$\chi_{obs}^2 = 0,46$$

In this case our null-hypothesis is accepted. From now on we will neglect the 8th measurement in the CD 6-test.

2.2.2. Analysis of the variance.

It is probable that between the different averages \bar{x}_i , some are contaminated by pointing errors, others are not. The former are an indication of the influence of pointing errors, the latter will be used to determine the additive constant. To separate these two kinds of data, we will proceed to an analysis of the variance.

Our null-hypothesis will now be the equality of the different averages :

$$H_0 : \bar{x}_1 = \bar{x}_2 = \dots = \bar{x}_p$$

The deviations within each measurement are defined by the within-group mean square (WMS)

$$WMS = \frac{\sum_{i=1}^p \sum_{k=1}^9 (x_{ik} - \bar{x}_i)^2}{N - p}$$

The deviations between the different measurements are defined by the between-group mean square (BMS)

$$BMS = \frac{\sum_{i=1}^p q (\bar{x}_i - \bar{x})^2}{p - 1}$$

with $\bar{x} = \frac{1}{p} \sum_{i=1}^p \bar{x}_i$

The ratio of the BMS to the WMS characterises the degree of falseness of the null-hypothesis H_0 .

$$F_{obs} = \frac{BMS}{WMS}$$

This ratio is a F-variable of Snedecor with $k_1 = p - 1$ and $k_2 = N - p$ degrees of freedom. At a risk level α of 5 % and for $k_1 = 9$ and $k_2 = 90$:

$$F_{0,95} = 1.985$$

After computing we found :

$$\text{For the MA 100-test : } F_{obs} = 158.04$$

$$\text{For the CD6-test : } F_{obs} = 2.6$$

In both cases the null-hypothesis is rejected because $F_{obs} > F_{1-\alpha}$

2.2.3. Multiple comparison of the averages.

After rejecting the null-hypothesis $H_0 : \bar{x}_1 = \bar{x}_2 = \dots = \bar{x}_p$ we are interested to know which are between the considered averages those that are significantly different. It seems logical to use a t-Student test by comparing two by two and reject the hypothesis of equality each time that :

$$t_{\text{obs}} = \frac{|\bar{x}_i - \bar{x}_{i'}|}{\sqrt{\frac{2WMS}{n}}} > t_{1-\alpha/2}$$

or :

$$|\bar{x}_i - \bar{x}_{i'}| > t_{1-\alpha/2} \sqrt{\frac{2WMS}{n}}$$

$|\bar{x}_i - \bar{x}_{i'}|$ is called the least significant difference.

However, by using for each t-test a risk level α , the global risk on making a type I error, i.e. to reject averages as significantly different when they are not, may be much higher. Therefore we preferred to use the **NEWMAN-KEULS** test. This test is based on the comparison of the amplitudes of groups of 2, 3.... p averages with a least significant range.

The least significant range is defined for a group of 2, 3.... p averages by the value $q_{1-\alpha} \sqrt{\frac{WMS}{n}}$. The value of $q_{1-\alpha}$ that replaces the value $\sqrt{2}.t_{1-\alpha/2}$ of the student test; is computed in such a way that for 2, 3.... p averages, the probability to pass beyond the least significant range is equal to α . With $\alpha = 0,05$ and for $N - p = 90$ degrees of freedom, the values of $q_{1-\alpha}$ are given in Table 3.

p	q
2	2,82
3	3,38
4	3,71
5	3,95
6	4,13
7	4,28
8	4,40
9	4,51
10	4,61

Applying the **NEWMAN-KEULS** test, we finally find that :

$$\text{For the MA 100-test : } \bar{x}_2 = \bar{x}_3 = \bar{x}_4 = \bar{x}_5 = \bar{x}_{10}$$

$$\text{For the CD 6-test : } \bar{x}_1 = \bar{x}_2 = \bar{x}_3 = \bar{x}_4 = \bar{x}_5 = \bar{x}_6 = \bar{x}_9 = \bar{x}_{10}$$

2.3. The additive constant; the pointing error.

2.3.1. For the MA 100-test.

The mean value that will be used for computing the additive constant is :

$$\bar{x}_m = \frac{\sum \bar{x}_i}{5} = 61,85 \text{ mm}$$

$$\sigma_m = \sqrt{\frac{\sum (\bar{x}_m - \bar{x}_i)^2}{4}} = 0,15 \text{ mm}$$

with $i = 2, 3, 4, 5, 10$.

The confidence interval at 95 % is :

$$\bar{x}_m \pm \frac{2\sigma_m}{\sqrt{n}} = 61,85 \pm 0,13 \text{ mm}$$

Or : $D_m = 52061,85 \pm 0,13 \text{ mm}$

The adopted additive constant is :

$$k = D_t - D_m = 51999,99 - 52061,85 = - 61,86 \text{ mm}$$

From the values in Table 1 we can see that errors up to 2 mm can be made if the instrument is not carefully pointed. It should be kept in mind, that when making measurements on short distances, more pointings should be carried out. The influence of the pointing error, characterised by its m.s.e. σ_p , has been computed as follows :

$$\sigma_p = \sqrt{\frac{\sum (\bar{x}_m - x_i)^2}{9}} \text{ with } i = 1, \dots, 10$$

$$\sigma_p = 0,84 \text{ mm}$$

2.3.2. For the CD 6-test.

In this case, the mean value that will be used for computing the additive constant is :

$$\bar{x}_m = \frac{\sum \bar{x}_i}{8} = 0,39 \text{ cm}$$

$$\sigma_m = \sqrt{\frac{\sum (\bar{x}_m - \bar{x}_i)^2}{7}} = 0,05 \text{ cm}$$

with $i = 1, 2, 3, 4, 5, 6, 9, 10$.

The confidence interval at 95 % is :

$$\bar{x}_m \pm \frac{2\sigma_m}{\sqrt{2}} = 0,39 \pm 0,04 \text{ cm}$$

Consequently the adopted additive constant is :

$$k = D_t - D_m = 5000,00 - 5000,39 = - 0,39 \text{ cm} = - 0,4 \text{ cm}$$

The influence of the pointing error, characterised by its m.s.e. σ_p , has been computed as follows

$$\sigma_p = \sqrt{\frac{\sum (\bar{x}_m - \bar{x}_i)^2}{8}} \text{ with } i = 1, 2, 3, 4, 5, 6, 7, 9, 10$$

$$\sigma_p = 0,07 \text{ cm}$$

As the m.s.e on the pointing error is of the same order of magnitude as the m.s.e on the phase measurement, the pointing of a CD 6-instrument becomes less critical.

3. The cyclic error.

3.1. Program of the measurements.

As can be seen in the fundamental distance equation, errors in the phase measurement will be repeated every half modulation wavelength. Already when the first E.D.M.-equipments were tested, a non-linearity in the phase detection system was found. The reason is not well known. Electronic coupling between the different detecting channels gives rise to a cyclic error with a half modulation wavelength period. By using a differential technique, we avoid the error made in determining the additive constant. The displacements of the reflector were measured with the HP-interferometer.

3.2. Tests with the MA 100-instrument.

For the MA 100 the cyclic error will have a period of 2m. To determine the cyclic error, the reflector was moved 8 times over exactly 250 mm. At each displacement a measurement, consisting of 5 different pointings, was carried out. The results are given in Table 4.

	Col 1	Col 2	Col 3
1	51807,80 ± 0,4 mm	249,6	- 0,4
2	51558,20 ± 0,6 mm	249,3	- 0,7
3	51308,94 ± 0,6 mm	249,3	- 0,7
4	51059,66 ± 0,9 mm	250,9	+ 0,9
5	50808,70 ± 0,8 mm	250,0	0,0
6	50558,60 ± 0,7 mm	250,6	+ 0,6
7	50308,09 ± 0,8 mm	250,2	+ 0,2
8	50057,90 ± 0,4 mm	249,9	- 0,1
9	49807,94 ± 0,9 mm		

Table 4

Col 1 : the MA 100-measurement with its confidence interval.

Col 2 : $D_i - D_{i+1}$.

Col 3 : $(D_i - D_{i+1}) - 250$ mm.

The differences between $(D_i - D_{i+1})$ and the interferometric displacements are very small. Taking the precision of the MA 100 measurements into account, we can state that the MA 100 n° 358 has no significative error. This implies that no systematic correction in function of the distance should be applied.

3.3. Tests with the CD 6-instrument.

The period of the cyclic error of the CD 6-instrument is 10 m. To determine this error the reflector was moved exactly for 1 or 2 m. At each displacement a measurement consisting of 5 different pointings was carried out. The results are given in Table 5.

	Col 1	Col 2	Col 3
1	5013,24 ± 0,09	200,37	+ 0,37
2	4812,87 ± 0,11	200,37	+ 0,37
3	4612,50 ± 0,09	99,94	- 0,06
4	4512,67 ± 0,04	99,89	- 0,11
5	4412,67 ± 0,02	199,59	- 0,41
6	4213,08 ± 0,03	99,94	- 0,06
7	4113,14 ± 0,10	100,03	+ 0,03
8	4013,11 ± 0,06		

Table 5

Col 1 : the CD 6-instrument with its confidence interval.

Col 2 : $D_i - D_{i+1}$.

Col 3 : $(D_i - D_{i+1}) - 1$ or 2 m.

Apparently a small cyclic error with a maximum amplitude of 4 mm exists. However the number of measurements is insufficient to make a definite conclusion about the corrections that should be applied in function of the distance. The technique for detecting the cyclic error still has to be improved.

References.

- H. KAHMEN und H. ZETSCHKE : Vergleichende Untersuchungen on elektro-optische Nahbereichsentfernungsmessern; Zeitschrift für Vermessungswesen, Heft 2, Februar 1974.
 - G. HEUPEL und B. WITTE : Messungen hoher Präzision mit dem Tellurometer MA100; Allgemeine Vermessungsnachrichten, Heft 2, Februar 1974.
 - D.J. HODGES : Callibration and testing of electro-optical distance measuring instruments; Department of Mining Engineering, University of Nottingham.
 - V. ASHKENAZI and A.H. DODSON : The Nottingham Multi-Pillar Base line; Department of Civil Engineering, University of Nottingham.
 - Pierre DAGNELIE : Théorie et Méthodes Statistiques - Vol 2; Les Presses Agronomiques de Gembloux.
 - The MA 100 and CD 6 operator's manual - Tellurometer.
-

THE PLANE MIRROR IN ELECTRO-OPTICAL DISTANCE MEASUREMENT

A.L. Allan, University College, London, United Kingdom
Presented by D. Proctor

Abstract

The plane mirror, used in early Geodimeter work, has been replaced as a reflector in EDM by the corner cube. The reasons for this are well known and need no elaboration here. However, if the plane mirror is mounted on the objective of a theodolite telescope normal to the line of sight, a very effective reflection system is obtained which has several advantages over the corner cube, if used directly, or if used in conjunction with the corner cube. In this paper we discuss two applications of the plane mirror mounted on the theodolite, there being insufficient space to consider all applications.

1.0 INTRODUCTION

1.1 Theodolite Telescope Attachments

For a number of reasons (accuracy of centering, accuracy of measuring slope and other angles, ease of pointing and measurement of steeply inclined lines etc.) the writer saw the advantages of attaching mirrors, corner cubes and small EDM instruments to the telescope of a theodolite. It was decided to use Watts instruments since these were available in abundance and because their objective glasses do not protrude beyond the telescope casing (in contrast to Wild and Kern instruments). It is a fortunate circumstance that all Watts instruments including old Vernier theodolites and levels, have telescopes whose outside diameters are identical; no doubt a deliberate policy on the manufacturer's part.

1.2 Telescope Mirrors

Aligning a mirror even over quite short distances is a time consuming and frustrating business, so much so that the writer gave some thought to the problem, eventually hitting on the happy idea of attaching a mirror to the front of a telescope. If the mirror has a clear portion (about 1cm diameter is convenient) the telescope can be used as a simple sighting device. Thus the use of plane mirrors became quite simple and direct.

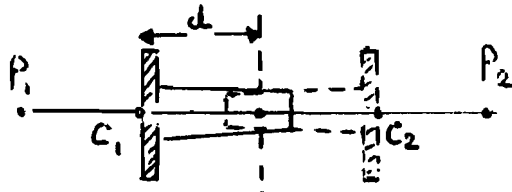
Although it served well, a rear silvered heliograph mirror was replaced by a front silvered mirror taken from a stereoscope. A hole was drilled through this mirror into which a plug is put after alignment to prevent unwanted light rays from the telescope itself from contaminating the signal. For transportation the metal covers of the stereoscope prove most useful. It is a commendable fact that the outside castings of the Watts instruments are aligned parallel to the lines of sight to a sufficiently high order of accuracy not to give trouble with interchangeability from one instrument to another. Once the mirror has been adjusted with the screws provided, the alignment problem is not serious.

The easiest way to adjust the mirror is to view a corner cube placed about 30m away until the image of the cube can be seen after reflection from the mirror. The hole in the mirror and the image can be centred on the corner cube by the telescope slow motions. If this direction is seriously different from the line of sight of the telescope, the mirror is adjusted by its screws. It has been found that this collimation

check can be carried out quite simply in the field each time the mirror is emplaced, and the effective line of sight established in relation to that of the telescope. This procedure is necessary when working alone. With the help of an assistant the mirror was easily aligned for distance measurement at a range of 518 metres.

1.3 Mirror Index

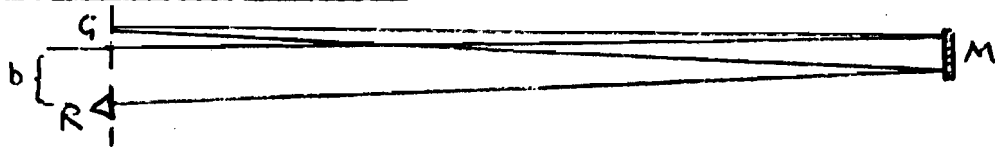
Because the distance between the mirror surface and the theodolite trunnion axis enters directly into the measurement, this distance has to be measured accurately, by the arrangement shown. Distances $P_1 C_1$, $P_1 P_2$ and $C_2 P_2$ were measured by scale, C_1 and C_2 being successive mirror positions 180° apart. Thus



$$2d = P_1 P_2 - (P_1 C_1 + P_2 C_2),$$

which is a simple system applicable in the field.

2.0 DOUBLE DISTANCE MEASUREMENT



If the distance $\langle GMR \rangle$ measured by the EDM instrument G is folded in two by a mirror M, the distance GM or RM is approximately $\frac{1}{2} \langle GMR \rangle$, thus any errors in the measurement system which are independent of distance will be halved. Provided that those errors which are distant dependent (refraction, scale) are not proportionately worse over the larger distance, there should be a gain of $\times 2$ in accuracy. The scaling effect will be unchanged, and refraction errors should be better than over a long line of similar length since the meteorological factors are samples at the "mid point" in this method.

In practice the $\frac{1}{2}$ beam width b must be less than the base GR. The Tellurometer MA.100 has a half beam width of $1/4^\circ$ or about 1 in 240 and the Geodimeter 6 about 1 in 4000. Thus R can be placed beneath the instrument for distances up to about 300m, and for longer distances the reflector R has to be placed to one side.

With the mirror M mounted on a theodolite telescope, pointing is achieved without difficulty by bisecting GR as seen through the telescope. The image of G reflected in R can then be seen at M, thus achieving a satisfactory pointing without the assistance of an observer at G. Obviously the visible light of the Geodimeter makes this whole procedure easier than with the infra red Tellurometer. In the latter case, the front of the optics has been painted in fluorescent paint to assist pointing. The theodolite also enables the necessary angles to be observed. The range limit will depend upon the size of the mirror M and the number of reflectors at R. The stereoscopic mirror has been used to measure a line 259m with three reflectors at R, intensity level of 40 on MA.100 scale. This same line was also measured with the AGA 12 Geodimeter using the same mirror, but only one corner cube at R.

In practice the highest accuracy will normally be required over lines less than 300 metres which is quite a feasible range with the present equipment.

2.1 The geometry of double distance measurement

In figures 1 and 2, G is the reference point of the EDM instrument, R is the reflector, and M is a plane mirror mounted on a theodolite telescope; Z' is the zenith of M (figure 2) and vertical angles to G and R are h_G and h_R respectively; α is the horizontal angle between G and R. The distance GR (measured by tape), has to be sufficiently long to avoid signal contamination from the mirror at M.

The measured distance <GMR> defines an ellipse whose foci are at R and G and whose major axis $2a = \text{<GMR>}$. The ultimate aim is to obtain the length of MG'.

Proceed as follows.

In figure 2, $\cos z = \sin h_G \sin h_R + \cos h_G \cos h_R \cos \alpha \dots (1)$

and β is obtained in a similar manner from the appropriate horizontal and vertical angles observed at R to M and G.

Refer to figure 1. Theoretically to achieve reflection of the ray from G to R at the mirror M, this mirror is tangential to the ellipse and its normal does not pass through O, the centre of the ellipse. However, the angles between G, O and R can still be measured by the theodolite at M and duly converted to the inclined plane from equation (1). In practice the plane MGR will not be seriously tilted, and angles in it may be measured directly by tilting the theodolite primary axis with the foot screws.

In figure 1 $z_3 = \beta - 90$, z , is measured or calculated as described, $\therefore H = z_2 + z_3$ is known.

Let $OM = r$, and the equation of the ellipse be $\frac{x^2}{a^2} + \frac{y^2}{b^2} = 1$

At M $y = x \cot H$ thus,

$$\frac{y^2 \tan^2 H}{a^2} + \frac{y^2}{b^2} = 1$$

Substituting for $b^2 = a^2(1 - e^2) = a^2 - s^2$ where $s = ae$, in equation yields

$$y^2 = \frac{a^2 - s^2}{1 + \left(\frac{a^2 - s^2}{a^2}\right) \tan^2 H} \dots (2)$$

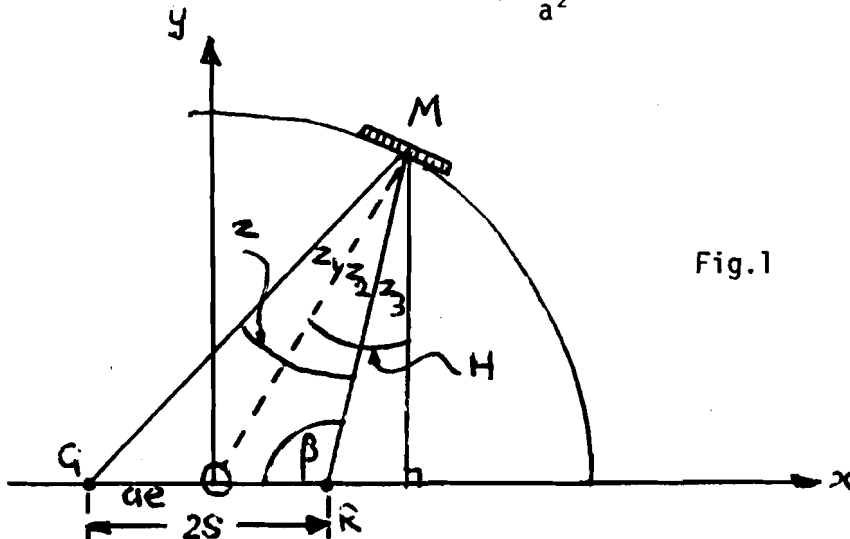


Fig.1

The double distances of serial DM7 were measured in the vertical mode to a single prism placed beneath the AGA.12. These measured values were as follows:-

518.523, .513, .519, .517, .515, .521, .518, .519
 518.516, .516, .519, .515, .525, .520, .512, .517

Mean 518.518 giving residuals in mm of

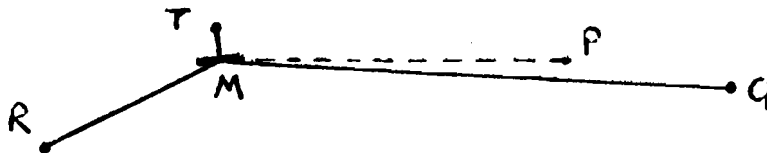
-5, +5, -1, +1, +3, -4, 0, -1,
 +2, +2, -1, +3, 17, -2, +6, +1 $\Sigma v^2 = +186$

and $\sigma_o = 3.5$ $\sigma_m = 1.$

The results from the AGA.12 are particularly gratifying.

3.0 INDIRECT MEASUREMENT OF A LINE

It sometimes happens that a very steep line has to be measured. To close out a traverse the distance was required for a line with a 44° slope. Since neither the MA.100 nor the Geodimeter 6 could be used directly without tilting the base, it was decided to use the mirror mounted on a theodolite T at the top end of the line.



Points G, T and R were traverse stations. Line GT was measured in the normal way, then lines $\triangle GMR$ from which the required distance TR was calculated. The whole procedure was repeated by a different group of students, both values agreeing to 1mm.

To assist alignment a plane mirror was also used at station R thus enabling its observer to direct the operator at T to align the mirror finally. The procedure began by setting TM to bisect the horizontal and vertical directions to G and R, which was followed by the observer at P looking into the mirror to obtain a view of R, mirror M being then moved until P's eye coincided approximately with G, the EDM instrument. By this time the observer at R would see the optic of the MA.100 which has been painted in fluorescent orange for this purpose. Only a slight adjustment was finally required at T for the measurement to proceed.

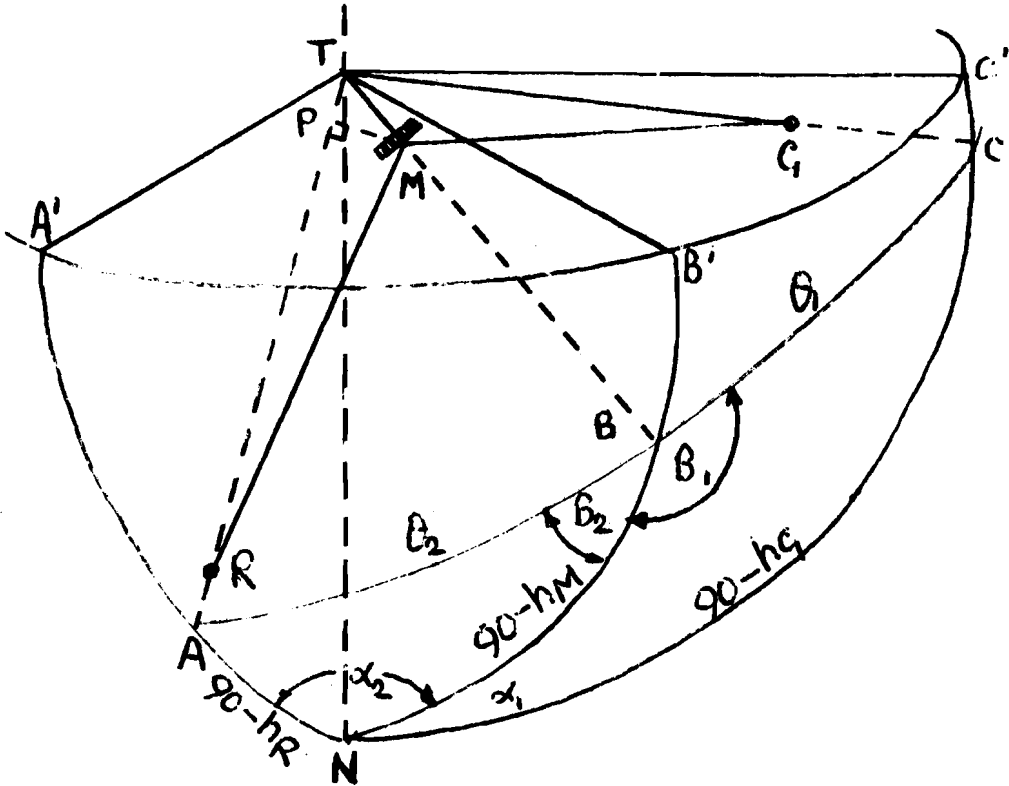
3.1 Measuring a distance indirectly using the plane mirror

G = EDM station - MA.100 Tellurometer

T = Theodolite with mirror M on objective

R = Reflector

TR = required distance



Observed angles

$$\alpha_1 = C' \hat{T} B'$$

$$\alpha_2 = B' \hat{T} A'$$

$$h_C = h_G = C' \hat{T} C$$

$$h_B = h_M = B' \hat{T} B$$

$$h_R = A' \hat{T} A$$

PRTMG are coplanar, and MB bisects angle GMR, $MP \perp RT$
 TG and $\angle GMR$ are measured lengths.
 $TM = d$

$$\cos \theta_1 = \sin h_G \sin h_M + \cos h_G \cos h_M \cos \alpha_1 \quad - (1)$$

$$\cos \theta_2 = \sin h_M \sin h_R + \cos h_M \cos h_R \cos \alpha_2 \quad - (2)$$

$$MG^2 = TG^2 + d^2 - 2d \cdot TG \cdot \cos \theta_1 \quad - (3)$$

$$PR^2 = MR^2 - d^2 \sin^2 \theta_2 \quad - (4)$$

$$TR = PR + d \cos \theta_2 \quad - (5)$$

3.2 Example 1

$$d = 0.090m, \quad TG = 57.394m, \quad \angle GMR = 105.423m.$$

$$h_G = -01^{\circ}35'30''$$

$$h_M = -27^{\circ}48'14''$$

$$h_R = -44^{\circ}44'16''$$

$$\alpha_1 = 28^{\circ}41'55''$$

$$\alpha_2 = 42^{\circ}44'07''$$

Whence $\theta_1 = 37^{\circ}832$

$\theta_2 = 37^{\circ}950$

TR = 48.171m,

The horizontal projection of which is 34.216m.

The complete measurement was repeated on a second day by entirely different observers yielding a result of 34.217m.

3.3 Example 2

Recently the method was used in the deformation analysis of a box girder bridge under test. Most sides of a network of six stations were observed indirectly without moving the MA.100 which was located outside the survey area. Precisions of 1mm were obtained throughout.

Some lines were also measured by the Double Distance method using the AGA.12, again giving 2mm precision.

4.0 CONCLUSIONS

For several reasons, we advocate the use of a theodolite as a base for EDM reflectors. Not only does this permit the very highest accuracy to be achieved, but it also enables this quality to be carried forward into the next stage of the survey, for example in setting out. The theodolite is not disturbed when removing the corner cube, it can be centered properly and be seen to remain so, and the various related angles may be measured to the required precision in a straight-forward manner. This is especially true when the plane mirror is used as a reflector.

Discussion (paper 5)

Remark 1. I think it is very inspiring what you can achieve with-let us say - relative small means and a sprankling mind. I think it is very brilliant and it shows that a lot of things and details with which, let's say - the ordinary people walk around and we have all the possibilities, a lot of mirrors in the world, a lot of theodolites and nobody has the ingenuity to make a combination.

Remark 2. The paper is very encouraging because everybody who tries to get top precision has to face such " simple " problems.

There are very encouraging ideas in this paper and they may be used for various practical purposes.



S h o r t a b s t r a c t

In connection to the 30-years celebration of the first Geodimeter AGA introduces a new member of the Geodimeter 6-family, the Geodimeter 600. It is a long-range EDM with an optimal range of about 40 km. Under very good weather conditions, 55 km has been measured. The instrument has a 1mW HeNe gas laser as a light source and the coaxial optical system from earlier Geodimeter 6 where the transmitter and the receiver "have changed places". A new phototube with a higher sensitivity also contributes to the reached longer range. By means of this together with the better optics and the laser which can be focussed at the measuring point the instrument also can be used for accurate deformation measurements up to about 200 m without any reflector and by means of a simple plastic reflector up to 1,5 km.

The Swedish AGA concern who exists since the beginning of this century and who has 50 years of experience in the fields of electronics, optics and precision engineering, celebrates in this year, 1977, the birth of the first electro-optical distance measuring instrument 30 years ago. It was in 1947 Dr. Erik Bergstrand offered the AGA to transform his prototype to a proper production unit. Since then a consistent product development based on experiences in laboratory and in the field has made the AGA Geodimeter instrument series one of the most economical and reliable EDM available for short, intermediate and long-range measurements.

Many of you have followed this development step by step from the Geodimeter 2 in 1952-53 via the Geodimeter 4 in 1959 to the big EDM brake-through with the Geodimeter 6 in 1964. This instrument was spread all over the world and regarded as the almost optimum EDM conception. Many Geodimeter 6 are even today still good working.

With the introduction of the Laser even for civil purposes in 1961, it was the beginning of a new epoch in the electro-optical measuring field.

This monochromatic and coherent light was very well suited as light source for the EDM instruments. The first experiences were made by the American "Coast Geodetic Survey" who with good results attached a laser to Geodimeter 4. The corresponding serial production version from AGA was the Geodimeter 8, a first order network EDM, with a maximum range over 60 km and the accuracy of 1×10^{-6} introduced in 1968.

For medium ranges, however, the Geodimeter 6, now in the modernized version 6A and later 6B, remained as the most used electro-optical instrument. In order to increase the daylight range and the maximum range in darkness the Geodimeter was equipped with a mercury lamp by means of which the maximum darkness range was increased up to 25 km. Of course, the question was posed if it was not possible to use a laser light source in the Geodimeter 6 instead of the mercury lamp. The disadvantage with this equipment was the highly required effect (6A and 50VDC). This energy was generated by means of a motor-generator.

In 1972 the technicians had overcome the difficulties to build in a laser in the Geodimeter 6B and you had the 6BL by means of which distances up to about 23 km were possible to measure even at daylight because of the monochromatic laser and the narrowband-filter.

In this instrument, however, the laser just replaced the tungsten lamp and you had the same transmitter and receiver optics as before. This meant that because of the very narrow coherent laser beam although a beam expander was used only a small part of the sender-optics was demanded. The kept receiver optics was dimensioned for the maximum range.

This instrument, the Geodimeter 6BL, has found good use for many geodetic applications, i.e. the St. Gotthard-network and measurements in Greenland.

Field experiences, however, showed that it was a demand of an EDM with the accuracy of 1×10^{-6} for ranges up to about 40 km over which it was rather difficult to keep the meteorological influences by normal measurements only at the endpoints of the measured distance, under this accuracy limit. This led to the fact that when AGA looked for a replacement instrument for the Geodimeter 8, we used the sum of the passed years experiences. The result of this is the Geodimeter 600 where you have the features of the coaxial optical system and where you use the 105 mm diameter optics as receiver. The weight of the instrument is only 15 kg and as required power supply a normal 12 V DC car-battery is sufficient. The power consumption is only 26 W.

The optical and electronical design can be seen in figure 1 and figure 2. Here we see that the beam coming from the laser will be two times deflected of 90° by prisms into the condenser-system and between the kerr cell electrodes. A polaroid filter is included in the condenser-system and so orientated that the laser light entering the kerr cell is polarized 45° with respect to the electrical field in the kerr cell. A second polaroid filter follows upon the kerr cell and normally so orientated that it's polarization plane is perpendicular to that one of the first polaroid. The light then passes two lenses used for focussing the light-beam and is then deflected 90° in the central prism. The divergence is then increased by a lens system so that the light illuminates the central objective.

The light will be focussed at the distance by the focussing knob.

In this respect it is perhaps necessary to say something about the chosed modulation-system. The HeNe-Gas laser needs an external modulator in order to be intensity modulated. In Geodimeter 600 as well as in the 6BL and the 700/710 a kerr cell has been chosen although one knows that the KD^+P modulator has a higher optical quality and better temperature properties compared with a kerr cell where the turbulence in the liquid nitrobenzene may introduce an undesirable amplitude of noise in the signal. However, experience has shown that this turbulence in most cases is small compared to the atmospheric turbulence. The kerr cell has the advantage of a shorter optical path length than the KD^+P which facilitates the optical layout. The light, which is returned from the reflector, is received by the main spherical mirror. The reflected light is deflected 90° in the central prism, passes then two thin glass-wedges and a thin glass plate tilted 45° (used for deflection of the calibration light-path) and before coming to the focal plane two focussing lenses. The spherical mirror can be tilted by turning the three knobs accessible on the mirror-end of the central tube. This makes it possible to change the orientation of the receiver optical axis so that it coincides with the optical axis of the transmitter.

During measurements, the light passes an adjustable diaphragm in the focal plane, then via a projection system to the cathode of the photomultiplier where it is focussed. The interference filter in front of the photo tube reduces most of the daylight influence, which makes a large diaphragm aperture possible.

A manual variable greywedge is inserted in the light-path for adjustment of the light intensity to a proper level.

In order to facilitate pointing of the instrument on the target the light-path can be deflected by switching in a plane mirror and observed through an eyepiece via a prism and lens system. The image observed in the eyepiece is however reversed sidewise. By means of a switch a red contrast filter can be used in order to further facilitate the pointing of the rather narrow laser beam (theoretical beam divergence 5 cm/km).

In this respect it perhaps could be of interest to mention a special method successfully used by the Geographical Survey Office of Sweden to locate a reflector at long distances. The method has been developed by working with the Geodimeter 3 but can in the following matter be applied to the operating with Geodimeter 600. The method presupposes that the reflector operator is equipped with a field-glass and a communication radio, enabling him to communicate with the Geodimeter operator. It is also assumed that the approximate bearings from both sides are known. The theoretical beam width of the Geodimeter 600, as already mentioned, corresponds to approximately 0,05 m per km, when focussed on infinity. If the beam is expanded by setting the focus control at e.g. 30 m, the beam will be focussed to a thinny point at 30 m but will diverge from that point on. The divergence will be $0.03:30 = 1 \text{ m}/1 \text{ km}$ where 0.03 is the laser beam diameter at the exit aperture.

The receiver is, however, automatically focussed at 30 m which makes it necessary to use the sighting telescope for a coarse orientation. The reflector operator now observes the Geodimeter station with his field-glass and will easily see the flash of the laser light when the Geodimeter beam is slowly swept along the horizon. By radio the Geodimeter operator is informed and reduces the beam divergence by gradually focussing for a longer distance and readjusting the pointing until he is able to make the final adjustment using the receiver optics of the Geodimeter, first visually and finally by looking at the control-instrument deflection.

The electronical design mainly corresponds to that of the Geodimeter 6BL where the phase comparisons between the transmitted and received signals is achieved with the mix-frequency of 1,5 kHz. The scale determining modulation frequencies are approximately 30 mHz and 750 kHz corresponding to the "unit lengths" of 5 m and 200 m respectively.

By means of a new "Hamumatsu" photo-multiplier the sensitivity of this is extremely increased compared with earlier models. This together with the larger receiver optics make the specified range of 40 km as a real optimum. Under extreme good conditions 55 km has been measured with 32 prisms and with a spread of only 4 mm between three independent measurements during 30 minutes.

A special instrument feature seen from the specification on figure 5 is that you - depending on the required accuracy - can chose the suitable measuring method (internal instrumental accuracy 1 mm - 10 mm).

In this respect it is also necessary to state some facts about the used laser and the output effects in order to clear the question if it is dangerous for the eyes or not.

The used laser is a 1mW HeNe gas-laser manufactured by Spectra-Physics or Siemens. Reduced by deflections and reflections along the transmitter light-path, the total output effect is about 200 μ W and the effective output area has a diameter of about 30 mm which corresponds to an effect density of about 28 μ W/cm². In many countries this value is good acceptable but in some countries where the limits have been stated very low e.g. in Germany, the Geodimeter operator have to act according to the actual regulations.

Finally, I wish you welcome to Sweden and the FIG-Congress and hope that you then will take the opportunity to visit AGA and participated at the 30-years celebration of the AGA Geodimeter.

Literature:

AGA Geotronics AB: Geodimeter 600,
Operating Manual.

Ragnar Schöldström: Various published papers
re Geodimeter 6A, 8 and 700.

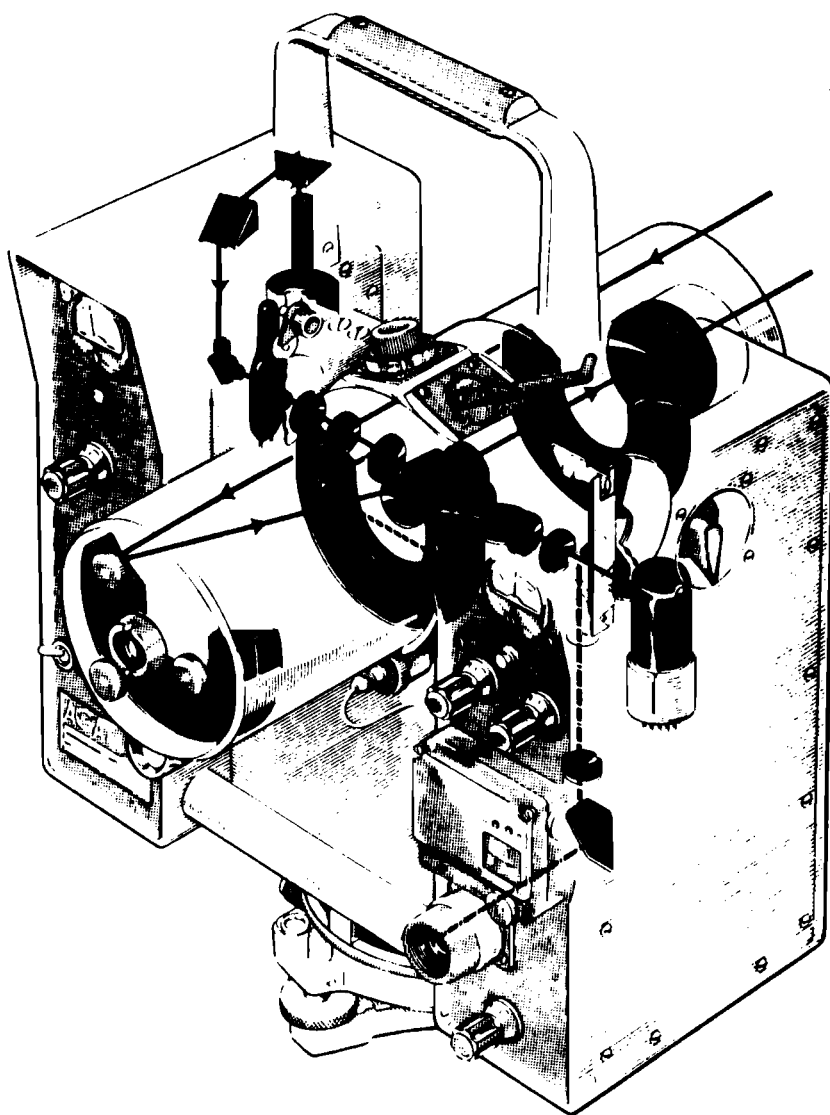


Fig. 4

Fig. 1
Geodimeter 600 optical layout.

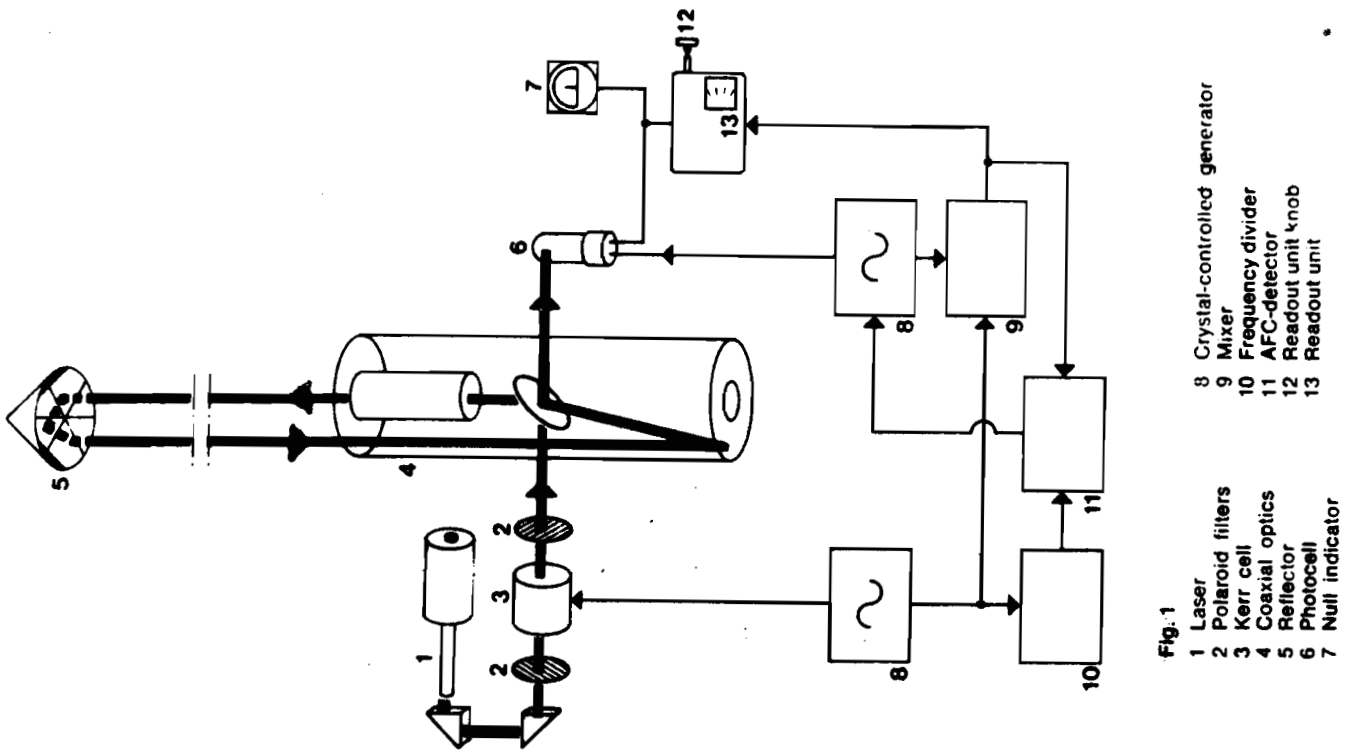


Fig. 1

- 1 Laser
- 2 Polaroid filters
- 3 Kerr cell
- 4 Coaxial optics
- 5 Reflector
- 6 Photocell
- 7 Null indicator
- 8 Crystal-controlled generator
- 9 Mixer
- 10 Frequency divider
- 11 AFC-detector
- 12 Readout unit knob
- 13 Readout unit

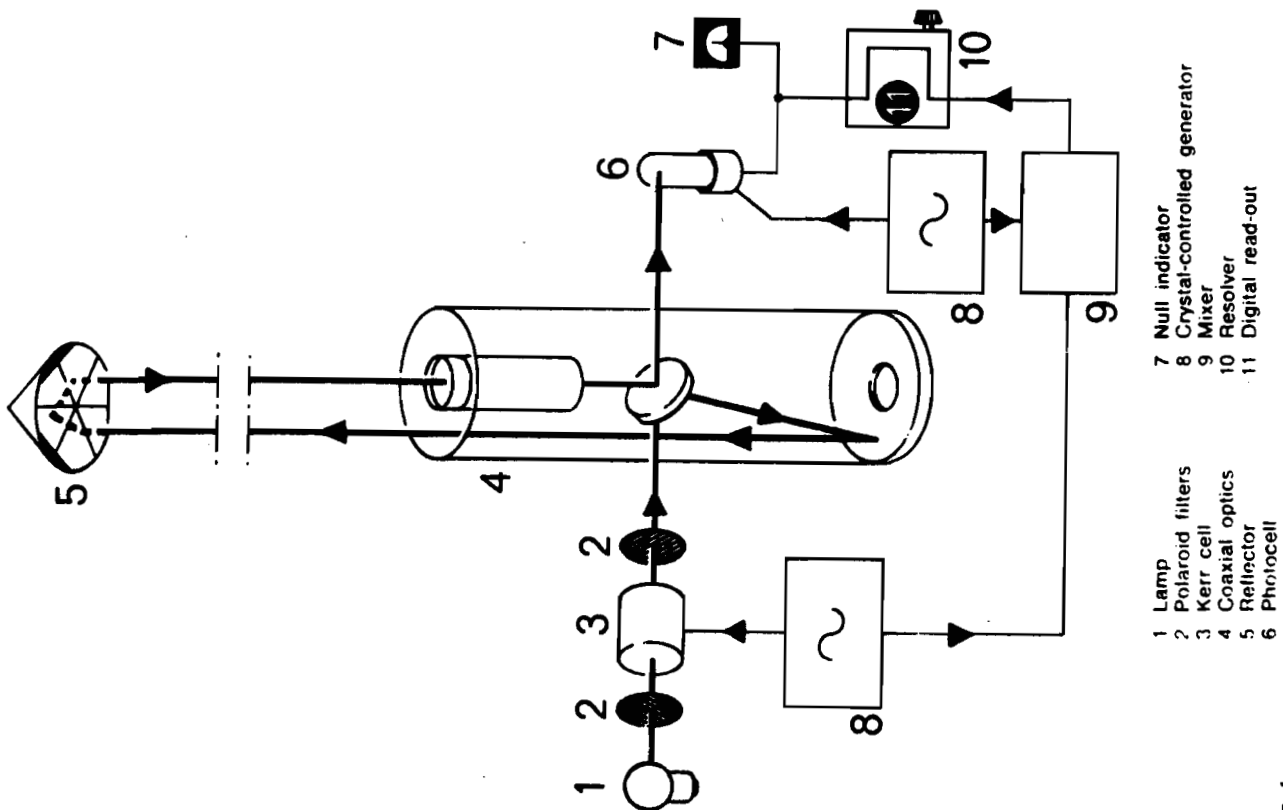


Fig. 1

- 1 Lamp
- 2 Polaroid filters
- 3 Kerr cell
- 4 Coaxial optics
- 5 Reflector
- 6 Photocell
- 7 Null indicator
- 8 Crystal-controlled generator
- 9 Mixer
- 10 Resolver
- 11 Digital read-out

Fig. 2
Optical and electrical design of Geodimeter 6A and Geodimeter 600.

AGA

Area **Svealand**
 Geodimeter: Nisse 68 serial No **3**

DISTANCE MEASURING

Time **1330** Date **15.12.70**

Geodimeter Lot **1023** Reflector **By 936**

Station name **Station No 936**

Station altitude **+36.27** **+81.43**

Instr height **1.25** **1.16**

Instr. altitude **+37.52** **+82.59**

Temperature **2.0** **4.0**

Bar press **753** **749**

Sum of corr **-0.160**

Zenith distance

Y-coordinate **23600**

Radius of earth **6387500**

Atm. corr $\cdot 18 \cdot 10^{-6} \cdot D$ **+0.075** m

Atm. corr **-0.085** m

Total sum of corr

Phase C B

1	F2	F1	F3	F4
2	F2	F1	F3	F4
3	F2	F1	F3	F4
4	F2	F1	F3	F4

Sum 2-3 **18429** **15517**

Sum 1-4 **18430** **15520**

Mean **18430** **15519**

0.5 x Mean **9215** **7759**

correct meter figure

Notes

Total sum of corr **0.085** m

Slope distance **4968459** m

Observer **J.A.**

Recorder **L.N.**

Approx. dist **5000 m**

Type of reflector **6x3**

Visibility **Good**

Fair **Good**

Poor

Example of one-phase measurement:

Geod Refl. No **1023** **936**

Height **1.25** **1.16**

Eccentr **0.750** **0.000**

Temp **20°C** **Press 760**

Atm. corr $+29 \cdot 10^{-6} \cdot D$ **+40**

Sum of corr **7.9.0**

F3 **5.0.3.2**

F2 **3.6.8.5**

F1 **1.3.4.7**

Slope dist **4916839.5**

Geod Refl. No **830** **831**

Height **1.20** **1.35**

Eccentr **0.750** **0.000**

Temp **20°C** **Press 760**

Atm. corr $+29 \cdot 10^{-6} \cdot D$ **+40**

Sum of corr **7.9.0**

F3 **5.0.3.2**

F2 **3.6.8.5**

F1 **1.3.4.7**

Slope dist **11316318.15**

Geod Refl. No **4.0.4.8.7.9.9**

Height **4.0.4.8.7.9.9**

Eccentr **4.0.4.8.7.9.9**

Temp **-6°C** **Press 772**

Atm. corr $-3 \cdot 10^{-6} \cdot D$ **-1.2**

Sum of corr **-1.2**

F3 **1.2.8.5.6**

F2 **8.7.9.9**

F1 **4.0.5.7**

Slope dist **4.0.4.8.7.9.9**

Phase C R

1	F2	F1	F3	F4
2	F2	F1	F3	F4
3	F2	F1	F3	F4
4	F2	F1	F3	F4

Sum 2-3 **18429** **15517**

Sum 1-4 **18430** **15520**

Mean **18430** **15519**

0.5 x Mean **9215** **7759**

correct meter figure

Notes

Total sum of corr **-0.245** m

Slope distance **4969908** m

Observer

Recorder

Approx. dist

Type of reflector

Visibility **Good**

Fair **Fair**

Poor

Fig. 3
 Geodimeter 600
 Example of one- and four-phase measurements.

The effects of the individual errors on the end result can be found in the following table:

	Mean square error mm	Proportional error $10^{-4} \cdot D$
1. Setting	± 2	—
2. Phase determination	± 3	—
3. Geodimeter constant	± 2	—
4a. Eccentricity, Geodimeter	± 1	—
4b. Eccentricity, Reflector	± 1	—
5a. Frequency setting	—	+0.6
5b. Frequency ageing	—	+0.5
6. Meteorological data	—	+1
Resulting mean square error	± 4 mm	$\pm 1 \cdot 10^{-4} \cdot D$

The methods described in the following will eliminate or reduce the contribution of the individual errors as follows:

Method 1: Error 2 is eliminated: $dD = 3 \text{ mm} \pm 1 \cdot 10^{-4} \cdot D$

Method 2: Errors 2, 3 are eliminated: $dD = 2 \text{ mm} \pm 1 \cdot 10^{-4} \cdot D$

Method 3: Only setting errors remain, $dD = \frac{2 \sqrt{2}}{\sqrt{n}}$, where n is the number of observations.

Fig. 4
Geodimeter 600
The effects of individual errors.

AGA Geodimeter 600

— a new long range instrument

Specifications

Range

Maximum distance 40 km
Minimum distance 15 m with AGA prisms 571.125.021

The range is dependent on visibility, light conditions and the reflectors. Daylight and after-dark ranges are practically the same. See diagram below.

Accuracy

One-phase measurement (measuring time = 1 min):
Mean square error is less than ± 10 mm + 1 mm/km
Standard method (measuring time = 3 min):
Mean square error is less than ± 5 mm + 1 mm/km
Special method (measuring time = 20-30 min):
Mean square error is less than 1 mm + 1 mm/km
The accuracy is unaffected by beam interruptions

General data

Light source 1 mW He-Ne laser
Power source 12VDC battery
Power consumption 26W
Elevation -55° to $+90^\circ$
Ambient temperature range -40°C to $+40^\circ\text{C}$
(up to $+50^\circ\text{C}$ with slightly lower frequency stability)

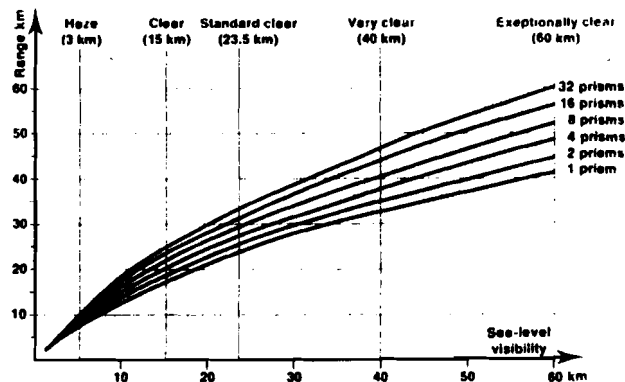
Optical data

Receiver:
Focal length 600 mm
Magnification $28\times$
Diameter 105 mm
Diaphragm infinitely adjustable between 0.5×0.5 and 0.1×0.1 mm
Corresponding 'projected' area $0.8 \times 0.8 - 0.15 \times 0.15$ m/km
Transmitter:
Focal length 600 mm
Diameter 53 mm

Dimensions and weights

Standard equipment No. 571.199.008:
Instrument unit with Kern tribr. 15 kg 220 x 360 x 530 mm
Transport case (including tool kit, operating manual, recording forms, battery cable) 8.5 kg 280 x 360 x 630 mm
Harness for transport case 1.1 kg

The greatly improved receiver optics and the laser light source enable you to measure distances of up to 200 meter directly against walls and other reflecting surfaces without reflector. Distances of up to 1.5 km can be measured using a plastic reflector. The main accuracy in connection with the above make the Geodimeter 600 suitable for displacement measurements.



Maximum range with AGA prisms (Part No. 571.125.021 or 571.125.001).
For long ranges a very solid instrument set-up is necessary, since AGA Geodimeter 600 has a small beam divergence.

First in electro-optical distance measuring

AGA have 50 years of experience in the fields of electronics, optics and precision engineering, and have been manufacturing electro-optical distance measuring instruments since 1947. Constant product development based on experience in the field has made the AGA Geodimeter instrument series one of the most economical and reliable available for short, intermediate, and long-range measurements.

Contact us to discuss your measuring work

AGA has subsidiaries and general agents with qualified service stations in every major country in the world. They, in turn, are backed up by a network of representatives.

To find out more about AGA Geodimeters and surveying accessories, contact the AGA representative in your area.

AGA

AGA Geotronics AB
S-181 81 Lidings, Sweden
Telephone: 08-767 00 20
Telex: 17781 AGAGEO S
Telegrams: Agafaros Stockholm

Scandinavia and Finland

AGA Geotronics, Scandinavia
181 81 LIDINGS, SWEDEN
Telephone (08) 767 00 20
Telex: AGAGEO S

W-Germany, Holland, Switzerland and Austria

AGA Optronik GmbH
D-6236 ESCHBORN/TS
Industriestrasse 4 W-GERMANY
Telephone (06196) 46041
46042
Telex: 417455 AGAOP

Italy

AGA Italia S.R.L.
Via Valassina 24
I-20159 MILANO ITALY
Telephone: (02) 6107 69, 60 30 76
Telex: 36540 TEKITAL (per AGA)

France, Belgium, Algeria, Tunisia and Morocco

AGA Geotronics S. A. R. L.
12, Ave du 8 Mai 1945
Les Flanades
F-95200 SARCELLES FRANCE
Telephone: (1) 990 45 98, 990 42 55
Telex: 220064 contract 4095

United Kingdom

AGA Geotronics
6, The Quay
St. Ives Cambridgeshire, U.K.
Telephone: St. Ives (0480) 64907
Telex: AGAGEO G

Eastern Europe (Comecon)

AGA Direct Exports
S-181 81 Lidings, Sweden
Telephone: (08) 765 27 35
Telex: 10821 AGADEX

Australasia

AGA Products Australia Pty Ltd
171, Fitzroy Street
ST. KILDA, Vic. 3182 AUSTRALIA
(Melbourne)
Telephone: 94 64 30
Telex: 44785 AGAMEL

AGA Products Australia Pty Ltd
P.O. Box 223 (275 Harbor Road)
BROOKVALE N.S.W. 2100 AUSTRALIA
(Sydney)
Telephone: 938 23 33
Telegram: AGAFAROS SYDNEY

USA

AGA Corporation
Geodimeter Division
80 Mark Drive
SAN RAFAEL
CALIF.
94903 USA
Telephone: (415) 479-3816
Telex: 349499 AMAFAROS

Canada

AGATronics Limited
41, Homer Avenue Unit 5
TORONTO 18, Ont. M8Z 4X4 CANADA
Telephone: (416) 252-4691
Telex: 06-967858 AGACAN

Japan, Taiwan, Korea

Gadexus AB
Dept. GEM-III
P.O. Box 1284
TOKYO C 100-91 JAPAN
Telephone: 03-403-21-41
Telex: 242-2075

Iran

Iran Swedish Co. AB
Sevom Esfand 29
TEHERAN IRAN
Telephone: 314161-69
Telex: 212407

Fig. 5
Geodimeter 600
General description - specifications

Discussion (paper 6)

- Q. Is the method of reading by an analogue read-out not somewhat old fashioned ?
- A. We have used the same electronics as in the model 6BL etc. and by means of this measuring principle you can choose what kind of accuracy you want to reach.
- Q. I know that there have been complaints about, let's say, the rather high built up shape of the models 6, and it ought to be physically more stable. Do you know something more about this or do you consider the instrument stable enough as it is ?
- A. Well, I understand. but I don't feel responsible for the research, and I regret I can't give you a proper answer.

Remark 1) I would personally say, that I am to a certain extent in favour of the analogue read out. In the digital read out, I have the feeling that the last digit is being chopped off, unless there is a special rounding off mechanism built in. So we would get a truncated reading instead of a rounded off one. One may of course add an extra digit, and use that for rounding. I favour the analogue read out, because I am not happy to have the same figures coming up again. This is of course psychological. But the digital read out has many advantages of one wants an automatic transfer of the reading for registration.

Remark 2) The development cost with regard to the digital read out would be higher. But from the standpoint of precision and truncation I think that usually digits are added, so that changes occur below the noise level. You don't see the truncation because the noise would usually dominate.

Remark 3) A good analogue read out may be more expensive today. I like to congratulate Aga that they eventually abandoned the idea of the high frequency delay line in the 6A model. It caused reasonable complaints from the user. It was very good on the old organ-like instrument because there it was used for interpolation.

In the model 3, which you did not show, as well as in the models 4 and the early model 6 it was difficult to calibrate this delay line. They were liable to all sort of influences.

Q. You mentioned a frequency of about 30 MHz and .750 KHz. The latter is a " virtual " frequency I trust. This is different from the previous instruments.

A. Yes, this touches on a question of EDM instruments in general namely the checking that the frequencies are correct. Of course you can use a frequency meter, and they can be very small today , but you can get a good value by using more than one crystal frequency, or - let's say - more than one passing frequency. It might also be a cavity resonator. Then you have more than one possibility having an independent check in the field; it will give you a redundancy. The AFC - detector more or less guarantees that your beat frequencies are correct. But still if the main crystal gives away, than the only way to check accurately is by applying an external frequency reference. For the people in the field it is simply a matter of how often we have to calibrate. We have tried, taking a portable frequency meter into the field. We found out it was very very correct. Still I think we would like you as ordinary users to give consideration to the thought that the instrument should show up if something goes wrong, in the form of an alarm, in preference of making the instrument absolutely foolproof.

HIGH PRECISION TRAVERSE OF FINLAND AND THE UTILIZATION OF IT

Teuvo Parm, Helsinki University of Technology, Department of Surveying,
SF-02150 Espoo 15, Finland.

During the years 1972...1974 the Finnish Geodetic Institute planned and measured through Finland the traverse seen in Fig. 1. The traverse consists of 25 sides, the directions of which were mainly obtained from earlier adjustments of the whole Finnish first order triangulation net. The directions of the rest sides were obtained from separate determinations. The heights of the stations of the traverse are either levelled, 14 cases, or determined from the observations of the vertical angles carried out in connection with distance measurements, 12 cases.

The distances were measured with the laser geodimeter, Geodimeter Model 8. 4-9 measurements on each side were carried out at different times of day and, in some cases, even in different years.

A detailed description of the traverse and the results were already published (Parm 1976).

The relative accuracy of the final result of the length of the geodesic line between the terminal points of the traverse is 1:7 400 000. This high accuracy achieved is due to the repeated calibrations of all instruments used, and especially by the measurement of the modulation frequency every day the distance measurements were carried out, and by the careful selection of observing conditions and procedures. For the geometrical reductions of the traverse legs the quality of the Finnish first order triangulation net is essentially important. The knowledge of the geoid in the Finnish area is reliable because both the astro-geodetic and gravimetric geoid were determined and the agreement between them is good. The flatness of the topography of Finland is favourable for these determinations.

A scale correction applied to the geodimeter results of the traverse measurement should especially be pointed out. In 1971 the Finnish Geodetic Institute carried out geodimeter measurements on the Niinisa-
lo 22.2 km long calibration baseline, the accuracy of which is about 1:10 000 000. These measurements indicated in the geodimeter measurement a scale error of ± 1.6 mm/22.2 km on average. The measurements before noon (AM) and after noon (PM) deviated from each other 7 mm. The distribution of the measurements was

AM	18 %
PM	82 %

So we see that there seems to be some systematic error still existing in the geodimeter results.

The results of the geodimeter measurements on the traverse were corrected with the scale correction -1.6 mm/22.2 km. On the traverse again, depending on the time of observations, there seems to exist systematic differences between results. On the traverse the distribution of the observations is, not only by chance,

AM	21 %
PM	79 %

Thus the observing procedures and the distributions of AM and PM measurements were similar on the calibration baseline and on the traverse. Thus the systematic errors in both cases are also similar and the application of the scale correction mentioned above eliminates the systematic error and the result of the length of the traverse is correct.

The utilization of the traverse is a work of current interest. As presented in (Parm 1976) the traverse is used for checking the scale of the first order triangulation net and the results of the first comparisons were already given in the same paper.

The differences between the geodimeter results and the side lengths obtained from the adjustment of the whole first order net were ± 11 cm on average, the greatest difference being 29 cm. On the whole length of the traverse, 888 km, the agreement is good: 1:4 500 000.

The traverse was recently included in the latest adjustment of the Finnish first order net (Hytönen 1977).

The traverse and whichever section of it is available for scaling the national stellar triangulation net of Finland.

The traverse and all sections of it are also available for calibrating instruments and method needing reference distances of 100-900 km. In addition it is worth mentioning here, that we have now the following calibration lengths of the following relative accuracies in Finland:

Nummela Standard Baseline	864 m	$\pm 0.69 \cdot 10^{-7}$
Niinisalo Calibration Baseline	22.2 km	$\pm 0.78 \cdot 10^{-7}$
High Precision Traverse	888 km	$\pm 1.3 \cdot 10^{-7}$

According to the advice given by Finnish geologists two sides of the traverse were selected to be measured repeatedly in order to indicate possible tectonic movements. The two sides were measured in 1974 and 1976. It is yet too early to conclude any changes in lengths.

Utilization of the high precision traverse for the international purposes is also going on. Professor Juhani Kakkuri (Kakkuri 1977) from the FGI has just completed the observations made simultaneously at both ends of the traverse with two Doppler receivers (Magnavox MX702A/GEO II). The receivers were kindly delivered for the measurement by manufacturer Magnavox. The observations are also affiliated with the European Doppler Campaign EDOC. Thus the traverse may serve in the scaling of the EDOC-network. Furthermore, the results may be used for calibration of the Doppler-instruments themselves.

Some other plans to utilize the traverse are under discussions as well. It would be recommendable to have new instruments or equipment for a measuring method, not yet well enough studied, brought to the traverse giving calibration distances right up to 900 km.

References:

- Kakkuri, J., 1977. Private communication.
- Hytönen, E., 1977. The National Report of Finland for the Commission for the New Adjustment of the European Triangulation. Reports of the FGI 77:2. Helsinki.
- Parm, T., 1976. High Precision Traverse of Finland. Publ. of the FGI No. 79. Helsinki.

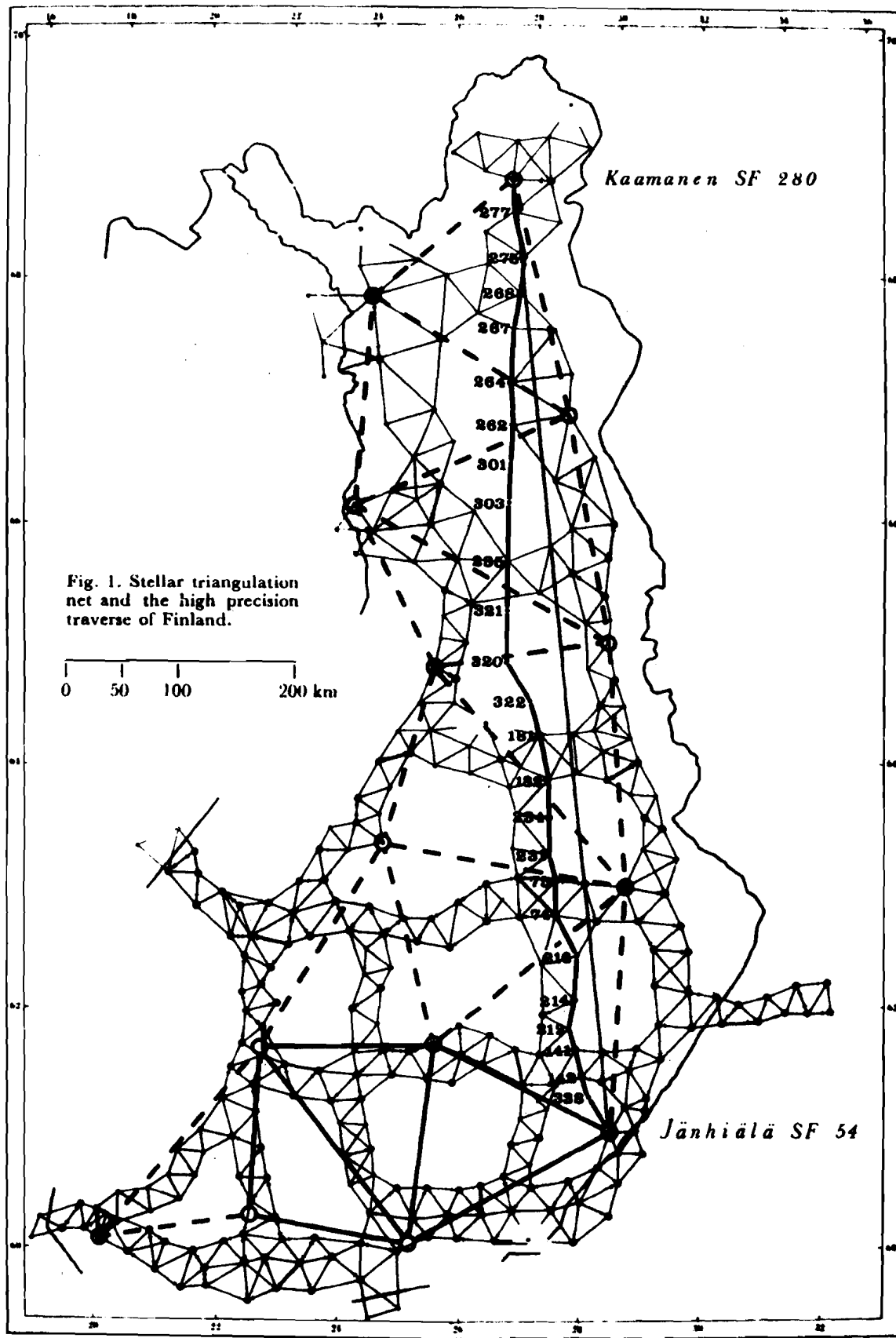


Fig. 1. Stellar triangulation net and the high precision traverse of Finland.

0 50 100 200 km

Kaamanen SF 280

Jänhiälä SF 54

Discussion (paper 7)

Q. I'm impressed by your confidence in applying a correction, which is considerably less than 0,1 or 1 part of a million to geodimeter measurements on 2 counts.

Firstly you have quoted the base-line as 0.78×10^{-7} , standard error of the base itself, which is about the same order I think as the 1.6 mm over that distance.

And, so quite apart from that factor itself I was wondering whether you did any significance tests or something like that of the results obtained, so that you could decide that this correction was significant.

I know you mentioned you could detect morning and afternoon differences and really it is quite impressive that you could produce something which was significant at all in that sort of realm.

A. I have no numerical indication at a frequency level or something like that. I can only tell that, as I have mentioned in my publication that there is a systematic change during the day in morning and afternoon measurements. But the mean of our measurements agrees with the result of the invar wires, the difference being this 0.6 mm. Again because this kind of difference really exist it would cause a systematic difference of errors on the traverse be it small or great. Therefore we have applied this kind of small correction. On the traverse measurements we observed this systematic change at different kinds of observation. There is some reason for systematic errors of course, since the conditions concerning the distribution of measurements and the observing procedures and the instruments are the same for the calibration measurements and the traverse measurements; therefore it is justified to conclude that the systematic error is eliminated even if it is very small.

Q. What is the cause of the systematic difference between the afternoon and the early -morning measurements ?

A. I don't know of any research on that. I can only guess as many others have guessed and conclude perhaps, that some influence of the refraction is left, effecting the EDM results anyway, but which is not compensated for.

If there is some constant error in the refraction left, it may be compensated, when using the scale correction, derived from the measurements on the calibration baseline.

Abstract:

By means of a rotatable plane mirror the transmitted signal of an electro-optical rangefinder can be transferred to an arbitrarily oriented spatial distance. This technique gives a better accuracy compared to distances directly determined, if the so called modified differential method is employed. Distances up to 250 m can be measured using this method, which is advocated for accurate measurements as well as for engineering work, where often vertical distances must be evaluated. Using the Tellurometer MA 100 the height of an 18 floor building has been determined with an accuracy of about ± 0.5 mm.

1. Introductory remarks

In engineering surveys it is quite often necessary to measure vertical and slope distances with high accuracy. In the following a method is therefore presented, by which it is possible to transfer the transmitted rangefinder signal by means of a rotatable plane mirror to an arbitrarily oriented spatial distance. This provides for a broader application of the rangefinder and in addition for increased accuracy.

It is well known, that the "precision" (inner accuracy or internal consistency) of various rangefinders is considerably higher than their "accuracy" (outer accuracy). Precision is understood to be the accuracy of the resulting distances obtained from repetitions observations without changing the set up of either the rangefinder or the reflector and, in addition, without changing the initial alignment of rangefinder and reflector. This higher precision is utilised in the already known differential method (compare e.g. the Tellurometer MA 100 handbook and ALLAN [2]) to increase the accuracy of the resulting distance, which is obtained as the difference of two distances. The rangefinder and the two reflectors have to be aligned in a straight line. Moreover, it is assumed that the reflectors have the same additive constant or are exchanged during the observation using forced centering.

Using this method it is very important, when forming the difference between the two observed distances, that the additive constant of the instrument cancels itself. In this way the long and short time variations of this "constant", which for this reason may also be called zero shift, are eliminated. The identical alignment for the two distance measurements provides, moreover, that the phase inhomogeneities of the wave front affect the "difference" distance to a lesser degree than direct obtained distances. The error due to the phase inhomogeneities cannot completely be eliminated, because the difference distance consists of a short and a relative long distance so that both reflectors do not reflect the same part of the wave front.

2. Description of the modified differential method

To make the method more universally applicable it is mandatory to abandon the condition of colinearity between rangefinder and reflector. This can be achieved by transmitting the signal to the terminal point of a distance via a gimbaled plane mirror, which can be turned around two axes. The length of the traverse P_1, P_2, P_3 is obtained according to the set up in figure 1. Replacing the mirror in P_2 with a reflector, the distance P_1P_2 can be measured and the distance P_2P_3 is obtained as the difference of the two measurements.

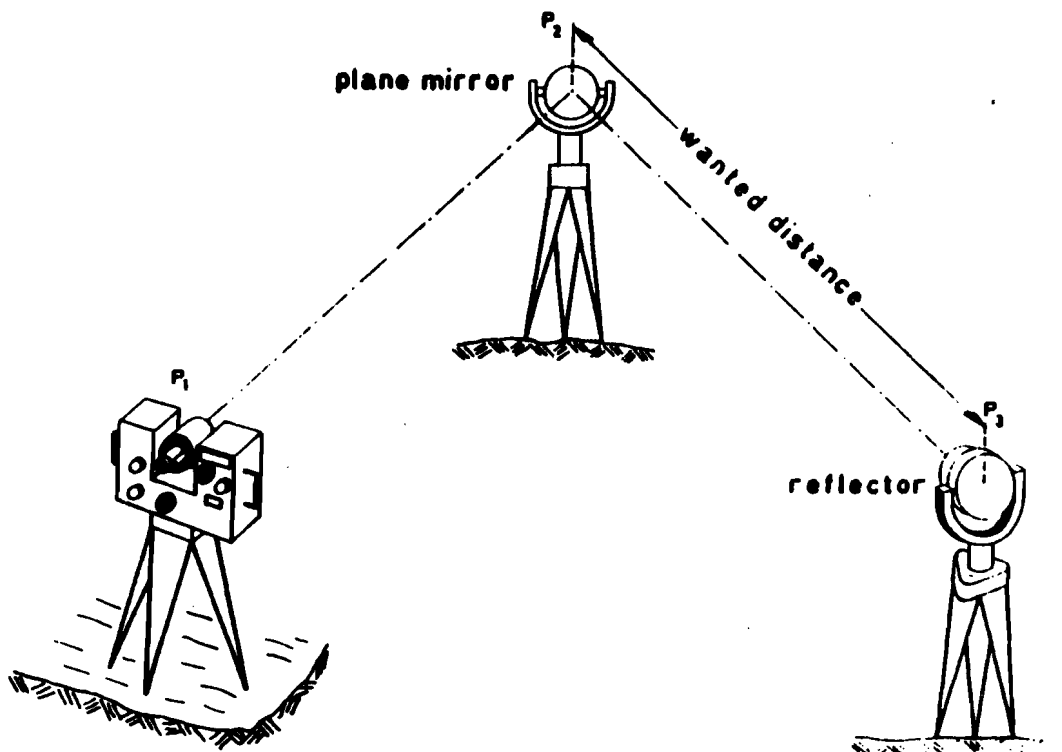


Figure 1

Examining this "modified differential method" for further error sources points to the dependence on the signal strength and the cyclic error. The effect of the signal strength on the measurement will be noticed when larger differences in signal strength appear which are caused by the length of the line P_2P_3 and the distance between rangefinder and mirror. HEUPEL and WITTE [5] have proved that such differences may cause an error of some tenth of a millimeter when using the Tellurometer MA 100, whereas using the Zeiss SM 11 an error of some millimeters may occur (HALLERMANN [4]). However, this error can be easily eliminated by applying proper corrections. The cyclic error, too, can be determined a priori and then accounted for. Moreover, the influence of this error can be reduced if the difference distance P_2P_3 is a multiple of integers of the basic periodicity for the used rangefinder (e.g. 2 m or 75 MHz for the Tellurometer MA 100). The remaining part of the difference distance has then to be measured in the conventional way. The amplitude of the cyclic error which is inversely

proportional to the received signal strength (e.g. GREENE [3]) varies from rangefinder to rangefinder. It depends also on the length of the measured distance (see also HÖLSCHER [6]) as tests, using the baselines of the Geodetic Institute at the University of Bonn, have shown. The signal strength of the received signal has been sufficient for these tests. Besides these error sources the range of a possible nonperiodical zero error's dependency on distance should be taken into account. Using seven different Kern DM 1000 instruments AESCHLIMANN and STOCKER [1] have shown that in a range between 30 m and 150 m the additive constant can vary between +6 mm and -4 mm against a mean value for this "constant". This dependency is caused by phase inhomogeneities and differs from instrument to instrument, but it can be determined in advance. If such nonperiodical errors become too large compared with the required precision, the use of a type of instrument having less or no nonperiodical errors would be suitable like for instance the MA 100. Because such a determination is also relative laborious it is furthermore easier to measure with an accurate instrument.

At a maximal distance of about 200 m, which is considered the upper limit of the differential method (see later), other error sources as e.g. the instrument scale error and the uncertainty of the mean atmospheric refractive index do not affect the accuracy obtainable with the tested rangefinders, because the frequencies show no greater deviations and the temperature can be observed sufficiently accurate. In any case, no undue deviations were found in the frequency checks routinely conducted by the Geodetic Institute.

3. Pointing procedure

Using instruments whose transmitter and receiver optics and their telescopes are set up coaxially, e.g. Zeiss SM 11, Zeiss Eldi 2, the alignment of the mirror can be obtained very easily with the line of sight of the built in telescope. With the aid of this telescope the mirror can be aligned with slow motion knobs for vertical and horizontal traversing such that the image of the terminal point P_3 appears in the center of the reticle. If the rangefinder does not have a coaxial telescope, e.g. Tellurometer MA 100, then the aiming procedure is reversed. Instead of a reflector a theodolite is set up in P_3 . But the vertical axis of this theodolite must have the same height as the used mirror and reflector. After aiming at the middle of the mirror with the theodolite's telescope the mirror is again turned around his axes such that the image of the transmitter and receiver optics appears in the center of the reticle. For an electronic fine adjustment both methods need a maximum returned signal, as indicated by the microamperemeter, in order to compensate a divergence between the line of sight and the transmitted signal for the first method, whereas the second method needs this adjustment as a proof that the transmitted signal reaches via mirror and reflector the receiver. This electronic alignment in vertical and horizontal direction is obtained from a small movement of the rangefinder's slow-motion drive screws. It can now be assumed that for both methods the transmitted signal will reach the receiver after being reflected in the middle of the mirror and the prism. Afterwards mirror and reflector are exchanged using forced centering so that the short distance can be measured without any alignment of the instrument.

For rangefinders with biaxially arranged transmitter and receiver optics, e.g. Tellurometer CD 6, the alignment, as indicated before, can be obtained from P_3 . With the aid of a special target, which may consist of white carton, the geometrical alignment can now be achieved.

Zeiss SM 11 is not equipped with temperature stabilised oscillator crystals a special scheme has been developed in order to use this instrument without any loss of accuracy. The exact procedure can be found in [7].

The field tests were performed on the test baseline of the Geodetic Institute, in the Kottenforst near Bonn. The sections of the base line, used for the tests, are 48 m and 96 m, respectively, long and have been determined to within ± 0.16 mm with two calibrated invar wires and one invar tape. The set up was the same as shown in fig. 1. The mean from four independent difference measurements differed only by 0.4 mm for the MA 100 from the results obtained with the invar wires for the 48 m and 96 m distance. The mean errors of the MA 100 for both distances were ± 0.3 mm, as computed from the observation discrepancies.

The Kern DM 1000 No 197746, the Tellurometer CD 6 No 1232, the Zeiss SM 11 No 78342 and the Zeiss (Jena) EOK 2000 No 240396 were also tested.

4. Test measurements

At first tests were performed with the Tellurometer MA 100 No 127 and the Zeiss SM 11 No 78347 in order to get an estimate of the precision of these instruments. These tests have shown a precision of ± 0.2 mm for the MA 100 and of ± 2.5 mm for the SM 11 respectively. For a quick check of the differential method, the prism tribrach was mounted on a cross-slide to allow for its moving along the line of sight, and set up in P_3 (s fig. 1). The displacement was measured to within ± 0.05 mm. With this device it is possible to prove directly the maximal obtainable accuracy of the differential method. From 10 independent difference measurements with shifts of 10 mm, an accuracy of ± 0.2 mm for the MA 100 and of ± 2.6 mm for the SM 11 was derived for a distance obtained from five individual measurements. Because of the fact that the Zeiss SM 11 is not equipped with temperature stabilised oscillator crystals a special scheme has been developed in order to use this instrument without any loss of accuracy. The exact procedure can be found in [7].

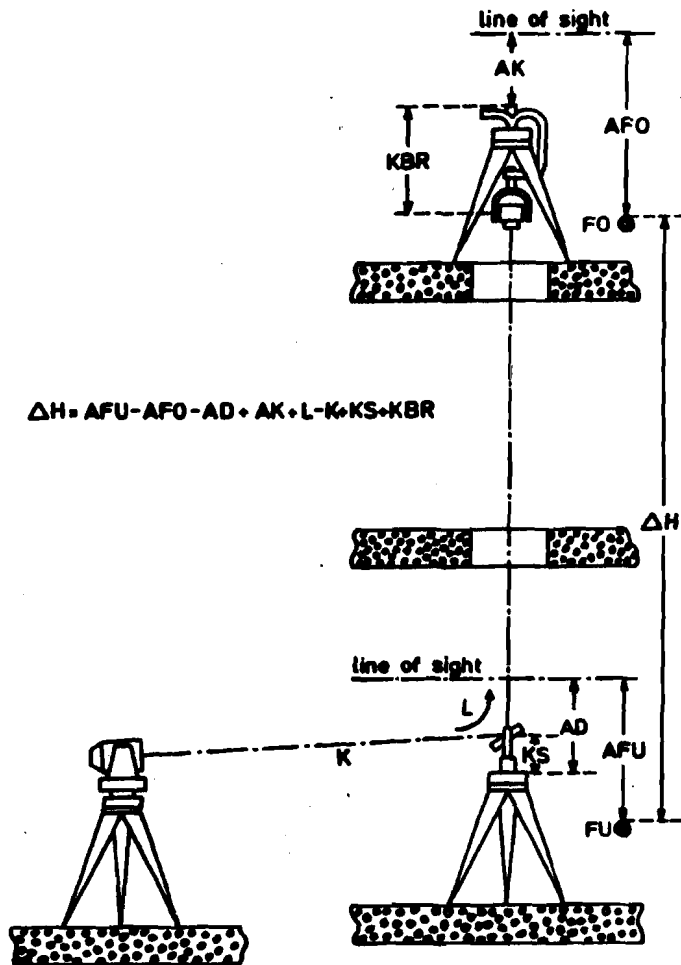
The field tests were performed on the test baseline of the Geodetic Institute, in the Kottenforst near Bonn. The sections of the base line, used for the tests, are 48 m and 96 m, respectively, long and have been determined to within ± 0.16 mm with two calibrated invar wires and one invar tape. The set up was the same as shown in fig. 1. The mean from four independent difference measurements differed only by 0.4 mm for the MA 100 from the results obtained with the invar wires for the 48 m and 96 m distance. The mean errors of the MA 100 for both distances were ± 0.3 mm, as computed from the observation discrepancies.

The Kern DM 1000 No 197746, the Tellurometer CD 6 No 1232, the Zeiss SM 11 No 78342 and the Zeiss (Jena) EOK 2000 No 240396 were also tested.

Summarizing one can say that their accuracy was improved by a factor of about 3.

5. Practical application of the method for elevation measurements

Elevation differences in high buildings can be measured either directly along the plumbline (see fig. 2) or indirectly by reducing a slope distance, and only the zenith distance associated with P_2P_3 (fig. 1) must be determined. Fig. 2 shows the set-up of instrumentation necessary for the determination of elevation differences between benchmarks in floors or mezzanines of buildings and which additional measurements have to be made.



$$\Delta H = AFU - AFO - AD + AK + L - K + KS + KBR$$

Figure 2

The total difference in elevation between the points is:

$$\Delta H = AFU - AFO - AD + AK + L - K + KS + KBR$$

ΔH = elevation difference between the two benchmarks

L = long distance

KS = constant height of the mirror's trunnion axis above tribrach

KBR = constant height of the reflector's trunnion axis

$\left. \begin{array}{l} AK \\ AFO \\ AD \\ AFU \end{array} \right\} = \text{readings on a levelling rod}$

As an accessory equipment a special bow is necessary so that the reflector can be attached below the tripod head within forced centering (fig. 3). The geometrical alignment

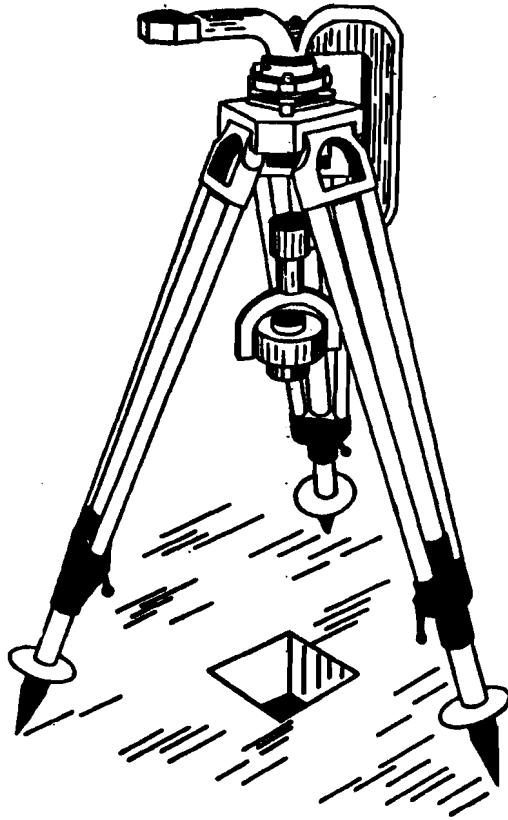


Figure 3

can now be obtained with the aid of an optical plummet, which can be exchanged for the bow using forced centering. This optical plummet serves here only as a telescope. The elevation differences between the benchmark and the highest point of the bow are determined by levelling. The constant height of the mirror's trunnion axis above the tribrach and the constant difference in height between the trunnion axis of the reflector and the highest point of the bow are evaluated in a laboratory. This method was applied to check the accuracy of elevation differences between several benchmarks on different floors of an 18 floor building obtained with a special levelling procedure using two rods screwed together on top of each other.

For this kind of levelling procedure it was not possible to give an estimate of the influence of systematic errors. But from the surveyor's point of view a standard deviation of only ± 5 mm for the elevation differences could be tolerated. Therefore the levelled elevation differences had to be checked by an independent method. In order to examine the accuracy obtained by levelling thoroughly, the accuracy of the differential method had here to be better than one millimeter. This could only be achieved with the Tellurometer MA 100 and its precision of ± 0.2 mm. The cyclic error could be eliminated because the distance between mirror and reflector, i.e. the difference distance, was tuned to a multiple of integers of the MA 100's basic periodicity by a corresponding high or low setting up of the used tripods.

On 4 different days 11 elevation differences were evaluated with the aid of the MA 100. The precision (inner accuracy) of all measurements could be determined, because every elevation difference was independently obtained two times. The standard deviation for the measurements is ± 0.2 mm and the biggest discrepancy between two independent measurements amounts to 0.4 mm. These discrepancies not only contain the standard deviations of all MA 100 measurements but also the standard deviations of the connecting levellings (2 instrument set ups for every elevation difference). But it should be pointed out that every distance (the long and short ones, see fig. 2) were determined five times. Using the differential method for this kind of elevation evaluation it is advantageous that the precision does not depend on the height of the elevation difference, because long (up to 200 m) and short distances are obtained with the same accuracy.

References:

- | 1| AESCHLIMANN, H. and STOCKER, R., 1974. Instrumental Errors in Electro Optic Distance Measurement. XIVth International Congress of Surveyors, Washington, D.C., Paper 505.4
- | 2| ALLAN, A.L., 1967. The Accurate Measurement of a Short Line by Geodimeter Model 6. Survey Review, XIX (145), 98 - 102
- | 3| GREENE, J.R., 1975. Accuracy Evaluation in Electro-optic Distance Measuring Instruments. Tellurometer Publication No. 2119; 1 - 6
- | 4| HALLERMANN, L., 1971. Untersuchungen des Tachymeter-Theodolits Reg Elta 14 der Firma Carl Zeiss, Oberkochen. Mitteilungen aus dem Geodätischen Institut der Universität Bonn, 1 - 90
- | 5| HEUPEL, G. and WITTE, B., 1974. Messungen hoher Präzision mit dem Tellurometer MA 100. Allgemeine Vermessungsnachrichten, 81 (2); 64 - 74
- | 6| HÖLSCHER, H.D., 1970. An Electro-optical Distance Measuring System of High Accuracy for Short Ranges. Survey Review, XX (157), 309 - 322
- | 7| WITTE, B.U., 1975. Genaue Messung von beliebig im Raum orientierten Strecken mit elektrooptischen Nahbereichsentfernungsmessern. Zeitschrift für Vermessungswesen, 100 (1); 21 - 29

A LASER SYSTEM FOR RANGING TO SATELLITES

F.W. Zeeman, Geodetic Institute, Delft University of Technology, The Netherlands

abstract

At the observatory for satellite geodesy in Kootwijk, The Netherlands the Geodetic Institute of the Delft University of Technology operates a laser ranging system since September 1976.

With this system distance measurements can be performed to all cooperative geodetic satellites presently in orbit. The measurements so far show an internal accuracy of 15 - 30 cm in satellite ranging and 3 - 6 cm on ground targets at short distance.

The purpose of this paper is to give a general description of the present system and its potentials for the next few years.

Introduction

The working group for satellite geodesy of the Delft University of Technology operates a geodetic satellite tracking station in Kootwijk, 30 km North of Wageningen, since the end of 1973. At the same time a project for design and construction of a laser system for ranging to satellites started in close cooperation with the Institute of Applied Physics (TPD) in Delft.

This project has been supported by the Royal Netherlands Academy of Sciences.

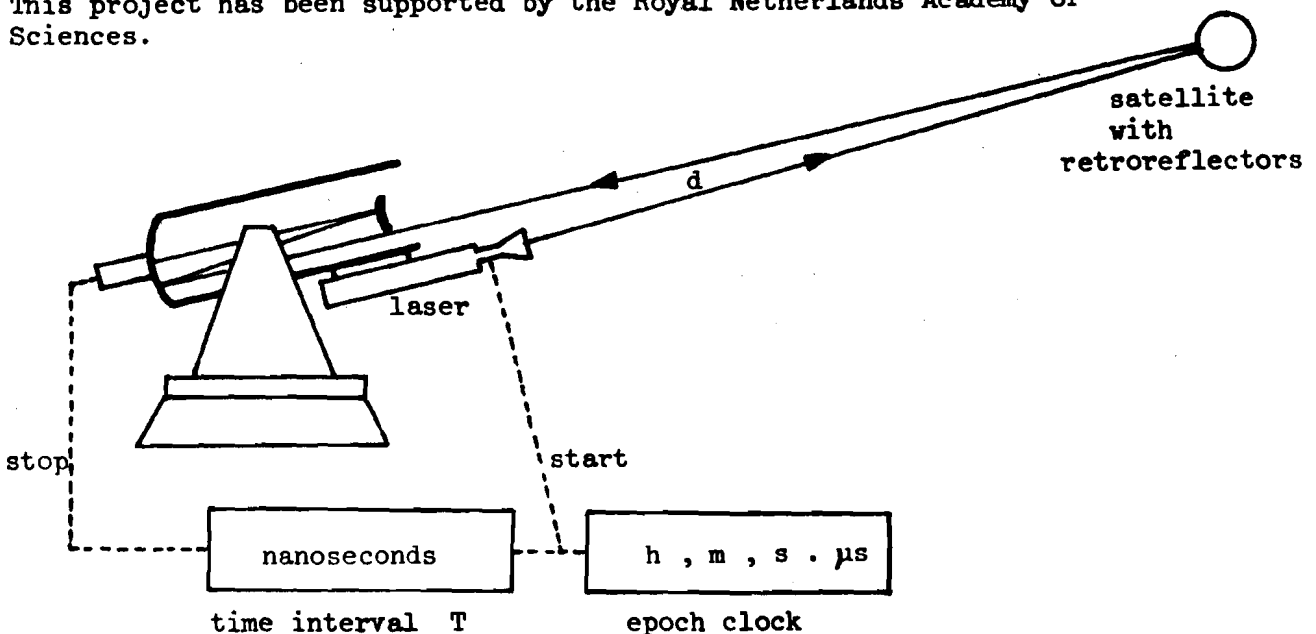


fig. 1

The principle used for ranging to satellites is that of a pulsed "optical radar".

The time-of-flight T of the light pulses from the transmitter, via the satellite to the receiver yields the distance d to the satellite according to $d = \frac{T}{2} \cdot c$.

The velocity of light c has to be corrected for the path through the atmosphere.

Only time-of-flight measurements together with the local meteorological data are recorded. The influence of the atmospheric refraction is implemented during geodetic network computations.

Before and after each satellite pass the measured values are compared with an identical distance measurement to a carefully surveyed fixed target at short distance. This method eliminates any delay caused by the internal optical path, cables, electronic equipment etc.

In order to define the position of the satellite in its orbit the epoch of the measurement, i.e. the instant when the satellite has been hit by the laser pulse, has to be recorded in UTC time scale.

The accuracy of this time measurement has to be compatible with the ranging accuracy. With a topocentric radial velocity of the satellite in its orbit of 5 km/s, 5 cm accuracy corresponds to a timing requirement of 10 μ s UTC.

Satellite	orbital altitude (km)	relative signal strength at 45 degr. elevation
GEOS - 1	1 950	0.03
GEOS - 2	1 530	0.13
GEOS - 3	930	10
Starlette	920	0.24
LAGEOS	5 900	0.005
Lunar arrays	360 000	3×10^{-8}

table 1

So far results have been obtained in routine nighttime ranging to the satellites Starlette, LAGEOS and the GEOS-1, GEOS-2 and GEOS-3 satellites. Daytime ranging on all these satellites except LAGEOS which has an orbital altitude of about 6000 km has been performed as a routine operation. Work is in progress however to obtain a fair output from LAGEOS daylight passes.

Internal accuracy of the measurements is 15 - 30 cm RMS.

Laser subsystem

The pulse laser is the most critical part in the ranging system. It requires much attention and for that reason it has been installed in an air-conditioned room.

This ruby pulse laser consists of the following parts:

- a Q-switched oscillator
- a spark-gap activated pulse chopper
- two amplifier stages
- a high voltage power supply, water cooling unit and control electronics

It has been built to our specifications by an American laser manufacturer.

The Q-switched oscillator consists of the laser head, a 100% reflector, a partially reflecting output mirror and the Q-switch, a combination of a vertical Brewster stack polarizer and a switchable Pockels cell polarizer. The output of this oscillator is a 25 ns wide light pulse of 6943 Å wavelength, horizontally polarized. From this 25 ns pulse a central part 4 ns wide is chopped out by means of an optical switch, again built with a Brewster stack polarizer and a Pockels cell. This short light pulse is then amplified by a two stage amplifier to a 1.5 Joule operational energy level (3 Joule max.). The maximum firing rate of this system is 15 pulses per minute.

Optical/ mechanical subsystem

The role of this subsystem is to point the laser beam to the satellite and to collect the laser light reflected by the satellite. The equipment is located in a dome on top of the building and has been designed specially for this application.

The transmitter and receiver optics have been combined in a theodolite type of structure. The absolute pointing of this mount is better than 20 arcseconds (1/3 of minimum laser beam divergence) with a windload up to Beaufort 8.

The mount's angular position is read out using absolute optical shaft encoders to a resolution of 0.001 degree. The mount control unit then compares the actual position with the desired position. The error signal generated is used to drive the DC servo motors.

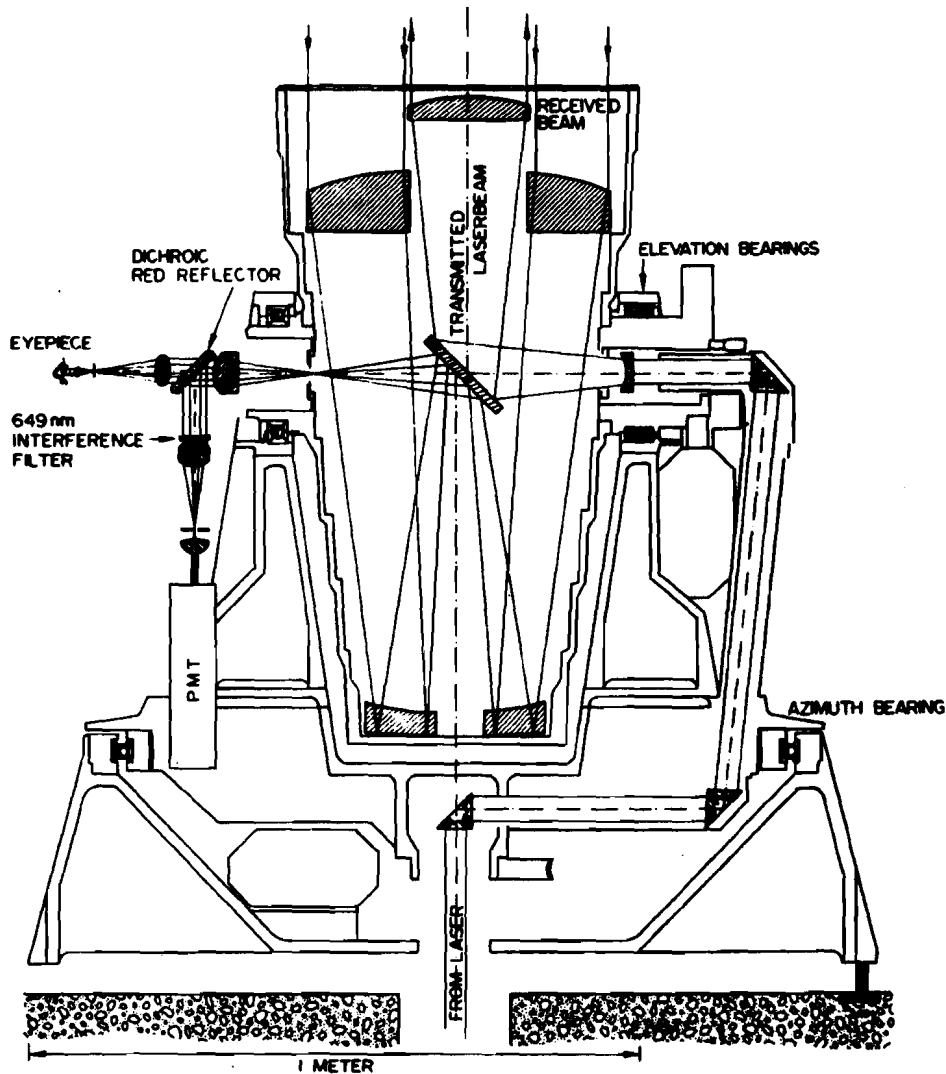


Fig. 2. Coudé telescope.

The laser beam is directed upwards through the hollow concrete pillar into the vertical axis of the mount. Via prisms the beam is directed to the elevation axis and into a 5 power Galilean collimator. The use of this collimator after the moving prisms in the optical train diminishes the alignment precision requirement of the coudé light path by a factor of 5.

The divergence of the laser beam after the collimator is 1 arcminute. By defocussing the collimator the divergence can be adjusted between 1 and 20 arcminutes; in order to adapt the system to the accuracy of the prediction of the satellite position at the time of laser firing. The receiving telescope is of a partial coude design (the optical path passes through the elevation axis only) with a catadioptric (lens - mirror) optical train. It has a 50 cm aperture and the field of view is adjustable between 1 and 20 arcminutes.

By means of a dichroic red reflector the received light is split into wavelengths $> 6500 \text{ \AA}$ which are directed to the photodetector and wavelengths $< 6500 \text{ \AA}$ going to an eyepiece. In this way the operator can see sunlit satellites to a visual magnitude of +13. This feature has shown to be very useful in acquiring satellites within a narrow beam.

The reflection of the laser beam on the second prism is directed via a secondary optical path (not shown in figure 2) and an adjustable attenuator to the photodetector. In this way it is possible to perform system calibrations without an external target.

Detector subsystem

The transmitted and the received laser pulses have to be converted to suitable electrical signals in order to perform a time interval measurement.

For the detection of the return light pulse a very fast vacuum photodiode (risetime 0.5 ns) is used.

For the detection of the return light pulse a very sensitive detector is needed. In our case we use a 12 - stage photomultiplier with a quantum efficiency of 5 - 6 %.

In addition to the return signal from the satellite the photomultiplier produces noise from the sky background and also internal (thermal) noise. Background noise is eliminated as much as possible by using a field stop in the telescope and a narrow band interference filter (adjustable 3 or 10 \AA bandwidth).

A narrow time window acts as an extra noise filter. In our case during only 10 μs around the predicted arrival time of the return pulse electrical signals are allowed to stop the time-of-flight measurement.

Timing subsystem

The purpose of this subsystem is to

- measure the time-of-flight of the laser pulse
- record the epoch (in UTC time scale) of the start of the time-of-flight measurement
- provide timing signals for the automatic operation of the system

All measurements are based on the output of a Rubidium vapor frequency standard with a stability of a few parts in 10^{12} .

The time-of-flight measurement is performed by a commercially available time interval counter with a resolution of 0.1 nanosecond. The measurement is performed between the leading edges of both the transmitted and the received pulses.

The epoch of laser firing is recorded with a resolution of 1 μs UTC.

The UTC time scale is maintained using daily time comparisons against the Netherlands national time standard UTC-(VSL). These comparisons are based on the so-called "TV sync. pulse technique", which has been described in several publications (1). The accuracy of our measurements is better than 1 microsecond.

Additional frequency monitoring is performed by means of phase comparison against the transmission of MSF (Rugby, England, 60 kHz).

Future improvements

The major improvement that will be implemented in the near future is the digital recording of the shape of both the transmitted and the received pulse. With this data corrections can be calculated for:

- time walk along the leading edges, caused by varying amplitude
- distortion of the shape of the return signal.

This technique will improve the accuracy to an expected 5 - 15 cm level. Further improvement of the accuracy, especially to higher satellites, can be expected from a decreased laser pulsewidth. This modification has been planned for 1979 - 1980.

Other modifications envisaged are:

- computer control of the operation
- improvement of the signal-to-noise ratio
- installation of a better photodetector

These latter actions will give only a slight increase in accuracy but they are intended mainly to improve the system efficiency.

Results

Shortly after each satellite pass the observations are subjected to an adjustment with respect to a best fitting elliptical orbit in order to have a first insight into the number of likely successful returns. After rejecting probable outliers each residual is individually tested statistically with respect to an a priori estimated single shot precision of 1.5 nanosecond (round travel time). Figures 3,4,5 give examples of the residuals of typical passes of the LAGEOS, Starlette and GEOS- 3 satellites under good atmospheric conditions.

On longer term, after having adjusted many passes of different satellites conclusions can be drawn about the quality of the system. At present the following statements can be made:

- under good atmospheric conditions the assumption of a single shot (internal) precision of 1.5 nanosecond is acceptable for all observed satellites.
- there is no evidence of any significant dependence of this precision on the range to the satellite.

As mentioned already before and after each observed satellite pass calibration measurements are carried out routinely over a given ground range (either a 6 m internal short-circuit light path, or an external 953 m), primarily to update the value of the system delay with respect to the reference point at the intersection of the two telescope axes.

The calibration measurements, being repeated at least 10 times in each series, give detailed (atmosphere independent) information on the overall system stability (standard deviation ~ 0.3 ns). Figure 6 shows residuals with respect to the adjusted mean value of a series of calibration measurements.

References

- (1) P.Parcelier, Time Synchronisation by Television, IEEE transactions volume IM - 19 , no. 4, November 1970.

L A G E O S
December 9, 1976

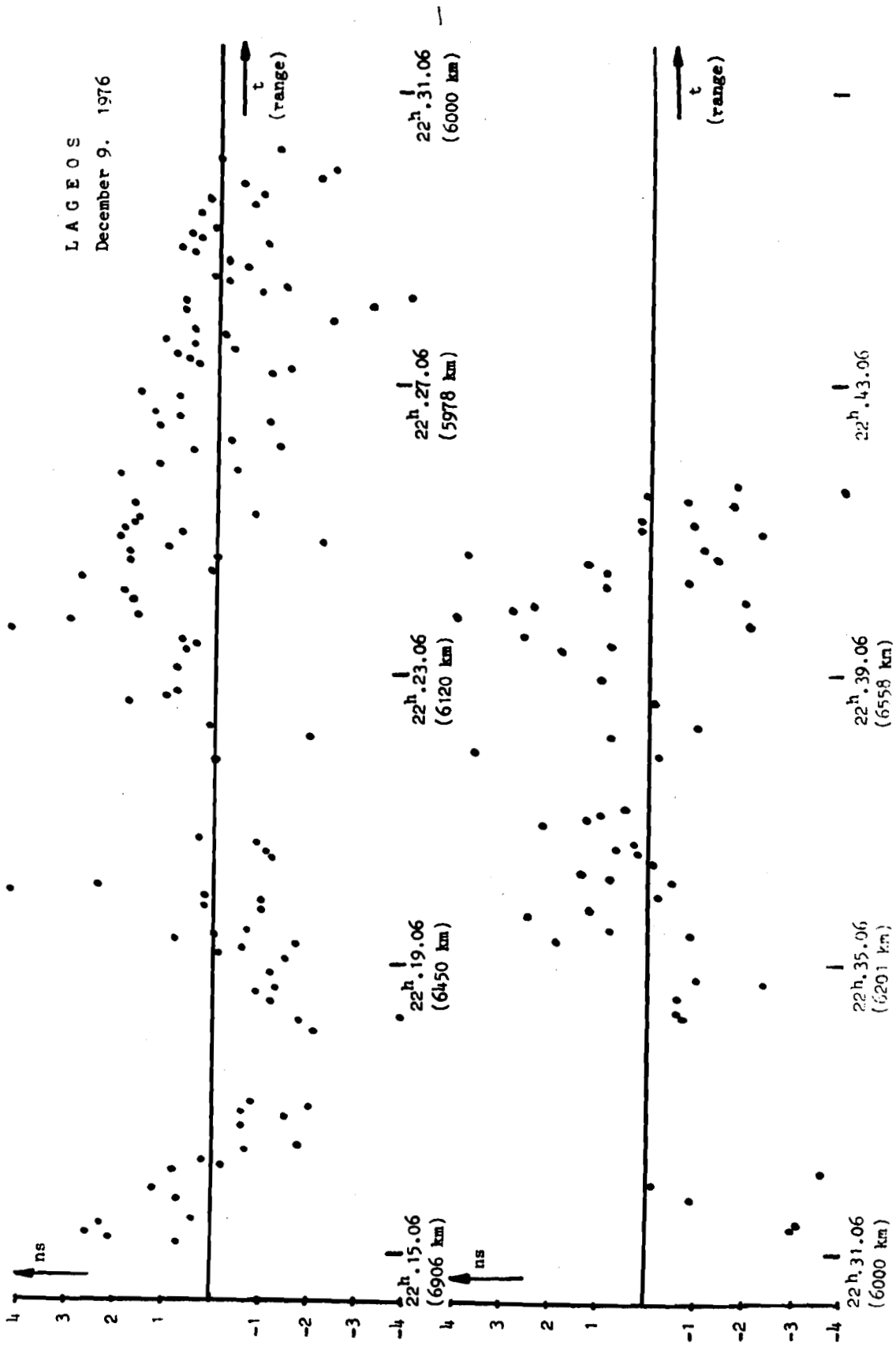


figure 3

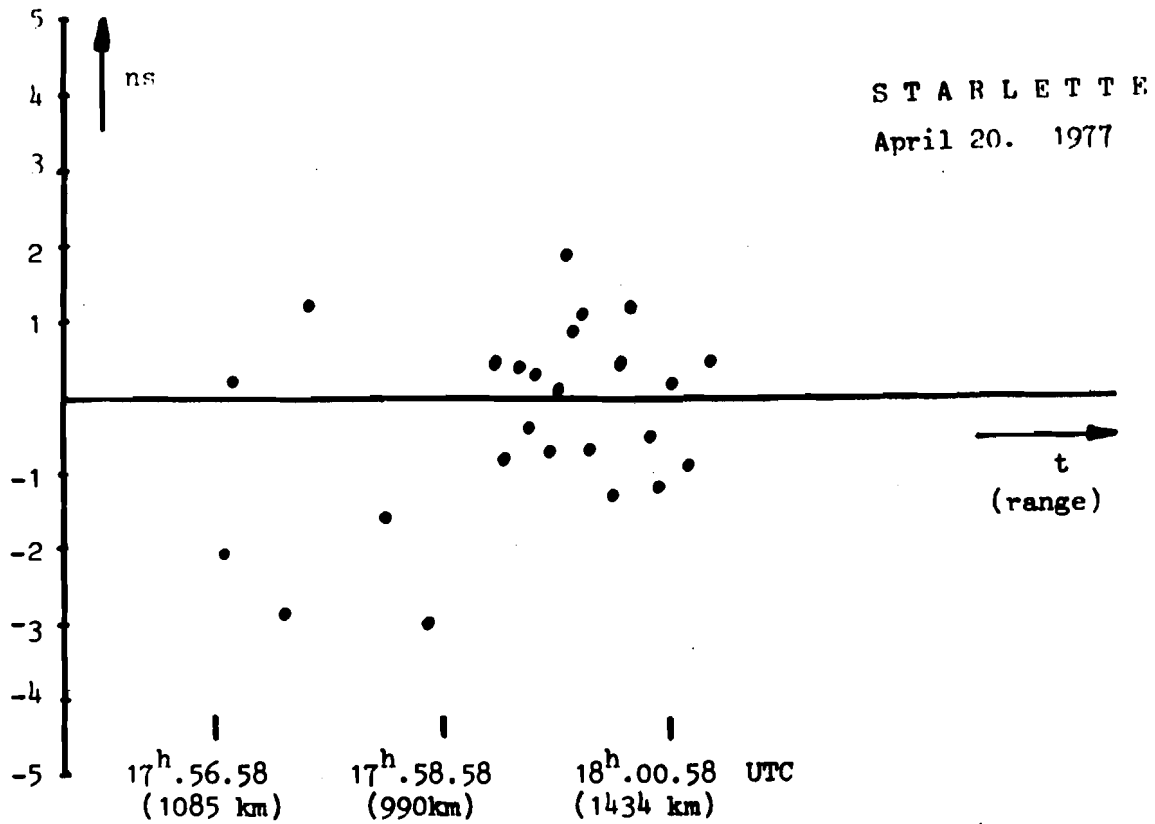


figure 4

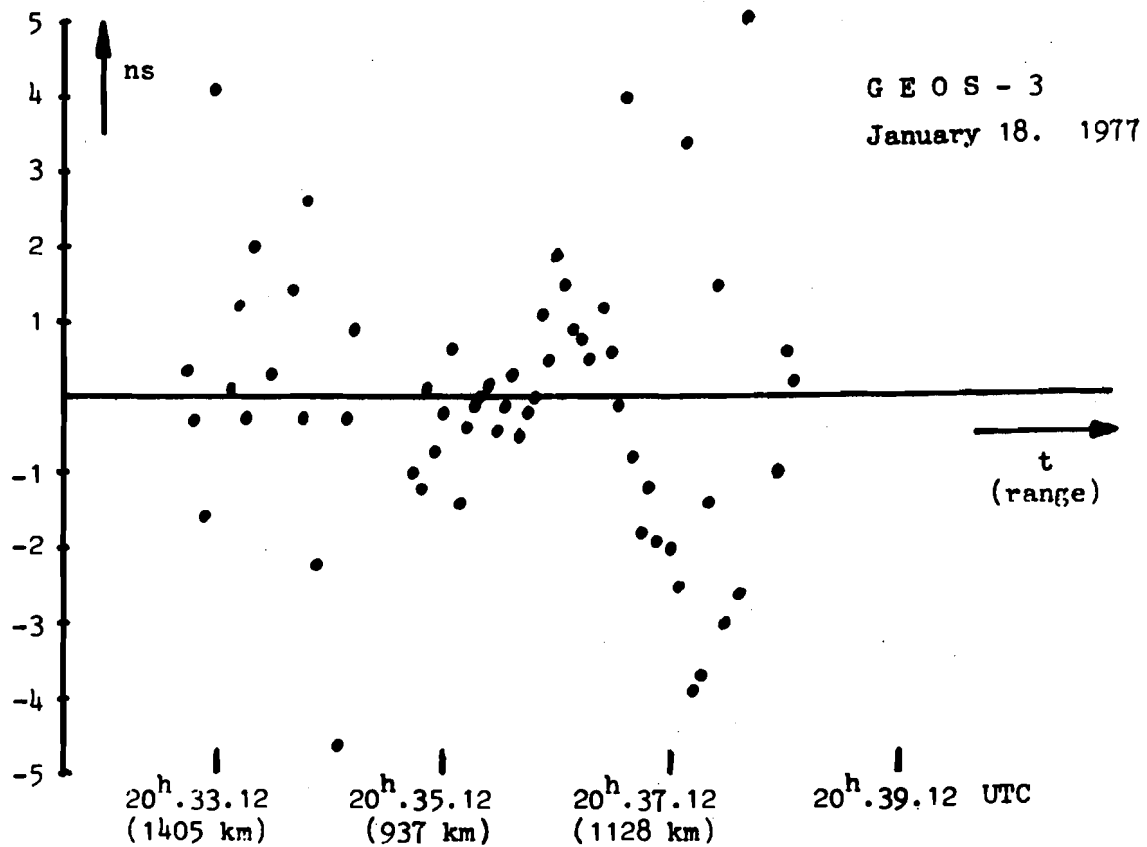


figure 5

Calibration
April 13, 1977

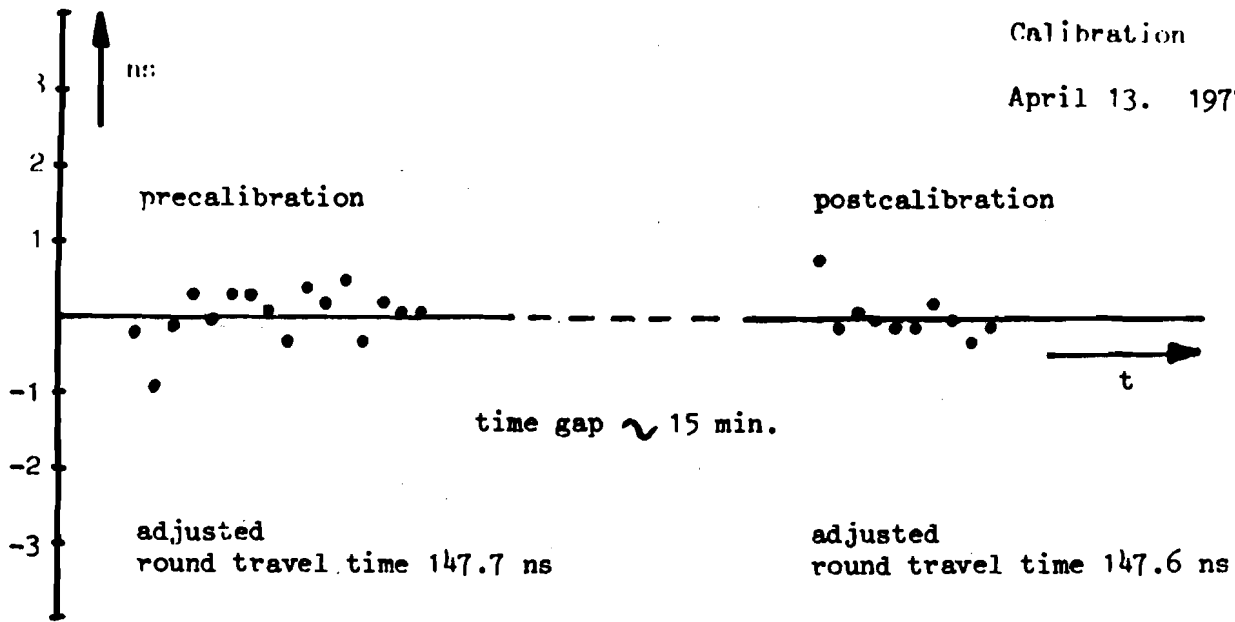


figure 6

Summary statistics

Station 7833

July 1976 - April 1977

	GEOS-1		GEOS-2		GEOS-3		Starlette		LAGEOS		total	
	obs	pas	obs	pas	obs	pas	obs	pas	obs	pas	obs	pas
total obs.	1799	21	534	9	534	30	998	67	1149	21	5014	149
rejected obs.	122		34		77		231		257		721	
accepted obs.	1677	21	500	9	457	30	767	67	892	21	4293	149

table 2

SOME ABSOLUTE TESTS OF THE RESULTS OF IDM-MEASUREMENTS IN THE FIELD WITH A DESCRIPTION OF FORMULAS USED IN THE TESTS

Erik Tengström, Uppsala, Sweden

Introduction.

During a sequence of years, the Institute of Geodesy at the University of Uppsala has been involved in experiments for determining terrestrial refraction. [1] [3]

Using continuous lasers of different wave-lengths (He-Cd UV 3250 Å, Argon blue 4880 Å and He-Ne red 6328 Å), carefully adjusted in height, so that each beam apex is lying in the same horizontal plane, and approximately in a straight line perpendicular to the line of sight, it was possible to determine the relative vertical position between the normals of the laser wavefronts at a distance of 20 km to within 0.1 centesimal seconds of arc. The dispersion between the UV- and the red beam is observed with a Cassegrain camera ($f = 6260$ mm), in front of which is placed a 6 slit grating with $d = 5$ mm spacing. The red apex and the UV apex have a horizontal distance of 1 m from each other, so on the exposed film, the interference patterns are sufficiently well separated to enable accurate comparator measurements to be made of the vertical distance z between the central fringes. z is obtained in microns (mean error per exposure $\pm 1\mu$) and then converted to angular measure δ , according to

$$\delta'' = \frac{\lambda_r}{d} \times \frac{z}{l_r} \times \rho' \quad (1)$$

where λ_r is the red wavelength, l_r the fringe distance of the red pattern, which is also measured.

In evaluating the mean error of δ , we accept realistic values of the mean errors in λ_r, d, z and l_r , and compute m_δ for normal conditions in the atmosphere. We have here assumed:

$$\begin{aligned} m_{\lambda_r} &= \pm 10 \text{ \AA} \\ m_d &= \pm 0.01 \text{ mm} \\ m_z &= m_{l_r} = \pm 1\mu \end{aligned}$$

Now $\lambda_r = 6328 \times 10^{-7}$ mm
 $d = 5$ mm

and we get from (1)

$$\frac{z}{l_r} = \frac{d}{\lambda_r} \times \frac{\delta''}{\rho''}$$

From (2) we know, that, neglecting any influences from humidity, the refraction angle for the D-line (yellow light)

$$\alpha_D = \kappa \delta_r^{UV} \quad (2)$$

the coefficient being computed from Barrell and Sear's formula for n_{0D} , n_{0r} and n_{0UV} as

$$\kappa = \frac{n_{0D} - 1}{n_{0UV} - n_{0r}} = 23.42 \quad (2')$$

Under normal conditions in dry air and at 20 km distance

$$\delta \sim 8''$$

Now, with $f = 6260 \times 10^3 \mu$

$$l_r = \frac{\lambda_r}{d} \times f = 792 \mu, \text{ and with } \frac{z}{l_r} = 0.1,$$

$$z \sim 80 \mu$$

From these numbers we see, that, with accepted mean errors in λ_r, z, l_r and d , their contribution to δ are in order

$$\pm 0''.01, \pm 0''.1, \pm 0''.01, \pm 0''.01 !$$

Even if we should have $m_{\lambda_r} = \pm 100 \text{ \AA}$, $m_d = \pm 0.1$ mm and $m_{l_r} = \pm 10 \mu$, the mean error of δ is only of the order of $\pm 0''.2$

In reality, however, $m_\delta \sim \pm 0''.1$, as stated above.

The accuracy of the refraction angle $\alpha_D = 23.42 \times \delta_{UV}^{(r)}$ depends also on the accuracy of the coefficient 23.42 !

Assuming realistically, that all n_0 :s have a mean error of $\pm 0.05 \times 10^{-6}$ [7], obtained from Barrell and Sears' formula (or Edlén's formula, which gives same values to within 10^{-8}), we get

$$m_\kappa \sim \pm 0.1, \text{ and consequently, at 20 km}$$

$$m_\alpha \sim \pm 2''$$

The n_0 :s have been determined for dry air at 0°C and 760 mm Hg-pressure. It is assumed, that this air contains the following main constituents: N_2 , O_2 , A and CO_2 with percents by volume equal to 78.09, 20.95, 0.93 and 0.03 respectively. [7] This composition seems to be rather constant up to a height of about 90 km except for a slow and small variation of the CO_2 -content, so our κ -value above should be sufficiently accurate to make our values for α and m_α realistic in dry air under all observation conditions in this part of the atmosphere. But further investigations are desired.

In [3] we have investigated the influence of humidity. We obtained

$$\alpha_D = 23.42 \delta + 2.37 Q - H \quad (3)$$

$$\text{where } Q = -3.36 \delta \frac{\bar{\theta}}{p} \left(1 - \frac{0.38}{1 + 0.29 \frac{dt}{dh}} \right) \quad (3a)$$

$\bar{\theta}$, p and $()$ being mean values over the distance $\overline{AP}^x)$

^{x)} A is the observer, P the nearest point on the ray, where the tangent is parallel to the chord AB, B being the lightsource.

$$H^* = -2\rho^* \overline{AP} \left(e \frac{dt}{dh} + t \frac{de}{dh} \right) \times 10^{-10}, \quad (3b)$$

the mean over \overline{AP} of the bracket-values being taken.

In the formulas above e , p are expressed in torr,
 $\frac{dt}{dh}$ in $^{\circ}/100 \text{ m}$, and $\frac{de}{dh}$ in mm/km

H^* could hardly reach values $> 0^*.01/\text{km}$ (see (3)) and might be neglected!

Q is normally small but might reach appreciable values during great negative humidity gradients, see (2) and Appendix I. However, it seems formally possible to evaluate Q by using a third laser.

We have chosen an Argon laser (see above) with $\lambda_b = 4880 \text{ \AA}$.

Observing δ_r^b we have an expression

$$a_D = \kappa \delta_r^b + k Q$$

where $\kappa = \frac{n_{0D} - 1}{n_{0b} - n_{0r}}$, and $k = \kappa \times 0.0083 \left(\frac{1}{\lambda_{0b}^2} - \frac{1}{\lambda_{0r}^2} \right) + 1.04 - \frac{0.0083}{\lambda_{0D}^2}$

We know $n_{0D} - 1 = 292.40 \times 10^{-6}$
 $n_{0r} = 1 + 291.76 \times 10^{-6}$

From Barrell and Sears' formula we obtain (wave index)

$$n_{0b} = 1 + 2876.04 \times 10^{-7} + \frac{16.288 \times 10^{-7}}{(4880 \times 10^{-8})^2} + \frac{0.136 \times 10^{-7}}{(4880 \times 10^{-8})^4}$$

which gives

$$n_{0b} = 1 + 294.68 \times 10^{-6},$$

and $\kappa = 100.14$

For k , we get the value 2.43.

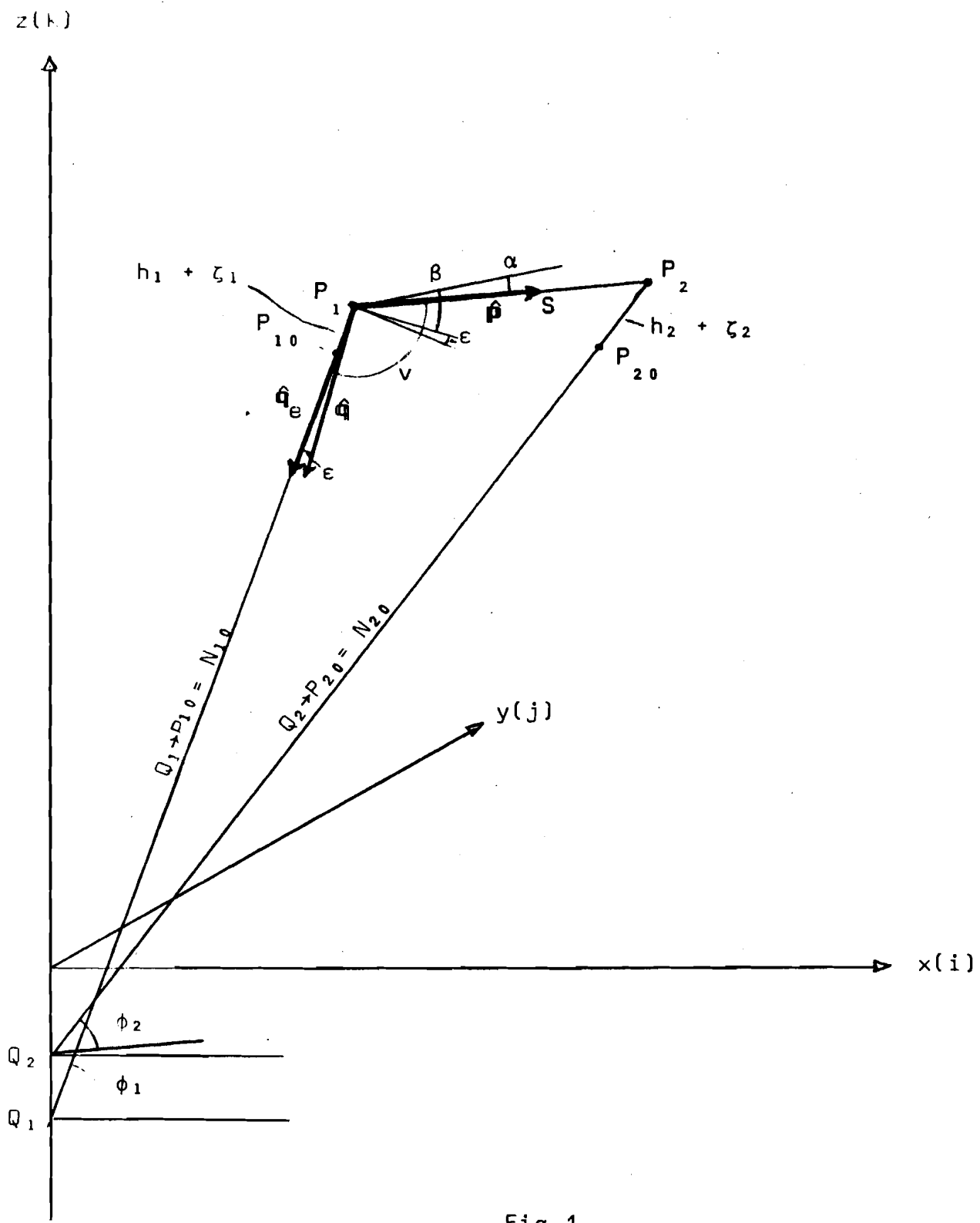


Fig 1

We should then have a nonzero value of

$$Q = (3.9 \delta_r^{UV} - 16.7 \delta_r^b) \times 10^2 \quad (4)$$

With obtainable accuracies in measuring δ , it is clear, that (4) is impossible to use in practise.

Possibilities of absolute tests of the IDM determinations of terrestrial refraction.

The results obtained, in using the observational means, and the theory described in the introduction, should be of minor value, if no method existed of absolutely checking them against values, computed from data, independent of the atmospherical conditions during the observation plus simultaneous observations of other kind, depending on these conditions. In fact, if we know the geoidal height difference between the IDM observer and the laser source, and the components of the deflection of the vertical at the site of the observer, we may calculate α_D , having vertical angle measurements made at the same time as the IDM exposures are performed. A formula for such an α_D -computation is given below. We have here accepted the ED-system for defining ζ, ξ, η .

In fig. 1 the unit vectors \hat{p} and \hat{q} are the true directions from observer P_1 toward the lightsource P_2 and the true nadir respectively. So \hat{p}, \hat{q} define a true vertical section in P_1 , which contains P_2 . The angle ν between \hat{p} and \hat{q} is given by

$$\hat{p} \times \hat{q} = \cos \nu$$

Let the ellipsoidal angular ED-coordinates for the P:s be given, that is ϕ_{ED}, λ_{ED} together with the orthometric height h , and the geoidal height ζ in the same system.

The ellipsoidal meridian through P , contains \hat{q}_e (the direction of ellipsoidal nadir of P_1), and the z-axis (k) of the ellipsoid. The x-axis (i) through the center of the ED-ellipsoid is perpendicular to k in this meridian plane. The ellipsoidal normal of P_2 intersects the z-axis at a point, and defines ellipsoidal $\phi_2, \lambda_2 - \lambda_1 = \lambda$, so λ_{ED} for P_1 equals 0 (λ_1) and λ_{ED} for P_2 equals λ (λ_2).

The y-coordinate for P_1 in this ellipsoidal system (with origin at O , see the figure) is therefore $= 0$, and we have

$$\begin{aligned} x_{P_1} &= (N_{P_{10}} + h_1 + \zeta_1) \cos \phi_1 \\ y_{P_1} &= 0 \\ z_{P_1} &= (N_{P_{10}} (1-e^2) + h_1 + \zeta_1) \sin \phi_1 \end{aligned} \quad (5)$$

where $N_{P_{10}}$ is the ellipsoidal normal radius of curvature of the orthogonal projection of P_1 on the ellipsoid (P_{10}), that is

$$N_{P_{10}} = \frac{a}{(1-e^2 \sin^2 \phi_1)^{1/2}}$$

For P_2 , $N_{P_{20}}$ is also given together with h_2 and ζ_2 .

For this point (P_2) we have

$$\begin{aligned} x_{P_2} &= (N_{P_{20}} + h_2 + \zeta_2) \cos \phi_2 \cos \lambda \\ y_{P_2} &= (N_{P_{20}} + h_2 + \zeta_2) \cos \phi_2 \sin \lambda \\ z_{P_2} &= (N_{P_{20}} (1-e^2) + h_2 + \zeta_2) \sin \phi_2 \end{aligned} \quad (5')$$

See fig. 2 : P'_1 and P'_2 are their orthogonal projections of P_1 and P_2 in the ellipsoidal equator.

In the i, j, k system we now have

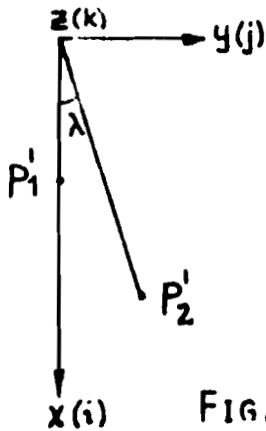


FIG. 2

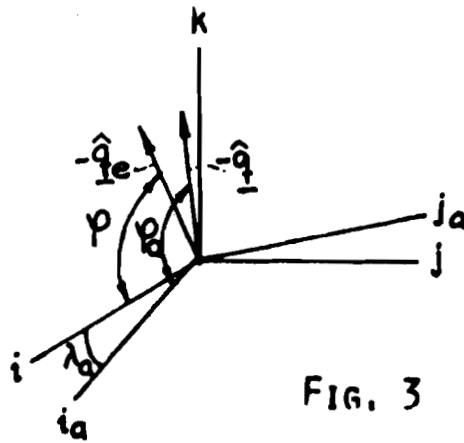


FIG. 3

$$\hat{p} = \frac{x_{p_2} - x_{p_1}}{s} \times i + \frac{y_{p_2}}{s} \times j + \frac{z_{p_2} - z_{p_1}}{s} \times k$$

(6)

with $s^2 = (x_{p_2} - x_{p_1})^2 + y_{p_2}^2 + (z_{p_2} - z_{p_1})^2$

The vector \hat{q}_e is acc. to fig. 1

$$\hat{q}_e = -\cos \phi_1 \times i - \sin \phi_1 \times k$$

What is then \hat{q} ?

Its direction-cosines are obviously in the i, j, k system :

$$-\cos \phi_a \cos \lambda_a, \quad -\cos \phi_a \sin \lambda_a, \quad -\sin \phi_a$$

where a denotes astronomical values (λ_a being defined as the angle between the ellipsoidal and astronomical meridians of P_1) counted positive eastwards.

From fig. 3 we get the components of \hat{q} in the form

$$-\cos \phi_1 + \xi \sin \phi, \quad -\eta, \quad -\sin \phi_1 - \zeta \cos \phi_1$$

$$\hat{q} = -\cos \phi_1 \times i - \sin \phi_1 \times k + \xi \sin \phi_1 i - \eta \times j - \zeta \cos \phi_1 \times k$$

(7)

and therefore

$$\begin{aligned}
\cos v = \hat{p} \times \hat{q} = \frac{1}{s} & \left[[(N_{p_{20}} + h_2 + \zeta_2) \cos \phi_2 \cos \lambda - \right. \\
& - (N_{p_{10}} + h_1 + \zeta_1) \cos \phi_1] \times (-\cos \phi_1 + \xi \sin \phi_1) + \\
& + [(N_{p_{20}} + h_2 + \zeta_2) \cos \phi_2 \sin \lambda] \times (-\eta) + \\
& + [(N_{p_{20}} (1-e^2) + h_2 + \zeta_2) \sin \phi_2 - (N_{p_{10}} (1-e^2) + \\
& + h_1 + \zeta_1) \sin \phi_1] \times -(\sin \phi_1 + \xi \cos \phi_1) \left. \right] \\
\end{aligned} \tag{8}$$

with $v = 90^\circ + \beta - \alpha$; $\cos v = -\sin(\beta - \alpha)$

$$\begin{aligned}
\sin(\alpha - \beta) = \frac{1}{s} & \left[(N_{p_{10}} + h_1 + \zeta_1) \cos^2 \phi_1 - \right. \\
& - (N_{p_{20}} + h_2 + \zeta_2) \cos \phi_1 \cos \phi_2 \cos \lambda + \\
& + (N_{p_{10}} + h_1 + \zeta_1) \sin^2 \phi_1 - (N_{p_{20}} + h_2 + \zeta_2) \times \\
& \times \sin \phi_1 \sin \phi_2 - N_{p_{10}} e^2 \sin^2 \phi_1 + N_{p_{20}} e^2 \sin \phi_1 \sin \phi_2 \left. \right] + \\
& + \frac{x_{p_2} - x_{p_1}}{s} \sin \phi_1 \times \xi - \frac{y_{p_2}}{s} \eta - \frac{z_{p_2} - z_{p_1}}{s} \times \\
& \times \cos \phi_1 \times \xi \\
\end{aligned} \tag{8'}$$

This can be written:

$$\begin{aligned}
\sin(\alpha - \beta) = \frac{1}{s} & \left[(N_{p_{10}} + h_1 + \zeta_1) - (N_{p_{20}} + h_2 + \zeta_2) \times \right. \\
& \times \cos(\phi_1 - \phi_2) + 2(N_{p_{20}} + h_2 + \zeta_2) \cos \phi_1 \cos \phi_2 \times \\
& \times \sin^2 \frac{\lambda}{2} - e^2 \sin \phi_1 [N_{p_{10}} \sin \phi_1 - N_{p_{20}} \sin \phi_2] \left. \right] + \\
& + \frac{x_{p_2} - x_{p_1}}{s} \sin \phi_1 \times \xi - \frac{y_{p_2}}{s} \eta - \frac{z_{p_2} - z_{p_1}}{s} \cos \phi_1 \times \xi \\
\end{aligned} \tag{8''}$$

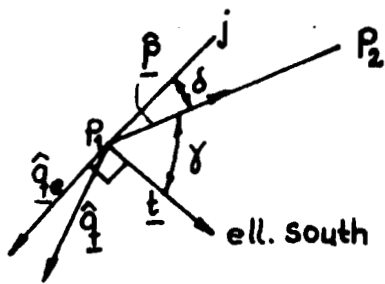


FIG. 4

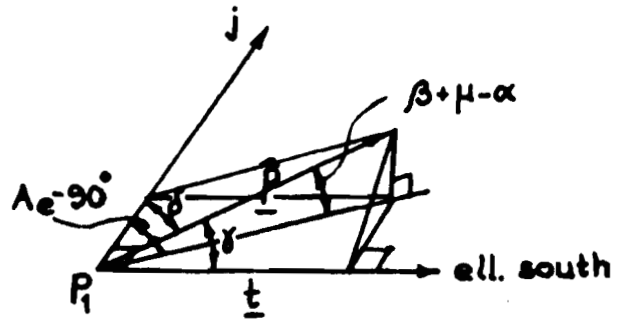


Fig. 5

We obtain from the figures 4 and 5

$$\underline{t} = \sin \phi_1 \times i - \cos \phi_1 \times k$$

$$\hat{p} \underline{t} = \cos \gamma = \frac{x_{P_2} - x_{P_1}}{s} \sin \phi_1 - \frac{z_{P_2} - z_{P_1}}{s} \cos \phi_1$$

$$\hat{p} j = \cos \delta = \frac{y_{P_2}}{s}$$

$$\cos \gamma = \cos(\beta + \mu - \alpha) \times -\cos A_e$$

$$\cos \delta = \cos(\beta + \mu - \alpha) \sin A_e$$

$\beta + \mu - \alpha$, where μ depends on ζ, η , is the true ellipsoidal elevation angle of P_2 in P_1 .

() can now be written:

$$\begin{aligned} \sin(\alpha - \beta) = & + \frac{1}{s} \left[(N_{P_{10}} - N_{P_{20}}) - (h_2 - h_1) - (\zeta_2 - \zeta_1) + \right. \\ & + 2(N_{P_{20}} + h_2 + \zeta_2) \sin^2 \frac{\phi_1 - \phi_2}{2} + \\ & + 2(N_{P_{20}} + h_2 + \zeta_2) \cos \phi_1 \cos \phi_2 \sin^2 \frac{\lambda}{2} - \\ & \left. - e^2 \sin \phi_1 [N_{P_{10}} \sin \phi_1 - N_{P_{20}} \sin \phi_2] \right] - \\ & - \cos(\beta + \mu - \alpha) \cos A_e \times \xi - \cos(\beta + \mu - \alpha) \times \\ & \times \sin A_e \times \eta \end{aligned}$$

Ordering the terms, we have:

$$\begin{aligned} & \frac{1}{S} \left[2(N_{P_{20}} + h_2 + \zeta_2) \left(\sin^2 \frac{\phi_1 - \phi_2}{2} + \cos\phi_1 \cos\phi_2 \sin^2 \frac{\lambda}{2} \right) - \right. \\ & - e^2 \sin\phi_1 [N_{P_{10}} \sin\phi_1 - N_{P_{20}} \sin\phi_2] + (N_{P_{10}} - N_{P_{20}}) - \\ & \left. - (h_2 - h_1) - (\zeta_2 - \zeta_1) \right] - \cos(\beta + \mu - \alpha) [\xi \cos A_e + \\ & + \mu \sin A_e] \end{aligned}$$

Observe: $\xi = (\phi_a - \phi_e)_{P_1}$; $\eta = ((\lambda_a - \lambda_e) \cos\phi_e)_{P_1}$

A_e is counted from ellipsoidal north clockwise.

Further $\cos(\beta + (\alpha - \mu)) = \cos\beta \times \cos(\alpha - \mu) + \sin\beta \times \sin(\alpha - \mu)$

Put e.g. $\alpha = 500''$ (great refraction: 50 km gives normally $350''$)

Then $\cos(\alpha - \mu) \sim 1 - \left(\frac{500}{636620}\right)^2 \times \frac{1}{2}$

$$\sin(\alpha - \mu) \sim \alpha - \mu - \frac{1}{3!} \left(\frac{500}{636620}\right)^3$$

That is $\cos(\beta + \mu - \alpha) = \cos\beta + \alpha \sin\beta$

$$\begin{aligned} \sin(\alpha - \beta) &= \sin\alpha \cos\beta - \cos\alpha \sin\beta = \frac{1}{S} \left[2(N_{P_{20}} + h_1 + \zeta_1 + \right. \\ & + (h_2 - h_1) + (\zeta_2 - \zeta_1)) \times \left[\sin^2 \frac{\phi_1 - \phi_2}{2} + \right. \\ & \left. \left. + \cos\phi_1 \cos\phi_2 \sin^2 \frac{\lambda}{2} \right] - e^2 \sin\phi_1 [N_{P_{10}} \sin\phi_1 - N_{P_{20}} \sin\phi_2] \right] - \\ & - \frac{1}{S} \left[(h_2 - h_1) + (\zeta_2 - \zeta_1) - (N_{P_{10}} - N_{P_{20}}) \right] - \\ & - (\cos\beta + \alpha \sin\beta) [\xi \cos A_e + \eta \sin A_e] \end{aligned} \tag{9a}$$

Here $s^2 = (x_{p_2} - x_{p_1})^2 + (y_{p_2} - y_{p_1})^2 + (z_{p_2} - z_{p_1})^2$

It is easily shown, that

$$\cos\alpha \sin\beta = \sin\beta$$

in all practical cases:

We have also

$$\cos\alpha \operatorname{tg}\beta = \operatorname{tg}\beta$$

and $\sin\alpha \times \rho'' = \alpha''$

$$\alpha'' = \rho'' \operatorname{tg}\beta + \frac{\rho'' \sec \beta}{s} \times T - \frac{\rho'' \sec \beta}{s} \left[(h_2 - h_1) + \right. \\ \left. + (\zeta_2 - \zeta_1) - (N_{p_{10}} - N_{p_{20}}) \right] - \left[\xi'' \cos A_e + \eta'' \sin A_e \right]$$

where $T = 2 \left[N_{p_{20}} + h_1 + \zeta_1 + (h_2 - h_1) + (\zeta_2 - \zeta_1) \right] \times$

$$\times \left[\sin^2 \frac{\phi_1 - \phi_2}{2} + \cos\phi_1 \cos\phi_2 \sin^2 \frac{\lambda}{2} \right] -$$

$$- e^2 \sin\phi_1 \left[N_{p_{10}} \sin\phi_1 - N_{p_{20}} \sin\phi_2 \right]$$

We have finally, if $\phi_1 > \phi_2$

$$\alpha = \rho \operatorname{tg}\beta + \frac{\rho \sec \beta}{s} \times \underline{T} - \frac{\rho \sec \beta}{s} \left[(h_2 - h_1) + \right. \\ \left. + (\zeta_2 - \zeta_1) - (N_{p_{10}} - N_{p_{20}}) \right] - \left[\xi \cos A_e + \eta \sin A_e \right]$$

where $\underline{T} = 2 \left[N_{p_{20}} + h_1 + \zeta_1 + (h_2 - h_1) + (\zeta_2 - \zeta_1) \right] \times$

$$\times \left[\sin^2 \frac{\phi_1 - \phi_2}{2} + \cos\phi_1 \cos\phi_2 \sin^2 \frac{\lambda}{2} \right] - \quad (9)$$

$$- e^2 \sin\phi_1 \left[N_{p_{10}} \sin\phi_1 - N_{p_{20}} \sin\phi_2 \right]$$

Here is $e^2 = \alpha(2-\alpha)$, with the flattening α , accepted in ED = 1/297

Observe: A_e is counted clockwise from ellipsoidal North in the ellipsoidal tangent plane, regarded as parallel to the ellipsoidal tangent plane at the Helmert projection P_{10} .

The formula (9) is meant to definitively, clearly and accurately realize the previous attempts to clarify the relation between refraction, observed vertical angle and geoidal data, done by Helmert [4], and by Baeschlin [5]. But I am grateful for all interest from my colleagues to criticize it.

In Appendix I a more convenient formula is given !

Field measurements with IDM since 1970. Various types of tests.

The photographic measuring campaigns have been the following (see [3]):

1970 (July, August, September)

with Mercury lamps and filters (6300 Å and 4400 Å) as light-sources, apochromatic optics with double slit ($f=1$ m) and careful adjustment of parallax. Base at Uppsala, 20 km. Mean error per pair (2 min. observation) of interchanged filters $\sim \pm 9''$. No vertical angle measurements, but reasonable magnitudes. Table 1 .

1971 (late September, one night)

with same light-sources and receiving optics. Filter calibration with He-Ne observations. Base at Niinisalo 17.5 km. Mean error per pair (see above) $\sim \pm 6''$. No vertical angle measurements but meteorological data. These were however, too inaccurate and not sufficiently representative for the whole base, so no reliable absolute tests could be made. Mean value of 4 observations (pairs) was $172'' \pm 3''$. Mean value of refraction, computed from the meteorological data was $189 \pm 25''$. See also fig. 6 .

Refraction, determined at Uppsala,
in the summer 1970, along the base
Örsundsbro - Alsike tower (20 km).

Date (night-observations)	Dispersion in μ on film	Refraction mean	No. of meas. pairs
June 2	33,1 \pm 1,0	54",6 \pm 1",5	2
July 9	24,2 \pm 1,3	39",9 \pm 2",0	4
July 23	30,6 \pm 1,3	50",5 \pm 2",0	2
Aug. 21	26,1 \pm 1,0	43",0 \pm 1",5	2
Sept. 2	29,0 \pm 0,9	47",8 \pm 1",3	1

The mean for all nights is 47",2. Using $k = 0,14$ as normal refraction coefficient, we obtain 45",4. Using $\frac{\partial t}{\partial h} = -1^{\circ},1/100$ m, Leijonhufvud in "On astronomic, photogrammetric and trigonometric refraction", RAK Medd. No. 13, 1950, obtains with his formulas 46",0.

During the night of 9 July, the 4 pairs of exposures were taken with about half an hour's time difference. A linear change in the 4 means, obtained from the measurements with an areal densitometer (film scanner) is clearly indicated (-5 /hour).

TAB. I

Time	Obs. elev. angle centesimal seconds	IDM refr. corr.	True elev. angle No humidity correction
21.30	- 16' 90" (int)	- 420" \pm 2"	- 21' 10"
21.45	- 17' 16"	- 392" \pm 2"	- 21' 08"
22.00	- 16' 70"	- 441" \pm 3"	- 21' 11"
22.15	- 17' 11"	- 401" \pm 4"	- 21' 12"

The precision, given for IDM-results is derived from the readings of the films by two persons (Stig Mårtensson and Sune Eklund).

TAB. II

Early August night 1974.

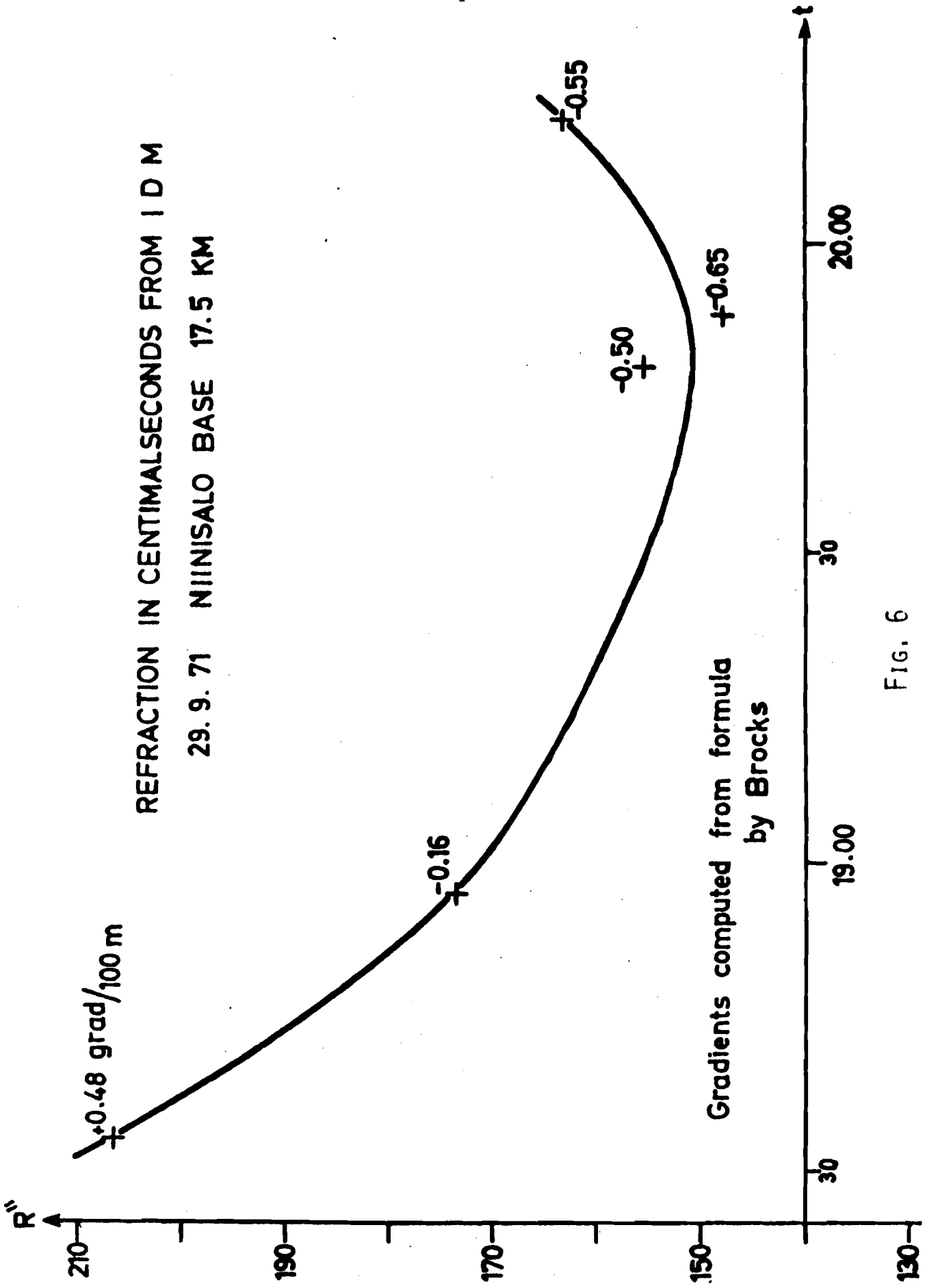


FIG. 6

1974 (early August, one night)

with laser-sources (He-Cd UV 3250 Å plus He-Ne 6328 Å) and reflecting optics (Cassegrain system $f=6.62$ m and 6-slit grating). New base at Uppsala 19.8 km. Simultaneous vertical angle measurements. Mean internal error in IDM refraction $\pm 3''$. Estimated mean error in the best observed vertical angles is $\pm 2''$.

Table 2 gives the IDM-refractions for the 4 most reliable angular measurements. As can be seen, the differences between the observed vertical angles and the corresponding differences of IDM-refractions is very good (to within $\sim 2''$).

The question, if each calculated elevation angle, equals the true one, however, still remains unanswered. To investigate this we used (9) with carefully determined geoidal and ellipsoidal data and obtained an almost constant difference (for this night) of $+ 24''$ between the values, computed from IDM and those calculated by means of (9).

A reason for this could be the one indicated in Appendix II.

1975-76

Due to problems with our UV-laser, we had to use only He-Ne and Argon in this period. Along the base of 1974, which is now our standard base, observations were made with same instruments as mentioned above, and under various but all the time very extreme atmospherical conditions. The k -value for these wavelengths is, of course, much greater, and will therefore decrease the accuracy in the value of "dry" refraction. Furthermore humidity is not taken into account, which is an additional source of error. The exposure-time is very short in all our experiments (0.2 seconds), so short-period variations in refraction will be clearly reflected in the results. We have detected great significant amplitudes (up to one minute of arc) in these variations. The vertical angle measurements have not yet been organized to follow the exposures closely enough in time, but it seems, that the smoothed IDM curve (20 seconds intervals) coincides with the vertical angle curve to within $10''$ as an average.

1977-78

It is very important, that the Uppsala group now considers aforementioned problems in its organizing continuous field measurements along the base, mentioned (which moreover runs about 30 m above the ground). It is also important, that it continuously draws conclusions from the experiences of other groups (Glissmann, Prilepin, Williams etc.) to be able to prove definitively, that the multiwave-method can achieve instantaneous values of refraction with the IDM-grating, which are good to 2[^], as indicated by my relative tests.

The problem of turbulence, causing systematical effects because of the spacing used (~ 1 m) at the laser station, I personally regard as of minor importance, but it must also be investigated in the future inside SSG 1.42.

During this symposium, the micrometeorological problems as regards wave propagation, will be dealt with, and I hope, that a special session could be devoted to this important area, the main theory of which is well established by Tatarski [6]. From the discussion during such a session, we would eventually catch points of view, which could be of importance for realistically introducing turbulence theory into the simple geometrical theory, underlying our IDM-experiments in Uppsala.

At the end of this paper, I like to mention, that the Michelson-magnification of determining δ , which I suggested at a very early stage of our experiments [1], is still of importance. The increase in the accuracy of determining δ (factor 10 or more), which demands by experience very stable atmospherical conditions, would facilitate a determination of δ to within 0.01[^] of arc, that is ten times the accuracy, talked about above!

In this connection, it should not be forgotten, however, that the accuracy of the κ -values must also be improved, either by new laboratory experiments of n_0 or still better by using more laser wavelengths during the observations. For the absolute tests in this case, the ellipsoidal and geoidal information as well as the necessary accuracy and continuity of verticle angle measurements have to be considered.

References:

- [1] E. Tengström: "Elimination of Refraction of Vertical Angle Measurements, Using Lasers of Different Wavelengths", ÖZfV, Sonderheft 25, Wien 1967.
- [2] J.C. de Munck: "The Theory of Dispersion, applied to Electro-optical Distance Measurement and Angle Measurement. Neth. Geod. Comm., Vol 3, No 4, 1970
- [3] E. Tengström: a) "Report on the results of IDM-experiments at Uppsala 1970, at the Finnish base of Niinisalo 1971, and of further experiments with He-Ne and He-Cd lasers",
b) "Appendix to Dr Tengström's letter to Dr Brein, January 10, 1969, concerning the influence of humidity on refraction determinations with the dual wavelength-method",
both appearing in the Proceedings of the International Symposium on Terrestrial Electromagnetic Distance Measurements and Atmospheric Effects on Angular Measurements", vol. 5, Stockholm 1977.
- [4] F.R. Helmert: "Theorien der höheren Geodäsie", Teil 1, Kap. 12, § 4, Leipzig 1880.
- [5] C.F. Baeschlin: "Lehrbuch der Geodäsie", § 54, Zürich 1948.
- [6] V.I. Tatarski: "Wave Propagation in a Turbulent Medium", (from Russian to English by R.A. Silverman), Dover publ. 1967.
- [7] US Air Force: "Handbook of Geophysics", New York, Mac Millan 1960.

APPENDIX I

The formulas, derived here for refr. α , are now definitively checked to be correct. However, the following presentation of the calculation of refr. α is, to my understanding more convenient and understandable, when compared to the spherical case:

By putting $\alpha_{\text{refr}} = 0$, we get from (9a) after new ordering of the terms, the refractionfree elevation angle β_0 , according to

$$\begin{aligned}
 \sin \beta_0 = & \frac{1}{S} \left\{ ((h_2 - h_1) + (\zeta_2 - \zeta_1) + (N_2 - N_1)) \right. \\
 & \left. \left\{ \cos(\phi_2 - \phi_1) - 2 \cos \phi_1 \cos \phi_2 \sin^2 \frac{\lambda}{2} \right. \right. \\
 (9') \quad & \left. \left. - 2(N_1 + h_1 + \zeta_1) \left(\sin^2 \frac{\phi_2 - \phi_1}{2} + \cos \phi_1 \cos \phi_2 \sin^2 \frac{\lambda}{2} \right) \right. \right. \\
 & \left. \left. - e^2 \sin^2 \phi_1 (N_2 \sin \phi_2 - N_1 \sin \phi_1) \right. \right. \\
 & \left. \left. + (\xi_1 \cos A_e + \eta_1 \sin A_e) (\cos \beta + \alpha_{\text{refr}} \sin \beta) \right\}
 \end{aligned}$$

Here P_1 is, as before, the point of observation, P_2 the position of the lightsource, S the refractionfree distance $P_1 P_2$, ϕ ellipsoidal latitudes, λ ellipsoidal longitudinal difference $P_1 \rightarrow P_2$, positive eastward, N radius of normal curvature of the international ellipsoid, a its equatorradius, $e^2 = a(2-a)$, where α is the flattening $1/297$, h_1 and h_2 "true" orthometric heights, ζ_1 and ζ_2 geoidal heights above the ellipsoid, ξ , η , the deflection components $\phi_a - \phi$ and $\lambda_a \cos \phi$ at P , with respect to the ellipsoid.

(9') is in principle to be iterated, but the unknown α_{refr} is usually so small, that the last term can be written as merely $\xi_1 \cos A_e + \eta_1 \sin A_e$

In (9'), the quantity

$$Q' = (N_2 - N_1)(\cos(\phi_2 - \phi_1) - 2\cos\phi_1\cos\phi_2\sin\frac{2\lambda}{2}) \\ - e^2\sin^2\phi_1(N_2\sin\phi_2 - N_1\sin\phi_1)$$

can be proved to be small (for 20 km meridional distance only about 10cm). Approximately it has the magnitude $\frac{ae^2}{2} \cos^2\phi$.

The term

$$T' = -2(N_1 + h_1 + \zeta_1)(\sin^2\frac{\phi_2 - \phi_1}{2} + \cos\phi_1\cos\phi_2\sin\frac{2\lambda}{2})$$

is the main curvature influence, Q' a correction for excentricity.

We could write (9') as

$$(9'') \quad \sin\beta_0 = \frac{1}{S} \left[\Delta(\cos(\phi_2 - \phi_1) - 2\cos\phi_1\cos\phi_2\sin\frac{2\lambda}{2}) + T' + \right. \\ \left. + Q' + \xi_1\cos A_e + \eta_1\sin A_e \right] \quad \text{with } \Delta = h_2 - h_1 + \zeta_2 - \zeta_1$$

This formula will be used for our base, when calculating α_{refr} . (9'') gives β_0 . Then :

$$\alpha_{\text{refr}} = \beta_{\text{obs}} - \beta_0.$$

We may now investigate the requirements as to the accuracy in the various pieces of information, needed.

For our base ($\phi \sim 60^\circ$, λ very small) we get, if β_0 shall be correct to within ± 0.5 :

$$\left. \begin{aligned} m_S &= \pm 5 \text{ m} \\ m &= \pm .2 \text{ cm} \\ m_{N_1 + h_1 + \zeta_1} &= \pm 2 \text{ km} \\ m_{\phi_2 - \phi_1} &= \pm 0.3 \end{aligned} \right\} \text{ to achieve } m_{T'} = \pm 1 \text{ cm}$$

$$m_{\xi_1} = \pm 0.5$$

$$m_{\phi_1} \text{ in } Q' = \pm 1$$

APPENDIX II

The expression (3) was derived in [3b], using Edlén's formula for $n - 1$ of humid air, as given by de Munck [2], and Barrel and Sears' formula for $n_0 - 1$ of dry air, which coincides accurately enough with Edlén's dry part. The total pressure coefficient $\kappa = 23.42$ corresponds to the wavelengths, used ($\lambda_{UV} = 3250 \text{ \AA}$, $\lambda_r = 6328 \text{ \AA}$). α_0 is the refraction angle at A for the Na-line 5900 \AA , which is usually valid for visual vertical angle measurements. The factor $k = 2.37$ is computed from the formula of Edlén as

$$k = 1.04 - \frac{0.0083}{\lambda_{D0}^2} + \kappa 0.0083 \left(\frac{1}{\lambda_{UV}^2} - \frac{1}{\lambda_r^2} \right)$$

The term H ought to be negligible!

The expression (3a) is derived in [3b] under the assumption, that Laplace's formula for the pressure in the atmosphere is correct, not only for p_{dry} , but also for the partial e-pressure.

All integrals in our theory have to be taken between A and P, P being the nearest point on the light-ray, where the tangent is parallel to the chord AB. As a first approximation, P is assumed to be situated halfway between A and B. This could be valid, of course, especially for horizontal sights.

In the original theory [1], I used the formula, accepted at that time, namely:

$$\begin{aligned} n - 1 &= (n_0 - 1) \cdot \frac{273}{760} \cdot \frac{p}{T} - 5.5 \cdot 10^{-8} \cdot \frac{273}{T} e = \\ &= (n_0 - 1) \cdot \frac{273}{760} \cdot \frac{p}{T} - 15.02 \cdot 10^{-6} \cdot \frac{e}{T} = (n_0 - 1)M_1 + M_2 \end{aligned}$$

where n_0 refers to zero-conditions of conventional dry air, M_1 and M_2 being independent of n_0 (λ_0).

I obtained

$$\alpha_D = (n_{o_D} - 1) \cdot \int_A^P \frac{\partial M_1}{\partial v} ds + \int_A^P \frac{\partial M_2}{\partial v} ds = (n_{o_D} - 1) R_A^P + Q_A^P,$$

v being the pos. normal of the ray! As Q_A^P is independent of λ , the dispersion, measured, should be

$$\delta = \Delta n R_A^P,$$

and

$$\alpha_D = \frac{n_{o_D} - 1}{\Delta n} \delta + Q_A^P = \kappa \delta + Q_A^P$$

$$Q_A^P = -15.02 \cdot 10^{-6} \cdot \int_A^P \frac{\partial}{\partial v} \left(\frac{e}{T} \right) ds = - \frac{15.02 \cdot 10^{-6}}{T_m} \left\{ \frac{\partial e}{\partial v} - \frac{e \partial T}{T \partial v} \right\} \cdot \overline{AP}$$

indicating mean values along \overline{AP} .

With de Munck's formula [2] for $n - 1$ we obtain (same Q_A^P as above)

$$\alpha_D = \kappa \delta + k Q_A^P - H,$$

where κ and Q_A^P are the same as above,

$$\delta = \Delta n R_A^P - 0.0083 Q_A^P \left(\frac{1}{\lambda_{02}^2} - \frac{1}{\lambda_{01}^2} \right)$$

λ in μm .

If, from meteorologic measurements Q_A^P is evaluated, the humidity correction is :

$$k Q_A^P - H,$$

where H should be very small.

The evaluation (3a) of Q was made as a prediction, assuming Laplace's formula for p_{dry} and e sufficiently accurate.

By constructing the example in [3b], $\bar{\alpha}_D'$ was, however, kept constant, equal to $50''$; which is, of course, wrong.

$\bar{\alpha}_D'' = (n_{o_D} - 1) R_A^P$ goes to zero with $\left\{ \frac{\partial p}{\partial v} - \frac{p}{T} \frac{\partial T}{\partial v} \right\}_m$ at the same time as the denominator $1 + 0.29 \frac{\partial t}{\partial h}$, and the false asymptotic behavior of Q disappears

For model computations, (3a) should be written

$$1) \quad Q = - 3.36 \Delta n \cdot R \left(\frac{e}{p} \right)_m \left\{ 1 - \frac{0.38}{1 + 0.29 \frac{\partial t}{\partial h}} \right\}_m$$

Δn is given. R may be evaluated from definition!

We have approximately, and good enough, for a horizontal beam, $S = 20$ km :

$$R = \frac{3.592}{T_m} \left\{ \left(\frac{\partial p}{\partial v} \right)_m \text{ mm/km} + \frac{10 p_m}{T_m} \left(\frac{\partial t}{\partial h} \right)_m \text{ }^\circ / 100 \text{ m} \right\}$$

so, in (3a) only $\left(\frac{\partial p}{\partial h} \right)_m$ and $\left(\frac{\partial t}{\partial h} \right)_m$ ought to be known, besides $\left(\frac{e}{p} \right)_m$ and T_m .

We could, of course, and preferably, directly calculate Q as it is defined, or approximately as

$$Q = - \frac{15.02 \cdot 10^{-6}}{T_m} \left\{ \frac{\partial e}{\partial v} - \frac{e}{T} \frac{\partial T}{\partial v} \right\}_m \cdot \overline{AP},$$

which in our case will be

$$2) \quad Q = - \frac{15.02 \cdot 10^{-5}}{T_m} \left\{ \left(\frac{\partial e}{\partial v} \right)_m \text{ mm/km} + \frac{10 e_m}{T_m} \left(\frac{\partial t}{\partial h} \right)_m \text{ }^\circ / 100 \text{ m} \right\}$$

In the first case, using the appropriate (3a)-formula, we accept the Laplace formula as valid for p_{dry} and e .

In the second case, we may either compute $\frac{\partial e}{\partial v}$ from accepted Laplace formula, or, which is the most realistic approach, insert also realistic measured values of $\frac{\partial e}{\partial v}$!

For my model in [3b], Laplace formula is accepted, so the results of 1) and 2) should coincide. And they do !

The information for the example was $p_m = 750$ mm, $e_m = 21.4$ mm, $T_m = 298^\circ\text{K}$, horizontal beam not too near the ground, where $T \sim 300^\circ\text{K}$. Our base has $h = 30$ m above ground.

The Laplace-approach gives

$$\text{in } 1) \quad \left(\frac{\partial p}{\partial v} \right)_m \text{ mm/km} \sim 34 \frac{p_m}{T_m} = 87 \text{ mm/km}$$

$$\text{in } 2) \quad \left(\frac{\partial e}{\partial v} \right)_m \text{ mm/km} \sim \frac{21 e_m}{T_m} = 1.51 \text{ mm/km}$$

Instead of the table of corrections, computed for the example in [3b], we should have the following list, which also contains $\bar{\alpha}'$: Laplace formula is still used.

$\frac{\partial t}{\partial h}$ °/100m	Humidity correction	$\bar{\alpha}' = 292.4 \cdot 10^{-6} R'' = 63'' (1 + 0.29 \frac{\partial t}{\partial h} \text{ °/100m})$
+4	-1.1	136
+3	-0.9	118
+2	-0.7	100
+1	-0.5	81
0	-0.4	63
-1	-0.2	45
-2	0	26
-3	+0.2	8
-4	+0.3	-10
-5	+0.5	-28

I ask the readers to correct the table in [3b] accordingly. Excuses for my blunder!

Experiences at the meteorological institute of Uppsala university show, however, that $|\frac{\partial e}{\partial h}|$ even at our base height (30m) can reach values more than 20 times those predicted from Laplace's formula. During inversions and strong negative $\frac{\partial e}{\partial h}$, the refraction is great, and the negative humidity correction, too. During the night in August 1974, the reported refraction was around 130'', and the correction (for humidity?) of the order of - 8''. To explain the observed result we should have had a humidity-gradient of \sim - 30mm/km and a temperatureinversion of around + 2°/100m. As a comparison, I can mention, that our IDM measurements in June of 1977, averaged over one minute (10 exposures), agree to within 5'' with the theoretical values, derived, using vertical angles and the formula (9''), in which now all geodetic information is checked. No significant Q-correction. Normal values $\alpha/\sim 60''$.

To obtain representative values, comparable with the theodolite anglemeasurements, it will be tried to use longer exposure-times (and slower films) in the next future. The present exposures (0.2-0.5sec) show considerable shortperiodic variations of the refraction, which cannot be detected by the eye. We have recorded fast changes between our exposures, which are made in intervals of 4 sec. Amplitudes of these changes can reach 5''.

Discussion (paper 10)

- Q. All instrumental errors in measuring vertical angles are asymmetric by reason of gravity, the bending of the instrument, the pivot that sinks down the oil etc. Could these errors not have influence on the errors you found in the absolute value ? If you measure with another instrument, the vertical angles may differ amongst them.
- A. Thank you very much. And with this suggestion: I liked to have an explanation., but I thought you should be happy with the humidity.
- Q. What is the reasonable shortest range of your method ?
- A. You know the first test we did was one km, but the refraction is small, so this did not interest us. Of course we can realise this under stable conditions and with a Michelson device with a base of 12 cm and a 0,5 cm. slit distance, giving a theoretical magnification of 24. We, however, did not use it in this experiment, only a 6 grid grating. In any case we can rely on a magnification of 10, which means that 2 sec. of an arc will be 0.2 sec. But it is very difficult to have such weather-conditions, that interference patterns in the Michelson device will be stable enough in order to make a good photograph. We made in the laboratory, as I told you that magnification with a big Michelson device, and when the airplanes from the military-base passed high over, everything disappeared in the interference. So we have to have, I think usually big refraction but stable refraction in order to be able to use it, but that doesn't matter, because what shall we use the refraction value for. That was my original aim and that was to determine the geoid, to fill in the gaps between the astrostations, we made and simple field method and get the geoidal undulations.
- Q. In the paper you wrote that this difference of 25 sec between the values computed from IDM and those by means of equation 9) is only for the night you observed the dispersion-angles. What was the difference at other nights ?
- I only want to ask you were there some changes in this constant difference for several nights ?

A. This is just a bad thing you know, because these are the only measurements, which could be made before the Rubylaser broke down and therefore I was hesitating to give you anything here, but I think already they are relative coincidences of importance for the future. I think that your group in Hannover and Williams group in NPL, you have also such correlation measurements made, but for much shorter days. But you haven't made any absolute test and we have to decide that this is absolutely necessary before we can convince the scientific community that we have really solved the problem. The accuracy I'm not thinking so much about.

But don't you think that what I demonstrated here from the old days at Uppsala, from the Niinisalo measurements and the subsequent improvement, this is some result in any case and now we have only to collect more and more data and perhaps, if we can see that these 24 sec, are constant we have to look at it in another way. But if it is reflecting the humidity, that is the temperature gradient, we will see that too.

Q. Could it be interesting to make simultaneous measurements with other instruments while using your instrument on the same base ?

A. I can tell you that, and Williams also, that in the Uppsala meeting it was planned to make measurements with their devices and with mine. But as I told you in the introduction here, there will be a combined astronomical union and association meeting on refraction, 1978 in Uppsala,

We have already talked about that. So we shall have real fieldwork during the working, Of course it is essential.

DIE ERFASSUNG DER REPRÄSENTATIVEN TEMPERATUR BEI LASER-STRECKENMESSUNGEN ÜBER DEN RHEINGRABEN

Udo Maier, Geodätisches Institut der Universität Karlsruhe, Federal Republic of Germany

Ein großer Teil der Strecken des Testnetzes Karlsruhe überquert den Rheingraben in einer Höhe von mehreren hundert Metern über der Grabensohle. Die Endpunkte dieser Strecken liegen auf Bergkuppen am Grabenrand. Die dort gemessenen Lufttemperaturen sind - wie allgemein bekannt - infolge der Bodennähe nicht repräsentativ für die Meßstrecke. Um die Genauigkeit von Lasermessungen solcher Strecken zu steigern, muß man daher nach Wegen suchen, die repräsentative Temperatur besser als durch bloße Endpunktmessungen zu erfassen.

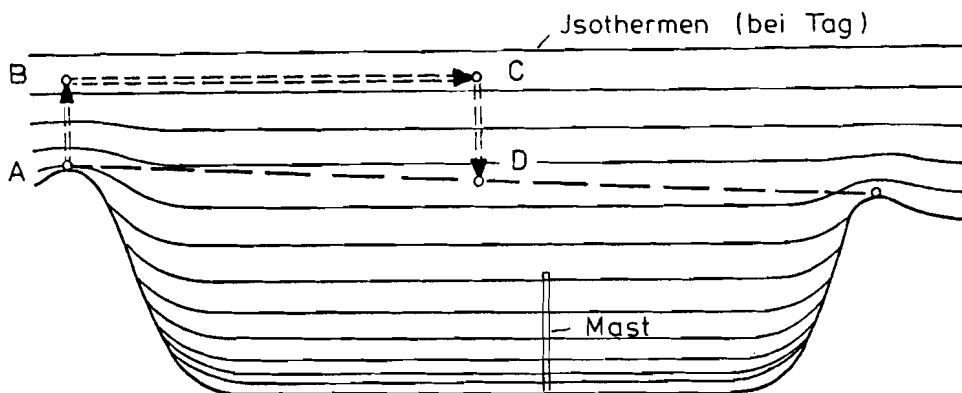


Abb. 1 Geländeprofil im Rheingraben

Einen guten Anhaltspunkt für die repräsentative Temperatur stellt die Temperatur in der Mitte des Meßstrahls (Punkt D in der Abb. 1) dar. Um sie aus der am Streckenendpunkt A gemessenen Temperatur zu ermitteln, benötigt man Informationen über die Temperaturverteilung im Rheingraben. Die Isothermen sind in der Nähe der Erdoberfläche dichter geschicht als in größerer Höhe; außerdem steigen sie an den Hängen etwas an, während sie in der Grabenmitte horizontal verlaufen. In größerer Höhe folgen die Isothermen dem Geländeprofil in abgeschwächter Form;

dieser Effekt wird mit weiter zunehmender Höhe kleiner und verschwindet schließlich ganz. Wählt man zwei Punkte B und C in einer solchen Höhe, in der die Isothermen bereits horizontal verlaufen, so bietet sich zur Berechnung der Temperatur am Punkt D der Weg A - B - C - D an. Das vertikale Temperaturprofil D - C ist in den meisten Fällen durch einen genähert konstanten Temperaturgradienten gekennzeichnet, der sich beispielsweise durch gleichzeitig mit der Streckenmessung vorgenommene Zenitdistanzmessung bestimmen läßt. Das Profil A - B dagegen liegt in der "bodennahen Luftschicht"; zu seiner Beschreibung ist man auf Modellvorstellungen angewiesen, weil es im allgemeinen nicht unmittelbar gemessen werden kann.

Eine solche Modellvorstellung wurde von BROCKS aufgrund von Profilmessungen an verschiedenen Orten empirisch entwickelt [1], [2]. Danach ist der Temperaturgradient in der "labilen Unterschicht" bei Tag durch folgende Gleichung zu beschreiben:

$$\frac{dt}{dh} = a \cdot h^b, \quad b < 0.$$

Oberhalb dieser "labilen Unterschicht" befindet sich nach BROCKS die "adiabatische Zwischenschicht", die sich bis in mehrere hundert Meter Höhe erstreckt. BROCKS gibt in Tabellenform mittlere Zahlenwerte für die Konstanten in Abhängigkeit von der Tages- und Jahreszeit an. Da das BROCKS-Modell nur einen statistischen Erwartungszustand beschreibt, kann man es nur mit Einschränkungen auf praktische Einzelfälle anwenden; auch ist man heute der Ansicht, daß die "adiabatische Zwischenschicht" bei weitem nicht von solcher Bedeutung ist wie BROCKS angenommen hat.

Eine weitere Modellvorstellung über das Temperaturprofil der bodennahen Luftschicht wurde von A.S. MONIN und A.M. OBUCHOV aufgrund von turbulenztheoretischen Untersuchungen entwickelt [3]. Aus der dort hergeleiteten Formel ergibt sich das Temperaturprofil im wesentlichen als eine Funktion des turbulenten Stromes fühlbarer Wärme. Da dieser nicht direkt gemessen werden kann, muß er im allgemeinen aus den übrigen Komponenten der Wärmebilanzgleichung der Erdoberfläche berechnet werden; zu diesen zählen vor allem die kurz- und langwelligen Strahlungsströme. Das MONIN-OBUCHOV-Modell gilt nur unter folgenden

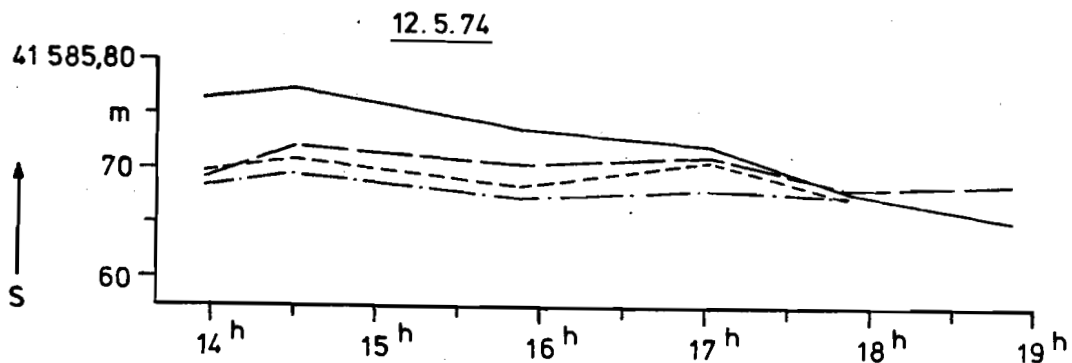
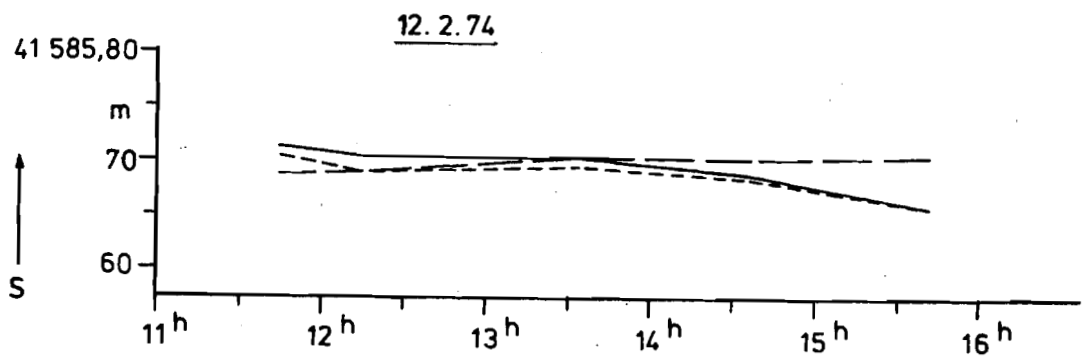
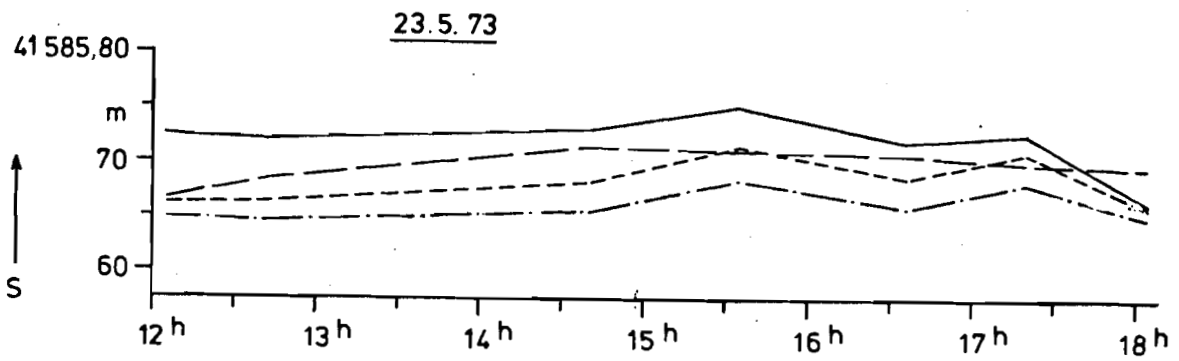
Einschränkungen bzw. Bedingungen:

1. Die bodennahe Atmosphäre ist labil geschichtet;
2. die Oberfläche ist eine horizontale, ins Unendliche ausgedehnte Ebene;
3. man erhält statistische Erwartungswerte, von denen sich der konkrete Einzelfall beträchtlich unterscheiden kann.

Die Bedingung einer unendlichen Ebene ist gerade auf Bergkuppen am wenigsten erfüllt, so daß das MONIN-OBUCHOV-Modell auf unser Problem - ebenso wie das BROCKS-Modell - nur unter großen Vorbehalten anwendbar ist.

Befindet sich auf der Talsohle ein meteorologischer Meßmast, so bietet sich eine weitere Möglichkeit zur Ermittlung der repräsentativen Temperatur. Ein solcher Mast ist an zentraler Stelle im Testnetz Karlsruhe günstig gelegen; mit seiner Hilfe wird das Temperaturprofil in sieben Höhen bis zu 200 m über Grund laufend registriert. Bis zur Meßstrahlhöhe muß das Temperaturprofil indessen noch verlängert werden. Diese Extrapolation ist im allgemeinen mit Hilfe des Temperaturgradienten in Höhe der Mastspitze vorzunehmen. Man erhält ihn aus der Temperaturdifferenz zwischen den beiden höchsten Meßstellen; damit sich die kurzperiodischen Temperaturschwankungen an diesen Meßstellen nicht als vergrößerte Schwankungen auf die extrapolierte Temperatur auswirken, ist eine Glättung des zeitlichen Verlaufs dieser extrapolierten Temperatur notwendig. Der Temperaturgradient oberhalb der Mastspitze läßt sich aber auch durch Messung von Zenitdistanzen während der Streckenmessung bestimmen. Eine ausgewählte Strecke des Testnetzes Karlsruhe, die an drei verschiedenen Tagen gemessen wurde, ist nach den erwähnten Verfahren ausgewertet worden; die Ergebnisse sind in der Abb. 2 dargestellt.

1. Es wurden die an den Streckenendpunkten gemessenen Temperaturen unverändert zur Streckenreduktion verwendet.
2. Aus diesen Temperaturen wurde unter Verwendung des BROCKS-Modells die repräsentative Temperatur für den Meßstrahl berechnet.
3. Eine entsprechende Berechnung wie unter Ziffer 2 wurde mit Hilfe des MONIN-OBUCHOV-Modells vorgenommen.



Erläuterung: — mit gemessenen Temperaturen (im Text Ziffer 1)
 - - - - BROCKS-Modell (im Text Ziffer 2)
 - · - · MONIN-OBUCHOV-Modell (im Text Ziffer 3)
 - - - - meteorologischer Mast (im Text Ziffer 4)

Abb. 2 Streckenmessungen Michaelsberg - Madenburg, reduziert mit verschiedenen Temperaturen

4. Das Temperaturprofil, das an dem erwähnten meteorologischen Meßmast im Gebiet des Testnetzes Karlsruhe registriert wird, wurde bis zur Meßstrahlhöhe verlängert; mit der so erhaltenen repräsentativen Temperatur wurden die Streckenmessungen gleichfalls reduziert.

Der Streckenverlauf nach Ziffer 1 ist an allen drei Meßtagen am stärksten vom Tagesgang beeinflusst. Auch die Ergebnisse nach Ziffer 2 und 3 zeigen einen - wenn auch gegenüber Ziffer 1 abgeschwächten - Tagesgang. Die beste Konstanz zeigen die Werte nach Ziffer 4; diese Werte zeigen auch die beste Übereinstimmung an den drei Meßtagen, wie aus der folgenden Tabelle ersichtlich ist.

Verfahren	Datum		
	23. 5. 73	12. 2. 74	12. 5. 74
1. mit gemessenen Stat.temperaturen	41585.719	.698	.735
2. BROCKS-Modell	.685	.658	.685
3. MONIN-OBUCHOV-Modell	.662	.698	.684
4. meteorol. Mast	.680	.698	.690

Tabelle: Tagesmittel der nach den Verfahren 1 bis 4 (siehe Text) reduzierten Strecken

Man ersieht daraus folgendes:

1. Die an den Endpunkten gemessenen Temperaturen führen zu den am wenigsten befriedigenden Ergebnissen.
2. Auch die Modellvorstellungen nach BROCKS und nach MONIN-OBUCHOV können nicht ganz befriedigen; dies leuchtet auch ein, wenn man die erwähnten Voraussetzungen und Einschränkungen für diese Modelle in Betracht zieht.
3. Bessere Ergebnisse als eine Modellvorstellung ergibt die Messung des Temperaturprofils, auch wenn dies nicht ganz bis zur Höhe des Meßstrahls reicht.

Befindet sich also ein Meßmast in der Nähe einer zu messenden Strecke, so wird die Verwendung der dort gemessenen Temperaturen empfohlen. Fehlt ein geeigneter Mast, so wäre in besonderen Fällen der Einsatz einer Radiosonde in Erwägung zu ziehen.

Literatur:

- [1] BROCKS, K. Ober den täglichen und jährlichen Gang der Höhenabhängigkeit der Temperatur in den unteren 300 Metern der Atmosphäre und ihren Zusammenhang mit der Konvektion. Ber. d. Deutschen Wetterdienstes in der US-Zone Nr. 5, Bad Kissingen 1948.
- [2] BROCKS, K. Temperatur und Austausch in der unteren Atmosphäre. Ber. d. Deutschen Wetterdienstes in der US-Zone Nr. 12, Bad Kissingen 1950.
- [3] MONIN, A.S.
 OBUCHOW, A.M. Fundamentale Gesetzmäßigkeiten der turbulenten Vermischung in der bodennahen Schicht der Atmosphäre. In: Sammelband zur statistischen Theorie der Turbulenz, Hrsg. H. Goering, Berlin 1958.
- [4] MAIER, U. Genauigkeitsuntersuchungen zur elektrooptischen Messung langer Strecken. (Dissertation in Vorbereitung)

STRENGTH OF TRILATERATION NETWORKS OBSERVED IN PAIRS

Kamal A. Atia, University of Newcastle upon Tyne, United Kingdom

ABSTRACT

Line pairs measurement has been suggested as a technique to improve shape determination in trilateration networks. The effect of the geometry of such networks on the accuracy of shape is not the same as in triangulation. Strength analysis is carried out by deriving a single formula for the accuracy of propagation of scale in a chain of triangles. The effect of geometry on orientation is also examined. Comparison with triangulation is made and general rules for reconnaissance are laid down.

1. INTRODUCTION

A great deal of work has been done in the past for the purpose of comparison between triangulation, trilateration and mixed networks. In these works pure trilateration was generally rejected for its weakness in shape determination. Chrzanowski and Konecny [3] found that combined triangulation - trilateration is the most accurate method; and that in contrast to either triangulation or trilateration, the combination of both does not depend on ideal configurations.

The introduction of line pairs technique [5] showed prospects of again considering pure trilateration [1]. It is interesting to investigate Line Pairs as a technique to improve the shape in pure trilateration. An immediate question arises concerning the meaning of "ideal configuration". In spite of the similarity and analogy in the formulation of geometrical conditions between triangulation and line-pairs trilateration, it can be easily seen that the sine rule is not used in the propagation of scale in the latter. It is not expected therefore that a configuration which is "ideal" for one system would be so for the other.

In the present treatment the strength of figure will be assessed using an approach similar to that used in traditional triangulation chains; i.e. using as a criterion the standard error of a computed length at the end of the chain. Although the main derivation is done for a simple chain of triangles and therefore not applicable to more complicated figures except, perhaps, after introducing some approximations, this approach was favoured over the alternative method of error ellipses for the following reasons:

(1) The computation to derive a single optimisation formula is feasible. In contrast the method of error ellipses requires particular numerical cases in order to be manageable. A general optimisation formula would provide an understanding of the favourable geometrical conditions so that general rules for reconnaissance could be reached.

(2) Ready comparison with triangulation would be available since the derived formula would be equivalent to the known triangulation formula of strength of figure .

(3) The derived formula can be used as a comparison criterion for alternative layouts; and as a specification formula for accuracy.

(4) One of the proposed schemes for line-pairs trilateration involves the measurement of selected bases for scale determination [1]. The assumption of a network extending between two bases is therefore a practical one.

The effect of geometry on orientation will also be investigated.

2. PRECISION OF AN ADJUSTED RATIO IN A SINGLE TRIANGLE

In the following derivation the notation of Richardus [5] is used. assume a single triangle measured using Line Pairs (figure 1), having side lengths a, b and c ; and all the three ratios

$$A' = \frac{b_1}{c_1}, \quad B' = \frac{c_2}{a_2} \quad \text{and} \quad C' = \frac{a_3}{b_3}$$

observed. Similar subscripts indicate instantaneous measurements.

Condition equation:

$$\frac{1}{A} v_A + \frac{1}{B} v_B + \frac{1}{C} v_C = t_a$$

$$\text{where } t_a = 1 - A'B'C' \quad [1]$$

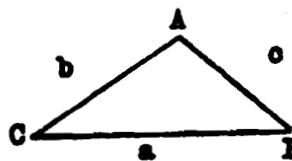


Figure 1

Weight coefficients for the three observed ratios according to the weighting system of [2] are

$$\epsilon_{AA} = \frac{1}{c^2} (1+A^2),$$

$$\epsilon_{BB} = \frac{1}{a^2} (1+B^2) \quad \text{and}$$

$$\epsilon_{CC} = \frac{1}{b^2} (1+C^2).$$

Correlative normal equation :

$$\left\{ \frac{1}{c^2} (1+A^2) \frac{1}{A^2} + \frac{1}{a^2} (1+B^2) \frac{1}{B^2} + \frac{1}{b^2} (1+C^2) \frac{1}{C^2} \right\} k_a = t_a$$

which can be reduced to

$$2 \left(\frac{1}{a^2} + \frac{1}{b^2} + \frac{1}{c^2} \right) k_a = t_a$$

Inverse matrix of normal equation is :

$$Q_{aa} = \frac{1}{2} \left(\frac{1}{a^2} + \frac{1}{b^2} + \frac{1}{c^2} \right)^{-1}$$

or, in terms of ratios and one side :

$$Q_{aa} = \frac{1}{2} \cdot \frac{c^2}{B^2 + A^{-2} + 1}$$

To obtain the weight coefficient " Q_{AA} " of the adjusted ratio "A", formula (7.27) in [4] is applied; leading, after some reductions, to

$$Q_{AA} = \frac{1 + A^2}{2\sigma^2} \frac{2A^2B^2 + A^2 + 1}{A^2B^2 + A^2 + 1} \dots \dots \dots (1)$$

3. PROPAGATION OF SCALE IN A CHAIN OF TRIANGLES

In a single triangle, the function used to compute side "a" from side "b" is

$$a' = b' C$$

The variance of a' will therefore be

$$\sigma_{a'}^2 = c^2 \sigma_{b'}^2 + b^2 \sigma_c^2$$

σ_c^2 according to (1) above is given by:

$$\sigma_c^2 = \frac{1 + C^2}{2b^2} \frac{2C^2A^2 + C^2 + 1}{C^2A^2 + C^2 + 1} \sigma^2$$

where σ^2 is the variance factor.

Therefore

$$\sigma_{a'}^2 = c^2 \sigma_{b'}^2 + (1+C^2) \frac{2C^2A^2 + C^2 + 1}{2C^2A^2 + 2C^2 + 2} \sigma^2$$

and the proportional variance is

$$\frac{\sigma_{a'}^2}{a^2} = \frac{\sigma_{b'}^2}{b^2} + \left(\frac{1}{a^2} + \frac{1}{b^2} \right) \frac{2C^2A^2 + C^2 + 1}{2C^2A^2 + 2C^2 + 2} \sigma^2$$

For a chain of triangles with a final computed base "d", if the correlation between ratios with common sides is neglected, the proportional variance of the end base will be

$$\frac{\sigma_d^2}{d^2} = \frac{\sigma_{b'}^2}{b^2} + \left[\left(\frac{1}{a^2} + \frac{1}{b^2} \right) \frac{2C^2A^2 + C^2 + 1}{2C^2A^2 + 2C^2 + 2} \right] \cdot \sigma^2 \dots \dots (2)$$

where the square brackets indicate summation for successive triangles.

Formula (2) requires for a strong network :

- (i) Large values for sides "a" and "b" in successive triangles; and
- (ii) A large value for the ratio $C = A / B$.

4. ORIENTATION OF THE CHAIN

The orientation error in a chain is obtained by the accumulation of errors in the vertex angles of successive triangles (γ). According to [1], γ is given by :

$$\cos \gamma = \frac{1}{2} \left(C + \frac{1}{C} + CA^2 \right)$$

For simplification assume the chain to be composed of isosceles triangles . Therefore

$$\gamma = \cos^{-1} \left(1 - \frac{1}{2} A^2 \right)$$

Applying the law of propagation of errors :

$$Q_{\gamma\gamma} = \left(\frac{d\gamma}{dA} \right)^2 Q_{AA} \quad (3)$$

From (1) and (3), after some reductions :

$$Q_{\gamma\gamma} = \frac{1}{a^2} \left(\frac{6 + 8A^2 + 2A^4}{8A^2 + 2A^4 - A^6} \right) \quad (4)$$

This formula shows the effect of geometry on the orientation. Comparison between two triangles with the same values for sides "a" and "b" but with different "c" represents a comparison between the layouts of figures 2 and 3 . The variation of the function between brackets in (4) is plotted against the vertex angle γ in figure 4 . The function is minimum at $dQ_{\gamma\gamma} / dA = 0$, which is a 9th. degree equation. The desired root of this equation has been obtained numerically as $A = 1.167$ corresponding to $\gamma = 71^\circ 23'$. The orientation function , however, is relatively flat between $\gamma = 40^\circ$ and $\gamma = 120^\circ$, and is dangerously steep outside this range.

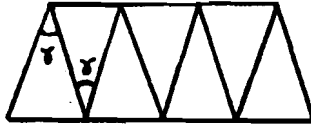


Figure 2

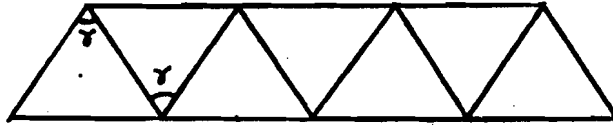


Figure 3

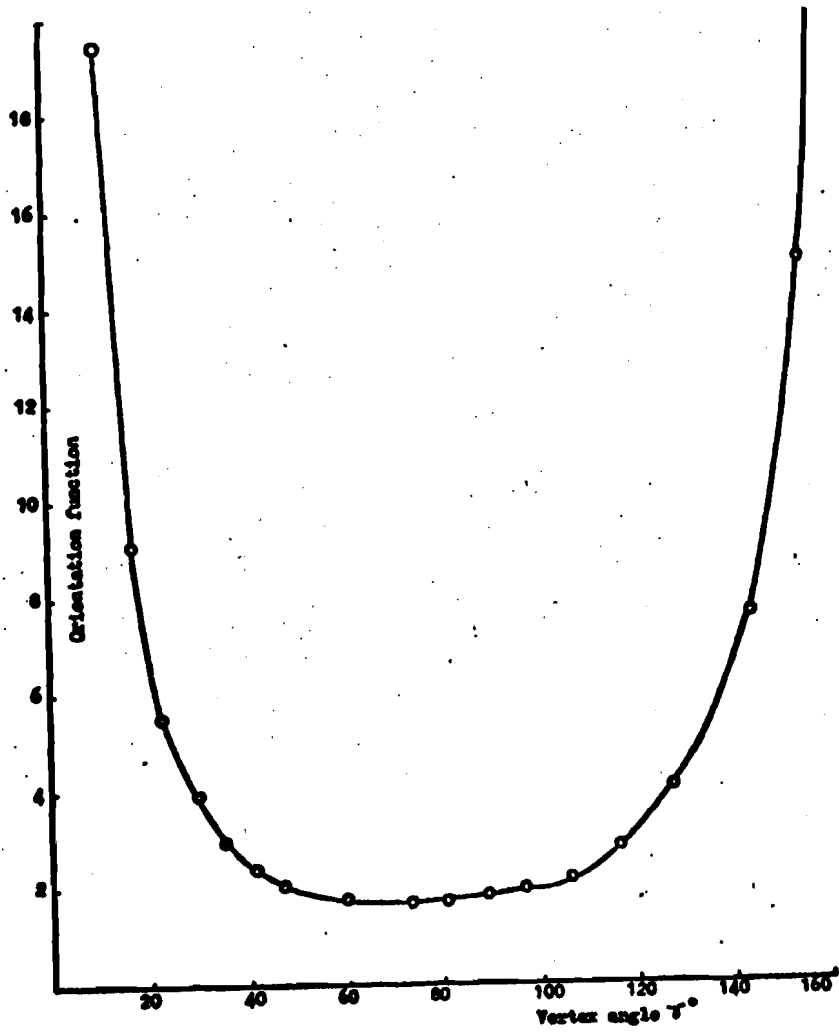


Figure 4

5. CONCLUSIONS

(1) Line-pairs trilateration provides a strong propagation of scale in the case of networks which grow in size as they extend; e.g. base extension networks.

(2) Small angles opposite to known and desired sides in a triangle have no adverse effect as in the case of triangulation. The layout of figure 3 is as good as that of figure 2 in scale propagation. The first with widely spaced stations would then be preferred due to the speed of propagation.

(3) The bigger the size of a network is, the smaller the standard error of a computed length (in proportional units).

(4) Orientation requirement imposes a limitation to (2) above. The angle γ should be kept between 40° and 120° . Serious degradation of orientation occurs outside this range. It is necessary to guard against this by applying a rigorous error analysis in suspected cases in the reconnaissance stage.

(5) A complete comparison between triangulation and line-pairs trilateration would depend largely on the particular instruments and field circumstances (a priori estimates of accuracy). The required estimates in such comparisons for edm need to be new (smaller) values specifically assessed for line pairs technique. Again the prospects of these stand in favour of trilateration, for the further major development of edm instruments is much more likely than that of theodolites.

REFERENCES :

1. Angus-Leppan, P.V., 1972. Adjustment of trilateration using length ratios. Survey Review, XXI(166):355-368.
2. Atia, K.A., 1976 . The adjustment of trilateration networks observed in pairs. Survey Review, XXIII(181):328-335.
3. Chrzanowski, Dr. Adam and Dr. Gotteried Konecny, 1965. Theoretical comparison of triangulation, Trilateration and traversing. Canadian Surveyor, XIX(4):353-366.
4. Richardus, P. and J. Allman, 1966. Project Surveying. North-Holland Publishing Company, Amsterdam.
5. Robertson, K.D., 1971. The use of line pairs in trilateration and traverse. Survey Review, XXI(165):290-306.

ACKNOWLEDGEMENT :

The author wishes to express his gratitude to the Egyptian Government for sponsoring him during his study.

RECENT ADVANCES IN MULTIWAVELENGTH DISTANCE MEASUREMENT

G.R. Huggett and L.E. Slater, Applied Physics Laboratory, University of Washington, Seattle, Washington, USA

ABSTRACT

A highly portable, multiwavelength distance-measuring instrument has been developed for field use. Its precision is better than 1 part in 10^7 . Simultaneous optical path-length measurements at different wavelengths and the dispersive nature of the atmosphere enable the corrected distance to be calculated without the need for the usual meteorological measurements. A minicomputer in the system allows real-time distance calculation (every 10 seconds), as well as mean value and standard deviation calculations. This instrument is currently being used to determine strain over baselines 3-9 km long. Strain episodes have been observed that are attributed to slip, at depth, on major faults in the area. There is a suggestion that this slip begins several kilometers down and propagates upward to the surface. Many of these strain episodes have coincided with magnitude 2.5-3.5 earthquakes in the region. Another strain episode indicates that the eastern end of the Sargent Fault may continue approximately 2-3 km past the point that it is currently thought to terminate.

INTRODUCTION

The solution to many geophysical questions would be greatly aided by the precise measurement of distance through the earth's atmosphere. While distances of a few meters or tens of meters can be measured with very high precision by interferometric techniques, it is generally not feasible to extend these techniques to baselines several kilometers in length. Standard triangulation techniques yield, at best, a precision of 1×10^{-5} , while the solution of many geophysical problems in a reasonable amount of time requires a precision of 1×10^{-7} or better (precision is defined here as the ratio of the standard deviation of the determinations to their mean value).

A variety of electromagnetic techniques are now in use for high-precision measurement. An excellent bibliography of such techniques is given by Wood [1971]. One of the major obstacles to an improvement of the precision is the uncertainty in the value of the index of refraction along the path. Despite this limitation, Parm [1973, 1975] in Finland and Savage and co-workers [Savage and Burford, 1973; Savage and Prescott, 1973] in the United States have made excellent distance measurements over baselines in the open atmosphere.

Savage and Prescott [1973] report a precision characterized by a standard deviation of measurements over a baseline of length L of $\sigma = (a^2 + b^2 L^2)^{1/2}$, where $a = 3$ mm and $b = 2 \times 10^{-7}$. The need for flying the line, however, not only makes the measurement expensive and time consuming but may actually prohibit measurements during the night. Higher precision and more rapid determinations require a direct method for determining the average index of refraction over the path rather than an approximation obtained by sampling.

Prilepin [1957] proposed a method using measurements at two wavelengths. Independently, Bender and Owens [1965] made a similar proposal. The method is based on the dispersive characteristic of air in the visible regions of the spectrum, which causes two optical signals of different wavelengths to propagate over the same path at slightly different velocities. Several authors have described the application of two-wavelength techniques [Huggett and Slater, 1975; Shipley, 1974; Birdsell, 1974]. The major noninstrumental source of error in the two-wavelength systems is uncertainty in the water vapor concentration along the path. An error of 1 mb in the determination of the partial pressure of water vapor causes an error of 1×10^{-7} in the calculated distance.

The index of refraction at microwave frequencies is about 100 times more sensitive to water vapor than the optical indices. By adding a third wavelength, microwave, to the instrument, the optical microwave dispersion can be used to determine the average water vapor density over the path being measured [Thompson, 1968]. Thayer [1967] analyzed the three-wavelength technique and determined that a precision of a few parts in 10^8 should be possible for path lengths of up to 50 km and temperatures of up to 30°C . The instrument described here is a combination of a dual-wavelength Fizeau type system and a direct phase-measuring microwave system.

THE THREE-WAVELENGTH DISTANCE EQUATION

The refractivity of the air N is proportional to the density of the air at the wavelength of the radiation used in the determination

$$N = n - 1 \quad N = \alpha \rho_s + \beta \rho_w, \quad (1)$$

where ρ_s is the density of dry air and ρ_w is the water vapor density [Owens, 1967]. A three-wavelength instrument measures the optical path lengths R_1, R_2, R_3 , at three wavelengths. It follows from (1) that $D = R_1 - DN_1$, $D = R_2 - DN_2$ and $D = R_3 - DN_3$. When any two of the difference terms are used, say,

$$\Delta R_{2-1}/D = N_2 - N_1 = (\alpha_2 - \alpha_1)\rho_s + (\beta_2 - \beta_1)\rho_w$$

and

$$\Delta R_{3-1}/D = N_3 - N_1 = (\alpha_3 - \alpha_1)\rho_s + (\beta_3 - \beta_1)\rho_w,$$

it is possible to solve for ρ_s and ρ_w . Substitution of these expressions for ρ_s and ρ_w in the distance equation

$$D = R_1 - D(\alpha_1 \rho_s + \beta_1 \rho_w)$$

yields

$$D = R_1 - \left[\frac{(\alpha_1 \beta_3 - \alpha_3 \beta_1) \Delta R_{2-1} + (\alpha_2 \beta_1 - \alpha_1 \beta_2) \Delta R_{3-1}}{(\alpha_2 - \alpha_1)(\beta_3 - \beta_1) - (\alpha_3 - \alpha_1)(\beta_2 - \beta_1)} \right] \quad (2)$$

The calculated distance is thus seen to be a function only of the measured optical path lengths R_1 and the two sets of dispersion coefficients α_1 and β_1 . The present three-wavelength instrument utilizes two optical lasers, a red He-Ne gas laser (632.9 nm) and a blue He-Cd metal vapor laser (441.6 nm). The third wavelength is a radio source operating in the microwave region. The subscripts in (2) are assigned as follows: 1 is red, 2 is blue, and 3 is microwave. Now $\alpha_1, \alpha_2, \alpha_3, \beta_1, \beta_2$ depend only on wavelength and hence, for a given instrument, are constants. Because of the polar nature of the water molecule, the β_3 coefficient is temperature dependent [Bean and Dutton, 1966]. Substituting the numerical constants and linearizing the temperature dependence yield the three-wavelength distance equation

$$D = R_1 - A(1 + A'T_c)\Delta R_{2-1} - B(1 + B'T_c)\Delta R_{3-1} \quad (3)$$

where $A = 20.9288$, $A' = -2.9184 \times 10^{-6}$, $B = -0.0198733$, $B' = 3.6243 \times 10^{-3}$, and T_c is the atmospheric temperature in degrees Celsius. The three-wavelength distance equation is only weakly dependent on atmospheric temperature; an error of 10°C produces an error of only 1×10^{-7} in the calculated distance. There is no need for atmospheric pressure or water vapor partial pressure measurements.

THE INSTRUMENT

A photograph of the three-wavelength distance-measuring instrument is shown in Figure 1 and a system block diagram in Figure 2. The basic concept of the instrument is that of the Fizeau velocity-of-light experiment. Light is passed through an optical modulator and returned to the same modulator after reflection from a distant retro-directive reflector. The return light reaches a photodetector only if the modulator voltage is in phase with the returning optical signal. This occurs when the optical path length is an integral number of modulation wavelengths ($2R = k\lambda$) or $R = kc/2f$, where R is the one-way optical path length, k is an integer, λ is the modulation wavelength, f is the modulation frequency, and c is the velocity of light in a vacuum.

The optical sources are a 5-mW helium-neon gas laser operating at 632.8 nm and a 5-mW helium-cadmium metal vapor laser operating at 441.6 nm. The two laser beams enter a Wollaston prism at the proper angle and polarization to make the outgoing beams collinear. The light passes through a microwave Pockels cell modulator that varies the ellipticity of the polarized light at 3 GHz and is transmitted by a 20-cm Cassegrainian telescope. The light traverses the path being measured and is returned

by a cat's eye retro-reflector, a 20-cm parabolic reflector with a plane mirror at its focal point. The beam is received by the same optics used for transmission and passes through the modulator a second time where the ellipticity of the polarization is increased or cancelled depending on the phase of the microwave modulator excitation. The returning light passes through the Wollaston prism (now used as a polarization analyzer), the output of which will be a minimum if the transit time is a half integral number of modulation periods. The beam emerging from the prism is both separated by color and directed to the photodetector by a dichroic mirror.

The instrument has two complete servo systems: One controls the modulation frequency on the red laser beam so that it is an integral number of half-wavelengths while the other system controls the modulation on the blue beam. The servos are identical and the common microwave elements and optical modulator are time-shared. The modulator is a potassium di-hydrogen phosphate crystal mounted in a re-entrant microwave cavity. The microwave portion of the system drives the modulator at a stable, accurately measured frequency.

The microwave power is pulsed on for about 25 μ sec to produce a large peak modulation index, while keeping the average power dissipation in the modulator low. The system is designed to deliver 20 W of peak power at a 5 percent duty cycle and the modulator is double pulsed at a repetition rate of 1000 Hz. The second pulse is delayed by a time equal to the transit time of the light over the path being measured.

The microwave modulation frequency at 3.005 GHz is derived from 5 MHz by an offset microwave phase-locked oscillator. In order to have a stable microwave frequency, the reference oscillator is phase-locked to the system clock and the computer-controlled 5-MHz frequency is added to it. The 5-MHz oscillator is a simple varactor-controlled LC oscillator. Tests have shown an output stability better than 1 part in 10^9 when the RF loop is phase-locked to a 5-MHz crystal test oscillator. The 3-GHz reference oscillator is phase-locked to the system master clock, a high-precision crystal oscillator with a stability of $\Delta f/f = 1 \times 10^{-11}$ rms per second and a long-term stability of $\Delta f/f = 5 \times 10^{-10}$ per day.

To follow fluctuations in the optical path length, a servo system adjusts the frequency of the microwave modulation to the optical path length such that the round-trip distance always remains a half integral number of modulation wavelengths. The 5-MHz oscillators are monitored by frequency counters that determine the average modulation frequency during each sample period, normally 1 or 10 seconds.

Simultaneously with the optical measurements, the radio path length is determined by standard direct phase measurement of a 9.6-GHz carrier frequency. This phase data and the modulation frequencies of the optical system are then input to the computer for the distance calculation. At the conclusion of each calculation (every 10 seconds), the corrected distance and all related data are output to magnetic tape and to various other peripheral devices at the operator's discretion. The operator can, at any time, request the computer to calculate the mean value and the standard deviation of the corrected distance. This information is displayed on a teletype.

FIELD DATA AND INTERPRETATION

Beginning in mid-September 1975, nine baselines radiating from Hollister have been measured daily with the MWDM system whenever possible. More lines were added to the network in early November 1975. The current network of 10 lines is shown in Figure 3, along with the approximate location of the major faults in the region. Data collected on the 10 lines from September 21, 1975, to April 17, 1976, are presented in Figure 4. Each point represents a daily mean value calculated from 30-100 consecutive 10-second determinations. The standard deviation of these 30-100 points (1 part in 10^7 or less from the mean) is a measure of the "visibility" on that particular line that day. The visibility is generally a function of both the clarity and the scintillation of the atmosphere and may vary considerably from hour to hour.

It became obvious by mid-October 1975 that the baselines Gambetta and Hollair-Easy had a considerably higher strain rate than the other lines in the array. The compression of the lines Gambetta and Hollair-Easy continued until mid-November 1975, when after about 1 μ strain of compression the rate abruptly decreased. Both lines are about 4 km long and extend northward from Hollister, ending on the east side of the Calaveras Fault. The MWDM instrument is also located just to the east of the Calaveras Fault. The close proximity of the MWDM instrument to the active trace of the Calaveras Fault is unusual for geodimeter lines, but the number of lines and radial pattern of the array make it easy to differentiate between movements of the instrument site and any of the retro-reflector sites.

This region had been seismically quiet for several months. On November 18, 1975, approximately one week after the decrease in strain rate, two earthquakes (magnitudes 3.1 and 2.8) occurred along the Calaveras Fault 7 km north of the northern ends of the two baselines (see Figure 5). A creep meter 1 km north of station Gambetta registered a moderate (3 mm) event on the Calaveras Fault on November 17, 1975 [R.O. Burford, personal communication, 19]. A creep meter 200 m from the instrument site has been monitored by us since the experiment began. During the time covered in this paper, it showed no appreciable change. No discontinuity is apparent in the strain data on the 17th or 18th.

A mechanism that may explain the observed strain episode is slip at depth on the Calaveras Fault north of Hollister. Note that the decrease in strain rate apparently occurred on baseline Hollair-Easy a few days before it appeared on baseline Gambetta. This may imply propagation of a slip episode from depth to the surface.

The detected "slip" terminated in early November, with surface creep and small earthquakes following within a week. These earthquakes may have resulted because the earlier, larger-scale aseismic fault slip episode loaded small, local zones of more difficult slip on the fault surface.

The second episode began abruptly on January 14, 1976, with baselines Knob, Goat, Gambetta, and Hollair-Easy all showing initial extension. The character of the event became clear within a few days; lines Knob and Goat continued to extend, while baseline Gambetta reversed its

FIELD DATA AND INTERPRETATION

Beginning in mid-September 1975, nine baselines radiating from Hollister have been measured daily with the MWDM system whenever possible. More lines were added to the network in early November 1975. The current network of 10 lines is shown in Figure 3, along with the approximate location of the major faults in the region. Data collected on the 10 lines from September 21, 1975, to April 17, 1976, are presented in Figure 4. Each point represents a daily mean value calculated from 30-100 consecutive 10-second determinations. The standard deviation of these 30-100 points (1 part in 10^7 or less from the mean) is a measure of the "visibility" on that particular line that day. The visibility is generally a function of both the clarity and the scintillation of the atmosphere and may vary considerably from hour to hour.

It became obvious by mid-October 1975 that the baselines Gambetta and Hollair-Easy had a considerably higher strain rate than the other lines in the array. The compression of the lines Gambetta and Hollair-Easy continued until mid-November 1975, when after about 1 μ strain of compression the rate abruptly decreased. Both lines are about 4 km long and extend northward from Hollister, ending on the east side of the Calaveras Fault. The MWDM instrument is also located just to the east of the Calaveras Fault. The close proximity of the MWDM instrument to the active trace of the Calaveras Fault is unusual for geodimeter lines, but the number of lines and radial pattern of the array make it easy to differentiate between movements of the instrument site and any of the retro-reflector sites.

This region had been seismically quiet for several months. On November 18, 1975, approximately one week after the decrease in strain rate, two earthquakes (magnitudes 3.1 and 2.8) occurred along the Calaveras Fault 7 km north of the northern ends of the two baselines (see Figure 5). A creep meter 1 km north of station Gambetta registered a moderate (3 mm) event on the Calaveras Fault on November 17, 1975 [R.O. Burford, personal communication, 19]. A creep meter 200 m from the instrument site has been monitored by us since the experiment began. During the time covered in this paper, it showed no appreciable change. No discontinuity is apparent in the strain data on the 17th or 18th.

A mechanism that may explain the observed strain episode is slip at depth on the Calaveras Fault north of Hollister. Note that the decrease in strain rate apparently occurred on baseline Hollair-Easy a few days before it appeared on baseline Gambetta. This may imply propagation of a slip episode from depth to the surface.

The detected "slip" terminated in early November, with surface creep and small earthquakes following within a week. These earthquakes may have resulted because the earlier, larger-scale aseismic fault slip episode loaded small, local zones of more difficult slip on the fault surface.

The second episode began abruptly on January 14, 1976, with baselines Knob, Goat, Gambetta, and Hollair-Easy all showing initial extension. The character of the event became clear within a few days; lines Knob and Goat continued to extend, while baseline Gambetta reversed its

many people who have kindly allowed continued access to their property. This work was supported by the U.S. Department of Interior, Geological Survey, under Contract 14-08-0001-15263.

REFERENCES

- Bean, B.R., and E.J. Dutton, Radio meteorology, Nat. Bur. Stand. U.S. Monogr., 92, 7, 1966.
- Bender, P.L., and J.C. Owens, Correction of optical distance measurements for the fluctuating atmospheric index of refraction, J. Geophys. Res., 70, 2461-2462, 1965.
- Bradsell, R.H., Georan 1, a new two-color laser ranger. Part 2: Technical description, Proceedings of the Int. Symp. on Terr. Electromag. Dis. Meas. and Atmos. Effects on Angular Meas., Stockholm, Sweden, 19-24 August 1974, Vol. 1, Paper No. 13.
- Huggett, G.R., and L.E. Slater, Precision electromagnetic distance-measuring instrument for determining secular strain and fault movement, Tectonophysics, 29, 19-27, 1975.
- Owens, J.C., Optical refractive index of air: Dependence on pressure, temperature, and composition, Appl. Opt., 6(1), 51-59, 1967.
- Pakiser, L.C., J.P. Eaton, J.H. Healy, and C.B. Raleigh, Earthquake prediction and control, Science, 166, 1467, 1969.
- Parm, T., Observing procedure and meteorological factors for electronic distance measurements, paper presented at International Symposium on Electronic Distance Measurements, Int. Ass. of Geod., Lagos, 1973.
- Parm, T., High precision traverse for scale determination of satellite and stellar triangulation and for controlling the first order triangulation, paper presented at General Assembly, Int. Ass. of Geod., Grenoble, 1975.
- Prilepin, M.T., Light-modulating method for determining the average index of refraction of air along a line, Trans. Inst. Geod. Aeron. Cartogr. USSR, Engl. Transl., no. 114, 127-130, 1957.
- Savage, J.C., and R.O. Burford, Geodetic determination of relative plate motion in central California, J. Geophys. Res., 78, 832-845, 1973.
- Savage, J.C., and W.H. Prescott, Precision of geodolite distance measurements for determining fault movements, J. Geophys. Res., 78, 6001-6008, 1973.
- Scholz, C.H., and T.J. Fitch, Strain and creep in central California, J. Geophys. Res., 75, 4447-4453, 1970.
- Shiple, G., Georan 1, a new two-color laser ranger. Part 1: Basic principles and preliminary results, Proceedings of the Int. Symp. on Terr. Electromag. Dis. Meas. and Atmos. Effects on Angular Meas., Stockholm, Sweden, 19-24 August 1974, Vol. 1, Paper No. 12.

Thayer, G.C., Atmospheric effects of multiple frequency range measurements, Tech. Rep. IER 56-ITSA 53, Environ. Sci. Serv. Admin., Rockville, Md., 1967.

Thompson, M.C., Jr., Space averages of air and water vapor densities by dispersion for refractive correction of electromagnetic range measurements, J. Geophys. Res., 73, 3097-3102, 1968.

Wood, L.E., Progress in electronic surveying, U.S. National Report, 1967-1971, Eos Trans. AGU, 52, IUGG17-IUGG21, 1971.

Wood, L.E., and M.C. Thompson, Jr., Technique for improving accuracy of air-to-ground radio distance measurement systems. Tech. Rep. ERL108-ITS 76, Environ. Sci. Serv. Admin., Rockville, Md., 1969.

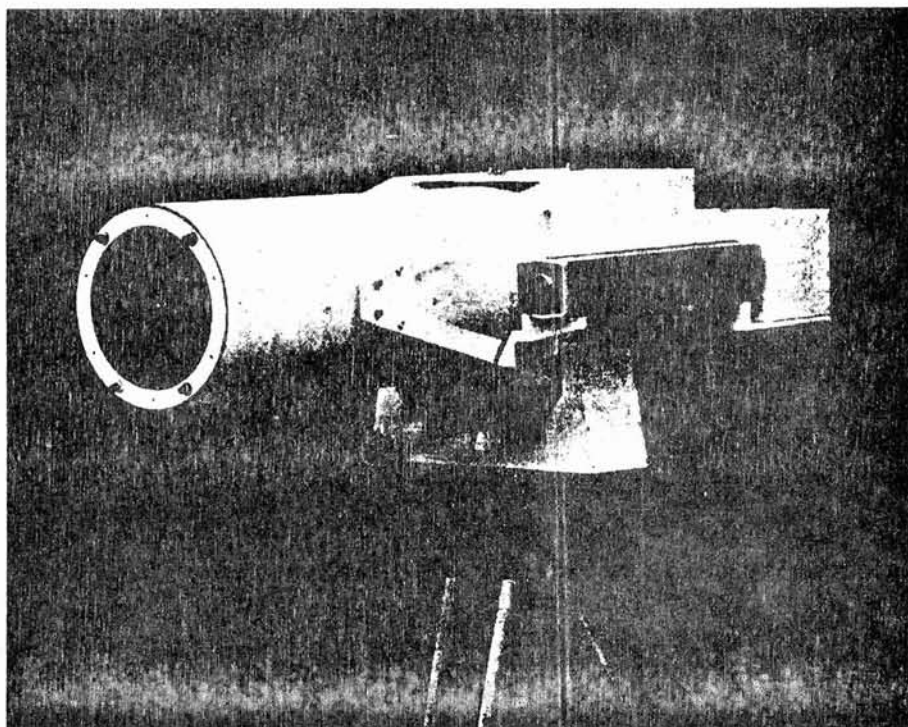


Figure 1. The multiwavelength distance-measuring instrument.

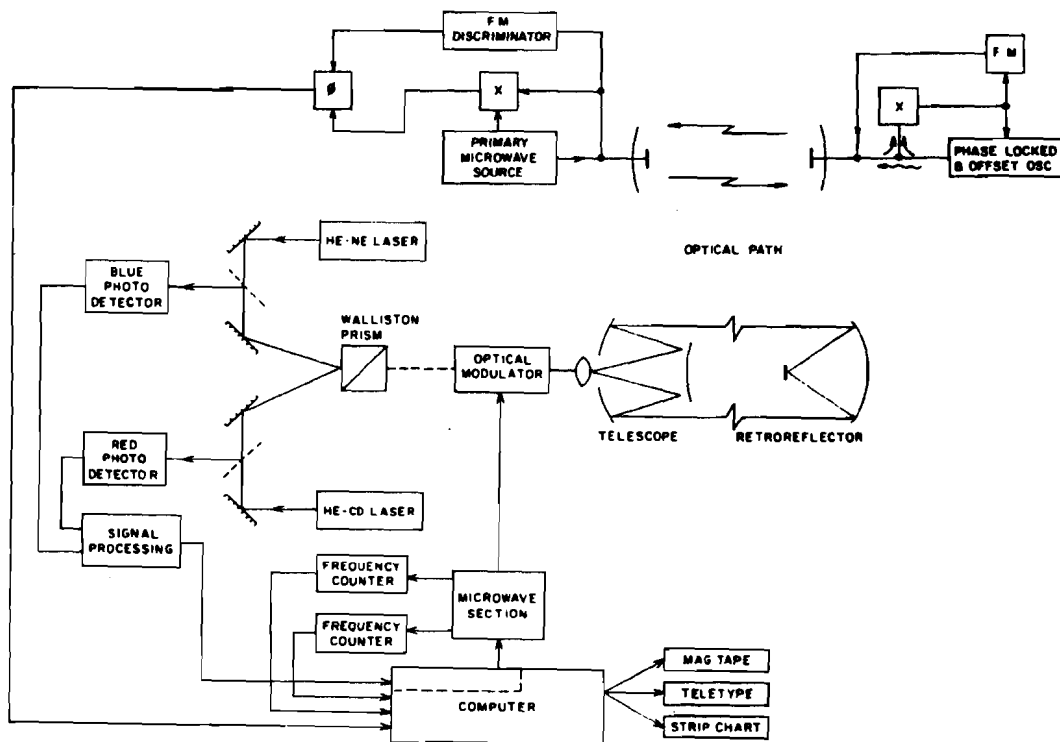


Figure 2. Block diagram of the multiwavelength distance-measuring instrument.

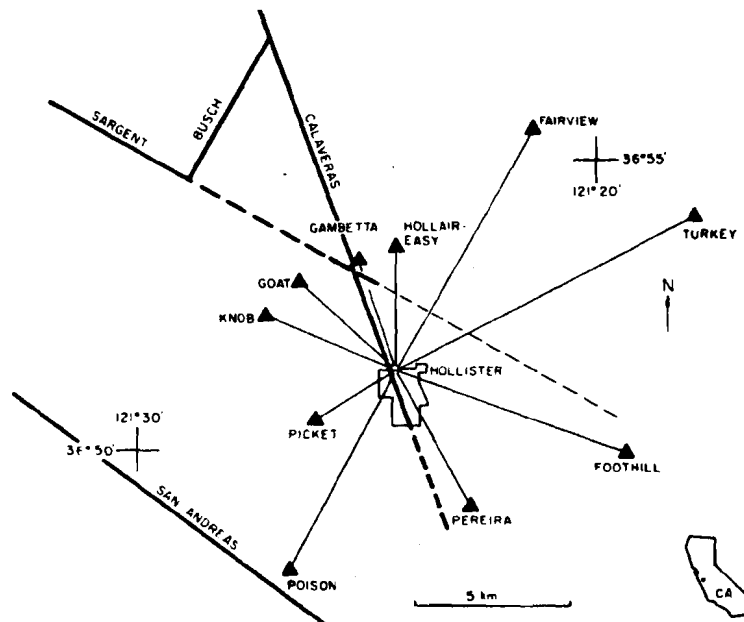


Figure 3. Map of the Hollister network showing its location relative to the major faults in the area (the faults are shown by the heavy lines). The instrument is located at the central station in the town of Hollister, California.

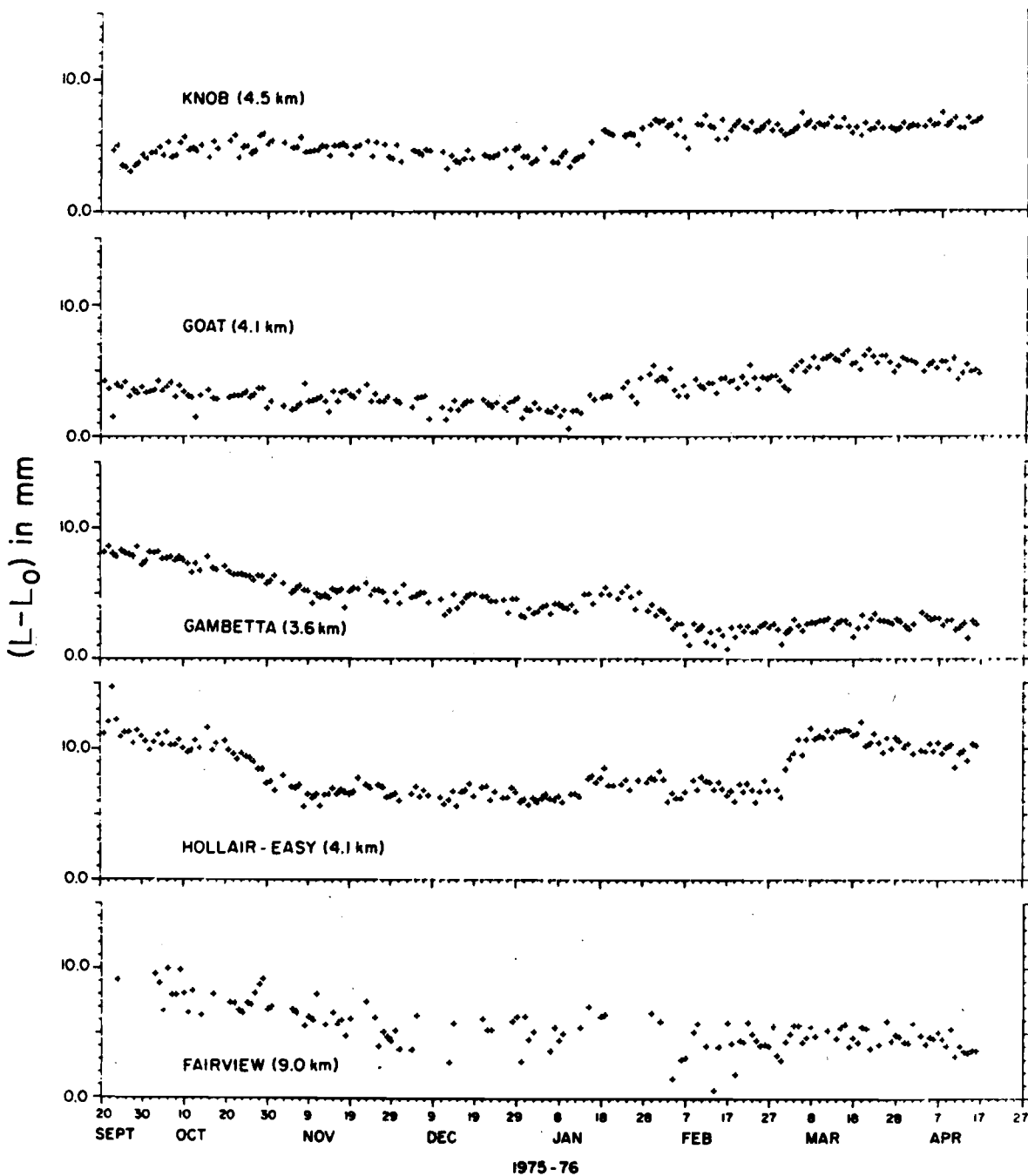


Figure 4. The difference between the measured length, L , and a constant nominal length, L_0 , as a function of observation time for those lines monitored from the central station in Hollister. Each point represents a daily mean value calculated from 30-100 consecutive 10-second determinations. The standard deviation of these 30-100 points is frequently less than 1 part in 10^7 from the mean.

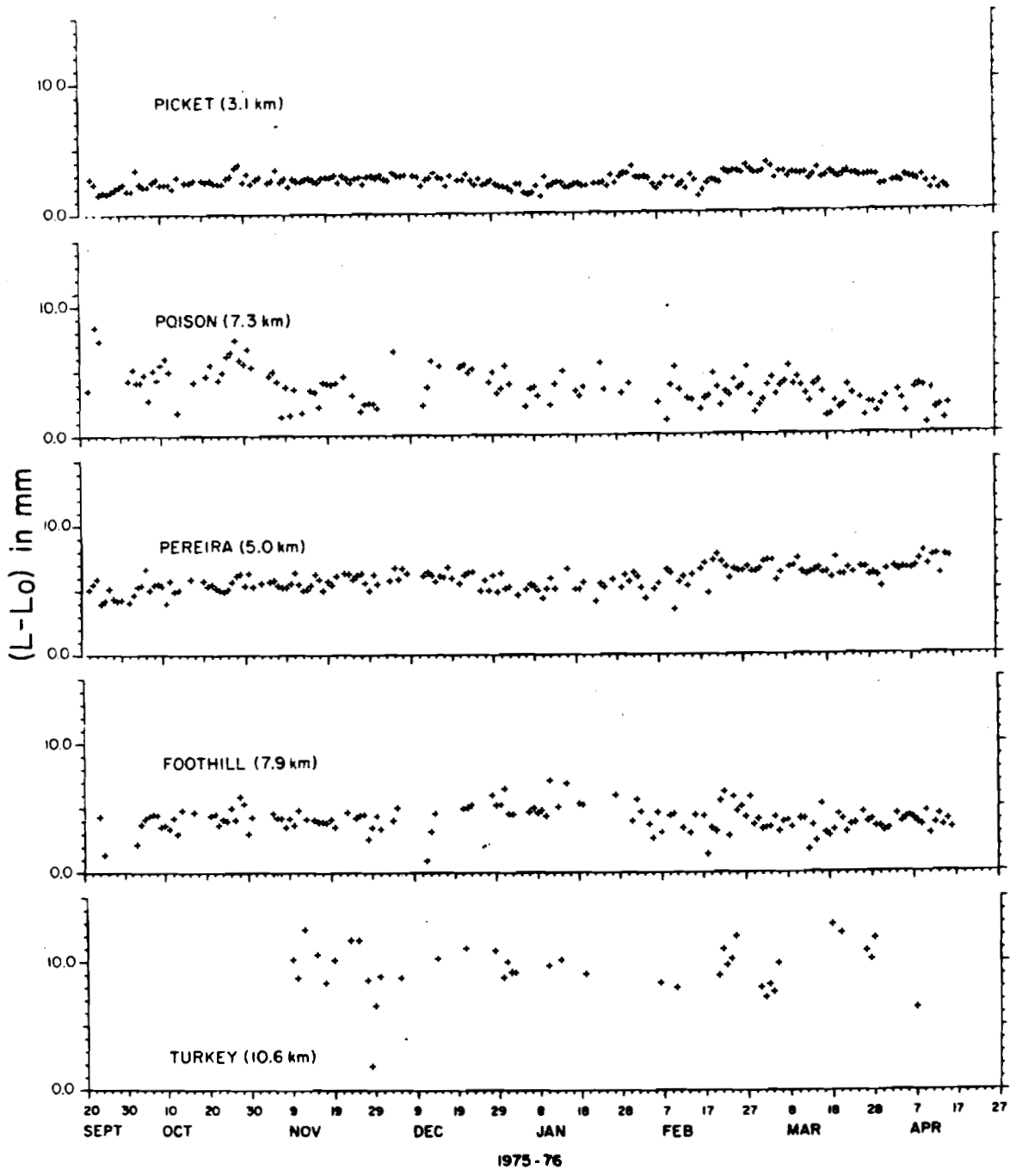


Figure 4, cont.

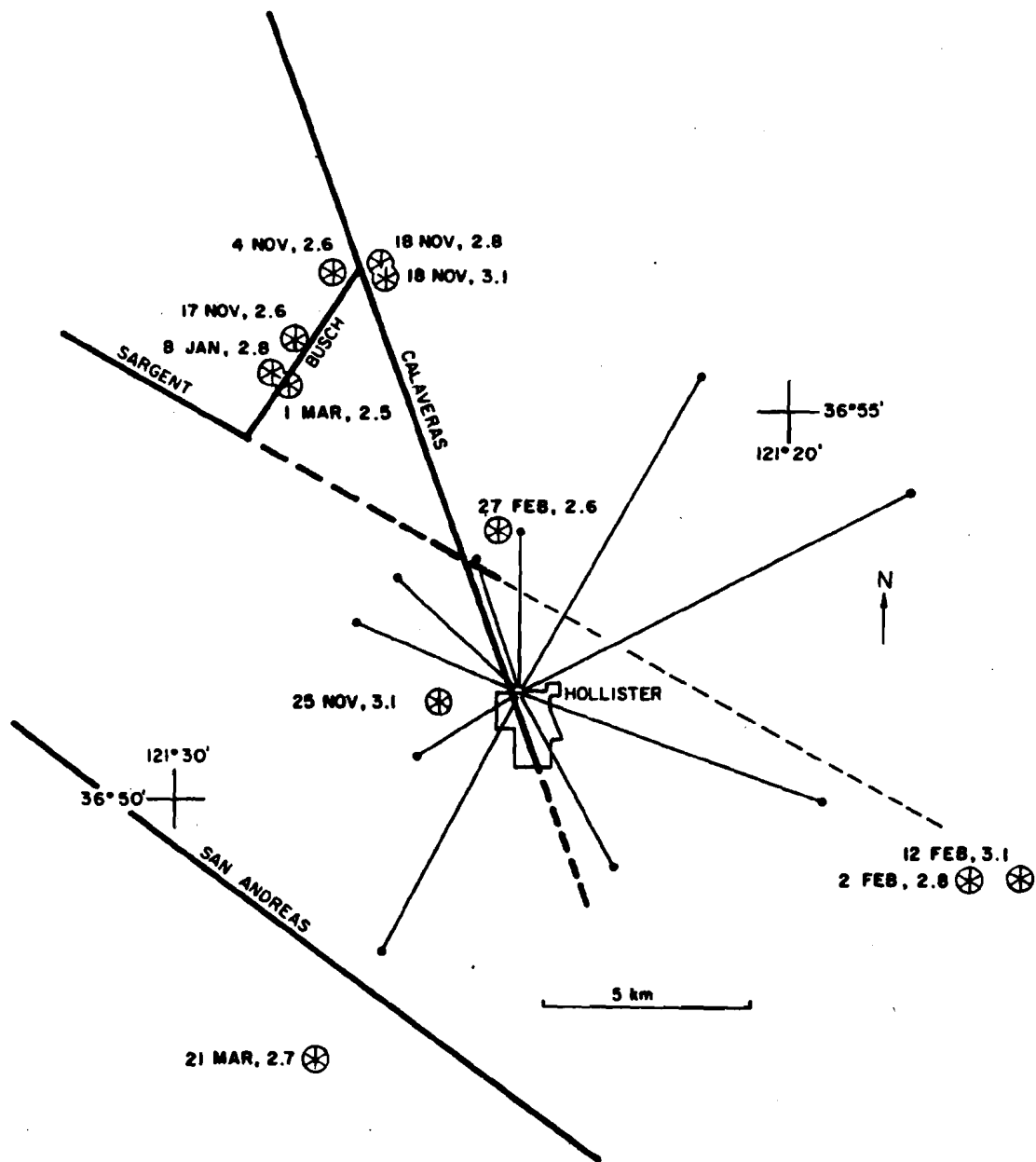


Figure 5. Map of the Hollister network showing epicenters of the earthquakes that have occurred in the area between the beginning of the strain measurements in September 1975 and April 1976.

PRECISION LEVELING WITH A TWO-FLUID TILTMETER

G.R. Huggett, L.E. Slater and G. Pavlis, Applied Physics Laboratory, University of Washington, Seattle, Washington, USA

Abstract. Thermally induced errors, dominant in a water-tube tiltmeter, are eliminated by using two adjacent tubes containing fluids with densities having different temperature coefficients. Simultaneous measurements of the apparent difference in height between two stations indicated by the two fluids are used to provide the required correction for the density changes. The application of this method could allow precise measurements over long baselines (a resolution of about 10^{-8} to 10^{-9} radians in a 1-kilometer instrument) without a level interconnecting tube or deep burial.

Introduction

The measurement of vertical displacement and tilt in active geophysical regions is an important yet difficult task. The advent of the theory of dilatancy has strengthened the need for high-precision measurements over baselines that are kilometers in length. Other fields with similar requirements are the detection of inflation phenomena in active volcanic regions, and the detection of subsidence in mining and geothermal resource areas.

Vertical displacement is generally determined using gravity meters or precision levels. The use of a gravity meter to infer vertical displacement assumes that the material beneath the instrument has a constant density; this may be a poor assumption, particularly in an active volcanic region. The measurement of level lines is subject to many systematic errors, and great care and expense are required to measure vertical displacements over kilometer-long baselines to a precision approaching a millimeter (an inferred average tilt of a micro-radian). The use of short-baseline tiltmeters is significantly limited by their great sensitivity to surface conditions near the pier. Fluid-tube tiltmeters with long baselines overcome many of these problems and have been used successfully for some applications [Eaton, 1959].

The most serious problem with a fluid-tube tiltmeter of considerable length (>50 m) is variations in the fluid's density caused by temperature changes along the path, particularly if the connecting tube between the stations is not kept horizontal. To illustrate, consider a column of fluid of height h . The pressure at the bottom due to the fluid is

$$P = \int_0^h \rho(T) g(y) dy \quad (1)$$

where $\rho(T)$ = density, $g(y)$ = acceleration of gravity, T = temperature, and h = height. The gravitational term can be assumed constant for reasonable values of h since the Bouguer gravity term, $\partial g/\partial y$, equals $-2\mu\text{gal/cm}$.

Copyright 1976 by the American Geophysical Union.

Assuming that the density varies linearly with temperature,

$$\rho(T) = \rho_0 (1 + \alpha T) ; \quad (2)$$

then

$$dP = g [\rho(T) dy + \rho_0 \alpha h dT] \quad (3)$$

at some height h in the column.

For a simple example that illustrates the thermal sensitivity, consider a water-filled tiltmeter. The temperature error is $\Delta y = \rho_0 \alpha h \Delta T = 1.5 \times 10^{-4}$ mm/deg C, where $\alpha = 1.5 \times 10^{-4}$ /deg C and $\rho_0 = 1$ gm/cm³. An average temperature change of only 1°C along a tube with $h = 10^3$ cm yields a temperature error of 1.5 mm.

This error is significantly larger than the height resolution usually desired. This temperature error, or apparent tilt, appears as "noise" on the tilt data.

The thermally induced noise can be reduced by burying the tube and keeping it perfectly horizontal, but this greatly increases the cost of installation and maintenance. In regions where deep burial at practically zero slope is impossible or impractical, the noise caused by thermal fluctuations will be the limiting factor controlling the precision of long-baseline tilt measurements.

Two-Fluid Tiltmeter

We suggest a new technique to overcome the thermal noise problem in liquid leveling: using two fluids with densities that vary linearly with temperature, each in a separate tube but in thermal contact so they experience the same thermal environment. This instrument is diagrammatically illustrated in Figure 1.

The pressure of a column of fluid is given by

$$P = \int_0^h \rho g dy , \quad (4)$$

where $\rho = \rho(y)$ = density of the fluid, and $g = g(y)$ = gravitational acceleration. It can be assumed that g is constant for reasonable values of h , since the Bouguer gravity term, $\partial g(y)/\partial y$, equals -2×10^{-6} cm/sec²/cm. In this case

$$P = \rho_0 g \int_0^h (1 + \alpha T) dy . \quad (5)$$

The pressure due to the column of fluid to station 2 is $P = \rho_0 g (h_2 + h_3) + \rho_0 g \alpha I_2$. P is also equal to the pressure caused by the column of fluid to station 1, so $P = \rho_0 g h_1 + \rho_0 g \alpha I_1$, where

Experimental Verification

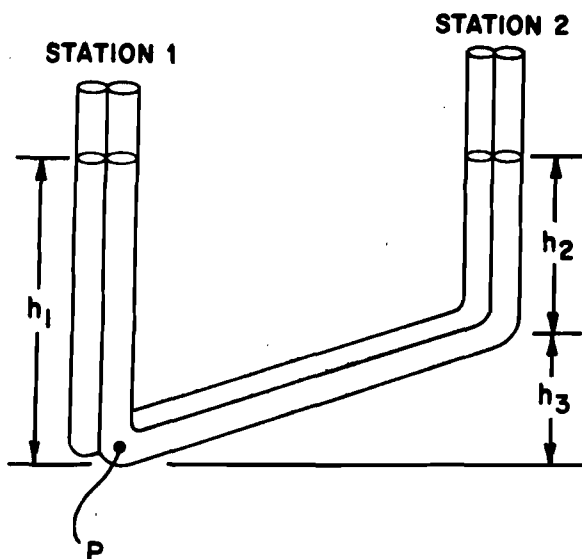


Figure 1. Diagrammatic sketch of two-fluid tiltmeter.

$$I_1 = \int_0^{h_1} T \, dy \quad (6)$$

The difference in the height of the liquid at each station is

$$\Delta = h_1 - h_2 = h_3 + \alpha(I_2 - I_1) \quad (7)$$

Assume two fluids a and b. Then

$$\Delta_a = h_3 + \alpha_a I \quad \text{and} \quad \Delta_b = h_3 + \alpha_b I \quad (8)$$

where $I = I_2 - I_1$. Then $\Delta_b - \Delta_a = (\alpha_b - \alpha_a) I$ and $(\Delta_a - h_3)/(\Delta_b - \Delta_a) = [\alpha_a/(\alpha_b - \alpha_a)]$.

The difference in height between stations is then simply

$$h_3 = \Delta_a - \frac{\alpha_a}{\alpha_b - \alpha_a} (\Delta_b - \Delta_a) \quad (9)$$

By measuring only the differences Δ_a and Δ_b , the relative height of two stations can be determined with no restriction upon station separation. It is thus possible to make a very long-baseline liquid-tube tiltmeter that compensates for temperature variations along the baseline. The height measurements could be accomplished in many ways, using optical sensors, differential transformers, capacitive coupling, mechanical indexing, etc.

There appear to be several suitable organic fluids with density coefficients that would yield an $\alpha_a/(\alpha_b - \alpha_a)$ term approximately equal to 2. This means that the column heights must be measured to a precision two times greater than would be required in a single-fluid tiltmeter. This should present no problem, and the instrument should provide a resolution of 10^{-8} to 10^{-9} radians. While this discussion has not addressed the dynamics of such a system, these are well presented by others [Eaton, 1959].

A simple two-fluid tiltmeter was constructed to experimentally verify the two-fluid concept. The arrangement is illustrated in Figure 2. The device consisted of two adjoining tubes, each composed of ten 1.2-m long sections of 8-mm diam glass tubing joined together with sections of plastic tubing 2-3 cm long. One tube contained methyl alcohol and the other ethylene glycol. Four 1.5-cm diam glass tubes with precision scales were attached to the four ends of the tubing and fastened side by side on a common reference stand. Thus any differential changes in liquid levels were due solely to temperature effects.

The two tubes contained an inclined section, the top of which could be raised to a height of about 2 m. On one side of this section the fluids were at room temperature; on the other side, the tubing passed through a 2.3-m water jacket which could be varied from 20° to 49°C. The inclined section with the large temperature difference between the two sides was designed to simulate the uncontrolled thermal and geometric conditions that exist in the field.

Figure 3 shows the difference in the levels of each fluid (thermally induced error) and the corrected difference as a function of water jacket temperature for two heights of the inclined section (1 m and slightly less than 2 m). Because both end stations were mounted on a common stand, the corrected difference should always be zero.

The results are quite dramatic. The corrected data have a standard deviation from the mean of 0.13 mm. Because all of the data were taken by visually sighting the meniscus of the liquids against the machinist's scale, this value could easily be improved with automatic level recording.

Note that the large temperature changes induced in this experiment reveal a slight nonlinearity in the fluids: the corrected values tend to be positive in the center of the range and negative at the low and high temperature extremes. $\rho(T) = \rho_0 (1 + \alpha T + \beta T^2)$ if the next higher term in the expansion of $\rho(T)$ is included. Applying the correction described above, the results will be in error by $[(\beta \alpha_a \alpha_b - \alpha_a \beta_b)/(\alpha_a - \alpha_b)] J$, where

$$J = \int_0^h T^2 \, dy \quad (10)$$

Using published values of α and β for methanol and glycol [International Critical Tables], the error is $(-4.0 \times 10^{-6}) J$. By selecting two fluids for which $\alpha_a/\alpha_b = \beta_a/\beta_b > 1$, this error could be reduced as much as three orders of magnitude.

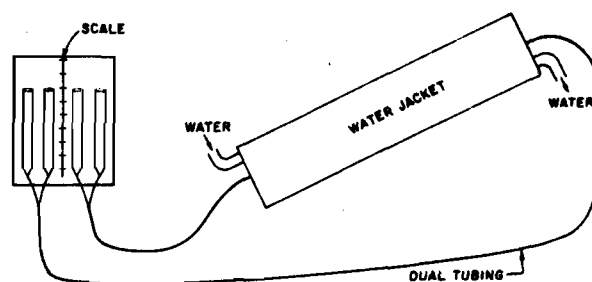


Figure 2. Test arrangement for two-fluid tiltmeter.

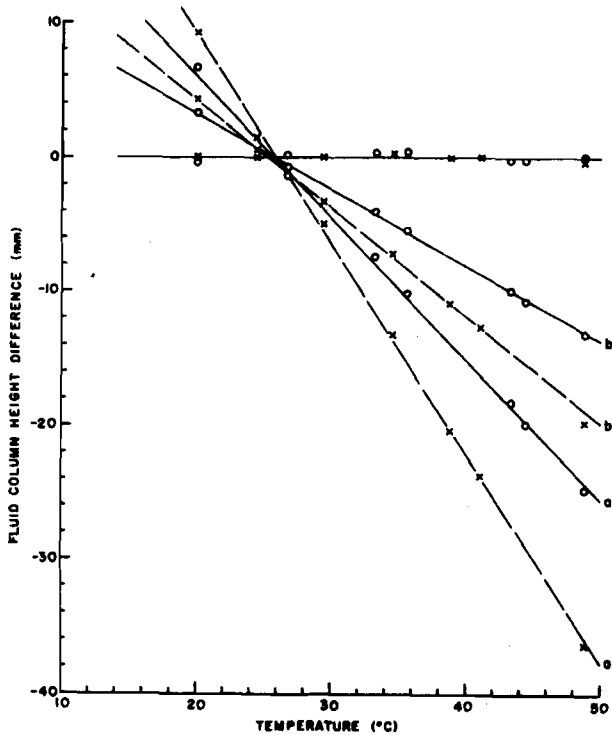


Figure 3. Test data for two-fluid tiltmeter. Thermally induced errors in methanol (a) and glycol (b) are shown for two incline elevations, 1 m (solid line) and approx. 2 m (dashed line) as a function of water jacket temperature. The upper horizontal line shows the corrected station height difference.

Conclusions

Minor local perturbations have a profound effect on small tiltmeters placed on a single pier, producing apparent secular tilting that is many times

larger than the actual secular tilting of the region [Hagiwara, 1947]. These perturbations have only a small effect on fluid-tube tiltmeters used to measure the relative changes of height of two piers many meters apart. The major shortcoming of the fluid-tube tiltmeter is its sensitivity to temperature. The temperature dependence requires that the tube be level and buried to reduce thermally induced errors.

The two-fluid tiltmeter eliminates thermal error from liquid-tube tiltmeter data. With the temperature sensitivity eliminated, precise long-baseline measurements are now possible, and may well result in considerable cost savings because deep burial and level tubing are unnecessary.

The two-fluid concept can be utilized to measure the relative height of two piers either by measuring the distance from the piers to the surface of the liquids, as discussed, or by measuring the pressure of the fluids. The pressure measurements can be used when there are large differences in elevation between stations. Both methods eliminate thermally induced errors.

References

- Eaton, J.P., A portable water-tube tiltmeter, *Bull. Seismol. Soc. Amer.*, 49, 301-316, 1959.
 Hagiwara, T., Observations of changes in the inclination of the earth's surface at Mt. Tsukuba, *Bull. Earthq. Res. Inst.*, Tokyo Univ. 25, 27-32, 1947.
International Critical Tables of Numerical Data, Physics, Chemistry, and Technology, McGraw-Hill, New York, 1928.

(Received September 27, 1976;
 accepted October 14, 1976.)

Discussion (paper 13)

- Q. Are the tests with the peculiar strainmeter collaborating with the tests with a gravimeter and with tiltmeters
- A. We do have some tiltmeters in the area, unfortunately most of the tiltmeters data are suspect. And then I found there has been a great deal of instrumental instability as well as an uncertainty as to the quality of the stations. It is not uncommon to find that with the small or common point measurement of tilt one can get the opposite of the original tilt, and they don't have a dense enough tiltmeter array to get good statistics.

The gravimeter work has not been done in this particular area, there is a large program, operating in Southern California near Los Angeles, where there is concern in the uplift area. They are doing a lot of gravimeter surveys and running a lot of levellines this summer, we have ours done on operating with the geodetic net as well. And there will be some correlation. We have now correlated with straingauges and gravimeters and we have increased the density of strainmeters around us.

- Q. I am interested in your work because even in Europe we are in need of the best solution for prediction nets, and I know that after the disaster in North Italy, you remember, the Italians woke up and understood that they had to pay a lot of money in order to do something and I just guess that they have got experience from you, but they are going to use suspensionmeters and tiltmeters and gravimeters mainly, but they probably don't know anything about your instruments,

A. This is possible.

- Q. You have to contact them, because it is very important.

A. I might point out that in the time that we have been in that area, we can say something about increased strain, I call it activity. I indicated that there was a temporal coherence between the earthquakes and our strain measurements.

We have no correlation, no special correlation as yet, because I think we don't have a dense net either, we just have one radial ray.

It is a start.

- Q. I wonder how such a high accuracy could be checked by an independent measure or something like that.
- A. Well, I guess it is difficult to check our instrument against any other system. I guess the biggest convincing argument would be, how multiple instruments on the same line, under as severe operating conditions as possible, would behave.
- Q. But in Europe there are such precise baselines, in Finland for instance, which are comparable in accuracy.
- A. I think that we must get on those lines, and I also would imagine that most of you would like to see that kind of comparison just as a very convincing argument. This device that has been talked about so long must be good, and in fact is.
- Q. What is your solution, how do you find it is the best way to resolve the instrument constant for the three-colour-system. What technique do you use ?
- A. The same technique you do. We simple set up a number of points in a line and measure combinations.
- Q. Do you in fact consider it's necessary to incorporate an instrument of this sort, that has the ability to measure the order of interference. Or do you really think that is not necessary ?
- A. I don't think it's necessary. The geodesist would disagree with me, but such a device, such a feature can be built in. An additional engineering complexity are the cost and we have not incorporated them. May I emphasize that the time has been of course for strain-there is no reason that it has limited the strain- as long as the base-line is known to 5 cm. So, with most systems, with most single wave-lengths, with reasonable fractions we know that one. So we decided that, because all these trade offs have to be made usually and we would not incorporate the ambiguity resolution. (? ed).

Q. You have an intelligent machine because it measures the water-vapour and corrects it. I have a question in this respect. Have you ever checked the water-vapour density, your " ρ_w ", against meteorological parameters, because we have made measurements in infrared and radiation measurements, close micro-wave propagation in the atmosphere and water-vapour density or the amount of water-vapour, what we get out is always different from the three methods we used, and it differed by the factor two or three or even more. We did it for the testing of the millimeter telescope, so we are no longer at the moment confident actually, which type of water-vapour we measured.

In this respect - if one turns around the instrument, you measure the water-vapour perhaps. So I have the question, have you ever checked this ρ_w against meteorological or water-vapour density, you derive from temperature, relative water-humidity and so on.

A. Yes, we have.

Q. May I ask you, do you find that the changes are the factor 2 in the correction or in the water-vapour determination ?

A. It is in the amount of water-vapour, I mean we try to calibrate our things as careful as possible in the water-vapour tank and so on, but even after that we have the confidence that something is happening in the atmosphere, which we don't detect.

Q. People studying propagation at let's say 300 microns and so, they discovered already that beside the water-vapour, there is something like a watervapour doubling molecule (? ed.), things like this, which starts to attenuate; it should alter the refraction in some way. So, my question is just whether you touched on this problem.

A. Yes, we did. We did not look specifically at the water-vapour determination itself. We determined the correction for the instrument both from a micro-wave measurement as well as from meteorological data measurements. We found in the regions we have operated, crossing over a large lake and also in the central California area, in both cases, that point meteorological measurements were adequate for the precision required for the "met" correction to the optical system.

I can't go on to say that this is going to be true in all cases, but we haven't moved this instrument to enough areas yet to rule out the necessity of the microwave path, but to answer your question briefly, yes we looked at it in our context, and the two results are the same.

- Q. In the astronomy and the meteorological section, one may have a sudden need to determine the water vapour amount more properly than just putting out a hair hygrometer or something like this. Do you think it is practical to get your ρ -w out with a certain confidence, by measuring a baseline of a certain known distance. Do you think it is possible to turn your instrument " around " in some way ?
- A. Yes. Also I think that, if one wants to look at profiles, one could set up a reflector on a sounding balloon, and look at vertical angles, which is probably easier than ranging.
- Q. I tell you that the meteorologists, when they started to study the micrometeorology by sounding, the principle was accepted that we could map all these meteorological factors by taking bases like this and then try to construct vertical temperature gradients etc. Now they are interested in using just vertical angles in the optical case to do the same. In the Uppsala test, where we make such meteorological studies, we will use angles. Then of course one makes meteorological observations at the same time, so we can be confident. As you say, I think it is very important even in his case that he always checks very different conditions in the beginning.
- A. I think you have to always convince yourself. For that matter we have been operating in California close to the Geological Survey, and until we operated, sensing right

at their location, they were rather sceptical about our results, primarily because of the appropriate comment, that there is said so much about the two-colour method, and very little came out of it. And I think that with the close cooperation with them now, our credibility is finally been established.

Q. I would like to ask how much consideration you have given to the question of the zero-constant, the instrument constant or index-error or what you like to call it, because more or less you are thinking in terms of an instrument that will cover a range of let's say, 10 km lines with an accuracy from atmospheric reasons of roughly 1mm, which means you should be able to maintain your instrument constant to at least 1 mm, probably 0,1 mm for at least a certain period of time. And this is, as seems with all other instrumentations also to be very near the attainable limit. Maybe it is the highest demand that is ever been put to an index error. I think this is a very vital point, when you consider this instrument, because it would be extremely difficult to use a difference of 2 mirrors-technique to eliminate the index error.

A. We cannot eliminate the index error.

Q. It will be very difficult to do it by the difference of two mirrors because your mirrors are very complicated involving a micro-wave transponder etc.

A. No, for the device itself the two wavelength portion of it we are not depending upon the micro-wave contribution to determine the instrument constant. It is the optical instrument-constant that we have to determine.

And you do that by simply moving one reticule from one position to another.

I have measured the differences, but it is not the micro-wave transponder, that enters into that determination. We have operated now for 2 years with that instrument and we do continue to monitor the master-crystal, which is as discussed.

You brought up earlier the necessity to really trust some master, some second rate standard if you will and we indeed do that.

I may also add that our components that determine the optical path-length are invar based.

I think I may have not stated clearly what I said.

It is obvious you will have to produce a crystal-oscillator good to somewhat better than one part in 10 millions - let's say one part in hundred millions.

This is quite feasible and this is not a real problem. What I think is, that you really are able to maintain a relation between the, let's call it, the physical center of the instrument and the optical centre of the instrument.

A. But that is mechanical.

Q. Yes, it is, but don't forget that no existing instrument to my opinion has been much better than one μm up till today. You should attain less than one μm to make 10 parts per million over sensible.

A. These kind of things are machine tool accuracies, that are required and known expansion coefficient of materials. And those things are known.

The electrical centre will not be translated from the mechanical centre.

Q. Maybe I'm not following the details, but is this something specific if you use 2 wave-lengths ?

A. No

Q. Then I wonder why the other makers haven't used the same technique to maintain their stability better than 1 μm .

Comment Dr. Bradsell

I would like to say that in fact we had 6 years experience with our prototype mekometer, where we had a resolution of 0,1 μm and we were very conscious of this problem and over that 6 years we read the term in the instrument constant and I think that over that total time it was only a change by a little over a tenth of a μm ., so I think mechanically this certainly is possible. Admittedly this was a small or lighter instrument. I don't know what the Kern-commercial prototype does, but I suspect it is a similar sort of stability. This is necessary with an instrument of this sort and we certainly confirm that in our experiences it can be done.

A. There is another thing before we stop, I have a peculiar feeling about it and that is that usually when we try to investigate how points on the earth-surface are moving, we are not interested to make an absolute determination of the distance between them. If there would be a possibility to just look at changes by some sort of a phase-modulating system, where refraction can be included as a part, then a lot of systematic errors could disappear. This is a strainmeter, which measures the absolute distance, but we are interested in the changes of the distance. Is it not possible to go directly to the difference method instead of making a absolute measurement and then taking the difference between that measurements ? If we take the geodimeter, and disregard anything but the most significant features, that is the phase measurement. Basically we have the 10 cm wavelength only. We really don't know the absolute length, we know only the delta phase if you will.

Q. But you get the absolute distance .

A. I expect we do with our instrument, but on the other hand one can say so does the geodimeter.

Remark: He is right, because you must have a good starting value, you cannot make a long distance measurement with this accuracy, without knowing anything before.

A. Right. Of all these lines we have showed here for example we do not know the absolute length.

Q. This should not be forgotten when we use your instrument. And that is why I ask how is the work, going on with Owens and Thomson in Boulder, because there it is just the direct determination of the distance.

A. No, they do the same thing. They did the same thing

Q. I thought that it was a distance-meter

A. No, it is this instrument. This instrument, is their effort, it started in Boulder and it moved to continuation of their work.

FIRST FIELD TESTS OF AN ANGULAR DUAL WAVELENGTH INSTRUMENT

D.C. Williams, Division of Mechanical and Optical Metrology, National Physical Laboratory, Teddington, Middlesex TW11 0LW, United Kingdom

In the NPL "dispersometer" for measuring angular refraction, combined beams from helium-neon red (633 nm) and helium-cadmium blue (442 nm) lasers are brought to a common focus by a reflecting telescope. Atmospheric refraction produces a small separation between the centres of the two images, which are chopped by a rotating grating. The resulting phase difference between photomultiplier outputs for red and blue is then detected, and serves as a measure of the total refraction.

Initial tests have been performed using a white light source over a 600 m folded path, 1.5 m above flat grass, on overcast evenings at dusk. These showed fairly good correlation between the actual random image wander (sometimes 15 arc seconds during a few minutes of time) and the red-blue difference signal.

Further trials are being carried out with the lasers over a 4 km suburban range at an average height of 30 m, for which the image wander is much smaller. Using a rotatable triple mirror arrangement fitted to the front of the telescope to eliminate systematic errors, some absolute measurements of refraction have been made, on cloudy afternoons in November 1976. Values obtained on different occasions were from 7 to 14 arc seconds, showing satisfactory agreement with published values of temperature gradients.

Systematic errors due to the imperfections of the mirrors appear to be small, confirming the predictions of a theoretical analysis. It has been found that the effects of turbulence can be reduced by dividing the signals by a third signal derived from the light before it is chopped; this should lead to an improvement in accuracy and enable the instrument to work in more adverse conditions.

The "dispersometer" being developed at the National Physical Laboratory for the measurement of angular refraction has been described previously [1,2]. Combined beams from helium-cadmium blue (442 nm) and helium-neon red (633 nm) lasers are brought to a common focus by a Cassegrain reflecting telescope (Fig.1); the aperture is 50 mm and the focal length 1.6 m. Atmospheric refraction produces a small separation between the centres of the images, which can be nulled by tilting a glass compensating plate. The angle of tilt then provides a measure of the refraction. To detect the separation, the images are chopped by a spiral grating rotated by a miniature synchronous motor. The resulting phase difference between photomultiplier outputs for blue and red is indicated by a meter, and can be recorded on a chart.

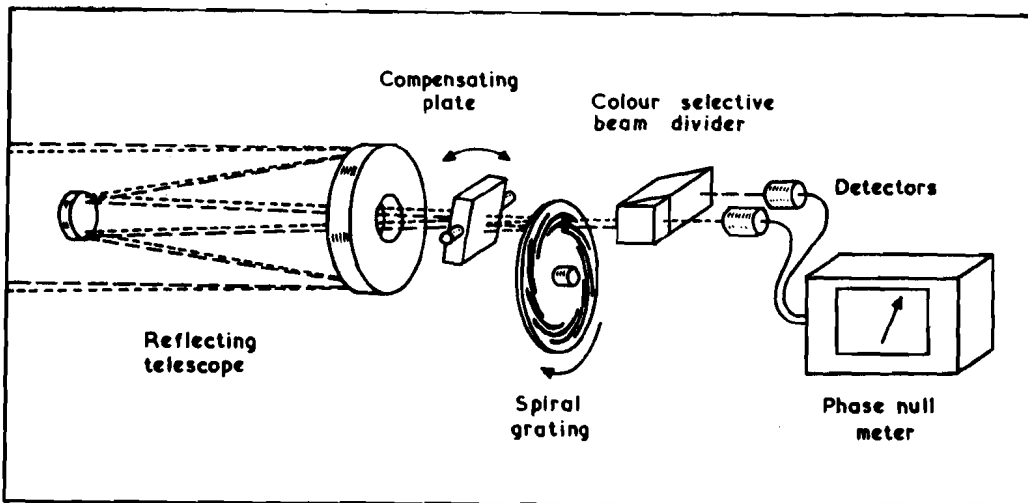


Fig. 1. Dispersometer principle

In the electronic system (Fig. 2), automatic gain control is applied to the a.c. components of the blue and red signals, and they are then subtracted. The difference signal is passed to two phase sensitive rectifiers switched by in-phase and quadrature reference square waves. The in-phase PSR output is used to ensure that the red signal is equal in amplitude to the blue. The quadrature PSR output is then proportional to the blue-red phase difference, and is displayed on the meter. The reference square waves are derived from a voltage controlled oscillator, which is phase locked to the blue signal using a third PSR. One of the references is fed to a divide-by-ten circuit, to produce a frequency equal to that of the sine wave driving the grating motor.

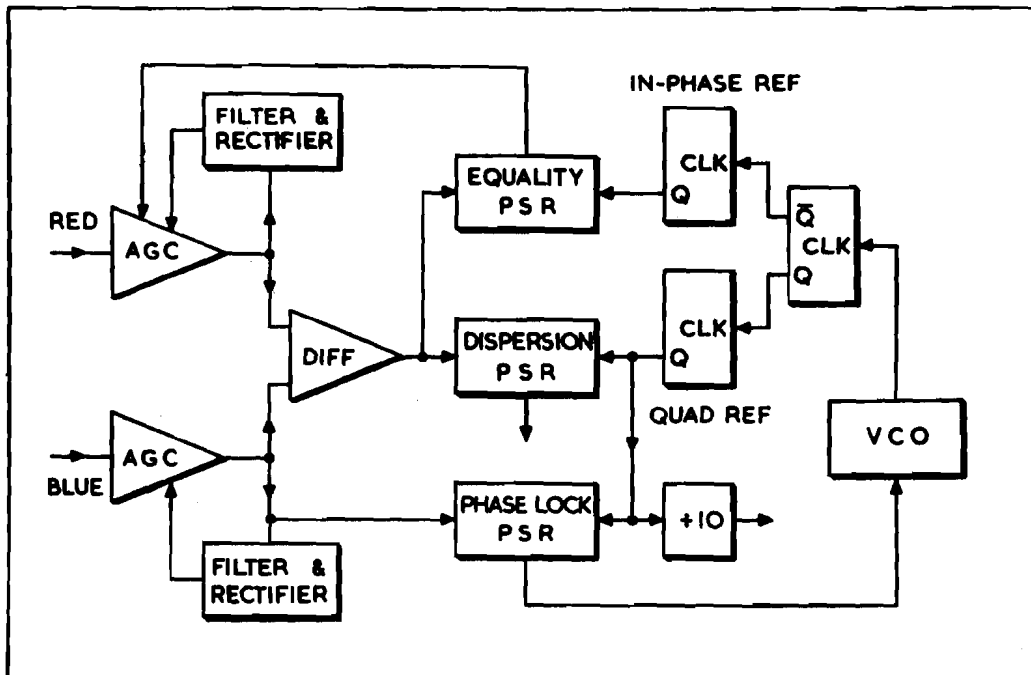


Fig. 2. Electronic system

TESTS OVER 600 m

The first outdoor tests were performed over a flat grass field adjacent to the Laboratory. The dispersometer was mounted on a concrete plinth with the source placed alongside it, the light being reflected from a mirror fixed to a second plinth 300 m away. Thus the effective range was 600 m, 1.5 m above the ground. The mirror surface was flat to better than 0.1 wavelength, and the aperture was 180 mm square, sufficiently large to give negligible edge diffraction effects.

The blue laser was not available for these tests, so the source used was a small tungsten halogen lamp at the focus of a collimating lens, giving an 18 mm diameter illuminated aperture. The geometrical size of the image formed by the instrument telescope was then 50 μm , comparable with the Airy disc diameter of 40 μm (at 540 nm wavelength) and with the grating line width of 55 μm .

When using a white light source, both receiver channels must accept broad bands of wavelengths in order to obtain an adequate signal-to-noise ratio. Unwanted background light then becomes more significant, and to minimize it the instrument has a field stop near the image plane, set to 1.5 mm across. Even so, it was only possible to operate within about one hour of darkness. The aperture has a diamond shape, which facilitates size adjustment and reduces any modulation of the unwanted light by the rotating grating.

The actual movement of the "blue" image due to refraction changes was recorded as well as the blue-red image separation. When the image moves at right angles to the grating lines, the divide-by-ten circuit output is shifted in phase relative to the synchronous motor drive. A further PSR was used to obtain a voltage proportional to this phase shift. The technique requires the dispersometer and mirror to be mounted rigidly, since small tilts would produce spurious image movements. Also, phase slip occurs if the phase locked loop is momentarily unlocked due to a burst of turbulence.

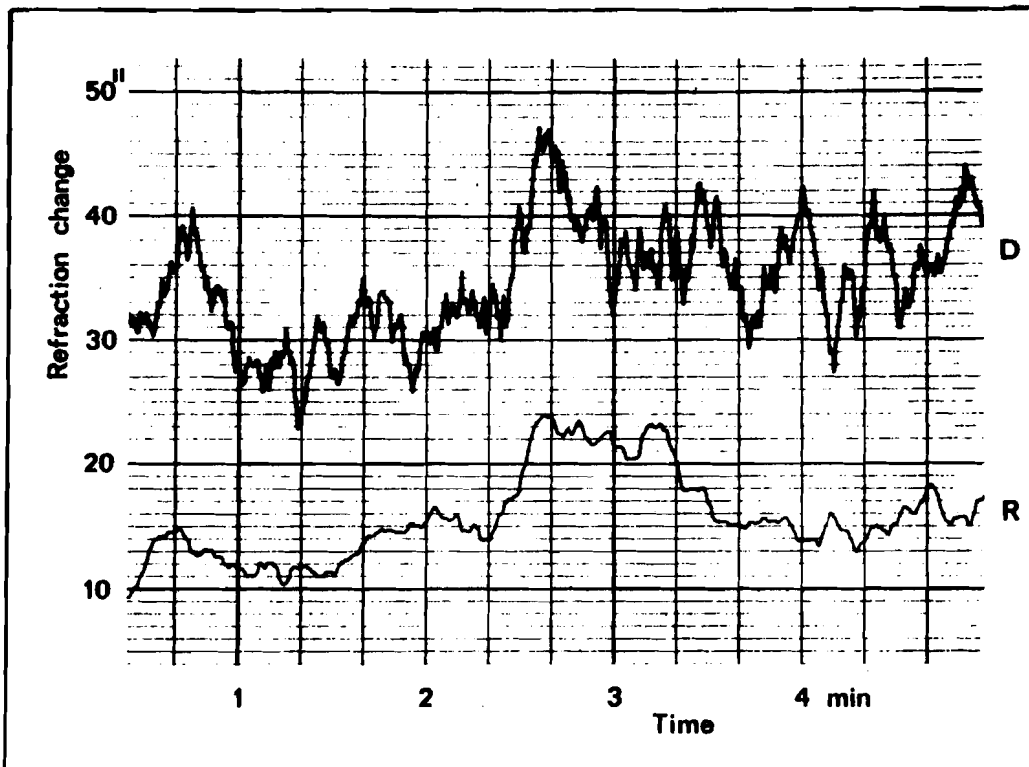


Fig. 3. Recording of dispersion (D) and refraction (R) over 600 m

Fig. 3 shows part of a typical recording (output time constant 4 s) obtained in July 1975 at 2100 GMT. The day and evening were overcast and the wind was fairly light. The random image wander shown by the lower trace is about 15" (arc seconds) peak-to-peak. This was confirmed by visual observation of the image with the grating stationary. In the upper trace, the blue-red difference is magnified by the reciprocal dispersive power of the air for direct comparison with the lower trace, and it can be seen that there is a fair degree of correlation between the two. On a particularly favourable night with gentle rain and a light wind, the image wander was reduced to about 8" and the noise on the blue-red trace was considerably less.

TESTS OVER 4 km

Further tests are being carried out over a range of 4.0 km, using lasers (Liconix model 401 for blue and Spectra-Physics model 120 for red). The dispersometer is located in the tallest building on the NPL site, 20 m from the ground. The lasers are in a building near the brow of Richmond hill, 45 m above the general ground level. The terrain is flat and mainly built-up away from the hill, and the line of sight crosses the river Thames 1.5 km from the receiver.

The power in each laser beam is about 6 mW, and the divergence is 1 mrad. A sighting telescope is provided for pointing the lasers approximately at the receiver, final alignment being accomplished by maximizing the light reflected from a cube corner. Interference filters of 10 nm bandwidth make it possible to operate the instrument in full daylight. With a clear atmosphere, the amount of light received is at least 50 times the minimum required.

The recording of Fig. 4 was obtained in April 1976 at 1800 GMT. Compared with the previous results, the wander of the image over a period of a few minutes was very much less — usually about 1".

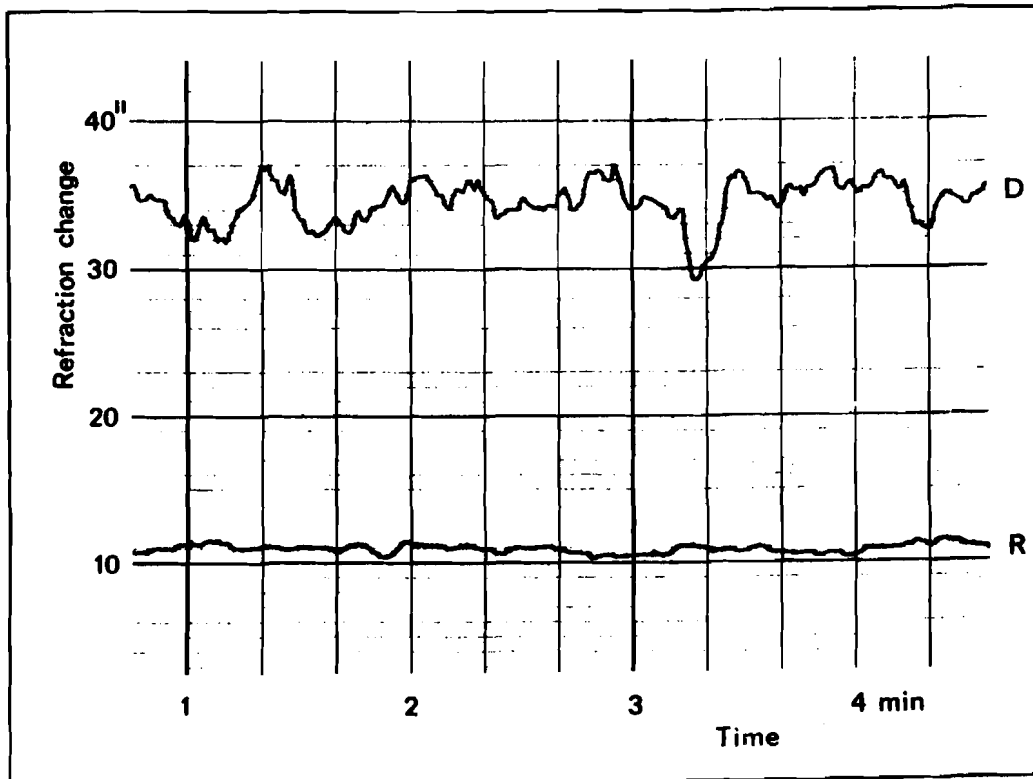


Fig. 4. Recording of dispersion (D) and refraction (R) over 4 km

On most occasions it was impossible to hold the phase lock and obtain a recording of the total refraction for more than about a minute, probably because turbulent gases from chimneys frequently drifted across the line of sight. However, the dispersion output was unaffected unless the phase slipped several times per second, since the circuitry recovers rapidly.

IMAGE ROTATOR UNIT

To make absolute measurements of dispersion, any apparent separation of blue and red images due to instrumental imperfections must be eliminated. This has been achieved by fitting to the front of the instrument telescope an assembly of three flat mirrors (Fig. 5). The assembly is mounted on a barrel held in a pair of ball bearings, so that it can be turned about the optical axis and set at various orientations.

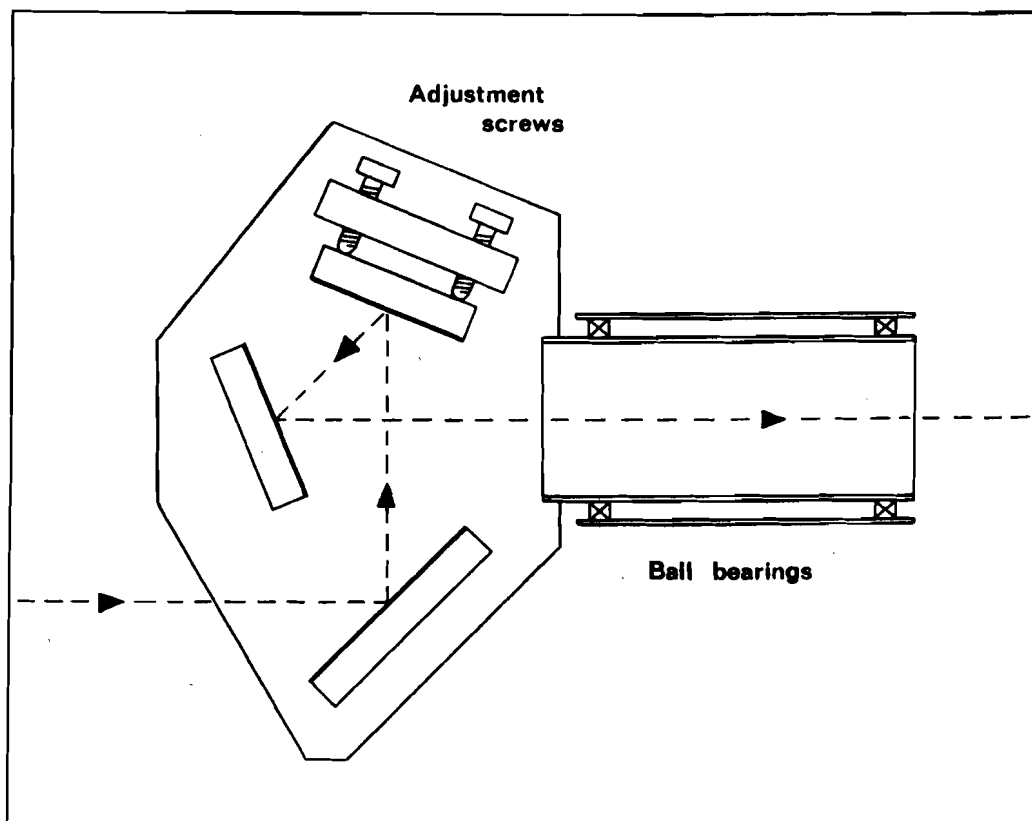


Fig. 5. Triple mirror unit

The output beams rotate through twice the angle of rotation of the unit, so there are two positions at 90° and 270° which do not affect the images, and two positions at 0° and 180° which invert them. Half the difference between readings taken at 0° and 90° thus gives a measure of the dispersion with the instrumental offset eliminated. A further pair of readings at 270° and 180° also eliminates errors due to the mirror assembly itself, and linear drift. The procedure is rather like performing the transit of a theodolite. Four intermediate positions at 45° , 135° , 315° and 225° allow measurement of horizontal refraction.

Any configuration of three mirrors which does not deviate the beam will produce the desired effect; the arrangement adopted affords a relatively compact construction with good mechanical balance. The lateral displacement of the input aperture does not matter, since it is small compared with the diameters of the arriving beams. One mirror can be tilted by two screws until the image returns to the same place on rotation of the unit through 180° , and a further pair of screws (not shown in Fig. 5) enables the rotation axis to be set parallel to the telescope axis.

ABSOLUTE MEASUREMENTS

The following table summarizes the results from some recent measurements, taken in the late afternoon on cloudy days with light wind. For each position of the mirror unit, the dispersometer output was recorded for 3 min and the average value was taken. The individual values are relative to an arbitrary zero.

Date (1976)	Half-way time	Individual results				Refraction VERTICAL
		0°	90°	270°	180°	
Oct 26	1610	-6	+8	+10	-4"	7"
Oct 27	1540	-9	+5	+12	-11	9
Nov 4	1510	-11	+16	+12	-17	14
Nov 4	1615	-11	+11	+10	-12	11
Nov 17	1415	-12	+16	+15	-12	14
		45°	135°	315°	225°	HORIZONTAL
Oct 27	1630	0	-4	0	+4"	-2"
Nov 4	1550	+2	-2	-1	+1	-2
Nov 17	1500	0	+3	0	-7	+2

The uncertainty in the final refraction values is about 2". The vertical measurements accord well with theoretical values calculated from the mean temperature gradients at this height given in [3] for the same months and times of day. The horizontal values obtained were all quite small.

There are appreciable differences between 0° and 180° readings, and between 90° and 270° readings, but they change randomly on different occasions and do not show a noticeable systematic bias. This confirms a theoretical analysis which has been made, indicating that spurious blue-red displacements due to the triple mirror unit and the telescope mirrors are likely to be small.

Suppose that the errors of figure of the mirrors are considerably less than a wavelength, and they are uniformly illuminated. The amplitude at any point on the transmitted wavefront can then be expressed as that due to a perfect undistorted wavefront plus a small component in quadrature representing the phase error. With this approximation, it is found that the position of the centroid of irradiance in the image formed is independent of wavelength, although the detailed distribution of light in the diffraction pattern will vary. The effective image position sensed by the NPL instrument does not correspond precisely to the centroid, but the result still leads one to expect quite small errors.

TURBULENCE EFFECTS

When the photomultiplier signals are displayed on an oscilloscope, the effects of turbulence are similar in character for both 600 m and 4 km ranges. The most favourable feature is that the amplitude fluctuations of blue and red due to turbulence always appear well correlated. This means that the noise level on the difference signal is sufficiently low to allow measurements of useful accuracy.

The fluctuations are usually quite large; 5:1 is typical with moderate cloud cover. In full sunlight, the signal amplitudes are very low for a large proportion of the time, with short bursts of large amplitude. It is thus unlikely that the instrument can be made to function satisfactorily on cloudless days. However, a considerable improvement is always observed towards sunset. The predominant frequencies in the fluctuations are related to the transverse wind speed. For a mean speed of 6 m/s, up to 200 Hz is typical for the 4 km range, considerably lower than the chopping frequency of 1.7 kHz.

It is possible to eliminate the effects of image intensity scintillation by splitting off a fraction of the blue light before it is chopped and passing it to a third detector. The signals after chopping are then divided by the signal before chopping in analog divide circuits. The resultant signals have constant mean levels, and the only remaining amplitude fluctuations are those due to spreading of the image so that it spans more than one grating line width.

This scheme has been successfully tested for the individual signals using one of the two existing photomultipliers for the unchopped light. It is planned to add a third photomultiplier so that both signals can be improved simultaneously. The improved signals do not reduce the tendency of the phase lock to slip, as had been hoped. However, they should make the dispersometer more accurate and allow it to work in more turbulent conditions.

REFERENCES

- [1] Dyson, J. "A method for the determination of the error due to refraction in the atmosphere." Proceedings of XIV International Congress of Surveyors, Washington, D.C., September 1974.
- [2] Williams, D.C. "A dispersometer for the measurement of angular refraction." Proceedings of IAG International Symposium on Terrestrial Electromagnetic Distance Measurements and Atmospheric Effects on Angular Measurements (Vol. 5, Paper 4), Stockholm, August 1974.
- [3] Best, A.C. et al. "Temperature and humidity gradients in the first 100 m over South-East England." Meteorological Office Geophysical Memoirs No. 89 (4th No., Vol. XI), 1952.

1. Einleitung

Für lange Strecken ($s > 5$ km) ist die Genauigkeit der Elektronischen Distanzmessung (EDM) eng mit der Genauigkeit der Erfassung des repräsentativen Brechungsindex längs der Meßstrecke verbunden. Durch Zweifarbenlaser (BRADSELL & SHIPLEY 1974) oder durch Registrierung meteorologischer Daten längs der Meßstrecke über den Einsatz von Flugzeugen (PRESCOTT & SAVAGE 1974) sind zwar Genauigkeiten bis nahezu in die Größenordnung 0.1 ppm möglich, aber mit großem Aufwand verbunden.

In dieser Arbeit soll deshalb untersucht werden, inwieweit das bisherige Verfahren der Endpunktmessungen, d.h. Messungen der Temperatur, Feuchttemperatur und des Druckes nur an den Endpunkten der Strecke, Genauigkeitssteigerungen zuläßt.

Mit Endpunktmessungen ausgewertete Strecken zeigen eine signifikante Differenz zwischen Licht- und Mikrowellenmessungen, die im Testnetz Karlsruhe etwa 2 ppm betragen (KUNTZ 1971). Das mathematische Modell der Auswertung - das sphärische Brechungsindexmodell (HÖPCKE 1964) - trifft größtenteils bei großem Bodenabstand des Meßstrahls zu. An den Endpunkten werden die Temperaturen (trocken und feucht) jedoch nicht repräsentativ für die Meßstrecke ermittelt, denn Ein- und Ausstrahlungsvorgänge über der Bodenoberfläche rufen starke negative wie positive Gradienten hervor, so daß die Temperaturen gegenüber der freien Atmosphäre gleicher Höhe zu hoch oder zu niedrig gemessen werden. Erst ab der Höhe von 30 m über Boden ist das Temperaturfeld nahezu ungestört (BROCKS 1948). Die durch die Temperaturverteilung in der bodennahen Luftschicht bedingten systematischen Modellfehler werden im folgenden mit Temperaturanomalien bezeichnet.

Für Endpunktmessungen mit einem Träger werden folgende Modelle untersucht:

- Messung der Temperaturen in 30 m Höhe.
- Messung in Instrumentenhöhe (1.50 m) und Extrapolation auf 30 m über Austauschbedingungen. Dazu sind weitere Messungen wie etwa die der Sonnenstrahlung, der Windgeschwindigkeit und der Verdunstung notwendig (MAIER 1974).

- Verwendung von statistischen Mittelwerten von Temperaturgradienten in der Unterschicht. Dabei interessiert besonders, unter welchen Bedingungen die Temperaturanomalien verschwinden.

2. Trocken- und Feuchttemperaturgradient

Nach BROCKS (1948) kann für den Temperaturgradienten in der Unterschicht

$$\frac{dt}{dz} = a_t z^{b_t} \quad (1)$$

mit $b_t = -1 \pm 0.2$ geschrieben werden. Der Faktor a_t ist am Tage von der Verdunstung, dem Bedeckungsgrad, der Windgeschwindigkeit, der Temperatur und besonders von der Sonnenhöhe h abhängig. Für Mittelwerte existiert folgende von der Jahreszeit unabhängige Funktion

$$a_t = a + b \sin h. \quad (2)$$

Durch Ausgleichung des Datenmaterials, das BEST (1952) und FRANKENBERGER (1955) über die bodennahe Luftschicht veröffentlicht haben, erhält man mit der Annahme $b_t = -1$ bis zur Höhe 30 m für die Zeit außerhalb der Inversion und für klare Tage, die besonders bei Lichtwellenmessungen zutreffen, die Konstanten a und b signifikant gesichert zu:

$$a = + 0.2 \pm 0.04$$

$$b = - 1.0 \pm 0.07.$$

Die Werte werden auch durch Gradientenmessungen auf den Bodenpunkten des Testnetzes Karlsruhe bestätigt.

Die Temperaturanomalie Δt bei Streckenmessungen am Tage (Abb. 1) kann durch Integration von (1) und dem Ansatz (2) im Mittel mit

$$\Delta t = - (0.2 - 1.0 \sin h) (\ln 30 - \ln z) + \gamma (30 - z) \quad (3)$$

angegeben werden. Hier ist h die mittlere Sonnenhöhe während der Meßzeit, z die Beobachtungshöhe der meteorologischen Daten über Boden und γ der Temperaturgradient oberhalb der bodennahen Luftschicht, deren Höhe im allgemeinen mit 30 m angegeben wird. Für γ gilt im Mittel ca. $-10/100$ m. Im Sommer gegen Mittag ist damit eine mittlere Temperaturdifferenz zwischen der Instrumentenhöhe (1.5 m) und 30 m von rund 2°C

vorhanden. Weiterhin läßt sich feststellen, daß für eine Sonnenhöhe von $h \approx 15^\circ$, d. h. etwa 2 Stunden vor Sonnenuntergang kurz vor Inversionsbeginn $\Delta t = 0$ wird. Damit werden zu diesem Zeitpunkt Lichtwellenmessungen frei von systematischen Fehlern.

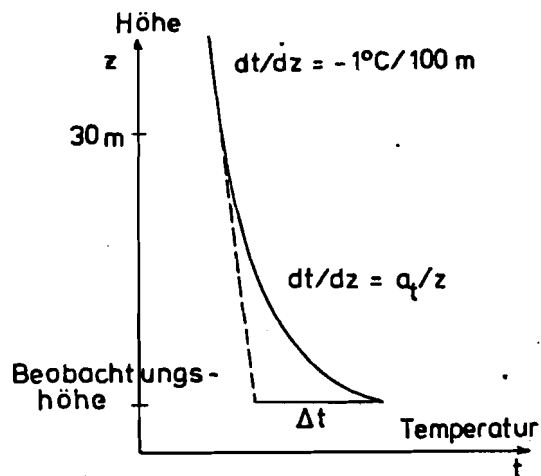


Abb. 1 Temperaturprofil

Zu (1) und (2) analoge Funktionen können auch für den Feuchttemperaturgradienten angegeben werden:

$$\frac{dt'}{dz} = a'_t z^{b'_t} \quad (4)$$

mit $b = -1$ und $a'_t = f(h)$. Für die Feuchttemperaturanomalie gilt mit den Daten von BÉST und FRANKENBERGER

$$\Delta t' = - (0.05 - 0.7 \sin h) (\ln 30 - \ln z) + \gamma' (30 - z) \quad (5)$$

wobei $\gamma' \approx -0.6^\circ\text{C}/100 \text{ m}$ ist.

Die Korrelation zwischen der Sonnenhöhe und den Feuchttemperaturgradienten ist jedoch nicht so ausgeprägt wie bei der Trockentemperatur, aber für den Bereich außerhalb der Inversion auch signifikant gesichert.

Für die Messung mit Mikrowellen kann kein günstiger Messungszeitpunkt angegeben werden, da im Mittel $\Delta t = 0$ und $\Delta t' = 0$ zeitlich nicht zusammenfallen.

Für die Zeit der Inversion können kaum empirische Formeln ähnlich (3) und (5) für die bodennahe Luftschicht bis 30 m Höhe entwickelt werden. Es ist fraglich, ob das vorgeschlagene Modell hier noch seine Gültigkeit besitzt, da die Inversionsschicht mehrere hundert Meter Höhe über Boden erreichen kann (JORDAN-EGGERT-KNEISSL 1966, KLEISS 1963)

und nur unsicher abzuschätzen ist, ob der Meßstrahl innerhalb der Inversionsschicht oder in der freien Atmosphäre verläuft. Deshalb sollten Messungen während der Nacht möglichst nicht durchgeführt werden.

Für Streckenmessungen in der Meßzeit Mittag/Nachmittag ergeben sich aus (3) und (5) folgende systematische Fehler, wenn die meteorologischen Daten in Instrumentenhöhe bestimmt werden: Mit Lichtwellen wird um 1 bis 2 ppm zu lang, mit Mikrowellen wird um 2 bis 4 ppm zu kurz gemessen. Bei der Beobachtungshöhe 10 m verringern sich diese Werte um die Hälfte.

Allerdings kann das oben skizzierte Temperaturmodell nur zur Fehlerabschätzung benutzt werden, da Mittelwerte verwendet werden, die nur für Messungen über ebenem Grasland zutreffen.

Für die Praxis wird deshalb vorgeschlagen, durch Gradientenmessungen von 1.5 m auf ca. 10 m mit mobilen Masten den Faktor a_t in (1) zu bestimmen und auf 30 m zu extrapolieren. Durch eine dritte Meßstelle in ca. 4 m über Boden könnte sogar der Wert des Exponenten b_t überprüft werden.

3. Parallelmessungen

Eine weitere Möglichkeit, systematische Fehler in der EDM bei Endpunktmessungen zu reduzieren, bietet sich durch die gleichzeitige Messung mit Licht- und Mikrowellen (Parallelmessungen) an (KUNTZ & MÖLLER 1971). Hierbei kann mit bereits vorhandenen Geräten (etwa Geodimeter 8 und Tellurometer MRA4) gearbeitet werden.

Bei der Parallelmessung sind zwei Informationen (Messungen), aber drei Unbekannte (s = gesuchte Strecke, Δt = Temperaturanomalie und $\Delta t'$ = Feuchttemperaturanomalie) vorhanden, wenn die Temperaturmessungen in der bodennahen Luftschicht ausgeführt werden. Eine dritte Information kann aus dem mit (1) und (4) beschriebenen Temperaturmodell entnommen werden: Danach ist in einem beliebigen Höhenintervall Δz innerhalb der bodennahen Luftschicht und außerhalb der Inversionszeit das Verhält-

nis $c = \Delta t / \Delta t'$ konstant. Mißt man an den Streckenendpunkten die Gradienten bis etwa 10 m Höhe und führt deren Verhältnis in die Rechnung ein, so kann eine von Temperaturanomalien weitgehend befreite Strecke hergeleitet werden. Die Temperaturanomalie ergibt sich aus:

$$\Delta t = - \frac{c \Delta \sigma}{a_p c - b_p} \quad (6)$$

$\Delta \sigma$ ist die Differenz zwischen den gemessenen Licht- und Mikrowellenstrecken in ppm, a_p und b_p sind von Temperatur-, Feuchttemperatur und druckabhängigen Größen, die bereits bei KUNTZ & MÖLLER (1971) vertafelt sind.

Wegen der großen Bedeutung für die Parallelmessung ist das Verhältnis c , dessen Mittel etwa 1.1 beträgt, auf Abhängigkeiten meteorologischer Parameter hin untersucht worden, um ohne Gradientenmessung auskommen zu können. Wesentliche signifikante Korrelationen sind aber nicht nachzuweisen.

Wie fehlertheoretische Untersuchungen zeigen (FELLETSCHIN 1974), braucht der Wert von c nur auf ± 0.5 bekannt zu sein, um eine Genauigkeit der von Systematik weitgehend befreiten Strecke von ± 0.5 ppm zu erreichen.

4. Messungen und Ausgleichungen im Testnetz Karlsruhe

Zur Überprüfung der oben angeführten Modellvorstellungen können die im Testnetz Karlsruhe durchgeführten Geodimeter-8- und Tellurometer -MRA4-Messungen herangezogen werden (KUNTZ 1971).

Weiterhin stehen zum Vergleich die meteorologischen Daten des Kernforschungszentrums Karlsruhe (KFZ) in ca. 200 m Höhe über Boden zur Verfügung. Diese Höhe entspricht der mittleren Zielstrahlhöhe der im Testnetz Karlsruhe gemessenen Strecken.

In Tab. 1 sind als Beispiel die Ergebnisse der Geodimetermessungen einer Strecke mitgeteilt:

Datum	Meßzeit	I	II	III	IV	V
25.4.69	17.00-20.30	41585.649	.692	.700	-	-
23.5.73	12.00-20.30	.719	.685	.662	.669	.680
12.2.74	11.30-16.00	.698	.658	.698	.684	.698
12.5.74	13.30-19.00	.735	.685	.684	.678	.690
Mittel		.700	.680	.686	.677	.689

Tab. 1 Ergebnisse auf der Strecke Michaelsberg - Madenburg in m

Darin bedeuten: I mit den Temperaturen an den Endpunkten in 1.5 m Höhe meteorologisch reduzierte Strecken;

II Strecken, für die nach dem Modell von BROCKS $\Delta t = 0$ ist;

III nach dem Modell von Monin-Obukhov verbesserte Strecken (MAIER 1974);

IV durch Parallelmessung verbesserte Strecken (FELLETSCHIN 1974);

V mit den Temperaturen des KFZ reduzierte Strecken.

Während die Werte mit den meteorologischen Daten in 1.5 m Höhe noch um 2.1 ppm streuen, differieren die ausgewählten bzw. verbesserten Werte nur noch um 1.0 ppm. Die Mittelwerte der Verfahren II bis V unterscheiden sich maximal sogar nur noch um 0.3 ppm. Das bedeutet, daß die verschiedenen Methoden zu praktisch den gleichen Ergebnissen führen. Die Temperaturanomalien sind durch die verschiedenen Verfahren weitgehend eliminiert worden, da keine signifikanten Unterschiede mehr zu erkennen sind.

Im folgenden sollen neben der normalen Auswertung (Tab. 1 unter I) besonders die mit der Methode der Parallelmessung (IV) erzielten Resultate diskutiert werden. Danach können die Ergebnisse in drei Punkten zusammengefaßt werden:

1. Geodimeterstrecken, die gegen Mittag und am frühen-Nachmittag gemessen wurden, sind im Testnetz Karlsruhe im Mittel um 0.6 ppm zu lang.
2. Durch Parallelmessung verbesserte Strecken und Strecken, die im Mittel 2 Stunden vor Sonnenuntergang gemessen wurden, zeigen keine Maßstabsdifferenz.
3. Bei ca. 5°C sind keine Unterschiede zwischen Licht- und Mikrowellenstrecken festzustellen, bei ca. 20°C sind es dagegen im Mittel 3 ppm, im Extremfall sogar 10 ppm.

Für die Ausgleichungen im Testnetz Karlsruhe (jetzt 11 Punkte) liegen 65 Tagesmessungen mit dem Geodimeter-8 und 145 Tagesmessungen mit dem Tellurometer-MRA4 vor. Davon wurden in den letzten Jahren 34 Tagesmessungen gleichzeitig durchgeführt. Als Gewichtsansatz für die Ausgleichung wird der folgende Ansatz benutzt (HÖPCKE 1965):

$$p = \frac{k}{m^2} \frac{n}{1 + r(n-1)} \quad (7)$$

n = Anzahl der Tagesmessungen auf einer Strecke

m_{GDM8} = ± 8 mm ± 0.7 ppm

m_{MRA4} = ± 9 mm ± 1.4 ppm

r_{GDM8} = 0.2

r_{MRA4} = 0.5

} a priori abgeschätzte Korrelationskoeffizienten.

Die Konstante k wird so bestimmt, daß für $n = 1$ und $s = 30$ km $p = 1$ wird. Die mittleren Fehler werden aus dem Messungsmaterial abgeleitet. Die Korrelationskoeffizienten sind mit dem empirischen Modell nach Gleichung (3) und (5) abgeschätzt unter der Annahme, daß die Temperaturanomalien Δt als "wahre Fehler" aufgefaßt werden können. Die hohen Werte sind darauf zurückzuführen, daß Wiederholungsmessungen sehr oft in gleicher Jahreszeit und von denselben Exzentrenausgeführt wurden. Kreuzkorrelationen sind a priori nicht nachzuweisen.

Mit den an den Endpunkten in Instrumentenhöhe gemessenen Temperaturen - zum Teil auch in 30 m Höhe auf Türmen - wurden folgende Resultate erhalten:

Gerät	m_0	durchschnittl. mittl. relativer Streckenfehler	durchschnittl. mittl. Punkt-lagefehler	Maßstab μ nach einer Helmertransf. zwischen Landes- u. Streckennetz +)
	mm	ppm	mm	ppm
GDM8	± 28	± 0.4	± 17	+ 11.1
MRA4	± 40	± 0.6	± 22	+ 9.0

Tab. 2 Ausgleichsergebnisse

Die Ergebnisse mit rund ± 0.5 ppm zeigen hohe innere Genauigkeiten; das Geodimeternetz mit mittleren Fehlerellipsen nach HELMERT ist in Abb. 2 dargestellt. Als Kriterium der äußeren Genauigkeit kann der signifikante Maßstabsunterschied zwischen beiden Netzen mit 2 ppm angesehen werden.

Wendet man an dieser Stelle das oben beschriebene Temperaturmodell nach Gleichung (3) und (5) an und berechnet aus den mittleren Meßzeiten und den mittleren Beobachtungshöhen der meteorologischen Daten die Anomalien Δt und $\Delta t'$, so erhält man im Mittel unter Verwendung der Differentiale der Formeln von ESSEN & FROOME für Mikrowellen bzw. von BARRELL & SEARS für Lichtwellen (KUNTZ 1971)

$$\Delta s_{\text{GDM8}} = + 0.3 \text{ ppm} \quad \text{bzw. } \mu_{\text{GDM8 Verb.}} = 10.8 \text{ ppm}$$

$$\Delta s_{\text{MRA4}} = - 1.6 \text{ ppm} \quad \text{bzw. } \mu_{\text{MRA4 Verb.}} = 10.6 \text{ ppm.}$$

Die systematische Differenz der Maßstabsfaktoren in Tab. 2 ist damit nahezu aufgehoben. Durch den Modellansatz können also Maßstabsverbesserungen für EDM-Netze angegeben werden. Die Maßstabsverbesserung für das Geodimeternetz ist deshalb so gering, weil das Mittel der Meßzeiten etwa bei drei Stunden vor Sonnenuntergang liegt und damit nur knapp vor der günstigen Meßzeit für Lichtmessungen.

+) Das Landesnetz entspricht dem Deutschen Hauptdreiecksnetz.

PROJEKT :

TESTNETZ KARLSRUHE GEODIMETERMESSUNGEN

MASSTAB $\overline{10 \text{ KM}}$

ELLIPSEN $\overline{2 \text{ cm}}$

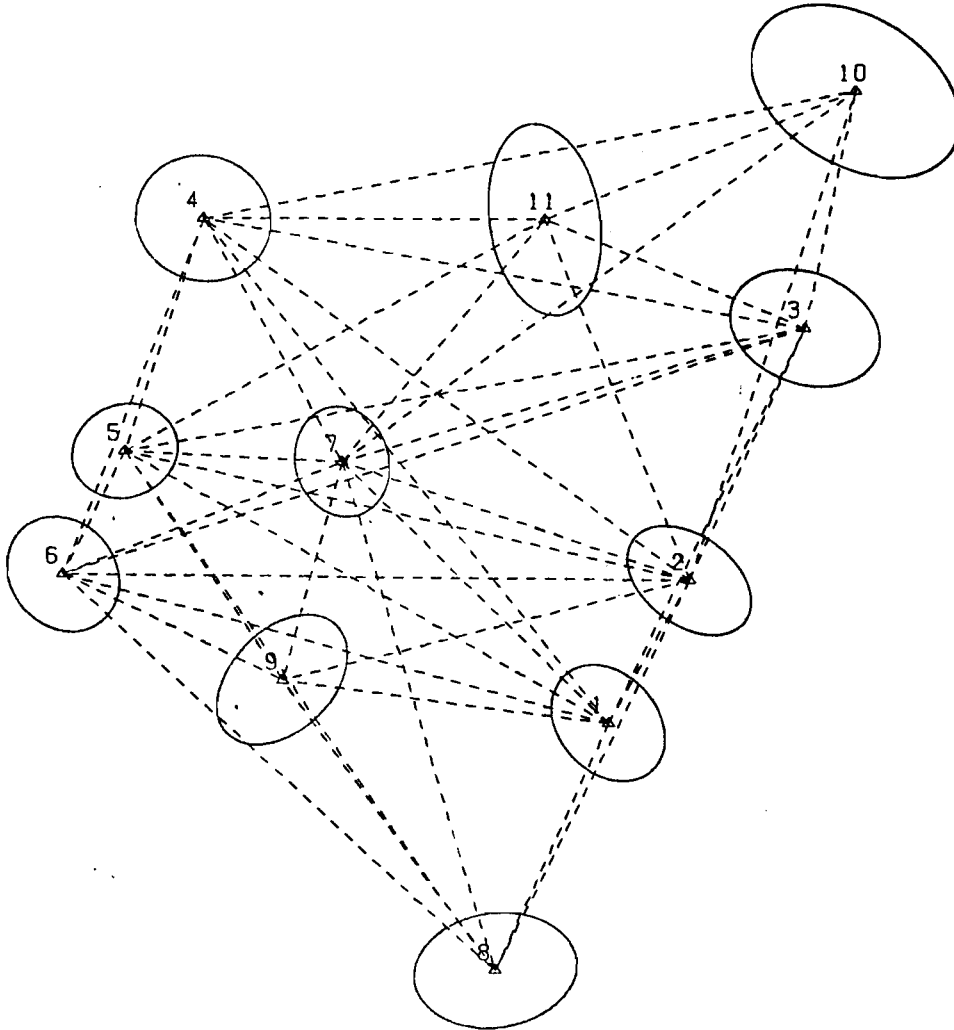


Abb. 2 Geodimeternetz mit mittleren Fehlerellipsen

Die Ausgleichung mit den nach (6) reduzierten Strecken und dem Gewichtsansatz (7) für $m_{\text{par}} = \pm 13 \text{ mm} \pm 0.5$ und $r_{\text{par}} = 0$ ergibt folgendes Resultat:

m_0	durchschnittl. mittl. relativer Streckenfehler nach der Ausgl.	durchschnittl. mittl. Punkt-lagefehler	Maßstab nach einer Helmerttransf. zwischen Landes- und Streckennetz
mm	ppm	mm	ppm
± 17	± 0.3	± 11	± 10.6

Tab. 3 Ausgleichungsergebnisse der Parallelmessungen

Der mittlere Gewichtseinheitsfehler bezieht sich wieder auf eine Tagesmessung bei der mittleren Streckenlänge von 30 km. Gegenüber dem unverbesserten Geodimeternetz ist sogar eine Genauigkeitssteigerung eingetreten, obwohl zur Reduktion wesentlich ungenauere Mikrowellenstrecken benutzt wurden.

Der nach einer Helmerttransformation erhaltene Maßstabsunterschied von 10.6 ppm entspricht den Werten, die durch Verbesserung der Netze mit Mittelwerten von Gradienten erhalten werden. Zum Vergleich können auch noch zwei weitere Werte angegeben werden: MAIER (1974) erhält als Maßstabsfaktor für die nach dem Modell von Monin-Obukhov verbesserten Strecken im Testnetz Karlsruhe 10.6 ppm; durch meteorologische Reduktion mit den Werten des KFZ erhält man als wahrscheinlichsten Maßstabsunterschied im Testnetz Karlsruhe zwischen Streckennetz und Landesnetz 10.7 ppm.

Mit der geschätzten Maßstabsunsicherheit von ± 0.3 ppm und den mittleren durchschnittlichen Fehlern nach der Ausgleichung von ± 0.3 ppm kann für die Strecken im Testnetz Karlsruhe als mittleren Fehler ± 0.4 ppm angegeben werden.

5. Restfehler und Korrelationen

Die aus der letzten Ausgleichung erhaltenen Strecken stellen die zur Zeit wahrscheinlichsten Strecken des Testnetzes Karlsruhe dar. Mit den Differenzen dieser ausgeglichenen Strecken zu den gemessenen Sätzen der Geodimeter- und Tellurometerstrecken sind Restfehleranalysen und Korrelationsuntersuchungen möglich. Die Differenzen können in erster Näherung als "wahre Fehler" angesehen werden.

Zunächst zu den Restfehleranalysen: Hier geht es um den Nachweis des empirischen Temperaturmodells, d. h. der Abhängigkeit der Restfehler von der Sonnenhöhe (bzw. Tageszeit) und von der Höhe der meteorologischen Beobachtungsstation über Boden.

Aus den Restfehlern der Geodimetermessungen (Abb. 3) läßt sich die Abhängigkeit von der Sonnenhöhe durch die signifikant gesicherte Funktion

$$\Delta s_{\text{GDM8}} = - 0.55 + 1.40 \sin h \text{ (ppm)}$$

angeben.

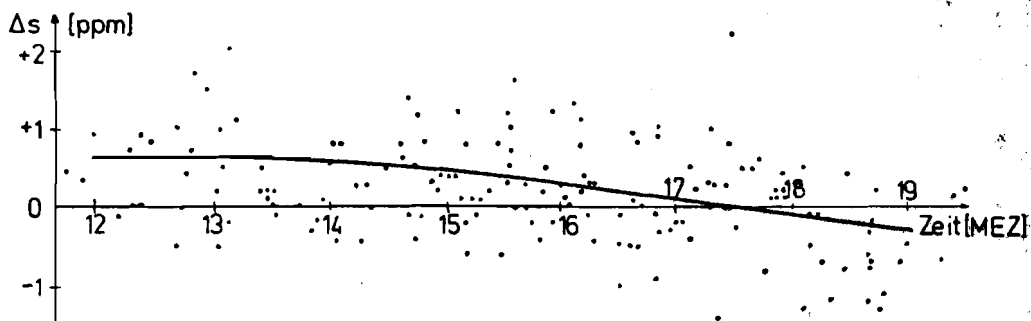


Abb. 3 Restfehler der Geodimetermessungen

Hieraus ergibt sich bei der mittleren Höhe der Meßstellen über Boden von 8 m, die durchschnittlich für die Punkte des Testnetzes Karlsruhe gilt, die Funktion

$$a_t = + 0.3 - 1.1 \sin h,$$

deren Konstanten mit denen aus Gleichung (2) identisch sind.

Während aus den Restfehlern der Geodimetermessungen eine Abhängigkeit von der Höhe der meteorologischen Meßstelle nicht signifikant nachzuweisen ist, kann aus den Restfehlern der Tellurometermessungen eine solche Abhängigkeit nachgewiesen werden.

Man erhält

$$\Delta S_{MRA4} = - 3.8 + 1.1 \ln z \quad (\text{ppm}) .$$

Hier ist die Abhängigkeit signifikant gesichert. Gleichung (3) kann damit für die Berechnung systematischer Temperaturfehler im Testnetz Karlsruhe benutzt werden.

Für die Feuchttemperaturanomalien nach Gl. (5) ist nur für die sich aus der mittleren Meßzeit ergebende Sonnenhöhe von 40°, nicht dagegen für andere Sonnenhöhen Übereinstimmung zwischen Modell und Praxis festzustellen. Hier spielen sicherlich mehrere Punkte eine Rolle:

1. Die aus den Restfehlern der Geodimetermessungen hergeleitete Abhängigkeit von der Sonnenhöhe muß auf die Tellurometermessungen übertragen werden, die im Mittel zu ganz anderen Zeiten ausgeführt wurden.
2. Die Korrelation zwischen h und a'_t ist nicht so stark wie zwischen h und a_t .
3. Bei GEIGER (1961) wird gezeigt, daß durch den täglichen Gang des Partialdampfdrucks und damit der Feuchttemperatur besonders am Nachmittag, der Hauptmeßzeit im Testnetz Karlsruhe, bis zu 70 m hohe Luftschichten beeinflusst werden.

Nach Elimination der signifikanten Zeit- und Höhentrends kann eine Berechnung der Korrelationen erfolgen, die dann nur noch vom Zeitunterschied $\Delta\tau$, und nicht mehr von der Zeit τ selbst abhängig sind.

Für Geodimetermessungen sind danach in den ersten zwei Stunden signifikante Autokorrelationen festzustellen (Abb. 4) die sich genähert durch eine Funktion von der Form

$$r(\Delta\tau) = a e^{-b^2 \Delta\tau^2} \quad (8)$$

mit $a \approx 0.9$, $b \approx 0.6$ und $\Delta\tau$ in der Dimension Stunden darstellen lassen.

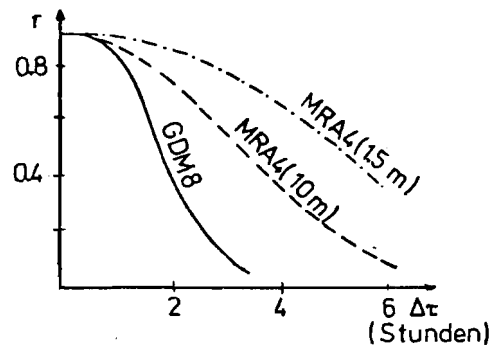


Abb. 4 Autokorrelationsfunktionen

Für Tellurometermessungen, deren meteorologische Daten in mindestens 10 m Höhe über Boden ermittelt werden, erhält man mit dem Ansatz (8) bereits $b \approx 0.25$: Der Autokorrelationskoeffizient fällt erst innerhalb von 6 Stunden von 0.9 auf 0.1 ab. Für Tellurometermessungen, deren meteorologische Daten in ca. 1.5 m Höhe gemessen werden, fällt r sogar nur von 0.9 auf 0.4 - hier ist $b \approx 0.15$ - .

Weitere Aussagen für $\Delta\tau > 1$ Tag sind wegen des zu geringen Beobachtungsmaterials und wegen der deshalb nicht signifikant feststellbaren Korrelationen problematisch. Allerdings decken sich die Werte, die aus den Messungen des Testnetzes Karlsruhe ermittelt wurden mit denen, die bereits an früheren Untersuchungen bekannt geworden sind (z. B. HÜPCKE 1965).

6. Zusammenfassung

Die Hilfe von verschiedenen Modellen (KUNTZ & MÜLLER 1971, MAIER 1974, FELLETSCHIN 1974) ist es möglich, Endpunktmessungen der Trocken- und der Feuchttemperatur zu verbessern und eine von Temperaturanomalien weitgehend befreite Strecke herzuleiten. Die Ergebnisse der verschiedenen Modellvorstellungen liegen sehr eng zusammen und lassen vermuten, daß Restfehler bei ca. ± 0.5 ppm liegen. Damit kann auch ohne großen Aufwand in der EDM eine Genauigkeit erreicht werden, die mit der von Zweifarbenlasern (BRADSELL & SHIPLEY 1974) vergleichbar ist.

Literatur:

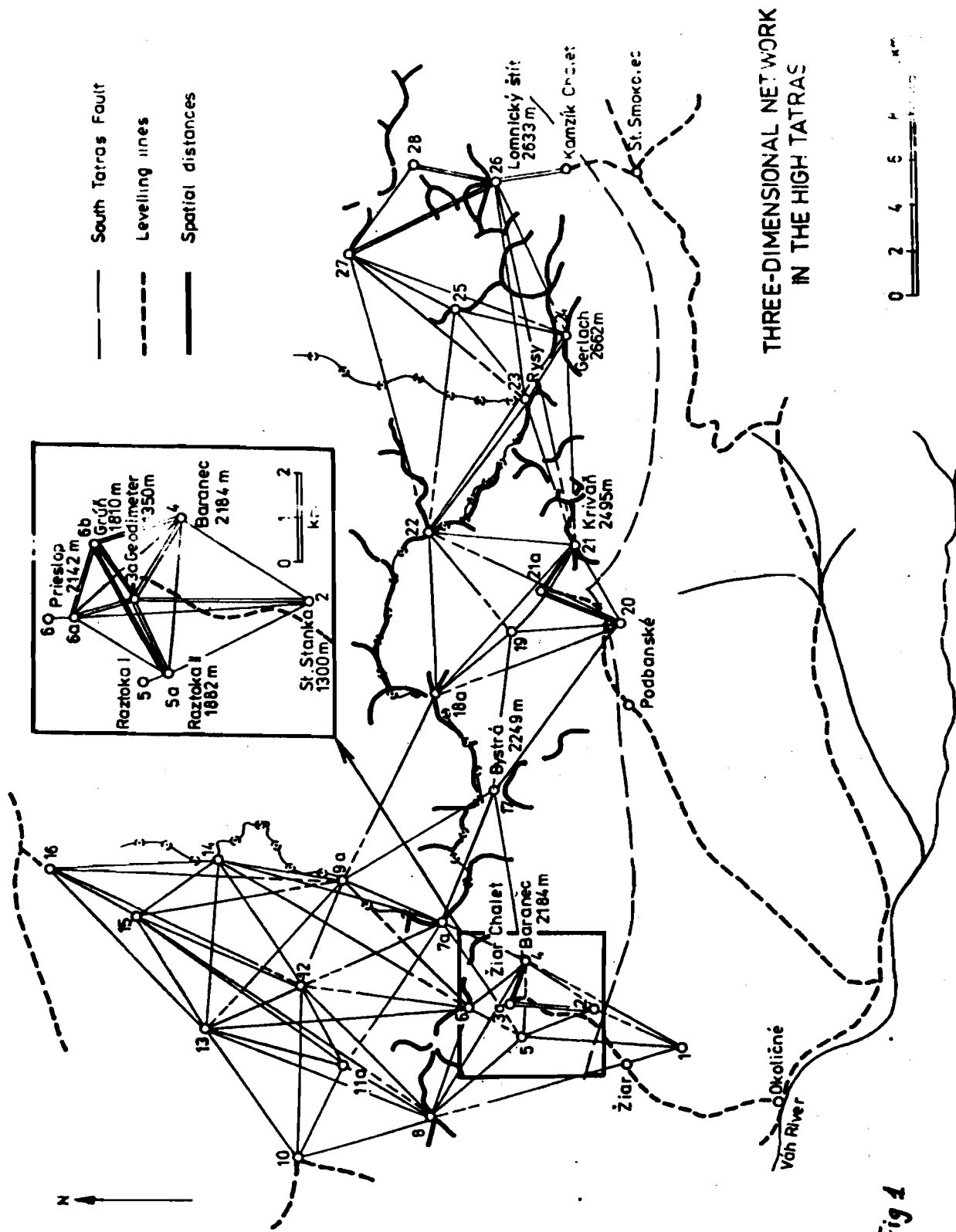
- BRADSELL, R.H. Georan I, a new two-colour laser ranger,
IAG-Kongreß Stockholm 1974
- BEST, A.C. Temperature and humidity gradients in the first
100 m over South-East-England
Geoph. Mem. 89/1952
- BROCKS, K. Über den täglichen Gang der Temperatur
Ber. des dt. Wetterdienstes 5/1948
- FELLETSCHIN, V. Comparison between light and microwave measure-
ments in the test area of Karlsruhe
IAG-Kongreß Stockholm 1974
- FRANKENBERGER, E. Über vertikale Temperatur-, Feuchte- und Windgra-
dienten in den untersten 7 Dekametern der Atmosphäre
Ber. des dt. Wetterdienstes 10/1955
- GEIGER, R. Das Klima der bodennahen Luftschichten
4. Aufl. Braunschweig, 1961
- HÖPCKE, W. Über die Bahnkrümmung elektromagnetischer Wellen
und ihren Einfluß auf die Streckenmessung
Zeitschrift für Vermessungswesen 6/1964
- HÖPCKE, W. Eine Studie über die Korrelation elektronmagne-
tisch gemessener Strecken
Allgemeine Vermessungsnachrichten 4/1965
- KLEISS, M. Inversionen in der unteren Troposphäre im Raum
Karlsruhe-Stuttgart
Ber. des dt. Wetterdienstes 90/1963
- KUNTZ, E. Elektronische Entfernungsmessung auf Teststrecken
und im Testnetz Karlsruhe
Deutsche Geod. Kommission, Reihe B 182/1971
- KUNTZ, E. Gleichzeitige elektronische Entfernungsmessung
MÖLLER, D. mit Licht- und Mikrowellen
Allgemeine Vermessungs-Nachrichten 7/1971
- JORDAN-EGGERT- Handbuch der Vermessungskunde
KNEISSL Band VI Stuttgart 1966
- MAIER, U. On estimation of the representative temperature
for the reduction of electro-optical distance
measurement
IAG-Kongreß Stockholm 1974
- PRESCOTT, W.H. Precision of Geodolite distance measurements
SAVAGE, J.C. IAG-Kongreß Stockholm 1974

DETERMINATION OF CRUSTAL MOVEMENTS BY THREE-DIMENSIONAL TRIANGULATION

Ludvík Hradilek, Faculty of Science, Charles University, Prague, Czechoslovakia

In the last 2 decades, different kinds of observational data have been tested at the Department of Applied Geophysics, Charles University [Hradilek, 1958a, 1958b, 1959, 1960, 1962, 1963, 1968a, 1968b, 1972, 1977] for precise evaluation of heights in mountainous areas. Steep distances measured by a geodimeter proved to be of a fundamental importance to create a basic pattern for a three-dimensional terrestrial triangulation. The three-dimensional triangulation can be considered a leading method for determination of mutual position of mountain peaks. In the years 1961/62, a three-dimensional network was established in the region of the Žiar-Valley in the West Carpathians (Fig.1). Spatial distances inclined as much as 30 degrees of arc were measured by a geodimeter NASM2A, horizontal and vertical angles were observed by Wild T2, T3 theodolites. Terrestrial refraction was overcome largely by a special observation, weighting and elaborating-procedure for vertical angles. Standard deviations of 9 and 13 millimeters in the estimates of horizontal and vertical coordinates of the peaks was a promising result with respect to the possibility of determination of the crustal uplift in this region. In the years 1963/64, the three-dimensional network was extended to the whole area of the High Tatras.

For the reconnaissance of the uplift, three spirit levelling lines were repeated in the year 1974. They proved a significant uplift of 50 mm in the Žiar-Valley within a time interval of 13 years. In the granite part of the High Tatras minor uplifts of 10 and 16 millimeters within 11 years were found. This result stimulated a renewal of spatial triangulation in the Žiar-Valley in the year 1975. The precision of the renewed network corresponds to that of the original one. Spatial distances were mea-



THREE-DIMENSIONAL NETWORK
IN THE HIGH TATRAS

Fig 1

sured by AGAS geodimeter. The observation time required for one distance dropped from two or three nights in the year 1961 to about 50 minutes in the year 1975. The changes in elevation differences determined by three-dimensional triangulation are given in Table 1.

Table 1. Changes in elevation differences determined by three-dimensional triangulation within 13 years

End point of levelling line	Point on the peak	Change in elevation difference	Standard deviation of the change in elev.dif.
Geodimeter - Baranec		+ 42.0 mm	16.5 mm
Geodimeter - Prieslop		+ 18.0	15.3
Geodimeter - Rasztoka		+ 17.0	19.5

The peak Baranec is formed by a special tectonic unit and the change in its elevation difference seems to be evident. The other two peaks are situated on another mountain ridge and the magnitude of their change in elevation equals to the estimates of standard deviations. The evidence for the reality of the changes is supported by the fact that all changes show the same positive sign and match the change in elevation of the end point of spirit levelling line, i.e. Geodimeter point in Fig.2. The change in elevation evaluated by spirit levelling is composed in its major of 58 mm/13 years, determined in the Žiar-Valley, and its minor part of 10 mm/13 years. The latter corresponds to the uplift of the nearest first-order levelling point Okoličné in the elevation system of the Slovak Socialist Republik. The total uplifts of the peaks surrounding the Žiar-Valley are estimated to be 6.6 mm/year and 8.4 mm/year, with a standard deviation 1.5 mm/year, i.e. roughly 7 mm/year above the Baltic- and Black-Sea levels. This value seems to be too large with respect to the uplifts of the Alps evaluated by releveling [Levallois,1972]. However, the results obtained by releveling in two other regions in the West Carpathians, i.e. in the Malé Karpaty and Nitrianská pahorkatina, support our results obtained in the Žiar-Valley [P.Marčák, Personal communications, 1976].

Further Investigations

The promising results in determination of crustal uplifts obtained by use of three-dimensional triangulation in the West

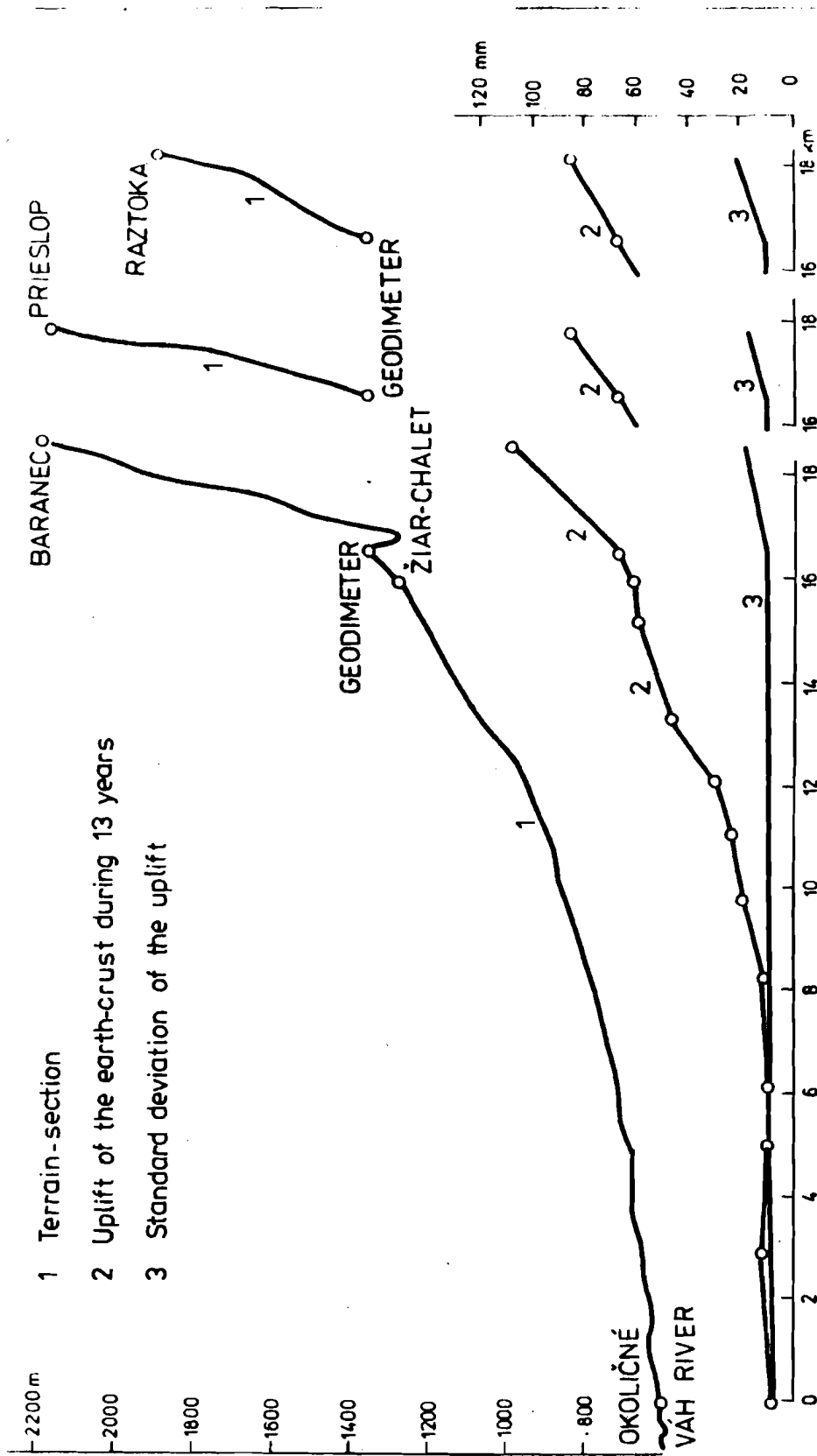


Fig 2 UPLIFT OF THE EARTH-CRUST IN THE ŽIAR-VALLEY

Carpathians are to be considered as preliminary ones. To verify the recent results and to improve the accuracy of the method used, further investigations are necessary.

i) Spirit levelling is to be investigated for systematic errors which play a much more important role in mountains than in plains.

ii) The method for evaluation of terrestrial refraction from vertical angles has its limits in elevation precision characterised by a standard deviation of about 13 mm and 25 mm for average distances of about 3 km and 6 km, respectively. For higher precision, the method should be completed or replaced by direct measurement of refraction angles designed by Tengström^{*)} or by Prilepin.

iii) The problem of vertical angles disturbed by terrestrial refraction may be avoided by total exclusion of vertical angles from our observations and by drawing the majority of information from spatial distances. This procedure may yield a significant increase of accuracy when top-precision ranging instruments are used, and one steep distance at least radiates from each point of the three-dimensional network; the inclination of the distance being about 15 degrees of arc or larger. A theoretical investigation has been made on the network in the Žiar-Valley simulating a standard deviation of 0.67 second of arc for all horizontal directions and an accuracy of 1 part per million for all spatial distances (with an alternative of 2 parts per million for steep distances radiating from the point 3a). The estimates of standard deviations of adjusted coordinates are given in Table 2.

Table 2. Standard deviations of coordinates estimated by the adjustment of simulated observations

Point No.	3a	4	5a	6a	6b
m_x	2.2 mm	2.5	2.3	2.2	2.2
m_y	2.1	2.3	2.3	2.2	2.2
m_z	3.2	7.1	6.4	4.5	4.8
m_x	2.2	2.6	2.3	2.3	2.2
m_y	2.2	2.3	2.3	2.2	2.3
m_z	4.7	9.8	9.2	6.1	6.2

The results given in the upper part of the table correspond to the standard deviation of 1 part per million, assigned to all

*) Prof. Tengström's IDM-observations show an agreement of the order of one centesimal second of arc with refraction angles calculated from simultaneous vertical angle measurements and from spirit levelling [E. Tengström, Personal communications, 1975].

spatial distances; in the lower part is an alternative solution with 2-parts-per-million accuracy for steep distances radiating from the point 3a.

iv) The spatial network in the Žiar-Valley has been adjusted as a "free network", i.e. four columns more, corresponding to the coordinates x_3, y_3, z_3, y_4 , have been incorporated into the observation equations matrix. The full rank of the matrix was completed by its bordering with four rows orthogonal to the original rows of the matrix. A new procedure has been developed to evaluate the elements of the bordering rows. The first three bordering rows consist from naughts and ones, and may be written without any computation immediately; the elements of the fourth row are evaluated from the orthogonality conditions by a simple computation.

R e f e r e n c e s

- Hradilek, L., Bestimmung der relativen Lotabweichungen und des Refraktionskoeffizienten beim Ausgleich trigonometrisch gemessener Höhennetze. *Studia geoph. et geod.* 2, 101-121, 1958a; 3, 334-359, 1959; 4, 217-232, 1960.
- Hradilek, L., Höhenbestimmung aus elektrooptisch gemessenen Längen. *Studia geoph. et geod.* 2, 206-212, 1958b; 6, 317-329, 1962.
- Hradilek, L., Space Triangulation in the Western Part of the High Tatras. *Studia geoph. et geod.* 7, 330-336, 1963.
- Hradilek, L., Spatial Triangulation in Mountain Regions. *Acta Univ. Carol. (Geogr.)* 1, 29-40, Praga, 1968a.
- Hradilek, L., Genaue trigonometrische Höhenmessung und Raumtriangulation in der Praxis. *Zeitschr. f. Verm.* 93, 404-410, 1968b.
- Hradilek, L., Refraction in Trigonometric and Three-Dimensional Terrestrial Networks. *Canad. Surv.* 26, 59-70, 1972.
- Hradilek, L., Bestimmung von Erdkrustenbewegungen durch dreidimensionale Triangulation. *Zeitschr. f. Verm.* 102, 57-63, 1977.
- Levallois, J.J., Sur la mise en evidence d'un mouvement de surrection des massifs cristallins Alpains. *Bull. Géod.*, No. 105, 299-318, 1972.

Discussion (paper 16)

Q. Professor Hradilek made sensation already in Vienna in 1967, by treating the refraction the way he did, and several other people have continued, not in mountainous areas. I know professor Ramsayer has treated a similar problem but in more flat areas, where he can make a different estimate of the refraction coefficient. You are forced to use the k-value at the observation site, but he prefers to make some more realistic mean values over the distance. You cannot do that because you cannot climb the peaks for local observations.

I have a question: You need spirit levelling, you have geometrical angles and distance measurements in your net. Have you taken into account your extensive material of gravity measurements in order to transfer the levelling results to be used in the geometrical system. You are in a favourable position there.

A. Yes. The gravity network is quite dense in this area. It was necessary to take it on the slopes, with two points about $1/3$ and $2/3$ on the slopes in order to complete the network. A computer programme has been designed, and the resulting values of the deflections of the vertical have been used to check our values, which have been estimated from astronomical measurements. The difference was about 1.5 sec. of arc. Professor Pick, however, assumes that the precision of the vertical measurements is satisfactory for the estimate of the refraction of the vertical angle as 0.5 sec. of arc and I believe that he is right. We have checked our results with his and the differences in the geoidal height, deduced from the three dimensional triangulation and by other methods and by Prof. Pick's gravity measurements are only 1.5 cm. (? ed) maximum.

Q. May I ask why you deliberately assumed the steep distances were only good to 2 ppm, where for the other distances you said 1 ppm.

A. I am not an expert in ranging, but I realised that the data taken at the end points are not representative enough for the steep distances, because there may be quite substantial

differences in the temperature, in the mid point of the line and the end-point.

I have used both of them, because I think the meteorology plays a significant role in this.

Q. I would say if you have a very strongly sloping line in EDM then of course you might be forced to take into consideration the second order derivative, with respect of the value of the refractive-index. But it turns out that if the line is just reasonably short, the proportionality factor is the difference of the height multiplied by the length of the line.

The length of the line is reasonably small here and therefore I think actually there is not much reason even if you use a very simple model of the atmosphere by just using the average value, corrected sufficiently for curvature and velocity, which is easy to do.

Then I think the short line should be measured quite as well as the long one just by the ordinary procedure, so my question is would they not be more homogeneous if you had assumed that your sloping lines also would be of a one part of the million quality ?

A. Absolutely, differences do exist. Only for shorter distance than 2 or 3 km it is convenient to use this refraction model.

Q. I would share your precautions about the meteorology measurement of EDM between valley and mountain peaks because, from meteorology you know that in the middle of the slope there will be the warmest zone because people grow the vinyards, because it is warm there; in the valley you would have an inversion-layer, which in many valleys can stay all year long.

And so, I would think that if you just take the average of the mountain and the valley, you are not getting a representative value for the line.

And so I think that those sloping lines, which you mentioned have to be treated very carefully, as you pointed out.

A. Yes, Thank you.

THE USE OF RADIOFREQUENCIES FOR ELECTRONIC POSITIONING SYSTEMS AND THE APPLICATION IN SERCEL'S SYLEDIS

S. Stellingwerff Beintema, Radio-Holland B.V., Amsterdam, The Netherlands

After World War II, the application of radiofrequencies for location of vessels and other crafts has found a wide-spread use.

A large number of systems have been developed for different applications.

For global navigation of merchant vessels the low frequencies (10 - 100 kHz) are used in Omega, Decca-Navigator, Loran C.

The used radio-waves follow the curvature of the earth, thus giving a coverage over a wide area.

Positional accuracies are low (upto 1 mile) and one is influenced by atmospheric conditions.

For a number of applications much higher accuracies are required, which followed to the development of systems, using the 2 MHz band.

This resulted in higher accuracies, but shorter ranges, due to the fact that the radio-waves do not follow the earth curvature as easily. Still one is influenced by atmospheric conditions.

The use of still higher frequencies, 200 MHz to 10 GHz, eliminated the influence of the atmosphere, but limited the range to the so-called line-of-sight.

Accuracies are very good (a few meters) but the requirement of long range forces the operator to seek high locations for the shore-stations.

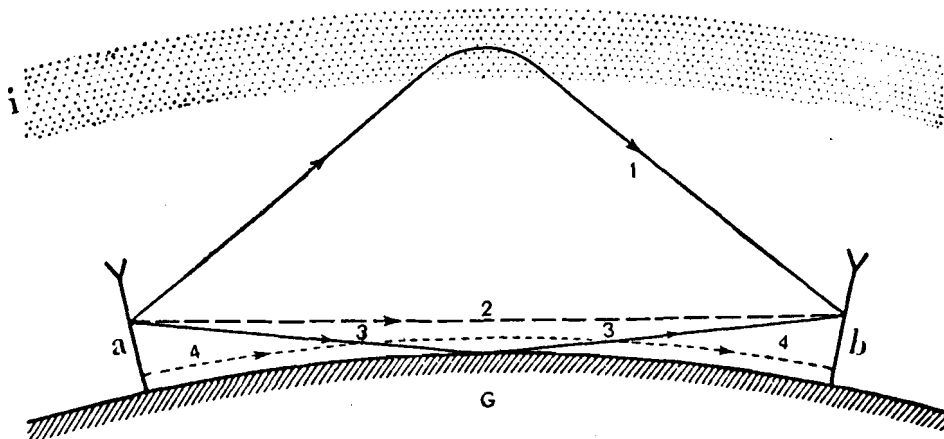
Sercel has developed the Syledis system, which operates in the 420 - 450 MHz band, and with which system it is possible to measure distances beyond the horizon. Special correlation techniques are used to compare the very weak received signals and process them to present ranges.

1. Propagation of radio-waves

The atmosphere has an important influence on the propagation of radio-waves. Radio-waves with a long period follow the earth quite easily, where short waves mainly follow a direct path and can therefore not be received at long distances from the transmitter, due to the curvature of the earth.

We will shortly describe the different waves.

We can divide the waves in the ground- and sky-waves, where the ground-waves are further subdivided in direct, surface and ground-reflected waves.



G = Ground	1 = Sky wave
a = Transmitting aerial	2 = Direct wave
b = Receiving aerial	3 = Ground reflected wave
i = Ionosphere	4 = Surface wave

figure 1

The path, followed by a radio-wave is a direct result of the frequency, and this results directly in the size of the area which can be covered from a transmitter.

1.1. Effects of ionosphere

An important effect on the propagation of radio-waves is the degree of ionisation. The ionosphere can be considered as consisting of different layers, each with an own degree of ionisation.

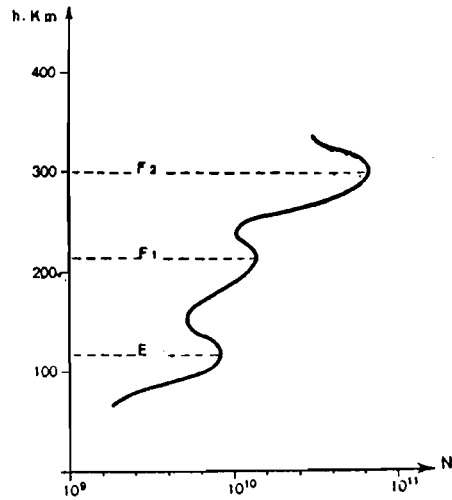


figure 2

Thus it is possible to regard the ionosphere in optical terms, where each layer has a refractive index, following the formula

$$n = \sqrt{1 - 81 \frac{N}{f^2}}$$

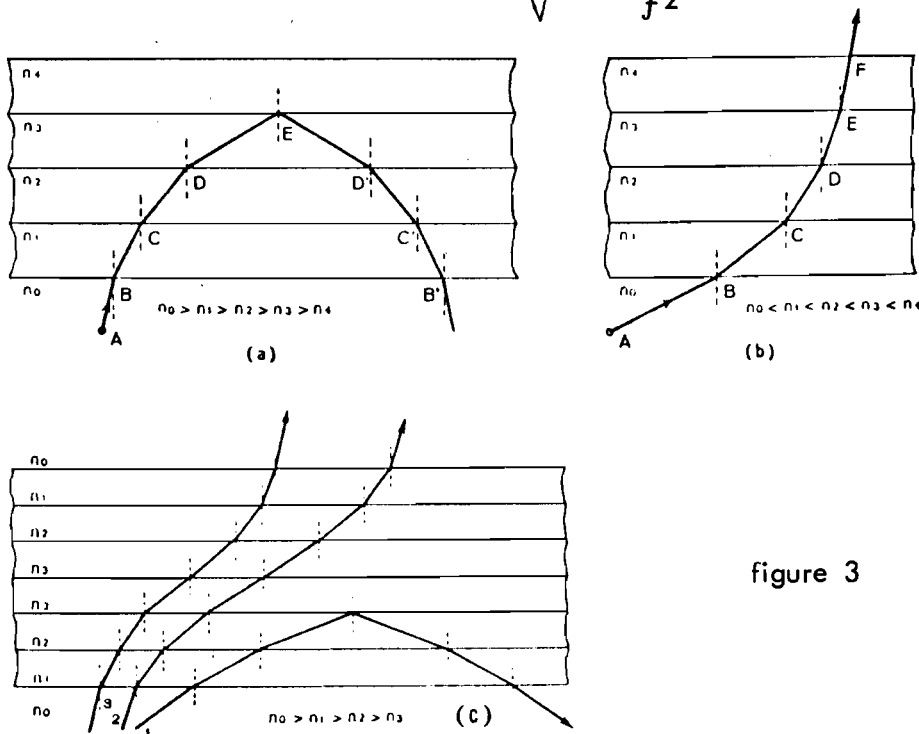


figure 3

Depending on the frequency, the wave will be refracted more or less by passing from one layer to the next. It can be seen in the formula that a higher frequency f will result in a figure n , closer to 1, and thus less refraction. It is then easy to understand that long waves will travel long paths between the ionosphere and the earth, where they are reflected again and up to the ionosphere again. These low frequencies will thus travel a long time, covering wide areas.

The shorter waves will penetrate further in the ionosphere, before returning to the earth.

During its path the radio-waves are attenuated, but the main attenuation takes place at the reflection to the earth. For shorter waves the attenuation is more than for longer waves, which is a second explanation for the wider coverage of longer waves.

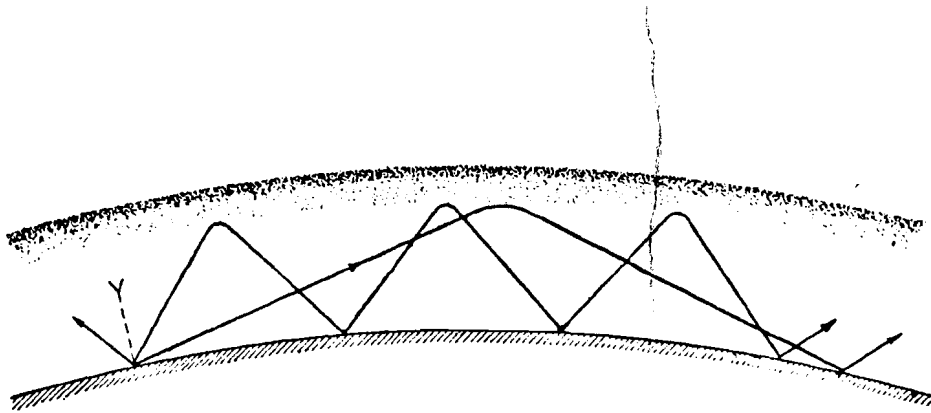


figure 4

Still shorter waves, shorter than 10 meters can be regarded as travelling linear, due to the refractive index which is now nearly 1.

1.2. Propagation of very short waves, effects of the troposphere

As the Syledis system, which is described later, uses wavelength of approximately 70 centimeters (frequency 420 to 450 MHz), we will develop the properties of propagation of such waves.

Usually one considers that 70 cm, or shorter, waves propagate up to the horizon or 10% beyond. In fact, up to the horizon, the signal-strength decreases with the distance, with an average rate corresponding to that in free space.

Signals are only effected by spatial pseudo-periodic increasing and decreasing, which corresponds to the interference between direct rays and those reflected on the soil.

The area of propagation to the horizon is often called the "interference zone". At the horizon one finds a so-called "intermediate zone" and beyond the horizon a "shadow zone". Works from 20 years ago show that the "shadow zone" can be split into two other zones: a "diffraction zone" and a "tropospheric scattering zone".

The first shadow diffraction zone is characterized by a very high rate of attenuation of signal strength versus distance. This rate corresponds to the theory of optical physics through Maxwell-equations near the "limit conditions", and applied to the sphere. This is rather complex and for practical use we have to remind mainly that the rate of attenuation in the diffraction zone is approximately:

$$\alpha = \frac{0.6}{\sqrt[3]{\lambda}} \text{ in which: } \begin{matrix} \alpha \text{ in dB/kilometers} \\ \lambda \text{ in meters} \end{matrix}$$

This means, for a Syledis wave-length of 70 centimeters: $\alpha = 0.7$ dB/kilometers.

Such an attenuation-rate would fastly limit the capability of transmission beyond the horizon. Fortunately, about 50 kilometers beyond the horizon, the rate of attenuation for this wave-length changes suddenly to become $\alpha = 0.12$ dB/kilometers: the "tropospheric scattering zone" begins here.

The reason of this phenomenon are still not very well known; they are supposed to correspond to the sum of a lot of complex factors, such as: heterogeneity of the lower atmosphere, variable rate of change of refractive index versus altitude, diffusion from irregularities of soil surface, etc.

The signals, observed in this zone due to tropospheric scattering are characterized by:

- a total independance of sunlight
- a relative independance of atmospheric conditions
- a fast and deep fading
- a strength, independant of the elevation of the antennas above the ground.

Roughly, if one disposes of a system able to reach the horizon, one has to find 30 to 40 dBs more to reach the "paradise zone" of tropospheric scattering where the rate of attenuation is only 0.12 dB/km. In that case one can reach very long distances.

The Syledis concept follows these propagation-laws, achieving accurate distance-measurements up to 10 times the horizon, using high-sensitivity receivers and high energies, through correlation techniques, high gain antennas and particular processes to fight fading. Propagation anomalies occur far beyond the horizon: they are the result of strong increases in signal-strength, due to effects of the so-called "ducts" between layer, caused by temperature-inversions in the lower atmosphere. This type of propagation is usable for distance-measurement, but cannot be regarded as a normal law. Reliable maximum range must be based alone on the tropospheric scattering.

2. Methods used in Electronic Positioning Systems.

Generally it is possible to separate the methods used in two classes, being measurement of phase differences or measurement of the time travelled by a signal from the transmitter to the receiver.

2.a. Phase comparison methods

These methods are mainly in use in public networks, where the user of the positioning system only needs to have a receiver on board, to receive the transmitted signals. The transmitters transmit the signals either on a time-sharing basis, or using more-or-less separated frequencies. Both systems have advantages and disadvantages. The use of only one frequency is an advantage in the always crowded frequency-spectrum, when one is talking to the government agency which has to allocate it. The advantage of the use of free running transmitters is that there is no influence due to obstacles in the pathes between the synchronisation-transmitter and those which come later. A second advantage is that a break-down of the synchronisation transmitter does not influence the performance of the other transmitters, as in a coupled network.

2.b. Pulse-measurement

In these systems the time is measured, which it takes for a short pulse of energy to travel between transmitter and receiver. Normally the interrogator on board transmits a signal, which is received by the shore-station, which on its turn transmits an answer. The total time-elapse is measured and, using the velocity of radio-waves, converted to a distance.

It is clear that this method requires very short pulses. (If the velocity is 300.000 km/sec, three meter is 10^{-8} sec.) Typically the duration of pulses is in the order of microseconds.

Normally the received pulses are processed to give them back their original shape, which has been distorted due to reflections and attenuation, after which a certain level on the pulse is used as a reference for the time-measurement. This principle requires rather high energies, and as high energies, transmitted in a short time result in a wide bandwidth, it is obvious that one can use this principle only in the Ultra and Super High Frequencies.

The great advantage of the measurement of time-difference lies in the fact that it does away with one of the drawbacks of the phase-comparison systems, namely the ambiguity of the phase and the resulting phenomenon of loosing of lanes. The transmission of short pulses of high energy requires the use of tubes as magnetrons or klystrons, where the systems using the principle of phase-comparison can be built completely solid state.

2.c. Evaluation of the different systems

As seen before both the phase-comparison and the pulse-measurement systems have advantages and disadvantages. It often depends on the type of work and the number of vessels that have to use the system in an area of a certain size and location which positioning system can be used.

No system existing nowadays is suitable for all applications and it seems rather unlikely that any system, other than the Navstar Global Positioning System, will satisfy all users.

It has been on purpose that no special system has been described, as there is much documentation available on this subject and it is not the intention to give a review of all positioning systems, before going over to the more interesting part of this article: The new Syledis System of Sercel.

3. Sercel and Positioning Systems

Sercel has been a manufacturer of positioning systems for many years. Being the daughter of a leading international geophysical contractor it has designed and constructed equipment that has found a worldwide use. A lot of this is geophysical equipment, which is used by many other geophysical companies other than Sercel's mother CGG.

One of its best-known products is the Distomat which Sercel builds for Wild. In the field of positioning Sercel has developed the well-known Toran system and which is in use in many countries all over the world.

An other product in this field is the Omega and differential-Omega receivers. The newest, and by far most interesting, product of Sercel is the positioning system Syledis, Systeme Leger de mesure de Distances.

4. Syledis

4.a. Use of frequency

Syledis operates in the 420 to 450 MHz band.

As seen before these frequencies are generally considered to propagate along nearly optical lines.

It has been found, however, that by using sufficient energy, one can receive these signals at distances beyond the horizon, at ranges of 3 times or more this previous considered horizon.

As said, this requires a high level of energy. At these frequencies this requires big amplifiers, which is a drawback if the system is to be operated in remote locations as this results in high consumption of power.

Older systems which use these frequencies and are used to measure beyond the optical horizon have always used very high power to transmit short pulses.

European frequency-boards have as a result often refused to allow the operation in their waters.

To transmit beyond the horizon the most important factor is the quantity of transmitted energy.

Instead of transmitting high power during a short period, Syledis transmits during a long period at a relatively low level. A Syledis pulse lasts for 2.6 msec. and has a level of 20 watts.

The total transmitted energy is $\int^t E$, which can therefore be compared with a pulse of 100 kW and 0.5 microsecond duration.

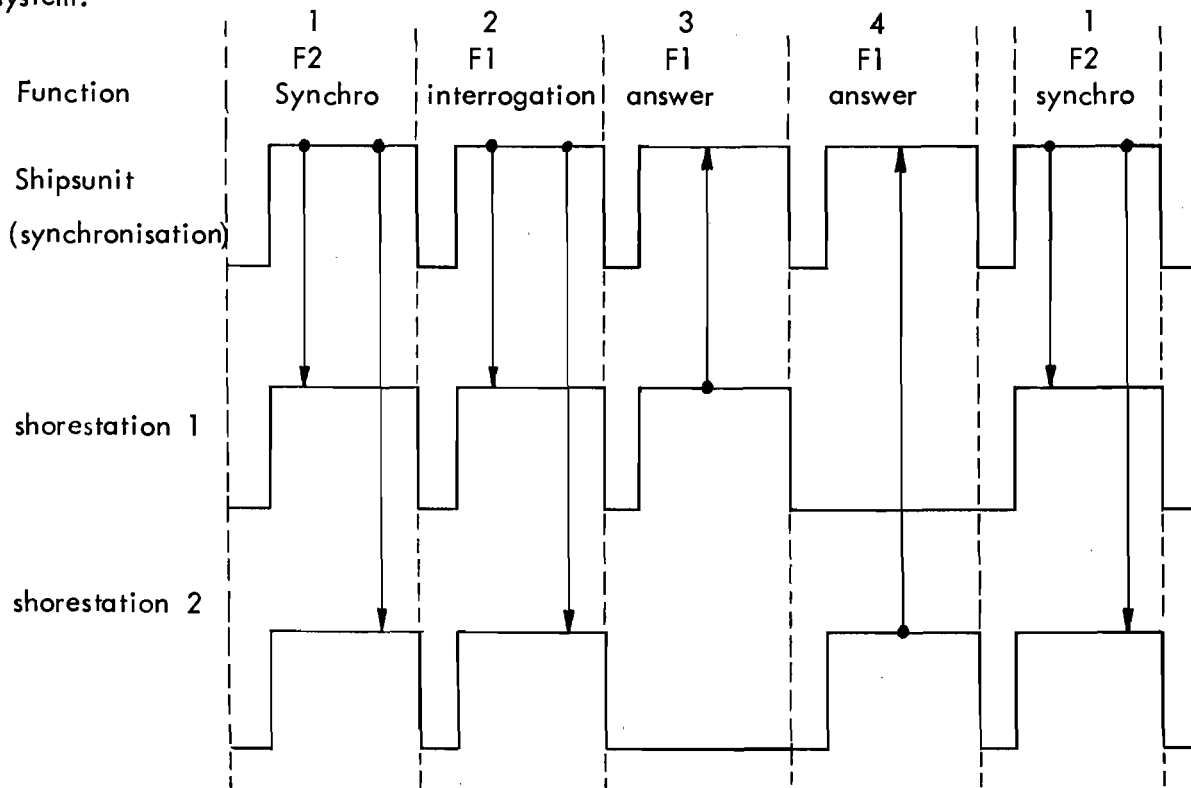
One of the advantages of the 420 - 450 MHz band is that transmitted signals are not influenced by the changing humidity and temperature of the earth. Therefore one does not find changes of the patterns at the coast.

4.b. Organisation of the measurements

Syledis works on the principle of time-sharing. The total period is divided in 30 parts, which parts are allocated to a special function.

The period starts with the transmission of the synchronisation pulse, which is received at the other transmitter stations as well as at the other receivers. This signal is used to tell all the other transmitters when it is their turn to transmit.

In case there is one ship using two shore-beacons one can have the following system.

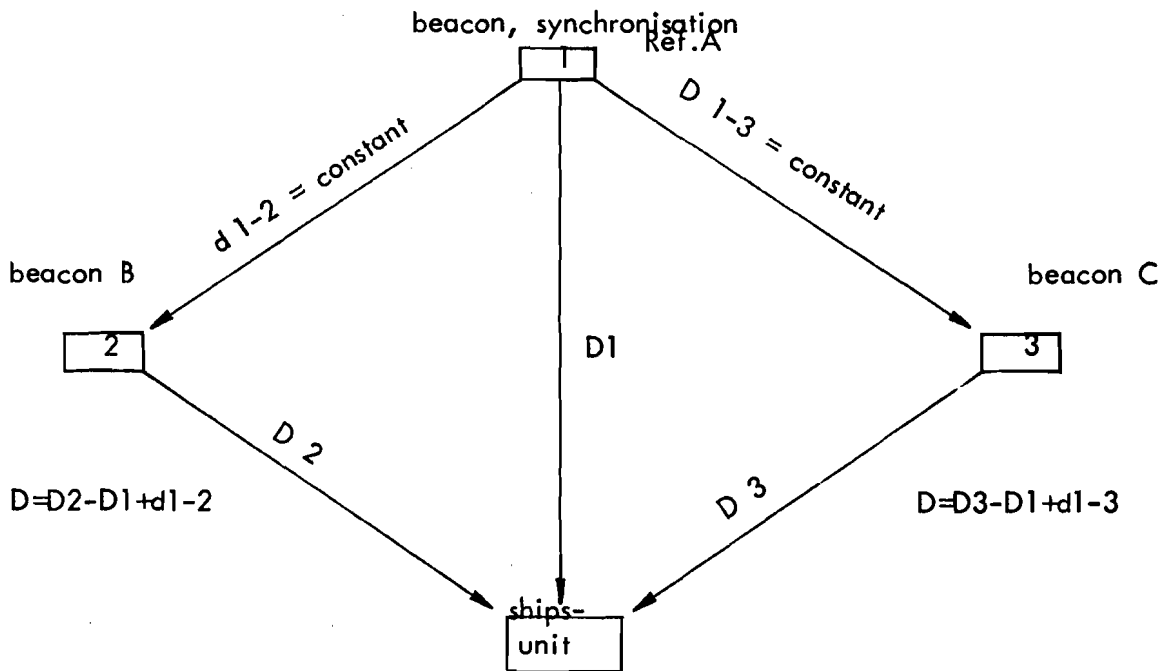


As there are 28 time-slots available for transmission the system can be very flexible.

If only the shore-stations transmit it is possible to set-up a hyperbolic network.

The ships are then only fitted with a receiver, in which the time-differences are measured between arrival of signals from the various transmitters.

The construction of a Syledis hyperbolic network follows from the following drawing:



A combination of the two modes-of-operation is possible. In such a "compound" network a number of ships can work in the range-range mode with the shore-stations, and at the same time an unlimited number of ships can receive the hyperbolic patterns.

We give the sequence-diagram for such a system:

4.c. Processing of the signals

The accuracy of a system is depending on the following factors:

- the pulse-length of the transmitted pulse or the equivalence after correlation
- the signal-to-noise ratio, which is directly depending on the transmitted energy of the transmitter
- the static and dynamic errors in the equipment.

Similar positioning systems use a signal which consists of an as small as possible pulse with a very high energy. The rising time of this signal determines the accuracy and the energy the maximum possible working distance.

Contrary to this the Syledis system uses a relatively wide pulse of 2.66 msec which due to special processing techniques gives a resolution to the signal that can be compared with a 0.52 microsecond pulse. This means that the Syledis transmits during 2.666 μsec a 20 watt signal, which has the same characteristic of a 0.52 μsec pulse of 100 kwatt power.

The basic Syledis code signal lasts 0.52 μsec . A complete code-sequence consists of 127 units and lasts 66.66 μsec . This code-sequence is repeated 40 times to derive a 2.66 millisecc. wide pulse.

The code-sequence is derived by phase modulating the carrier with the discrete values 0 and π , controlled for each 0.5 msec. clock-period by the logic levels 0 and 1 from a pseudo-random code-generator.

This code-sequence can be generated easily in all the units and thus can be compared with the code-sequence generated locally. The auto-correlation function of this sequence has got one maximum, when the two sequences are in coincidence. It is now possible to measure the required shift, which is a measure to the distance travelled by the sequence, thus giving the range or the difference in range.

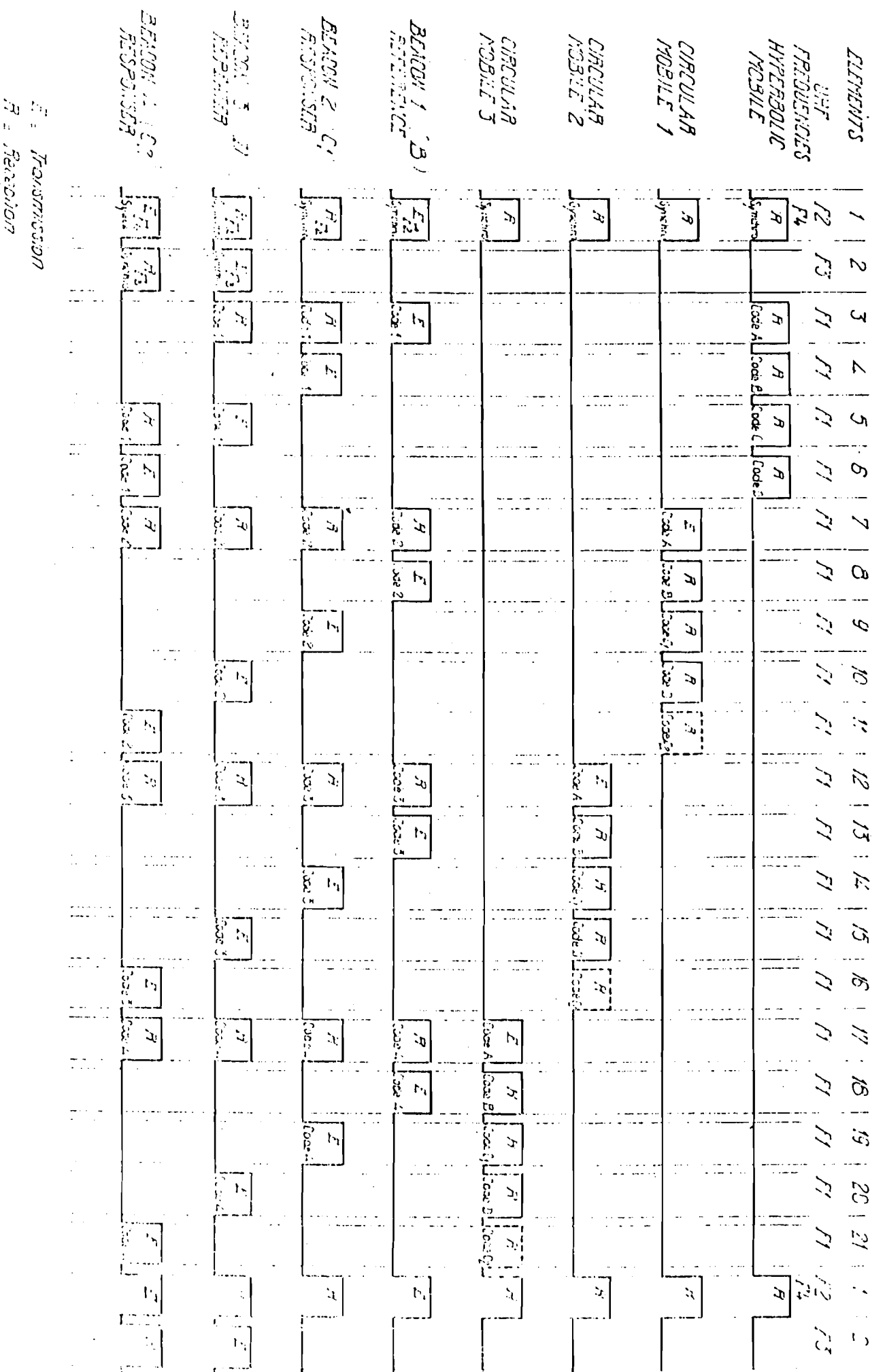


FIG. 6 Timing signals
Compound mode network, 4 beacons, 3 circular mobiles
Ref. Text: § 1.6.5

Discussion (paper 17)

Q. I think this is an important work, just to try to select frequencies which are at an optimum value for the accuracy to achieve, and I would like to ask you what accuracy approximately can you achieve in your measurements using this band ?

A. In this system you can have about one meter at ranges up to the horizon. It is not good enough, but it is better than 10 meters anyway. It is an improvement when you realise that you are on a moving boat, and have the antenne in the mast so you don't know where you are actually measuring

Q. Why is the band of 400 MHz given as approximate ?

A. In this kind of equipment you sometimes have problems with the authorities to get the frequency clearance.

Q. Why did you state that the 420-450 MHz band is not affected by the changing humidity and temperature of the earth. I don't believe that.

A. I said for our practical purposes, that means if you measure with an accuracy of say 1 meter, 1.50 or even 2 meters you would not worry about half a meter more or less.

Remark: You know Mrs. Hopfield has dealt very much with the problem of tropospheric refraction, dividing it into a humid and a dry part. She is not very happy about the humid part.

A. That is why I think it is a pity that they from the factory are not here, because we have done some operational trials with the equipment, and we have seen that, when you are sitting in a certain place, a rain shower at a 30 km distance would not cause difference in the readings

final remark: " I don't mean rain showers ".

Introduction Chairman - Mr. de Munck.

Ladies and Gentlemen, this morning we will speak about the atmosphere, about spatial and temporal variations in the atmosphere. What varies in the atmosphere is the pressure, (of which we do not speak often because the model is well known); temperature (somewhat less well known).

We can do direct measurements with balloons and construct a model of the temperature. Another method perhaps not known to everybody is by acoustic means. One measures temperature profiles, by transmitting acoustic waves into the atmosphere and tracking them with radar waves of the same length and of course one knows the dual wavelength method to find something about temperature gradients.

The humidity is more difficult to handle. Water vapour is the limiting factor for dual wavelength, angle and distance measurements and for the use of microwaves. Also the variations are irregular.

As you know scintillation is a practical limit to most geodetic measurements, but sometimes we can use scintillation to measure terrestrial distances far beyond the horizon up to several hundreds of km. on short radio waves of 400 MHz. from the forward scatter. This type of irregularities is very little known, and I think they deserve more interest.

TROPOSPHERIC CORRECTION OF ELECTRO-MAGNETIC RANGING SIGNALS TO A SATELLITE:
STUDY OF PARAMETERS

Helen S. Hopfield, The Johns Hopkins University, Applied Physics Laboratory,
Laurel, Maryland, United States of America

ABSTRACT

An all-weather satellite tracking system must use a radio signal frequency. A two-frequency system can correct for ionospheric effects on range measurement but not for the troposphere, since un-ionized air is not dispersive at radio frequencies less than (approximately) 30 GHz. A tropospheric range correction must be based either on local measurements involving the whole atmosphere above the tracking station (radiometer data, meteorological balloon data, etc.) or on surface data and an atmospheric model. A "two-quartic" refractivity model that treats the "dry" and "wet" components of refractivity separately as fourth-degree functions of height was proposed earlier by the author. The present paper reports some improvements in the model. Specifically, the height parameters are re-examined on the basis of meteorological balloon data from more locations, over a longer period of time. As before, the height parameter for dry air is found to be consistent with theory and predictable from surface temperature, globally. The water vapor height parameter h_w varies with both position and time and its behavior is not very well understood. Evidence is presented here to show that it varies diurnally (h_w larger at night), seasonally (h_w larger in summer) and possibly also with the sunspot cycle. The value of h_w is especially important for correcting low-elevation-angle observations. Since the parameter h_w involves the height distribution of water vapor, its variation is significant not only for range measurement but perhaps also for weather forecasting.

At low angles the range effect of signal path bending is important. This is neglected in the model, but a correction is being developed; results will be published in a later paper.

These studies were supported by the Defense Mapping Agency Topographic Center and the U. S. Department of the Navy.

I. Introduction

The lower, un-ionized part of the atmosphere (troposphere and stratosphere) delays the passage of an electromagnetic signal and introduces an error into an apparent satellite range. Most of this delay occurs in the troposphere proper, below the tropopause, and for brevity, the term "tropospheric effect" will here include the stratospheric effect except where specified.

Ionospheric effects will not be discussed here.

Un-ionized air is dispersive in the optical range of wavelengths, but not appreciably so in the radio region, up to frequencies of approximately 30 GHz (in spite of the water vapor absorption line at 22.2 GHz). Thus it is possible to correct range measurements for tropospheric effects by using two optical frequencies, but not two radio frequencies. On the other hand, optical signals are rapidly attenuated by clouds, while radio signals are little affected. For an all-weather satellite tracking system, it is necessary to use radio frequencies and to get a tropospheric range correction either from local measurements involving the upper air, or from an atmospheric model.

The present paper will report further work on height parameters for an earlier model.^(1,3) Variations of water vapor distribution are examined especially. Path-bending effects on range are mentioned briefly.

II. Background and Procedures

The index of refraction n of air is a function of temperature, pressure and water vapor content. A measured range is the magnitude of the integral $\int_{\text{path}} n ds$ along the signal path. Thus the atmospheric effect is

$$\Delta\rho = \int_{\text{path}} n ds - \rho \quad (1)$$

where ρ is the slant range. If signal path bending is small enough to be negligible, the integral can be taken along the slant range vector. This approximation is

$$\Delta\rho = \int_{\text{vector}} (n-1) d\rho \quad (2)$$

A model must at least provide a value of (2) that matches the real atmosphere at any angle, and needs parameters suitable for the location and time involved.

At low elevation angles, the model should also provide an evaluation of eq (1). This is under study, but will be mentioned only briefly here and will be presented in a later paper.

The refractivity ($\equiv 10^6 (n-1)$) for air is⁽²⁾

$$N = \frac{77.6}{T} \left(P + \frac{4810 e}{T} \right) \quad (3)$$

in which T is the Kelvin temperature and P and e are, respectively, the total pressure and the partial pressure of water vapor, both in millibars. The two components of N in eq (3), the "dry" and "wet" components, will be subscripted d and w respectively. The N profile model used here is the sum of separate N_d and N_w profiles with different height parameters. Horizontal gradients are assumed negligible. The fourth-degree form of the profile is theoretically justified for dry air; (1) it is used for water vapor also, for lack of a better expression.

The two-quartic model for the refractivity profile (Fig. 1) is:

$$\begin{aligned}
 N &= N_d + N_w \\
 N_d &= \frac{N_{ds}}{(h_d - h_s)^4} (h_d - h)^4 & h \leq h_d \\
 N_w &= \frac{N_{ws}}{(h_w - h_s)^4} (h_w - h)^4 & h \leq h_w
 \end{aligned} \quad (4)$$

where h is height above the geoid, the subscript s refers to the surface, and h_d and h_w are parameters to be determined.

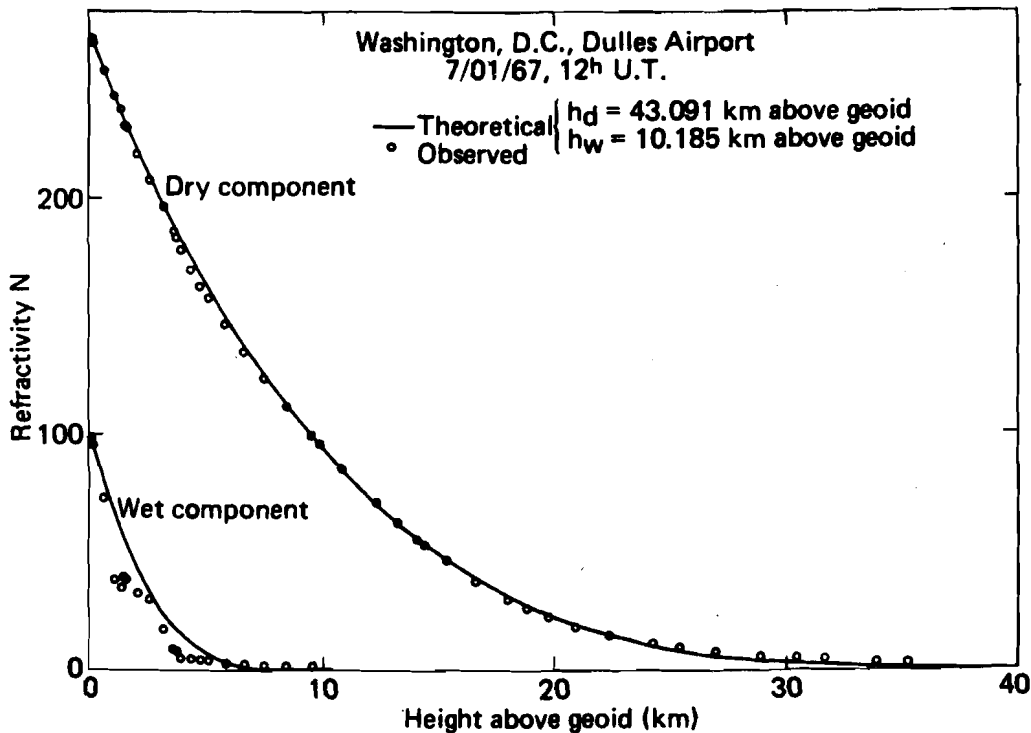


Fig. 1 Refractivity Profile, Dry and Wet Components, Theoretical and Observed

Theoretically, ⁽³⁾ $h_d - h_s$ is a linear function of the surface temperature:

$$h_d - h_s = (h_{d0} - h_s) + a_{hd} T_c \quad (5)$$

where $(h_{d0} - h_s)$ is the value of $(h_d - h_s)$ at 0°C and a_{hd} is its temperature coefficient.

No comparable expression has been found for h_w . It is assumed constant for a given data set, but its variation with time and place will be discussed below.

The parameters h_{d0} , a_{hd} and h_w were determined from meteorological balloon data by a least squares method. ⁽³⁾

The profile model of eq (4) yields an expression for $\Delta\rho_{\text{model}}$ that can be integrated in closed form ⁽¹⁾ or otherwise evaluated ⁽⁴⁾ not only at the zenith but at any elevation angle of the vector ρ . $\Delta\rho$ of eqs (1) and (2) at different elevation angles were studied by tracing signal paths through the observed, layered atmospheres: (1) tracing a curved path by using Snell's law, assuming that the ray path in each layer is an arc of a circle (radius of curvature changing between layers); and (2) assuming a straight-line path to the same end-point.

III. Results

Table I gives the list of locations studied, and supplements earlier lists. ^(3,5) Data were processed for all balloon flights (00 and 12 hours U.T.) but were screened for completeness before being used further. Special procedures were developed for estimating the unmeasured contribution of the atmosphere above the balloon flight.

The stations listed here and in Refs. (3) and (5) provide sampling from more than half the globe; however, Table I is weighted toward the U.S.A.

TABLE I
LOCATIONS AND DATES OF OBSERVATIONS

Station	Latitude	Longitude	Height, m.	Dates
Ship E, Ocean Weather Station	35° N	48° W	6	1970-1973
Caribou, Maine, U.S.A.	46°52' N	68°01' W	191	1970-1974
Washington, D.C., U.S.A., Dulles Airport	38°59' N	77°28' W	85	1970-1974
St. Cloud, Minnesota, U.S.A.	45°35' N	94°11' W	316	1970-1974
Monett, Missouri, U.S.A.	36°53' N	93°54' W	438	1970-1974
Lander, Wyoming, U.S.A.	42°49' N	108°44' W	1697	1970-1973
Denver, Colorado, U.S.A.	39°46' N	104°53' W	1611	1970-1973
Ely, Nevada, U.S.A.	39°17' N	114°52' W	1908	1970-1973
Albuquerque, New Mexico, U.S.A.	35°03' N	106°37' W	1620	1970-1974
El Paso, Texas, U.S.A.	31°48' N	106°24' W	1194	1970-1974
Vandenberg Air Force Base, U.S.A.	34°45' N	120°34' W	100	1970-1974
Point Barrow, Alaska, U.S.A.	71°18' N	156°47' W	8	1970-1974
Wake Island	19°17' N	166°39' E	5	1970-1974
Majuro Island	7°05' N	171°23' E	3	1970-1974
Pago Pago, Samoa	14°20' S	170°43' W	5	1970-1974

The parameters were computed separately for each one-year set of balloon data (6-month set for the year 1970), and for seasonal or diurnal subsets in some cases.

A. Dry Component Parameters

The dry component parameters appear to be global in nature and invariant with time. Their global mean values and standard deviations σ are listed in Table II, computed from all the data. Agreement between all stations is surprisingly close, as indicated by the small value of σ . When the two locations nearest the equator are separated from the rest of the stations, there is a small difference between the two subsets, as shown. For continental stations, no consistent difference was found between low-elevation and high-elevation stations.

The dry component of the tropospheric range effect at the zenith can be estimated within 1 or 2 mm (0.1 percent or less) with the quartic model and suitable dry parameters; or less) with the quartic model and suitable dry parameters; or from the surface pressure alone.^(3,5) At low angles, the model has the advantage.

Extrapolating from the values in the table, $(h_{do} - h_s)$ would vanish at a temperature close to 0°K . This approximation is poorest for the tropical stations, where the assumption that the dry component can be treated as a dry atmosphere is most in error.

TABLE II

DRY COMPONENT HEIGHT PARAMETERS

Data Set	$h_{do} - h_s$, km		a_{hd} , km/deg		$\frac{h_{do} - h_s}{a_{hd}}$ deg K
	Mean	σ	Mean	σ	
All Data (70 sets)	40.152	0.114	0.14795	0.00296	271.39
Marine Tropical Data : Majuro Is. & Samoa (10 sets)	40.402	0.097	0.14281	0.00330	282.91
All Other Data (60 sets)	40.110	0.040	0.14881	0.00180	269.54

B. Wet Component Parameter h_w

The water vapor effect is seldom more than 10% of the total range effect at high angles, but it is extremely variable. The value of h_w was found to be variable also, both with location and with time. It was usually between 8 and 13 km above the station. A higher-than-average value of h_w for a data set indicates that the amount of water vapor aloft was greater than the average expectation on the basis of surface conditions. Figure 1 illustrates the case of a humid surface layer and an irregular water vapor profile.

1. Geographical Variations of h_w

There are large; e.g., the annual mean of h_w was 8 km in California and 12.6 km in Texas (USA) in the same year, 1971, if both were measured above the station. The difference was even more if h_w was measured above sea level. Stations in similar latitudes or climates showed similar values of h_w in some cases, but not always. No general rule has yet been found.

2. Seasonal Variations

Data from a few locations were examined in seasonal sets (winter, spring, summer, autumn). An annual variation in h_w was found at most locations. The peak value generally (but not always) occurred in local summer, with the winter value 2 or 3 km smaller (15 to 25%). Figure 2 shows three samples of the effect, two from the northern and one from the southern hemisphere. The 180° phase difference is clear. The indicated 1σ deviations from the mean are large but do not mask the seasonal effect.

3. Diurnal Effects

The balloons at all locations were launched at 00 and 12 hours U.T., therefore at different local times. With only two data points per day, a diurnal effect would not be equally evident at all longitudes, but should be visible at longitudes near 0° and 180° . Figure 3 shows the diurnal change of h_w along with the seasonal variation for two mid-Pacific and one Atlantic station. The seasonal effect is out of phase for the two Pacific stations since one was north and one south of the equator (cf. Fig. 2). But the diurnal effect is the same for both, with the night value of h_w (12 hours U.T.) greater than the daytime value. In the Atlantic, the value of h_w was less at 12^h U.T. than at 00^h U.T., but here 12^h U.T. was in the daytime (9 a.m.).

Data from continental stations also suggested a diurnal effect, but the local times of observation made this less clear.

4. Relation to Sunspot Cycle

The balloon data on hand for two stations covered almost the duration of one sunspot cycle. Figure 4(a) shows the annual mean of the Zurich relative sunspot number for the years 1963-1975 inclusive. There was a minimum in 1964; the next minimum had not quite been reached in 1975.

Parts (b) and (c) of the figure show the annual mean values of h_w for Ship E and Wake Island respectively, over the same time interval (data not available for every year). For Ship E especially, a low value of h_w appears to be correlated with high sunspot numbers, with perhaps a small time lag. The effect for Wake Island is less definite but is at least suggested by the figure. Further data are needed to determine whether a real correlation exists, and if so, what is the mechanism. For example, does the greater amount of solar wind that accompanies high sunspot number in some way affect the distribution of water vapor; and by what means? Understanding such relations may contribute to our understanding of climate and weather.

C. Low-Angle Studies

The ray-tracing procedure mentioned above was used to compute signal paths through some samples of observed atmospheres based on balloon data. For each case, $\Delta\rho$ from eqs (1) and (2), also, $\Delta\rho_{\text{model}}$, and the total angular bending τ along the signal path of eq (1) were computed. Figure 5 shows the mean $\Delta\rho$ from eqs (1) and (2) as a function of signal path elevation angle, for a one-month winter sample of balloon-measured atmospheres. Figure 6, on a larger scale, shows the curvature effect on range for a summer sample, for the lower angles, i.e., the differential effect ($\Delta\rho_{\text{vector}} - \Delta\rho_{\text{path}}$); and also the quantity ($\Delta\rho_{\text{model}} - \Delta\rho_{\text{path}}$).

The two curves of Fig. 6 would coincide for a perfect model of $\Delta\rho_{\text{vector}}$. Agreement was excellent at the lowest angle, with the parameters used, but there was a small bias at other angles. The bias can be minimized by adjusting parameters. However, the 1σ scatter of the model prediction is much larger than the bias, and is largely a water vapor effect. The water vapor parameter studies were undertaken with the hope of reducing this scatter.

Even if the model matches $\Delta\rho_{\text{vector}}$, the path bending effect should still be considered at low angles, as shown by Fig. 6. The effect on satellite range is greater than 1 meter at elevation angles below 2° , and several meters at 0.5° . Although the curved path is geometrically longer than a straight path, it is electromagnetically shorter, as indicated by Fig. 6 (Fermat's principle). The procedure that is being developed for estimating the bending correction to range will be presented in a later paper.

Acknowledgement

Discussions with Harold D. Black, and the collaboration of Harry K. Utterback in making the numerical studies, are acknowledged with appreciation.

The meteorological balloon data were supplied by the National Climatic Center of the National Oceanic and Atmospheric Administration, U. S. Department of Commerce.

References

1. Hopfield, H. S., Two-quartic tropospheric refractivity profile for correcting satellite data, J. Geophys. Res., 74, 4487-4499 (1969).
2. Smith, Ernest K., Jr. and Stanley Weintraub, The constants in the equation for atmospheric refractive index at radio frequencies, Proc. I.R.E., 41, 1035-1037 (1953).
3. Hopfield, Helen S., Tropospheric effect on electromagnetically measured range: predictions from surface weather data, Radio Science, 6, 357-367 (1971).
4. Yionoulis, S. M., Algorithm to compute tropospheric refraction effects on range measurements, J. Geophys. Res., 75, 7636-7637 (1970).
5. Hopfield, H. S., Tropospheric range error parameters: further studies," APL/JHU report CP 015 (June 1972); also published as Goddard Space Flight Center preprint X-551-72-285 (August 1972).

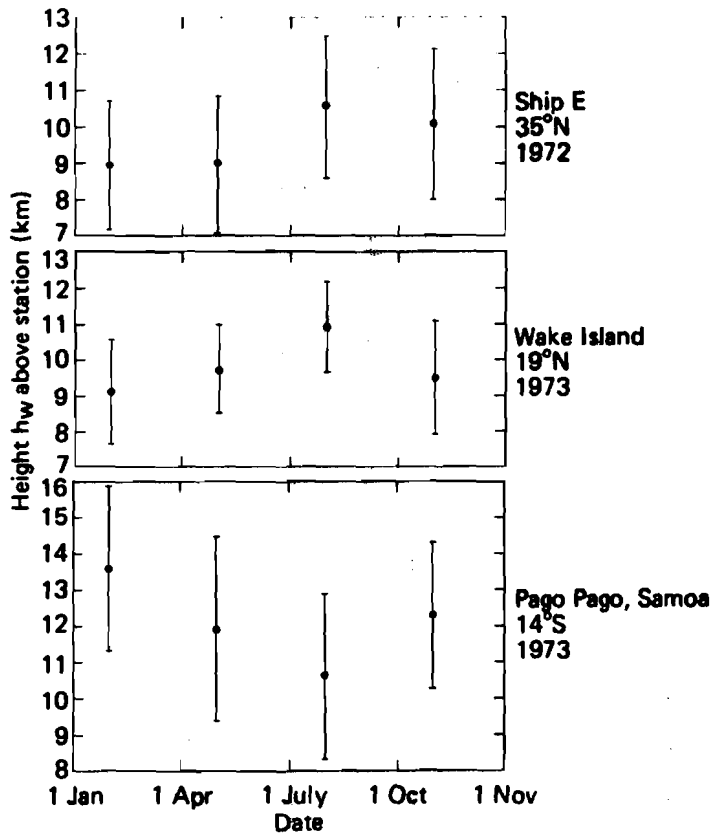


Fig. 2 Seasonal Variation of the Wet Height Parameter h_w

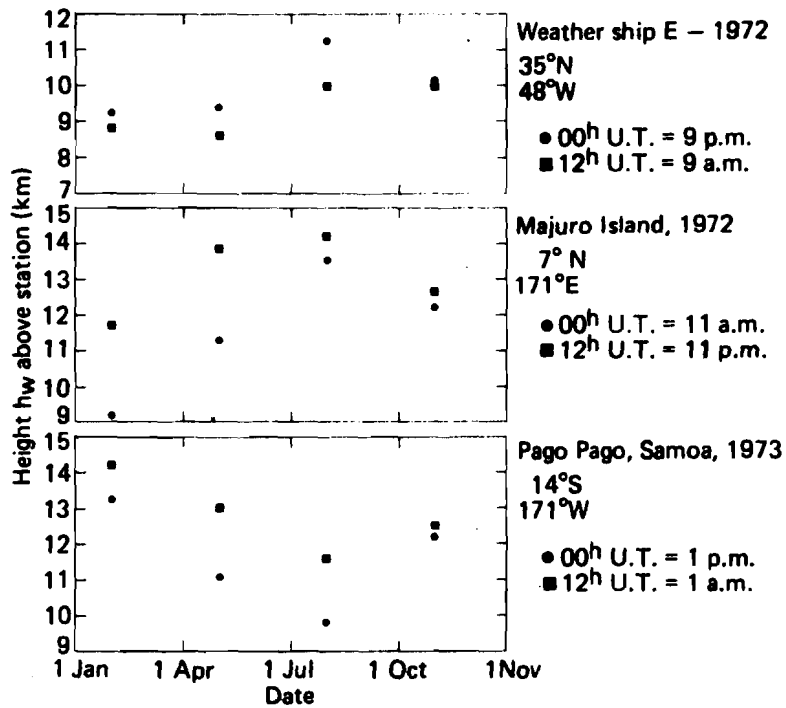


Fig. 3 Diurnal and Seasonal Effects on the Wet Height Parameter h_w

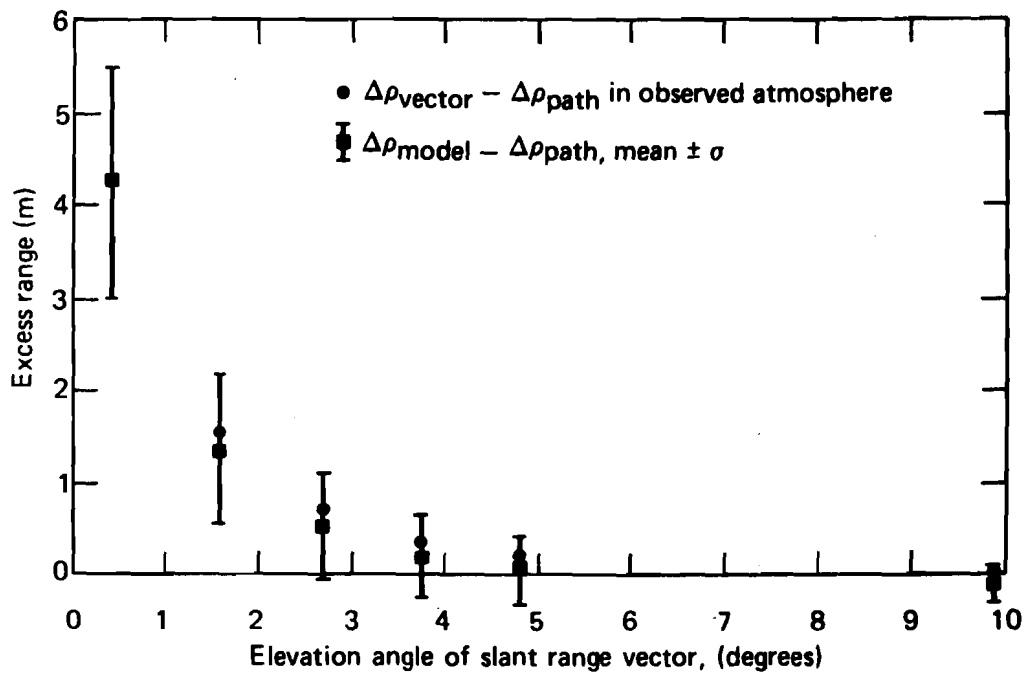


Fig. 6 Tropospheric Path Bending Effect on Radio Ranging
Excess Range, Straight Line Path – Curve
Washington, D.C. (Dulles Airport), July 1967

Discussion (paper 18)

- Q. Is it possible that some of the effects you found are due to the inaccuracy ?
- A. I looked at that and I think they are not, but the plots that I showed with the variation in HW are based on all the data, because of the insufficiency of profiles otherwise, but I did look at some and found the same trend, even if we threw out the high humidity profiles.
- Q. It would appear to me that if you use the very low elevations - you are talking about a few degrees elevation - the meteorological observation at your point of observation is not representative any more for the pass. Have you taken into consideration changes in the atmospheric conditions away from your point of observation. Would you comment on that ?
- A. I am sure that, to a greater extent from more angles it is more or less rather surprising how sometimes the trend of the vertical integral shows about the same pattern for stations that are quite a distance apart. I have no slides to show that, I may have a report with me, which shows some samples like that, if you would like to look after, but I have no slides.
- Q. Do you think this effect you found for the radio wave-lengths, can there be also some sort of effects, if you use optical light for ranging to satellites ? I mean seasonable and annual
- A. That is quite possible, but I have not looked at it.
- Q. You are showing in one of your slides the refractivity integral of the wet and the dry components and one could see for the months january and july, there was an ondulation of about ten to eleven days. Have you more data than these two months to proove sudden ondulation ?

A. I have more data, but I have not done any spectrum calculations on it. There just has not been time to go all direction, that might be interesting and that is one. So I have not done that.

- They could be probably interesting for the prediction of the measured data, if you know the period of 10 to 11 days and the wet and dry components.

A. I agree, there might be interesting information there. About the time you have that information although, the time for prediction is much passed. Well, I mean you haven't the balloon data at up to date bases. You think of, I suppose, a systematic formula that could be used at any time. You may look at weather-maps and they show a certain periodicity in weather systems following each other, perhaps it shows more clearly when you get these integrals. I haven't done it anyway.

Q. There is one point mentioned before, this is the low elevation ray tracing. I found that this low elevation ray tracing is so uncertain, that one should not rely upon any data at the present. The reason for it is the " concentric sphere " model, and at such low elevation angles the sine of the angle S has such a strong influence. The sine S has a considerable variation at these lower elevation angles sometimes of a magnitude of several hundreds of percent.

Thus, this error would enter proportionally into the ray bending, and the ray bending would be off by some hundreds of percent either.

A. I would not trust the ray tracing at very low angles either. I agree.

SOME CONSIDERATIONS ON THE STOCHASTIC BEHAVIOUR OF THE ANGLES OF REFRACTION AND OF THE REFRACTION INDICES, CONCERNING LASER- AND MICROWAVE DISTANCE MEASUREMENTS

Heribert Kahmen, Geodätisches Institut der Universität Karlsruhe, Federal Republic of Germany

Summary: A consideration of the meteorological field shows that the fluctuations of the angles of refraction and of the refraction index, concerning laser- and microwave-measurements, may be described by a stochastic process: a two-component process. The process is not stationary. The stochastic behaviour of the process however can be described by the first and second order central moments of a stationary process, if the two components are considered separately. The calculations show, that there is no fundamental difference between the statistical functions describing effects of refraction on measured distances and its effects on observed vertical angles. The parameters of the central moments are estimated using parameters of the meteorological field, which were registered over a period of years on towers at different heights.

1. Introduction

For vertical angle measurement and electronic distance measurement instruments of such a high precision are available, that the accuracy of the measuring procedures depends mainly on the estimation of the meteorological field along the ray path. However as the external conditions can not be estimated exactly, the single values of time series are not always independent, but correlated. If the correlation factors are neglected the adjustment of geodetic networks may result in apparent alterations of coordinates, which simulate seeming point shiftings. Tests with trilateration networks have shown, that these apparent point shiftings may become two or three times larger than standard errors of positions, if correlation coefficients $> 0,5$ are neglected (SCHÖLLER, K., 1973).

Normally it is difficult to estimate the correlation functions directly from the geodetic measurements, since for economic reasons only a small number of repeated measurements can be performed. Therefore an attempt shall be made to estimate the physical causes of the fluctuations from the meteorological field and then to derive from these values the fluctuations of geodetic observations by linear transformations. With these model studies no absolute values of the parameters of the correlation functions shall be estimated but we can gain more experiences about the functional behaviour of the correlation factors. If the functional behaviour is well known, the absolute parameters can be estimated by only a small number of direct geodetic measurements.

2. The Stochastic and Functional Behaviour of the Field of Refraction

The basic equations for the coefficients of refraction and the angles of refraction are (FEARNLEY 1884/85):

$$k = \frac{2}{s} \int_0^s \frac{s-s'}{s} \kappa(s') ds' , \quad (1)$$

$$\delta = \frac{\rho}{R} \int_0^s \frac{s-s'}{s} \kappa(s') ds' \quad (2)$$

where $\kappa = \kappa(s')$ is the local refraction coefficient, R is the radius of the earth, s is the length of the ray path (the difference between the



arc-length and the chord-length is neglected) and s' denotes the coordinates along the light ray
Fig. 1.

Fig. 1

For low elevation angles, as is usually the case with geodetic observations, the local refraction coefficients are obtained from (BROCKS, K., 1973):

$$\kappa = 17.19 \frac{p}{T^2} \left[1 - 0.2925 \frac{\partial T}{\partial z} \right] \quad (3)$$

where p [mbar] is the barometric pressure, T is the absolute temperature and z [unity: 100 m] is the height.

The accuracy of vertical angle measurements is limited due to the inadequate mathematical model of the atmosphere. The meteorological field of the parameters p and T shows in different regions of the earth a different stochastic and functional behaviour. Considering the meteorological process - e.g. in Germany - we can assume, that the variance spectrum of the fluctuations

$$\Delta k(t) = k_m - k(t) \quad (4)$$

will have three frequency bands with higher variances. In equation (4) k_m denotes the average $M[k(t)]$. The first maximum, extending from low frequencies to frequencies of some hundred Hz (Hertz) is mainly caused by optical effects of the turbulent medium. A second frequency band is influenced by the daily alterations of the position of the sun and the short-periodic climatic variations with periods of about one to five days. The third maximum of the spectrum will be caused by the yearly climatic variations. The fluctuations of the refraction coefficients are smallest during the time of maximum downward radiation and they become a maximum during midnight. Generally the amplitudes of the fluctuations increase with the length of the ray path and they decrease with height above sea level.

Similarly for long distances in electronic distance measurement the accuracy of the path length depends essentially on precision of the atmospheric model, which is applied for reduction of the distances. Normally refraction indices for reduction can only be calculated from endpoint measurements near the ground. The refractive indices n_e , calculated from endpoint measurements, generally differ from those, being averaged along the ray path

$$n_i = \frac{1}{S} \int_0^S n(s') ds' , \quad (5)$$

where $n(s')$ are the local refractive indices. The refractive index is a function of the parameters: dry temperature, wet temperature and pressure. Considering the meteorological process - e.g. in Germany - we can assume that the variance spectrum of the fluctuations

$$\Delta n(t) = n_i(t) - n_e(t) \quad (6)$$

of the refractive indices will also have three frequency bands with higher variances. The causes are analogous to those, which influence the fluctuations of the refraction coefficients.

The fluctuations, being influenced by the optical effects of the turbulent medium shall not be discussed here, as they can easily be eliminated by

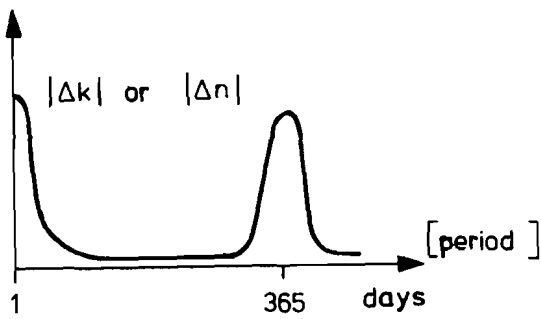


Fig. 2

Generally, the fluctuations of the refraction coefficients and those of the refractive indices are stochastic functions of the coordinates x, y, z of the station and of the parameter time t :

$$\begin{aligned} \Delta k &= \Delta k(x, y, z, t), \\ \Delta n &= \Delta n(x, y, z, t). \end{aligned} \quad (7)$$

The dependence on the position is mainly given by the topographical features, the nature of the soil and the vegetation. In the following consideration, however, only the dependence on time shall be analysed.

3. The Statistical Analysis of the Field of Refraction

The first and second order moments

$$M[\xi(t)] = \lim_{T \rightarrow \infty} \frac{1}{T} \int_0^T \xi(t) dt, \quad (8)$$

$$M[\xi(t+\tau) \xi(t)] = \lim_{T \rightarrow \infty} \frac{1}{T} \int_0^T \xi(t+\tau) \xi(t) dt, \quad (9)$$

of a random process can easily be estimated by applying the stationary and ergodic hypothesis. $\xi(t)$ denotes a random variable and τ is the time delay. The random variables $\Delta k(t)$ and $\Delta n(t)$ however are neither stationary nor ergodic since the averages and variances are a function of the time of day and of the time of year. The stationary and ergodic hypothesis however can be applied if the process is split up into two components where one component $\xi_1(t)$ is characterized by the first maximum of the spectrum and the other component $\xi_2(t)$ by the second maximum (Fig. 2). With further

time averaging. The following considerations only base on those frequency bands of the spectrum, which are influenced by the daily and yearly alterations of the climate Fig. 2.

specialisations of the calculations then the first and second order moments can be estimated by means of equations (8) and (9). Imposing certain limitations, then the moments of the total process may be calculated from the moments of the components of the process. In case the two components superimpose additively, we have

$$\Phi_{\xi_S \xi_S}(\tau) = \lim_{T \rightarrow \infty} \frac{1}{T} \int_0^T [\xi_1(t) + \xi_2(t)] [\xi_1(t + \tau) + \xi_2(t + \tau)] dt,$$

$$\Phi_{\xi_S \xi_S}(\tau) = \Phi_{\xi_1 \xi_1}(\tau) + \Phi_{\xi_2 \xi_2}(\tau) + \Phi_{\xi_2 \xi_1}(\tau) + \Phi_{\xi_1 \xi_2}(\tau). \quad (10)$$

If the two components are uncorrelated, we obtain

$$\Phi_{\xi_S \xi_S}(\tau) = \Phi_{\xi_1 \xi_1}(\tau) + \Phi_{\xi_2 \xi_2}(\tau). \quad (11)$$

The two components can be separated by using transversal filters of the form

$$X(t) = \int_{-\infty}^{+\infty} g(\nu) \cdot \xi_S(t + \nu) d\nu. \quad (12)$$

$X(t)$ is the filtered random variable. $g(\nu)$ is the function of the weight, which is defined for $-\infty < \nu < +\infty$, where

$$\left| \int_{-\infty}^{+\infty} g(\nu) d\nu \right| < \infty.$$

The frequency characteristic $G(\nu)$ of the filter is obtained by means of a Fourier-Transformation of $g(\nu)$:

$$G(\nu) = \int_{-\infty}^{+\infty} g(\nu) \exp(i2\pi\nu\nu) d\nu. \quad (13)$$

For the following calculations the Gaussian function

$$g(\nu) = \frac{1}{\theta \sqrt{\pi}} \exp\left(-\frac{\nu^2}{2\theta^2}\right) \quad (14)$$

is used for estimating the weights, where 2θ denotes the interval of the time average. Then the frequency characteristic of the filter is also a Gaussian function:

$$G(\nu) \exp(-\pi^2 \nu^2 \theta^2) . \quad (15)$$

4. Calculation of the Realisation Funktionen of the Random Processes from the Meteorological Field

Meteorological data, recorded on a tower near Munich at heights of 2 m, 5 m, 10 m, 20 m and 50 m shall be used to calculate realisation functions of the random processes. The following studies base on the idealized assumption that the recorded data will be homogeneous all over the test area. For the calculations, instead of equation (1), the summation equation

$$k = \frac{\sum_{\nu=1}^n (2n-2\nu+1) \cdot \kappa_{\nu}}{n^2} \quad (16)$$

is used, where ν denotes the number of the intervals beginning at the observation station and n is the total number of the intervals.

The correlation function of the random signal (4) is

$$\Phi_{\Delta k \Delta k}(\tau) = \lim_{T \rightarrow \infty} \frac{1}{T} \int_0^T \Delta k(t) \Delta k(t+\tau) dt .$$

As we find from (1) and (2) the linear relationship

$$\delta = \frac{S_p}{2R} k \quad (17)$$

the correlation function of the $\Delta \delta$ is

$$\Phi_{\Delta \delta \Delta \delta}(\tau) = \lim_{T \rightarrow \infty} \frac{1}{T} \int_0^T \left\{ \frac{S_p}{2R} \Delta k(t) \cdot \frac{S_p}{2R} [\Delta k(t + \tau)] \right\} dt, \text{ or}$$

$$\Phi_{\Delta \delta \Delta \delta}(\tau) = \left(\frac{S_p}{2R} \right)^2 \Phi_{\Delta k \Delta k}(\tau) . \quad (18)$$

As the fluctuations $\Delta h(t)$ of the trigonometric determined heights are derived from the fluctuations $\Delta k(t)$ of the refractive indices by

$$\Delta h(t) = - \frac{s^2}{2R} \Delta k(t) \quad (19)$$

the correlation function of the $\Delta h(t)$ is

$$\begin{aligned} \Phi_{\Delta h \Delta h}(\tau) &= \lim_{T \rightarrow \infty} \frac{1}{T} \int_0^T \left[\left(- \frac{s^2}{2R} \right) \Delta k(t) \cdot \left(- \frac{s^2}{2R} \right) \Delta k(t+\tau) \right] dt, \text{ or} \\ \Phi_{\Delta h \Delta h}(\tau) &= \left(\frac{s^2}{2R} \right)^2 \Phi_{\Delta k \Delta k}(\tau) . \end{aligned} \quad (20)$$

The random signal $\Delta n(t)$ - see equ. (6) - can be calculated by the meteorological field (dry temperature t_t , wet temperature t_f) if the differences Δt_t and Δt_f between the averages calculated with endpoint measurements and the integral averages along the ray path may be estimated. For the estimation of the Δt_t and the Δt_f also temperatures recorded on towers at different heights can be used, if an idealized model is assumed (KAHMEN, H., 1975).

For a given set of meteorological conditions (dry temperature, wet temperature and pressure) the refractive index n of microwaves can be computed by the formulæ of ESSEN and FROOME and the refractive index of Lasers by those of BARREL and SEARS. A simplified form of the law of propagation of errors for the refractive indices is

$$dn_L = - a dt_t \quad (\text{for light waves}) , \quad (21)$$

$$dn_M = - a' dt_t + b' dt_f \quad (\text{for micro waves}) , \quad (22)$$

where a , a' and b' can be computed with the meteorological parameters. Thus we find for the correlation functions of the fluctuations of the refractive indices if light is used as carrier oscillation

$$\begin{aligned} \Phi_{\Delta n_L \Delta n_L}(\tau) &= \lim_{T \rightarrow \infty} \frac{1}{T} \int_0^T [(-a) \Delta t_t(t) \cdot (-a) \Delta t_t(t+\tau)] dt, \text{ or} \\ \Phi_{\Delta n_L \Delta n_L}(\tau) &= a^2 \Phi_{\Delta t_t \Delta t_t}(\tau) , \end{aligned} \quad (23)$$

and if micro waves are used as carrier oscillations

$$\Phi_{\Delta n_M \Delta n_M}(\tau) = a'^2 \Phi_{\Delta t_t \Delta t_t}(\tau) + b'^2 \Phi_{\Delta t_f \Delta t_f}(\tau) - a'b' \Phi_{\Delta t_t \Delta t_f}(\tau) - \left[\begin{array}{l} - \\ - \end{array} \right] b'a' \Phi_{\Delta t_f \Delta t_t}(\tau) \cdot (24)$$

With the expression

$$ds = - \frac{dn}{n} \cdot s \approx - dn \cdot s \quad (25)$$

($n \approx 1$)

the correlation functions of the fluctuations Δs of the distances become

$$\Phi_{\Delta s \Delta s}(\tau) = \lim_{T \rightarrow \infty} \frac{1}{T} \int_0^T \{ [(-s) \Delta n(t)] \cdot [(-s) \Delta n(t + \tau)] \} dt, \text{ or}$$

$$\Phi_{\Delta s_L \Delta s_L}(\tau) = s^2 \Phi_{\Delta n_L \Delta n_L}(\tau) , \quad (26)$$

$$\Phi_{\Delta s_M \Delta s_M}(\tau) = s^2 \Phi_{\Delta n_M \Delta n_M}(\tau) . \quad (27)$$

5. Numerical Estimation of the Correlation Functions

For the numerical calculations meteorological data are used recorded on a tower near Munich. The data are: dry temperatures recorded at heights of 2 m, 5 m, 10 m, 20 m and 50 m, wet temperatures recorded at heights of 2 m, 20 m and 50 m and barometric pressure recorded at a height of 2 m. The tower is surrounded by grassland. The temperatures were measured every ten minutes. In order to eliminate the daily sinusoidal behaviour of the refractive indices and of the refraction coefficients, only one mean hourly value of every day is used for the single series of observations. Extensive tests have shown that for many measuring dispositions no significant alterations of the refractive indices and

of the refraction coefficients do occur even if the observation time extends from 9 a.m. to 4 p.m. (see e.g. RINNER, K., 1971; BROCKS, K., 1973).

The random processes, characterized by the first maximum of the variance spectrum (Fig. 2) may be considered stationary if only data of a limited day time (e.g. mean hourly values) are used and if moreover the time series are limited to certain periods of the year. The periods must be chosen in such a way that during this time the physical causes of the fluctuations will remain constant. For these time series the ergodic hypothesis also can be accepted since the tendency of conservation of the short periodic climatic variations will last about one to five days and consequently the correlation coefficients of the $\Delta n(t)$ and $\Delta k(t)$ will tend to zero after a few days.

The computations of the moments of the short periodic random processes base on mean hourly values plotted daily from January 1962 to December 1963. Three series of observations have been calculated, the first using values recorded between 9 a.m. and 10 a.m., the second using values recorded between 12 a.m. and 1 p.m., the third using values recorded between 3 p.m. and 4 p.m. The single series of observations have been limited to a period of two months. The results show, that already for a time-delay of one to two days the correlation coefficients of the $\Delta k(t)$ and $\Delta n(t)$ are smaller than 0,5. For a minimum time-delay τ_{\min} of at least some days we get

$$\Phi_{\Delta k \Delta k}(\tau) = \begin{cases} \Phi_{\Delta k \Delta k}(0) \\ 0 \text{ elsewhere,} \end{cases} \quad (28)$$

$$\Phi_{\Delta n \Delta n}(\tau) = \begin{cases} \Phi_{\Delta n \Delta n}(0) \\ 0 \text{ elsewhere.} \end{cases} \quad (29)$$

The variances $\Phi(0)$ become maximum in winter.

The random processes, characterized by the second maximum of the variance spectrum (Fig. 2) can be approximated by a Gaussian narrow-band noise

$$r(t) = r_0(t) \cos [\omega_0 t + \varphi(t)] \quad (30)$$

which is superimposed by a signal

$$s(t) = A \cos \omega_0 t . \quad (31)$$

ω_0 is the center frequency of the noise.

Equation (30) is suitable for the physical interpretation of the random signal. The statistical behaviour of the random process however can better be described, if equ. (30) is transformed into

$$r(t) = r_1(t) \cos \omega_0 t - r_2(t) \sin \omega_0 t \quad (32)$$

with

$$r_1(t) = r_0(t) \cdot \cos \varphi(t) \text{ and}$$

$$r_2(t) = r_0(t) \cdot \sin \varphi(t),$$

where $r_1(t)$ and $r_2(t)$ follow a two-dimensional Gaussian distribution

$$w(r_1, r_2) = \frac{1}{2\pi\sigma^2} \cdot e^{-\frac{1}{2\sigma^2} (r_1^2 + r_2^2)} .$$

Then, with (31) and (32) we get for the total process:

$$s_g(t) = [A + r_1(t)] \cos \omega_0 t - r_2(t) \sin \omega_0 t \quad (33)$$

or

$$s_g(t) = \rho_0(t) \cos [\omega_0(t) + \psi(t)], \quad (34)$$

where

$$\rho_0^2(t) = [A + r_1(t)]^2 + r_2^2(t) \text{ and}$$

$$\psi(t) = \text{arc tg } \frac{r_2(t)}{A + r_1(t)} .$$

The probability density of $\rho_0(t)$ and $\psi(t)$ is

$$p(\rho_0) = \frac{\rho_0}{\sigma^2} \cdot I_0 \left(\frac{A\rho_0}{\sigma^2} \right) \exp \left(- \frac{\rho_0^2 + A^2}{2\sigma^2} \right) \quad (35)$$

and

$$p(\psi) = \frac{1}{2\pi} \exp \left(- \frac{A^2}{2\sigma^2} \right) + \exp \left(- \frac{A^2 \cdot \sin^2 \psi}{2\sigma^2} \right) \left\{ 1 + \text{erf} \left(\frac{A \cdot \cos \psi}{\sqrt{2}\sigma} \right) \right\} \frac{A \cdot \cos \psi}{\sigma\sqrt{8\pi}} \quad (36)$$

for the interval $0 \leq \psi(t) \leq 2\pi$, where I_0 is the Bessel-Function with the index $n=0$ and $\text{erf}(x) = \frac{2}{\sqrt{\pi}} \int_0^x e^{-u^2} du$.

The probability density (35) is called Rice distribution. The form of the Rice distribution depends on the relation between the energy of the signal and the energy of the noise on the same frequency. If the energy of the signal is much greater than the energy of the noise on the same frequency the Rice-distribution changes into a Gaussian distribution. Then the phase angles are limited to a small part of the interval $0 \leq \psi(t) \leq 2\pi$. Such a process is not ergodic and not stationary. Consequently for the estimation of the second order moments equ.(9) cannot be used. Besides equations (35) and (36) show, that, even if idealized models are used the probability density functions become very complicated.

If the energy of the noise on the frequency ω_0 predominates, the Rice-distribution tends to a Rayleigh distribution

$$p(\rho_0) = \frac{\rho_0}{\sigma^2} \exp \left(- \frac{\rho_0^2}{2\sigma^2} \right) , \quad (37)$$

and the probability density function of the $\psi(t)$ tends to

$$p(\psi) = \frac{1}{2\pi} [\sigma_r(\psi) - \sigma_r(\psi - 2\pi)] \quad (38)$$

(σ_r : normed step function).

Then the phases $\psi(t)$ are equally distributed over the interval $0 \leq \psi(t) \leq 2\pi$. A random process characterized by the probability density functions (37) and (38) can exactly be described by equations (8) and (9) (SCHLITT, H., 1960; TAUBENHEIM, J., 1969).

Correlation functions, characterized by (37) and (38) can be approximated by the function

$$\Phi(\tau) = C_0 \exp(-a_0^2 \tau^2) \cos \omega_0 \tau, \quad (39)$$

where C_0 and a_0 are constants. The correlation function has the form of a cosine-function whose amplitude slowly decreases.

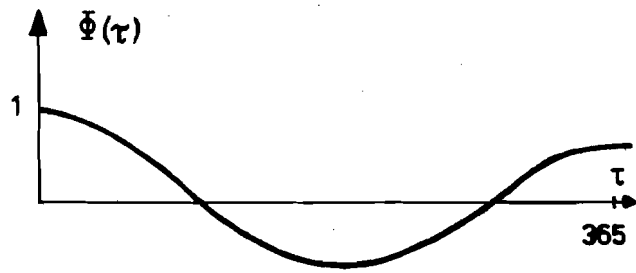


Fig. 3

In the following we shall analyse how closely the correlation functions of the long periodic fluctuations $\Delta k(t)$ and $\Delta n(t)$ can be approximated by the model function (39). The tests base on time series of the $\Delta k(t)$ and $\Delta n(t)$ computed from mean hourly values of meteorological parameters recorded during the time from January 1962 to december 1971. Four time series have been calculated, the first using values recorded every fifth day between 1 p.m. and 2 p.m., the second using values recorded every fifth day between 3 p.m. and 4 p.m., the third using values recorded every fifth day alternately between 1 p.m. - 2 p.m. and 3 p.m. - 4 p.m., the fourth using values recorded every tenth day about two hours before sunset. All the calculations verify that the correlation functions may be approximated by the model function (39). Consequently we can write

$$\Phi_{\Delta k \Delta k}(\tau) = C_1 \exp(-a_1^2 \tau^2) \cos \omega_0 \tau, \quad (40)$$

$$\Phi_{\Delta n \Delta n}(\tau) = C_2 \exp(-a_2^2 \tau^2) \cos \omega_0 \tau. \quad (41)$$

C_1, C_2 and a_1, a_2 are constants.

Hence we get for the correlation functions of the total processes

$$\phi_{\text{tot.}}(\tau) = \left. \begin{array}{l} \phi^{(P1)}(\tau) \\ \phi^{(P2)}(\tau) \\ \phi^{(P3)}(\tau) \end{array} \right\} + \phi^{(1)}(\tau) \quad (42)$$

where the indices (P1),(P2), ... denote the correlation functions of the short periodic fluctuations calculated for different periods of a year and the index (1) denotes the correlation function of the long periodic fluctuations.

6. Conclusions

The measurements being used in this paper are limited to a special topographic situation. Therefore the author intends to do further studies considering different conditions. These further investigations and more detailed discussions of the results will be published.

Literature:

- BROCKS, K.: Ausgewählte Schriften über Terrestrische Refraktion, Wechselwirkung Ozean-Atmosphäre und Radiometeorologie. G.M.L. Wittenborn Söhne, Hamburg, 1973.
- FEARNLEY, C.: Zur Theorie der terrestrischen Refraktion. Verhandlinger: Videnskabs-Selskabet; Christiana 1884, Christiana 1885.
- KAHMEN, H.: Numerical filtering of trilateration networks. Prepared for presentation at the XVI General Assembly of the IAG, Grenoble, 1975.
- RINNER, K.: Erster Vergleich zwischen Mikrowellen- und Lasermessungen im Testnetz Steiermark. Mitteilungen der geodätischen Institute der technischen Hochschule in Graz, Folge 10, Graz, 1971.
- SCHLITT, H.: Systemtheorie für regellose Vorgänge. Springer-Verlag, Berlin/Göttingen/Heidelberg, 1960.
- SCHOLLER, K.: Korrelationsänderungen und scheinbare Punktverschiebungen im Trilaterationsnetz. Mitteilungen aus dem Institut für Theoretische Geodäsie der Universität Bonn, Nr. 19, Bonn, 1973.
- TAUBENHEIM, J.: Statistische Auswertung geophysikalischer und meteorologischer Daten. Akademische Verlagsgesellschaft Geest & Portij K.-G., Leipzig, 1969.

Discussion (paper 19)

- Q. How long are the short period processes, how many minutes or something like that ?
- A. I took time at intervals of about 2 months
- Q. Two months, and is that the shortest period possible ?
- A. Yes, if there is a time-delay of about 2 days, the correlation coefficient will be about 0.4 or 0.3. It depends on the signal, you use to eliminate the trend. And if you take a time-delay of about 5 days, you will get the correlation-function be nearly a delta-function.
- This is very interesting: if you have at least 2 correlation-functions you can use least squares collocation to adjust for instance trilateration networks or three-dimensional networks.
- Q. Did you look for measurements at certain moments of the day only ?
- A. Yes. My experience shows that these very short fluctuations can only be caught by direct measurements, and my task was to estimate the correlation functions for a period for which direct measurements are very uneconomical.
- It is very difficult to get direct measurements over such long periods.
- Q. I'm wondering in how far those functions compare with each other at the various levels. You mentioned that you used data on a tower at levels of 2 m, 5 m, 10 m and 15 m. Did you take the average of these data or did you treat them separately.
- A. I took the mean values
- Q. Did you take each level separately
- A. The difference of the levels, yes.
- Q. and then averaged at 200 m.
- A. at 15 m; I calculated the local refraction coefficients for the different surfaces.

SCINTILLATION MEASUREMENTS OF A LASER - BEAM

R. Bruckner, Geodetic Institute, University of Hannover, Federal Republic of Germany

Summary:

The angle of elevation without the influence of refractivity can be measured with the dispersometer. The so found angle-variation depends - besides other factors - on the character of the amplitude - and frequency-spectrum of the scintillation of direction, too. This cognition was the inducement to examine the scintillation of direction and intensity. A beam of a He-Ne-laser modulated by 1 kHz is received by the telescope system of the dispersometer. In the focal plane of which a position sensing photodetector is. The horizontal and vertical alternations of direction as well as the fluctuations of intensity of light are registered by an analog taperecorder. The evaluation after the digitalization (250 data/s) shall be done in the frequencies 0 - 100 Hz. Besides this dry and wet temperatures are measured in different heights at little temporale disintegration as well as the velocity of the wind.

1. Introduction:

A beam of light propagating through the atmosphere of earth is altered by different processes for example by scattering caused by atmospheric molecules as well as by mist, haze and aerosols, or by refraction from unhomogeneities of the density of the atmosphere. Contrary to the propagation in the vacuum where a beam of light, for example a laser beam, propagates exactly rectilinearly from source to receiver, in the real atmosphere the wave of light becomes more or less deflected. In the following the propagation of a laser-beam in a turbulent medium shall be described (plane waves), then will be reported about a system of measurement registering in direction and intensity caused by atmospheric turbulence, and finally results of measurement not yet exploited shall be set out.

2. Propagation of a laser-beam in a turbulent medium

According to the Fermat Principle every electro-magnetic wave propagates so that the transite time becomes a minimum.

$$\int_A^B n(x,y,z,t) ds \rightarrow \min. \quad (1)$$

In (1) n is the refractive index of the air which is a function of space and of time. The fluctuations of the refractive index as a function of dry- and wet-temperatures and of the air-pressure and its gradients now cause a non-linear propagation, respectively a propagation disturbed by effects of turbulence. On the other hand the fluctuations of the parameters mentioned depend on the weather conditions and the time of day and season, on the topographic conditions of the profile and on the ground distance. Thus [LEE and HARP, 1969] registered changes in the temperature up to 5 K within fraction of seconds in about 1.5 metres above the ground.

The processes of fluctuation have a frequency-spectrum that can reach up to several hundreds cps [HÖHN 1969]. Everyone knows the effect, if a star is observed through a telescope with a small aperture: the star seems to dance continuously and to fluctuate in its intensity. Astronomers speak of scintillation. Many works especially within the English-speaking part of the world dealt with scintillation of intensity during the last fifteen years. Beyond this the geodesist is interested in scintillation of direction, specially its reactions within the ground near field of refraction. With the Hannover dispersometer [GLISSMANN 1976] the effect of a gradually altering field of refractivity on the angle of elevation can be investigated. The indicated small alternations during the time of observation manifest in the imageplane for example of a theodolite as a shivering of the target, as fluctuations in intensity of light and as defocussing of the image of the target. According to the fundamental work by [TARTARSKI 1961] in the statistic theory of turbulence the structure function of the refractive index is used to describe its spatial distribution:

$$S_n(\underline{r}) = \langle [n(x) - n(x + \underline{r})]^2 \rangle \quad (2)$$

Practically it represents the geometric mean value of all differences of refractive indices between two points which are remote the distance of r . Thereby the square brackets signify the mean value of the sample by a constant vector \underline{r} (x, y, z). Besides this in many works also a spatial and temporal correlation-function of the alternation of the refractive index is used.

$$K_n(\underline{r}) = \langle \Delta n(\underline{x}) \Delta n(\underline{x} + \underline{r}) \rangle = \langle \Delta n_1 \cdot \Delta n_2 \rangle \quad (3)$$

$$K_n(\tau) = \overline{\Delta n_1(t) \cdot \Delta n_2(t + \tau)} \quad (4)$$

$$S_n(\underline{r}) = 2[K(0) - K(\underline{r})] \quad (5)$$

The connection between (2) and (3) follows from relation (5). According to this $S_n(\underline{r})$ can also be calculated from the autocovarianzfunction $K_n(\underline{r})$. The structure function depends only on the difference between two functional values. This means that the statistic field is isotrop and homogeneous only within a small region. The mean values of the refractive indices may still alter linearly within this region. The theory of turbulence coined the outer scale L_0 for the distance at which this is no longer valid. Elements of turbulence larger than L_0 are unisotrop and unhomogeneous. On the other hand the inner scale l_0 amounts to few mm (up to cm) near the ground thus corresponding to the scale of the smallest element of turbulence. According to [TARTARSKI 1961] the temporal spectrum of a statistic variable quantity can be described by the geometric optic as long as condition (6) is valid.

$$\rho = \sqrt{\lambda \cdot L} \ll L_0 \quad (6)$$

L_0 = diameter of the largest element of turbulence,

λ = wave-length,

L = distance between source and receiver,

ρ = correlationlength.

Practically this means "freezing" the spectrum of quantity of the elements of turbulence. [HODARA 1966] found empirically for the dependences of figure L_0 on h up to 400 m:

$$L_0[m] = \frac{0,4 h_{[m]}}{1 + 0,1 h_{[m]}} \quad (7)$$

Following the same work also an estimation of the dependences on h of the fluctuations of the refractive index results:

$$\langle \Delta n^2 \rangle = 10^{-12} \exp\left(-\frac{h}{1600}\right) \quad (8)$$

Specially within the first 100 m of the atmosphere of turbulence from several mm up to some decimetres exist.

According to [TARTARSKI 1961] the structure function of the refractive index can be estimated following (9):

$$S_n(\underline{r}) = \begin{cases} C_n^2 \underline{r}^{2/3} & l_o \ll \underline{r} \ll L_o \\ C_n^2 l_o^{2/3} \left(\frac{\underline{r}}{l_o}\right)^2 & \underline{r} \ll l_o \end{cases} \quad (9)$$

Here C_n is the structure constant of the fluctuations of the refractive index. It represents a measure for the quantity of the turbulence concerned [DAVIS 1966] and serves as statistic for the description of the atmospheric turbulent reciprocal effect with optical waves.

weak turbulence: $C_n = 8 \cdot 10^{-9}$

mean turbulence: $C_n = 4 \cdot 10^{-8}$

strong turbulence: $C_n = 5 \cdot 10^{-7}$.

This arrangement is a rather subjective one, for the proportional factor C_n in (9) depends on many factors, as on the average time of day, when the observations are made, on the height above ground, on the local ground and so on. Regarding relation (9) the structure function that represents a mean value of differences of the refractive index depends on the magnitude of the elements of turbulence and on the distance between the observation-points.

However, horizontal and vertical refractive index gradients insert in both functional values, causing an alternation of the speed and direction of the parallel light. In many works the behaviour of C_n were confirmed by other authors. In [CLIFFORD 1976] some examples of the reactions of the structure constant are mentioned. Following this low values are received in the morning while the maximum is reached in the afternoon. Then the ground gives the warmth received during the day to the air-layers near the ground. A minimum comes again at sunset.

Within the English-speaking part of the world the bubbles in which the refractive index varies from the average value are also called EDDIES. Their effect can be shown roughly by the following division.

Elements of turbulence with medium diameter l_0 in which the refractive index can reach different values, too, are regarded.

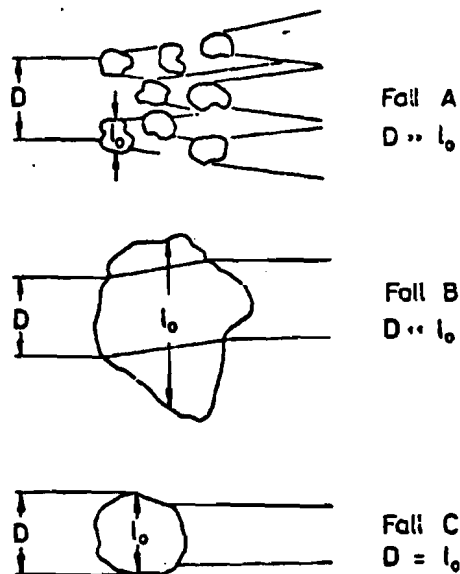


Fig. 1: Effect of the elements of turbulence on the propagation of laser beams

D = diameter of beam

l_0 = diameter of an element of turbulence

In case A the diameter D of the beam is very large in relation to the diameter of an element of turbulence. Each element exercises an influence on a partial bundle and causes a broadening of beams, a splitting of beams as well as fluctuations of phases and amplitudes. In case B the whole beam is deflected, the distribution of intensity over the cross-cut of radiation remains constant while in case C the beam is bundled like by a lense or widened, deflected or deformed. In the real atmosphere this separation is not possible, however. There all sizes are found as well in horizontal as in vertical direction of propagation. However, the effect also depends on the situation of the elements of turbulence in relation to source and receiver. As already mentioned the other meteorologic parameters exercise a more or less large influence on the scintillation-behavior of a laser beam, whereby all quantities have to be regarded as functions of space and time. Here only solar radiation, velocity and the grade of clouding shall be mentioned. Concerning

the instrumental conditions to measure phenomena of scintillation many experiments were done. However, general methods of only little common currency were deduced. But the opening of the receiver-system should not be too small according to [FRIED 1967] about 10 cm. [HODARA 1966] mentions an estimation of the mean elevation deviation, too,

$$\langle \Delta \theta^2 \rangle = 2 \cdot \Delta n^2 \cdot \sqrt{\frac{L}{L_0}} \quad (10)$$

which [HOLTZ 1968] converts to values of the beam-displacements in the distance L from the source,

$$\overline{\Delta x_E^2} = \overline{\Delta y_E^2} = \overline{\Delta n^2} \cdot \frac{L^3}{3L_0} \quad (11)$$

$$\Delta r_E = \sqrt{\overline{\Delta x_E^2} + \overline{\Delta y_E^2}} \quad (12)$$

by which Δr_E gives the distance between the axes of the disturbed and the undisturbed signal.

3. Source, receiver, test-ranges

In this paragraph some dates about the Hanover tests are reported. A modulatable He-Ne-laser of the firm of LICONIX serves as source:

wavelength :	632,8 nm
power:	5 mW
beam diameter:	1,0 mm
beam divergenze:	0,8 mrad $\hat{=}$ 50 mgon
coherence length:	20 cm
modulation:	1 kHz

The telescope-system described in [GLISSMANN 1976] serves as receiver, here with a focal length of 6,8 m. An iron tube contains a Cassegrain-system. A position-sensing photodetector is in the focal plane.

relative aperture of the telescope-system M:

$$M = \frac{\text{focal distance } f_{\text{ges}}}{\text{diameter of primary mirror}} = \frac{6,8 \text{ m}}{0,11 \text{ m}} = 62 \quad (13)$$

After an electronic treatment of the signals from the detector the total intensity, the horizontal and the vertical position of the received laser-beam and a signal of 50 cps as a marking of time are registered on four tracks of an analog tape recorder. The digitalization for the exploitation with a computer is done at the Bundesanstalt für Geowissenschaften at Hanover, at 256 datas per second and per channel what corresponds to a Nyquistfrequency of 125 cps. However, the filter of the receiver-set allows a resolving up to 90 cps. Illustrations 4 and 5 show measurements on a 2 km long test-range roughly running in east-west direction. Thereby the laser-beam propagates in a height of about 2 m above the ground. The source is on a very heavy wooden tripod standing on iron tubes of about 0,75 m length that are driven into the ground. The receiver stands on a brick pillar, unshakeable as well. In contrary to the short test-range above the ground of the 22 km long range from the Nordmannsturm (Deister) to the Geodätisches Institut (Hanover) is very unhomogeneous (see fig. 2).

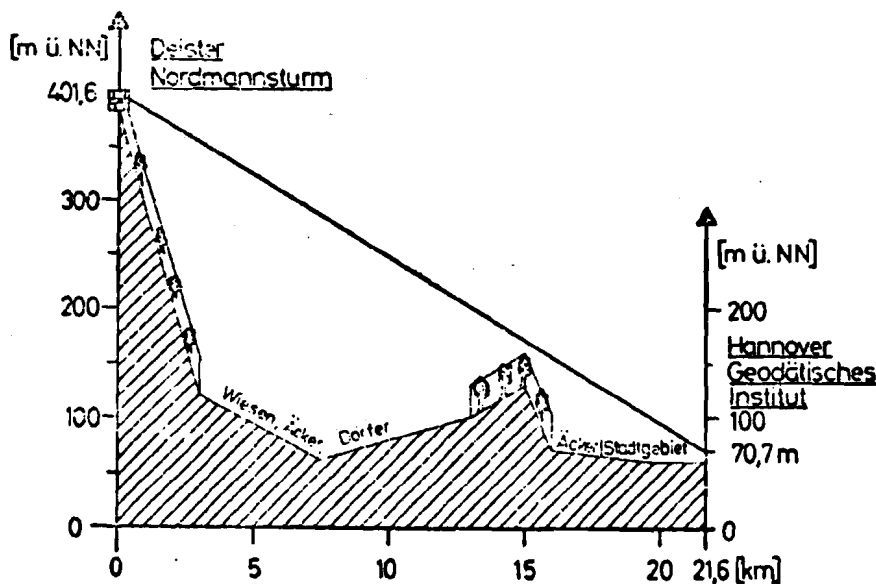


Fig. 2: Profile of the test-range Deister - Hanover

The distance between the beam and the tree-tops, respectively the ground, is from 10 ($s_1 = 1,5$ km distance from source) up to 230 m ($s_2 = 5,4$ km distance from source). Now the values of some of the parameters mentioned in chapter 2 for the described test-ranges

shall be summarized in tabular form (tab. 1). According to this the elements of turbulence have to be considerably larger than 0,4 m, if the statistic field to be figured cannot be described by geometric optic any longer. The radial deflection between the disturbed and the undisturbed laser-beam has to be expected to be about 0,3 m for the 2 km-distance and 4,9 m for the 22 km-distance - according to the theoretic statements.

	2-km - Teststrecke 2-km-testrange	22-km - Teststrecke 22-km-testrange
1. Kohärenzlänge (Gl. (6)) coherence length (Eq. (6))	$\rho = 0,11 \text{ m}$	$L = 5,4 \text{ km } \zeta = 0,18 \text{ m}$ $L = 15,0 \text{ km } \zeta = 0,31 \text{ m}$ $L = 22,0 \text{ km } \zeta = 0,37 \text{ m}$
2. Abschätzung für L_0 (Gl. (7)) Value for outer Scale L_0 (Eq. (7))	$h = 2 \text{ m}, L_0 = 0,67 \text{ m}$	$h = 10 \text{ m } L_0 = 2,0 \text{ m}$ $h = 230 \text{ m } L_0 = 3,8 \text{ m}$
3. Abschätzung für Δr_E (Gl. (12)) Estimation for Δr_E (Eq. (12)) $\Delta n^2 = 1 \cdot 10^{-12}$	$L_0 = 0,7 \text{ m}$ $\Delta r_E = 0,28 \text{ m} \hat{=} 9 \text{ mgon}$	$L_0 = 3,0 \text{ m}$ $\Delta r_E = 4,9 \text{ m} \hat{=} 14 \text{ mgon}$
4. Strahldurchmesser am Empfänger beam diameter in the receiver plane	$b = 1,6 \text{ m}$	$b = 17,3 \text{ m}$

Tab. 1: Abschätzung einiger Turbulenzparameter für die Teststrecken.

Tab. 1: Estimations for some parameters of turbulence for the two test-ranges

4. Registration of the position of the laser-beam

a) 2 km-test-range

The first measurements on the 2 km long test-range Vahrenheide were made every full hour between 1 and 8 p.m. on May 29th 1976 for four minutes each time. The general weather conditions were marked by a slight, cloudy high-pressure-area enclosing rain and thunder-showers. Indeed it remained dry during the time of observation. Besides temporary rather strong clouding there were short sunny periods. At the receiver-station dry- and wet-temperatures were registered at pole in the heights of 1.7, 3.7 and 5.7 m above the ground at intervals of about 10 seconds. The gradient of air pressure was not measured. He calculated refractive values N_L show a variation from 302 to

309 within 6 minutes at 2 p.m., while at 8 p.m., shortly before sunset, the values were between 307 and 308. Similar observations cannot be made for wind velocity, which is observed at 6 m above the ground. At 2 p.m. the values within the 6 min. long time of observation are between 2.0 and 6.0 m/s, at 8 p.m. still between 1,5 and 5.0 m/s. Illustrations 4 and 5 show parts of the measurements of scintillation of 2.5 s each at 2 p.m. and 8 p.m., the uncorrected values are shown. A comparison leads to the following statement first: The maximum amplitudes of the oscillations of position nearly decrease to half the amount between the two dates of observation, horizontally from 14 mgon down to 8 mgon, vertically from 11 mgon down to 7 mgon. A decrease in turbulence can be read off the refractive values of fig. 3, too.

b) 22 km-test-range

For these experiments the laser was on a heavy wooden tripod on top of the Nordmannsturm in the Deister hills. The receiver-telescope was fixed on an iron tripod on the top of the Geodätisches Institut. The weather conditions for this experiment on August 5th 1976 were marked by short clearing ups with very intensive sunshine and, besides that, by very heavy rain and showers of hail. The observations were made within a period, when a shower passes through from west to east about in the middle of the range. However, source and receiver remain dry. For some minutes the signal interrupts completely, neither continues the visible contact between the two stations. After the shower passed through the registration is continued. A cut of about 3.5 s of this is shown in fig. 6. Hereby the maximum oscillations in vertical and horizontal direction are near 6 mgon and lay in the sun. Meteorologic dates were not found, for their importance would have been negligible in comparison to the 2 km-range.

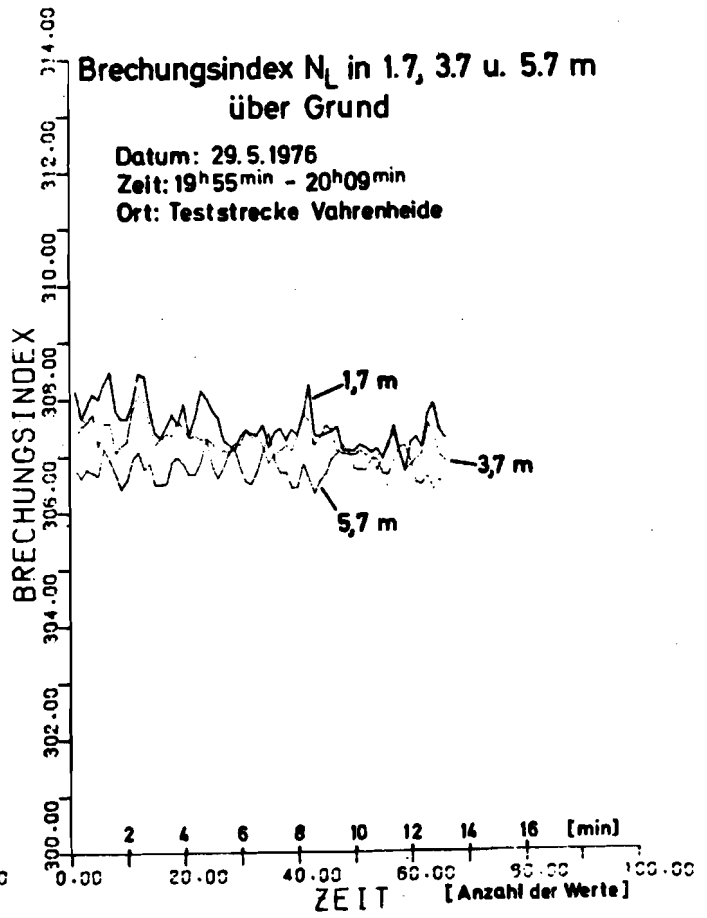
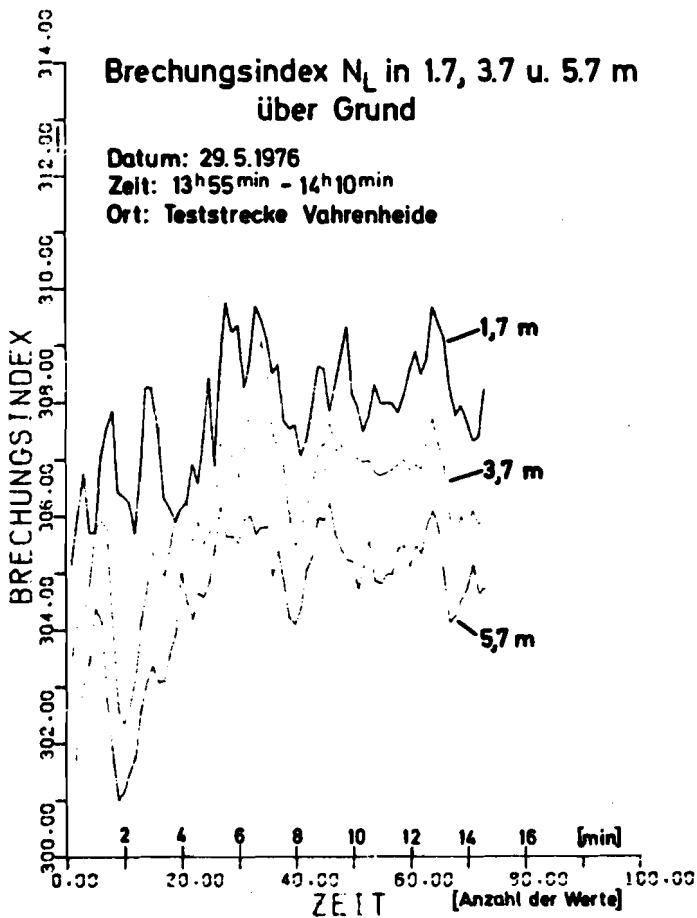
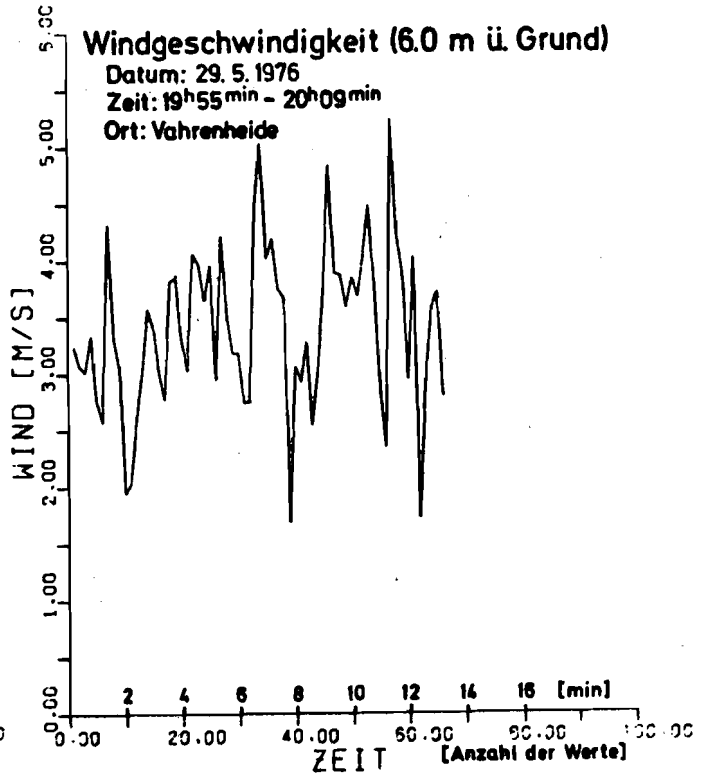
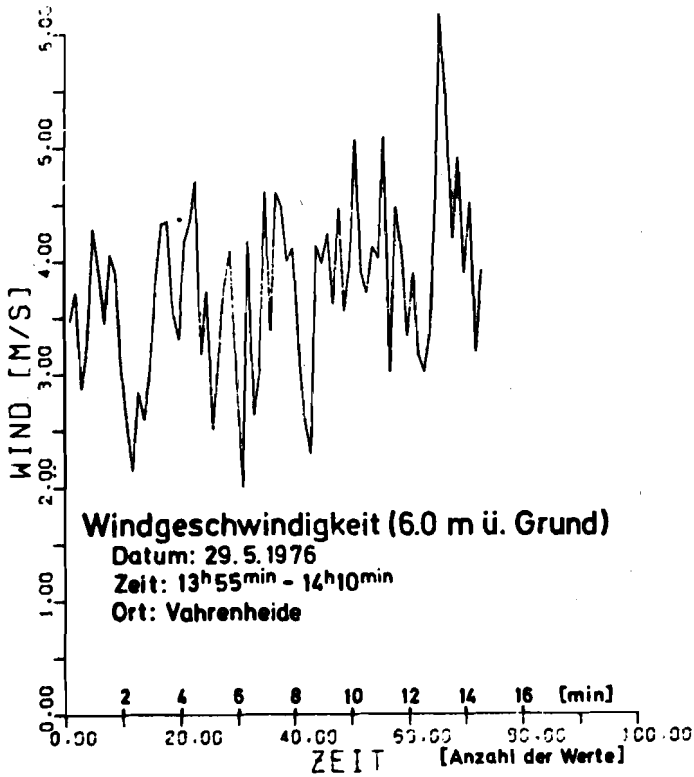


Abb. 3: Brechungsindex N_L in verschiedenen Höhen und Windgeschwindigkeit: 29.5.1976, 14^h und 20^h, Teststrecke Vahrenheide

Fig. 3: Refractive index N_L in different heights and the wind-velocity: May 29th 1976, 2 p.m. and 8 p.m., Vahrenheide test-range

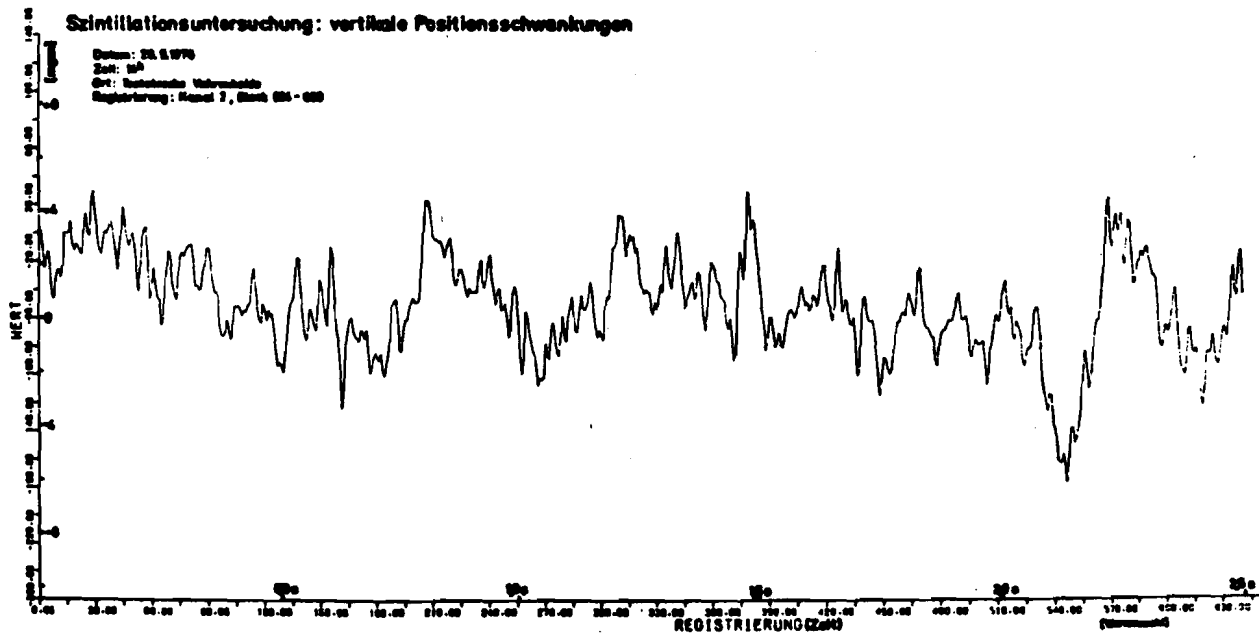
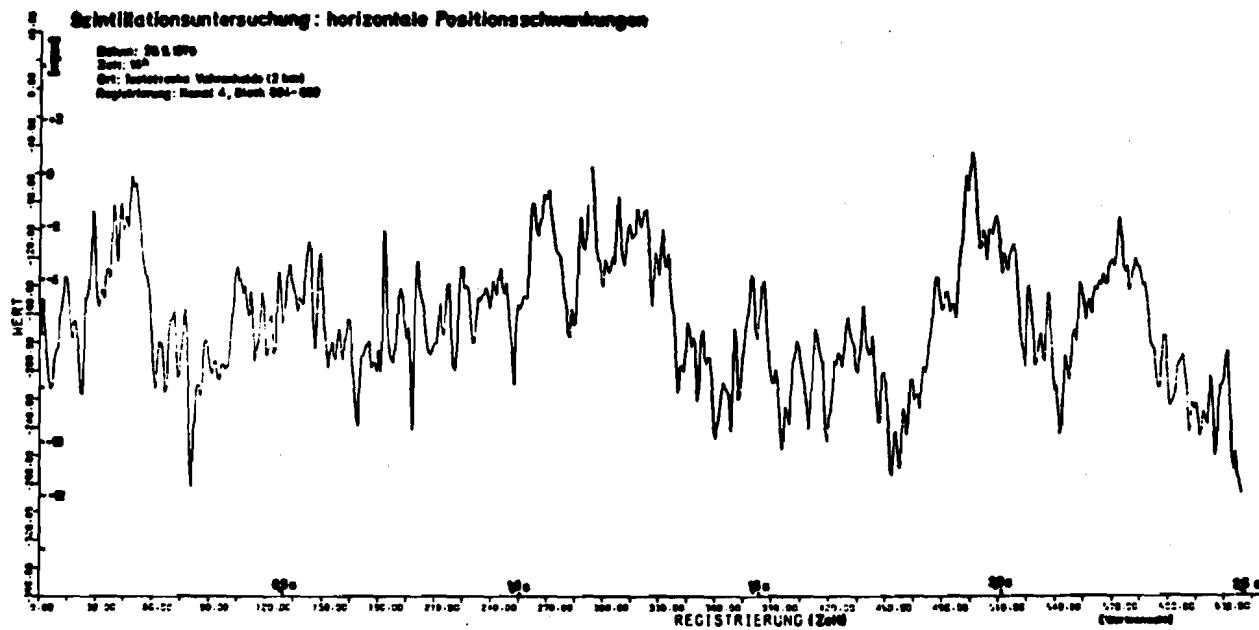


Abb. 4: Schwankungen eines Laserstrahls infolge turbulenter Atmosphäre: 29.5.1976, 14^h, 2 km - Teststrecke

Fig. 4: Oscillation of a laser-beam due to turbulent atmosphere: May 29th 1976, 2 p.m., 2 km - test-range

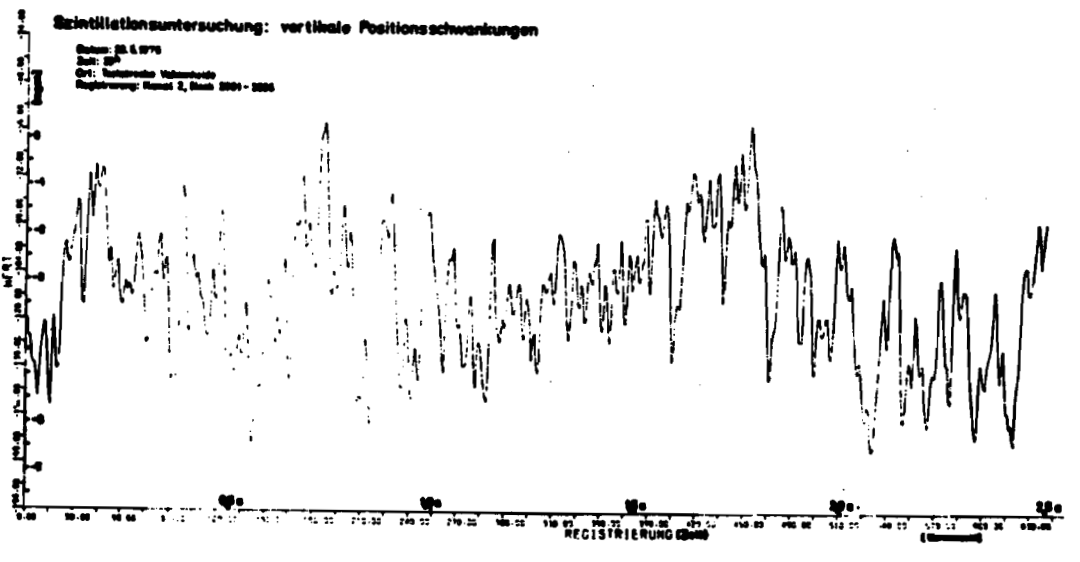
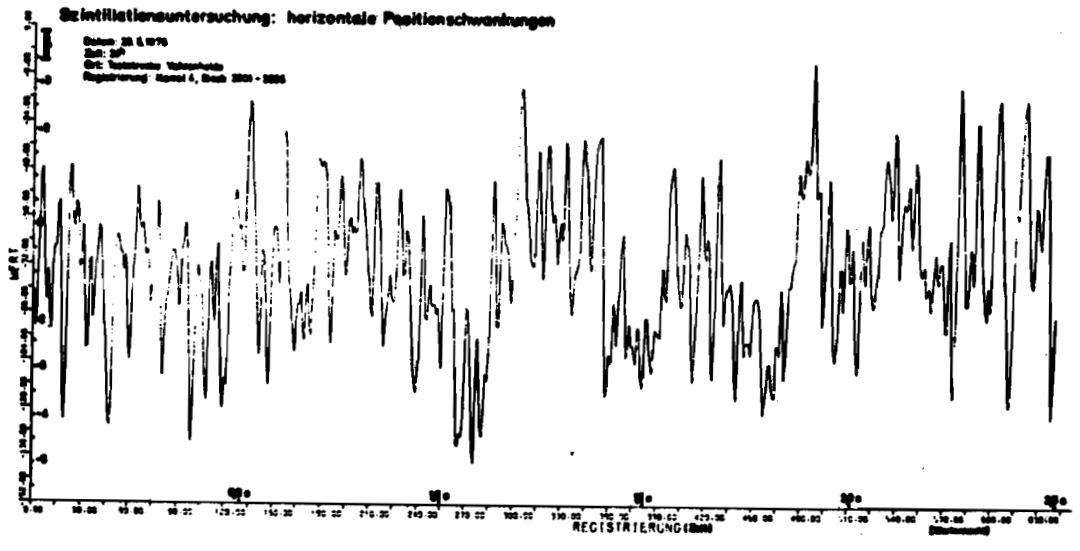
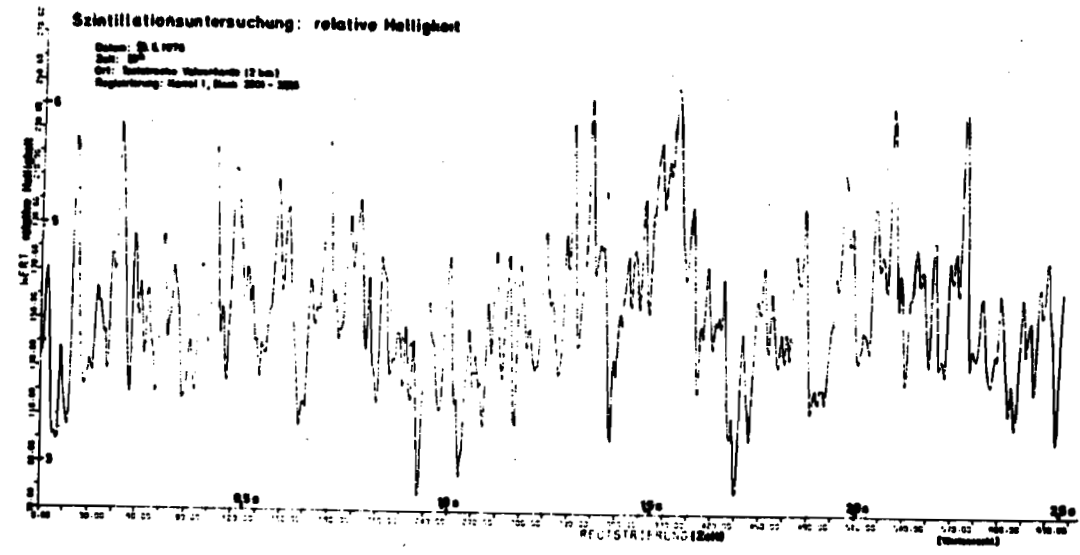
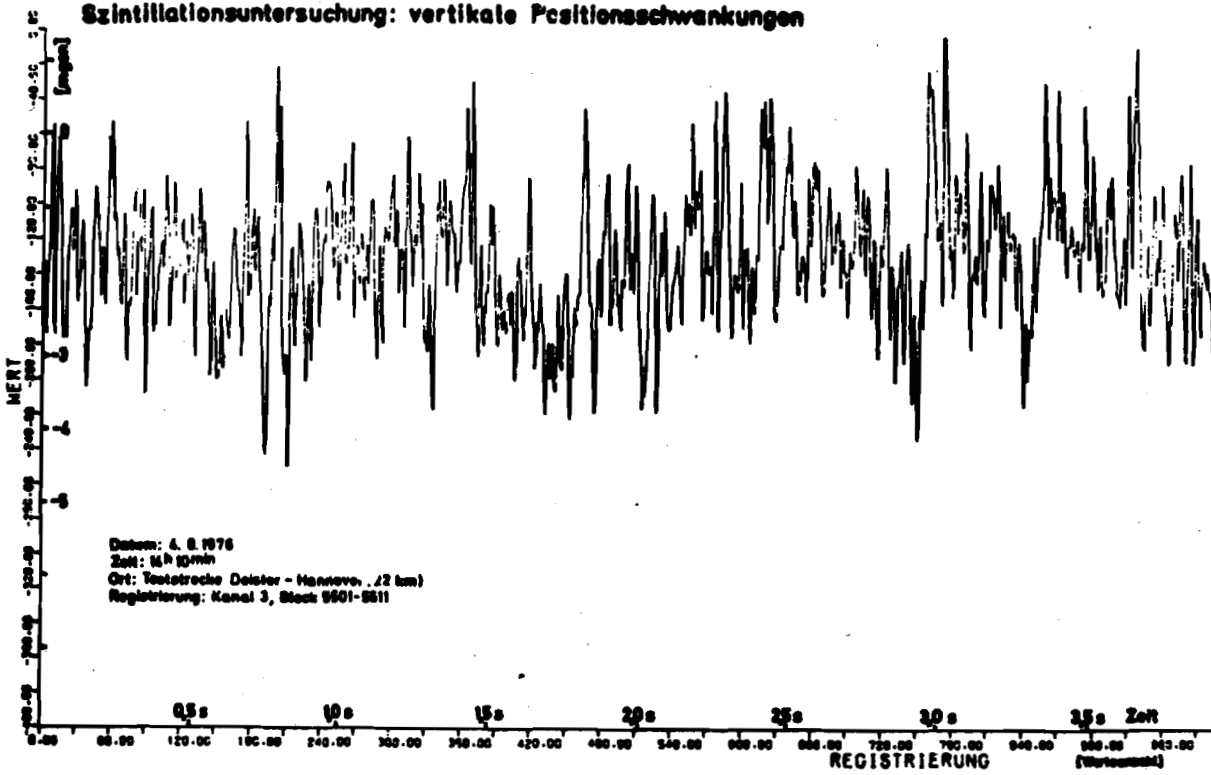


Abb. 5: Schwankungen eines Laserstrahls infolge turbulenter Atmosphäre: 29. 5. 1976, 20^h, 2 km-Teststrecke
Fig. 5: Oscillations of a laser-beam due to turbulent atmosphere: May 29th 1976, 8 p.m., 2 km-testrange

Szintillationsuntersuchung: vertikale Positionsschwankungen



Szintillationsuntersuchung: horizontale Positionsschwankungen

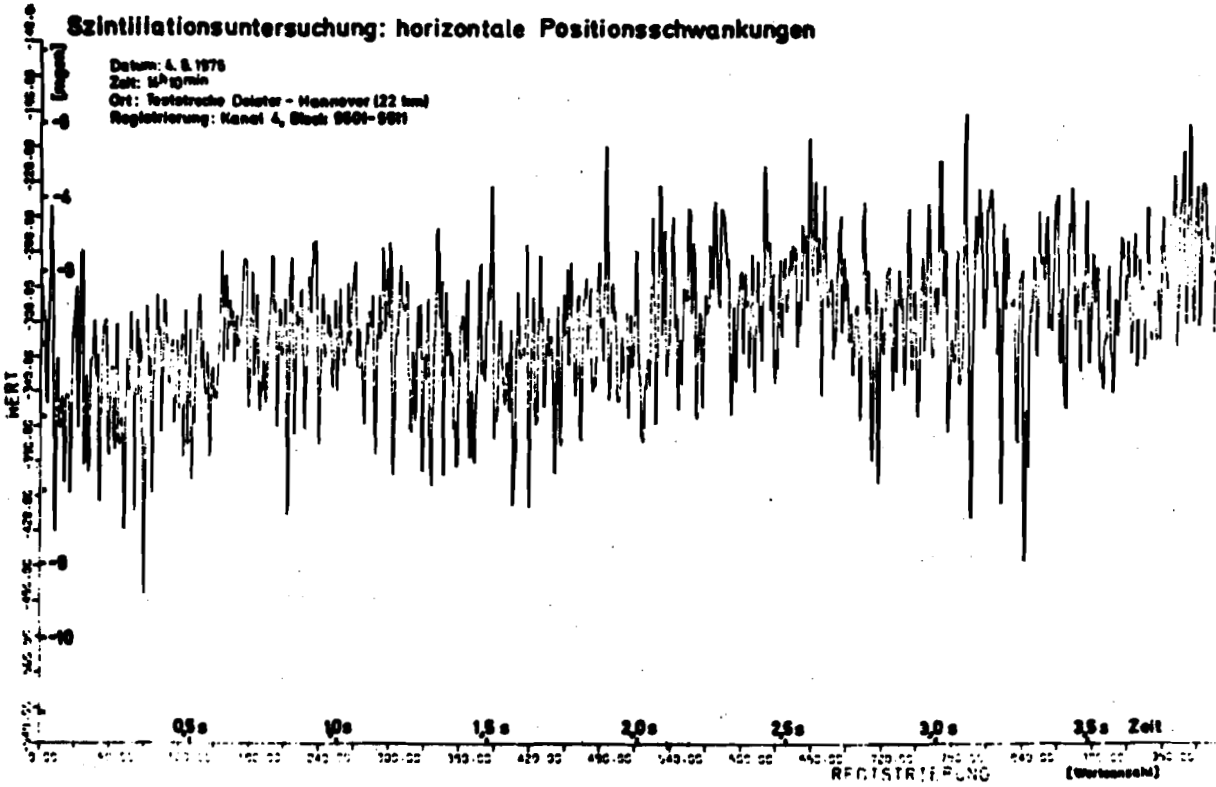


Abb. 6: Schwankungen eines Laserstrahls infolge turbulenter Atmosphäre: 5.8.1976, 14^h 10 min, 22 km - Teststrecke

Fig. 6: Oscillations of a laser-beam due to turbulent atmosphere: August 5th 1976, 2 p.m., 22 km - test-range

REFERENCES:

1. G.K. Born
R. Bogenberger
K.D. Erben
F. Frank
F. Mohr
G. Sepp
Phase-front distortion of laser radiation
in a turbulent
Applied Optics, Vol. 14, Nr. 12, 1975
2. A.L. Buck
Effect of the Atmosphere on Laser Beam
Propagation
Applied Optics, Vol.6, Nr.4, 1967,
S. 703 - 708
3. S.F. Clifford
Physical properties of the atmosphere in
relation to laser probing
Optical and Quantum Electronics 8 (1976)
S. 95 - 104
4. J.I. Davis
Consideration of Atmospheric Turbulence in
Laser Systems Design
Applied Optics, Vol.5, Nr.1, S. 139 - 147
5. D.L. Fried
G.E. Mevers
M.P. Keistner
Measurements of Laser-Beam Scintillation in
the Atmosphere.
Journal of the Optical Society of Amerika,
Vol.57, Nr. 6, 1967
6. T. Glissmann
Zur Bestimmung des Refraktionswinkels
Über die Dispersion des Lichtes mittels
positionsempfindlicher Photodioden.
Wiss.Arb. der Lehrst. für Geodäsie,
Photogrammetrie u. Kartographie an der
TH Hannover, Nr. 62, 1976
7. E. Grafarend
Elektromagnetische Entfernungsmessung
im Konzept stochastischer Prozesse
AVN 1971, S. 41 - 49
8. H. Hodara
Laser Wave Propagation Through the
Atmosphere.
Proceedings of the JEEE,
Vol. 54, Nr. 3, 1966
9. D.H. Höhn
Zur Ausbreitung eines Laserstrahls in
der Atmosphäre.
OPTIK 30, 1969, S. 161 - 170
OPTIK 30, 1969, S. 234 - 256
10. E. Holtz
Entwicklung eines Laser-Nivelliersystems
Diss. TH Aachen, 1968
11. D. Paperlein
Influence of Wind and Cloudiness on
Terrestrial Scintillation.
J.Opt. Sc.Am., Vol. 57, 1967,
S. 1157 - 1158
12. V.I. Tatarski
Wave Propagation in a Turbulent Medium
Mc Graw-Hill, New York, 1961

Discussion (paper 20)

- Q. You have reported about the deviation of the direction of the laser-beam perpendicular to the direction. For me it is of interest to know the variation of the optical path, the integral of the refractive index and ds ; and the dependence of the time or with other words, the fluctuation-spectrum of the distance between 2 points. Can you give me any information or perhaps anyone else in this room.
- A. What we did is to determine the fluctuation of the laser on the axis of the detector. We looked for the variations in the angle and not in the distance.
- Q. Have you any idea what to do with these measurements. Are you trying to do more measurements in other regions, and correlate with other things ?
- A. We tried to find the frequency spectrum within the time of a few minutes.

EXPERIMENTAL DETERMINATION OF THE COEFFICIENTS OF REFRACTION FROM HEAT FLUX MEASUREMENTS

F.K. Brunner, Department of Geodesy, The University of New South Wales, Sydney, Australia

ABSTRACT

The uncertainty associated with the determination of vertical refraction is still the limiting factor in the precision attainable with trigonometric levelling. The atmospheric temperature gradient is the vital component in the calculation of the coefficient of refraction. A relationship between heat flux and the temperature gradient, based on the energy balance at the earth's surface has been established in the literature.

In order to study the nature and prediction of the refraction coefficients, a field experiment was set up. A 480 m test-line was established on a grassy slope in Berry, NSW, Australia. Reciprocal refraction coefficients were determined by zenith distance observations as well as via the heat flux approach, at every 15 minutes during the time period 0600 to 1900 hours. Values of heat flux were determined by direct measurements of net radiation, heat flux into the ground, and through application of the combination method. The measured coefficients of refraction show high numerical values, with a range of +1.5 to -0.8. The correlation coefficient between the values determined independently by the two different methods is found to be 0.88. It is shown that the profile of the line is essential in the determination of the absolute values of individual refraction coefficients, and that the sun/shadow conditions at the observation station play an important role in the modelling of refraction coefficients.

The results presented encourage further testing of the heat flux method for the determination of refraction coefficients, and these tests should now be extended to longer lines of sight.

1. INTRODUCTION

1.1 Aims of the Investigation

There are advantages in replacing spirit levelling by the more economical trigonometric levelling, where the lines of sight may be both inclined and much longer (> 400 m), depending on the topography. However, the effects of atmospheric refraction over longer lines of sight reduce the precision of trigonometric levelling. Consequently, it is appropriate that research should concentrate on the determination of the vertical refraction in trigonometric levelling.

The gradient of temperature is the key factor in the calculation of the coefficient of refraction. To date, the representative measurement of the gradient of temperature using temperature sensors has met with limited success in geodetic applications, especially because of the turbulent character of the atmosphere close to the ground. The use of the relationship between heat flux and the temperature gradient, which was established by micrometeorologists [9], [10], [12], [14], has therefore been proposed. The heat flux can be calculated by the combination method using the measurements of net radiation, heat flux into the ground, water vapour pressure, air pressure, mean wind speed and mean air temperature. These parameters show smaller fluctuations than the measured temperature gradients, and the gradients derived by this method are therefore expected to be more representative for the refraction of the light path.

A theoretical discussion of the heat flux approach as a method for the determination of the coefficient of refraction has been given in the literature [1], [2]. In the present paper, modifications to this method are discussed and experimental test measurements are reported and analysed. The line over which the experimental measurements were taken was reasonably short (500 m), with the underlying vegetation distribution being homogenous over the profile. In order to limit uncertainties which accompany empirical formulae, most of the required meteorological parameters have been measured directly.

1.2 Trigonometric Levelling

The height differences between two points A and B, ΔH_{AB} , can be calculated from observations of the zenith distance z_{AB} and the slope distance S by the formula [4]:

$$\Delta H_{AB} = S \cos z_{AB} + \frac{1}{2} (S \sin z_{AB})^2 r^{-1} (1 - k_{AB}) \quad (1)$$

where r is the radius of the spheroidal section in the azimuth A to B, and k_{AB} the refraction coefficient for the line of sight A to B. The effect of the deviation of the vertical on the height differences which are determined by measuring zenith distances and slope distances may be neglected for the present investigation, according to the previous work of the author, [4], [5]. The refraction coefficient k_{AB} in Eq.(1) is defined as the ratio of the refraction angle $\Delta\beta_{AB}$ at the station A, to half of the centre angle of the spheroidal section:

$$k_{AB} = 2 \Delta\beta_{AB} r (S \sin z_{AB})^{-1} \quad (2)$$

For reciprocal zenith distance observations the mean height difference $\overline{\Delta H}_{AB}$ is calculated from the formula, [4]:

$$\overline{\Delta H}_{AB} = \frac{1}{2} S (\cos z_{AB} - \cos z_{BA}) - \frac{1}{4} (S \sin z_{AB})^2 r^{-1} \Delta k \quad (3)$$

where $\Delta k = (k_{AB} - k_{BA})$. From this equation it is obvious that besides observation errors of distance and zenith distance, the height difference will be affected by the difference of the reciprocal refraction coefficients. Research should therefore concentrate on the difference of reciprocal refraction coefficients Δk rather than on the absolute values of k . Investigations should also be extended to determining the allowable time differences between the reciprocal zenith distance observations. This would further make organization of the trigonometrical levelling operation easier. In seeking a fuller understanding of the

behaviour of Δk , the investigation of the individual refraction coefficients appears to be the appropriate starting point.

In the following sections, derivations are carried out for the direction AB only, and similar equations for BA may be found by simple substitution of the appropriate values. Throughout this paper pressure is taken in mb, but all other quantities are expressed in SI units.

2. DETERMINATION OF REFRACTION COEFFICIENTS

2.1 Geometrical Method

The individual refraction coefficient k_{AB} can be determined by a geometrical method, if in addition to the zenith distance z_{AB} and the slope distance S , the (true) height difference $\Delta \tilde{H}_{AB}$ has also been measured, for example by spirit levelling. From Eq. (1) it follows that:

$$k_{AB} = 2r(S \cos z_{AB} - \Delta \tilde{H}_{AB}) (S \sin z_{AB})^{-2} + 1 \quad (4)$$

The mean refraction coefficient can be determined without knowing $\Delta \tilde{H}_{AB}$, [6], but this aspect will not be dealt with in the present context.

2.2 Meteorological Method

An expression for the refraction angle $\Delta \beta_{AB}$, based on the solution of the eikonal equation for geometrical optics by MORITZ [11], has been given in [7]:

$$\Delta \beta_{AB} = - 10^{-6} S^{-1} \sin z_{AB} \int_0^S \left(\frac{dN}{dh} \right) (S - X) dX \quad (5)$$

where (dN/dh) is the vertical gradient of the refractivity (N) of light waves, and X an integration variable, see Fig. 1. It should be noted, that the integration in Eq. (5) is carried out along the chord. Using the formula of BARRELL and SEARS, the gradient of refractivity can be derived as [7]:

$$(dN/dh) = - 0.79 pT^{-2} [3.416 + 100(dT/dh)] \quad (6)$$

where p is the air pressure, T the air temperature (H), and (dT/dh) is the vertical gradient of temperature. In the derivation of Eq. (6), the effect of the water vapour pressure gradient on the curvature of

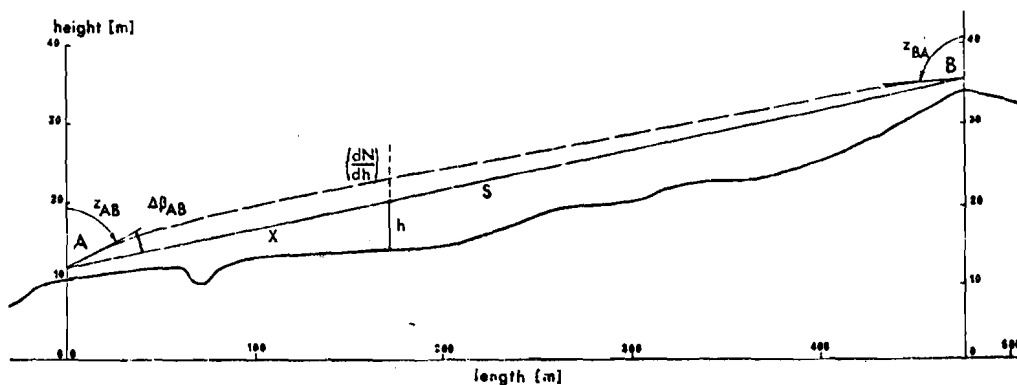


Fig. 1: Geometry of trigonometrical levelling, and ground profile of the line of the experiment.

light waves has been considered insignificant. However, this assumption is only valid for light rays at heights more than one metre above the ground, which is generally the case for ordinary theodolite observations.

Substitution of Eq. (6) into Eq. (5), and then into Eq. (2) yields the required value of k'_{AB} from meteorological measurements, considering p and T constant along the light path:

$$k'_{AB} = 5.032p T^{-2} \left[3.416 + 200 S^{-2} \int_0^S \left(\frac{dT}{dh} \right) (S-x) dx \right] \quad (7)$$

where r has been taken as $6.37 \cdot 10^6$ m. For the practical application of Eq. (7), the determination of (dT/dh) has to be restricted to the terminals only, and hence (dT/dh) along the chord will be predicted from the terminal values.

It has been shown [3], [12] that the potential temperature gradient close to the ground can be expressed by the equation:

$$(d\theta/dh) = -\alpha h^\beta \quad (8)$$

where α is the potential temperature gradient at 1 m height, and β an exponent which changes with atmospheric stability.

The potential temperature is calculated from the well known equation:

$$\theta = T(1000/p)^{0.286} \quad (9)$$

and the relationship between $(d\theta/dh)$ and (dT/dh) is then given to sufficient accuracy by:

$$(d\theta/dh) = (dT/dh) + \Gamma \quad (10)$$

where Γ is the adiabatic lapse rate, 0.00977 km^{-1} .

If the potential temperature gradient at 1 m height has been derived at the station A as α_A , and is assumed constant for the line AB, then Eq. (7) can be rewritten:

$$k'_{AB} = 5.032 p T^{-2} \left[2.439 - 200 S^{-2} \alpha_A \int_0^S h^\beta (S-x) dx \right] \quad (11)$$

For the measured profile of a line of sight, and for a known exponent β , the integration in Eq. (11) can easily be carried out by numerical integration methods. (The value of β will be discussed in the next section). Introducing the equivalent height h_{AB} :

$$h_{AB} = \left[2S^{-2} \int_0^S h^\beta (S-x) dx \right]^{1/\beta} \quad (12)$$

yields the final form for the refraction coefficient k'_{AB} :

$$k'_{AB} = 5.032p T^{-2} \left[2.439 - 100 \alpha_A h_{AB}^\beta \right] \quad (13)$$

3. EVALUATION OF $(d\theta/dh)$ FROM HEAT FLUX MEASUREMENTS

3.1 General Remarks

A determination of (dT/dh) can be made by measuring either temperatures

or temperature differences at a few levels on meteorological masts. In geodetic literature, air temperature differences between two points, vertically separated by a small distance, are often referred to as temperature gradients. More reliable estimates of (dT/dh) can be derived from multi-level temperature recordings. This is the common practice in meteorology. However, because of the effects of fluctuations in small-scale atmospheric turbulence, representative mean temperature gradients can only be derived from measurements close to the ground when recordings are integrated over a few minutes. Turbulent fluctuations can reach amplitudes of 2K, during unstable atmospheric conditions.

3.2 Formulae for the Evaluation of $(d\theta/dh)$

An alternative way for the evaluation of $(d\theta/dh)$, using the sensible heat flux through the atmosphere, has been proposed by ANGUS-LEPPAN and WEBB in [2]. It is thought that the sensible heat flux, which is subject to less fluctuation, will yield more representative mean potential temperature gradients.

Turbulent transfer of sensible heat H (heat flux) forms one component of the energy balance equation [9], [13] which can be given in the form:

$$H = (R - G) - \lambda E \quad (14)$$

where R is the net radiation; G the heat flux into the ground; and λE is the latent heat flux of evaporation or condensation, λ being the latent heat of this change of phase. The determination of $(R - G)$ values has been proposed [2] from empirical formulae using qualitative observations of prevailing weather conditions, cloud type, surface material, vegetation, soil type and moisture. For the present investigation, the values of $(R - G)$ were measured directly using commercially available net radiometers and heat flux plates. The direct measurement was chosen in order to eliminate inaccuracies of the input data for the heat flux approach. The principles of measurement of evaporation E have been extensively discussed in literature [13], [15].

Of the many methods employed, the so-called 'combination method' appears to be most suitable in the evaluation of Eq.(14). The heat flux H may then be expressed as:

$$H = \frac{\gamma}{\gamma + s} (R - G) - c_p \rho \eta \bar{u} (D - D_s) \quad (15)$$

where γ is the psychrometric constant ($\gamma = c_p/\lambda$); c_p the specific heat at constant pressure; s the gradient of saturation specific humidity with temperature; ρ the density of air; \bar{u} the mean wind speed at height z ; D and D_s the wet-bulb depressions at height z and at the surface, respectively; and η a non-dimensional bulk aerodynamic coefficient. The combination method is vulnerable to an inadequate knowledge of the appropriate value of η for a particular surface. η is a function of both surface roughness and thermal stability and values given to date [1] appear to be only tentative. The major advantage of the combination method in the prediction of evaporation, is the fact

that Eq.(15) is defined in terms of standard meteorological data only. In geodetic fieldwork, measurements of dry- and wet-bulb temperature are generally made with aspirated psychrometers, and wind speed measurements can easily be carried out using cup anemometers.

Formulae for the vertical gradient of potential temperature ($d\theta/dh$) have been derived from the transfer equation of turbulent heat flux [12]:

$$H = -c_p \rho K_H (d\theta/dh) \quad (16)$$

where K_H is the eddy transfer coefficient for sensible heat.

These formulae take different forms for different (neutral, unstable, stable) stability regimes and are also height dependent, WEBB [15]. The present experiment has been specifically designed such that only a few of these formulae are to be applied. By limiting the zenith distance observations to usual daylight observation times and keeping the ray path between 1 to 10 m above the ground, only formulae relevant to unstable and neutral stability conditions are required. For the unstable period, the ray path can be assumed to be fully within the middle region (Region II) of the turbulent regime, WEBB [14], [15], [8]. Stability regimes are identified in the present investigation by use of the sensible heat flux value, H. If H assumes either very small positive or negative values, near-neutral conditions are indicated. Unstable conditions are identified by a positive (upward) heat flux.

For region II of the unstable regime WEBB [15] has given an expression which yields values of the parameters α and β of Eq. (8), appropriate when $H > 0$:

$$\alpha = [H^2 \theta (c_p \rho)^{-2} g^{-1}]^{1/3}, \quad \beta = -4/3 \quad (17)$$

where g is the acceleration due to gravity. It is important to note that for unstable conditions the gradient ($d\theta/dh$) is not dependent on the wind speed, see Eq. (17), as the sensible heat flux H plays the governing role.

During neutral conditions the gradient of potential temperature is dependent on the wind's shearing stress, and sensible heat flux. An expression for ($d\theta/dh$) has been derived from dimensional analysis of wind and temperature profiles during adiabatic conditions [12]. For neutral stratification ($H \lesssim 0$), the parameters α and β can be expressed as:

$$\alpha = H (c_p \rho u_* K)^{-1}, \quad \beta = -1 \quad (18)$$

where u_* is the friction velocity; and K von Karman's constant, with numerical value 0.4.

The friction velocity u_* is a reference velocity, which characterises the particular turbulent regime. The magnitude of u_* is dependent on the wind's shearing stress and on air density. u_* can be calculated for neutral conditions from the well-known logarithmic wind profile [12]:

$$u_* = \bar{u} K / \ln(z/z_0) \quad (19)$$

where \bar{u} is the mean wind speed measured at height z , and z_0 the roughness length. The value of the roughness length z_0 corresponding

to various natural surfaces can be estimated with sufficient accuracy from tables [12], or read from graphs [14]. At the roughness length z_0 , the value of \bar{u} , according to Eq. (19) becomes zero. For surfaces whose characteristics do not alter markedly with changing wind speed, z_0 may be considered as more or less a constant surface property [13].

4. FIELD EXPERIMENT

4.1 Measurements

The site of the experiment was at Berry, NSW, Australia. The test line runs north-south on a west-facing slope with smooth topography and reasonably homogenous grass vegetation. The measurements were carried out on February 9, 1977 which was the first day of fine weather after several days of rain.

The *ground profile* of the test line AB, shown in Fig.1, was determined to sufficient accuracy in order to evaluate the equivalent heights for each terminal. The *height difference* was determined by levelling between the two terminal reference marks with an automatic level Zeiss Nil and invar staffs, using lines of sight limited to 15 m in order to eliminate refraction errors. From these measurements the height difference between the transit axes of the theodolites at A and B was derived as 24.0775 m, with an estimated precision of 0.5 mm. The *slope distance* between A and B was measured at three different times with a HP 3805 Distance Meter. A value of 479.446 m was obtained after correction for atmospheric effects. The precision of the distance can be estimated at 5 mm.

The following measurements and observations were carried out at both terminals between 0600 and 1900 hours Eastern Standard Time, starting at every 15 minutes. *Simultaneous reciprocal zenith distances* were observed with Wild T2 theodolites (automatic index) using the three-wire method. These observations were carried out from tripods, set at both stations to an instrument height of 1.50 m. Special sighting targets were fitted to each theodolite allowing for simultaneous reciprocal observations. The precision of the mean zenith distance (three-wire method) has been estimated from all observations as $\pm 0.9''$. *Dry and wet-bulb temperatures* were measured by specially manufactured aspirated psychrometers with an electronic read-out system. The psychrometers were mounted on a small mast at heights of 1.5, 3 and 6 m above the ground. The wet-bulb depression at the surface was measured with a hand held Assmann psychrometer. *Air pressure* was measured using mechanical barometers. *Horizontal wind speed* was measured with a Rimco three-cup sensitive anemometer at the 1.5m level. The revolutions were counted for periods of 3 minutes. *Net radiation* was measured with Swissteco net radiometer S-1, at 1 m above the ground. *Heat flux into the ground* was measured with Solar Radiation soil heat flux plates. Three plates were connected in series, and placed about 8 cm below the natural surface. *Cloudiness* was estimated in oktas. The *sun/shadow condition* at each station was also recorded by noting whether the observation station was subject to the full strength of the sun's radiation, subject to variable strength radiation through passing clouds, or in total shadow.

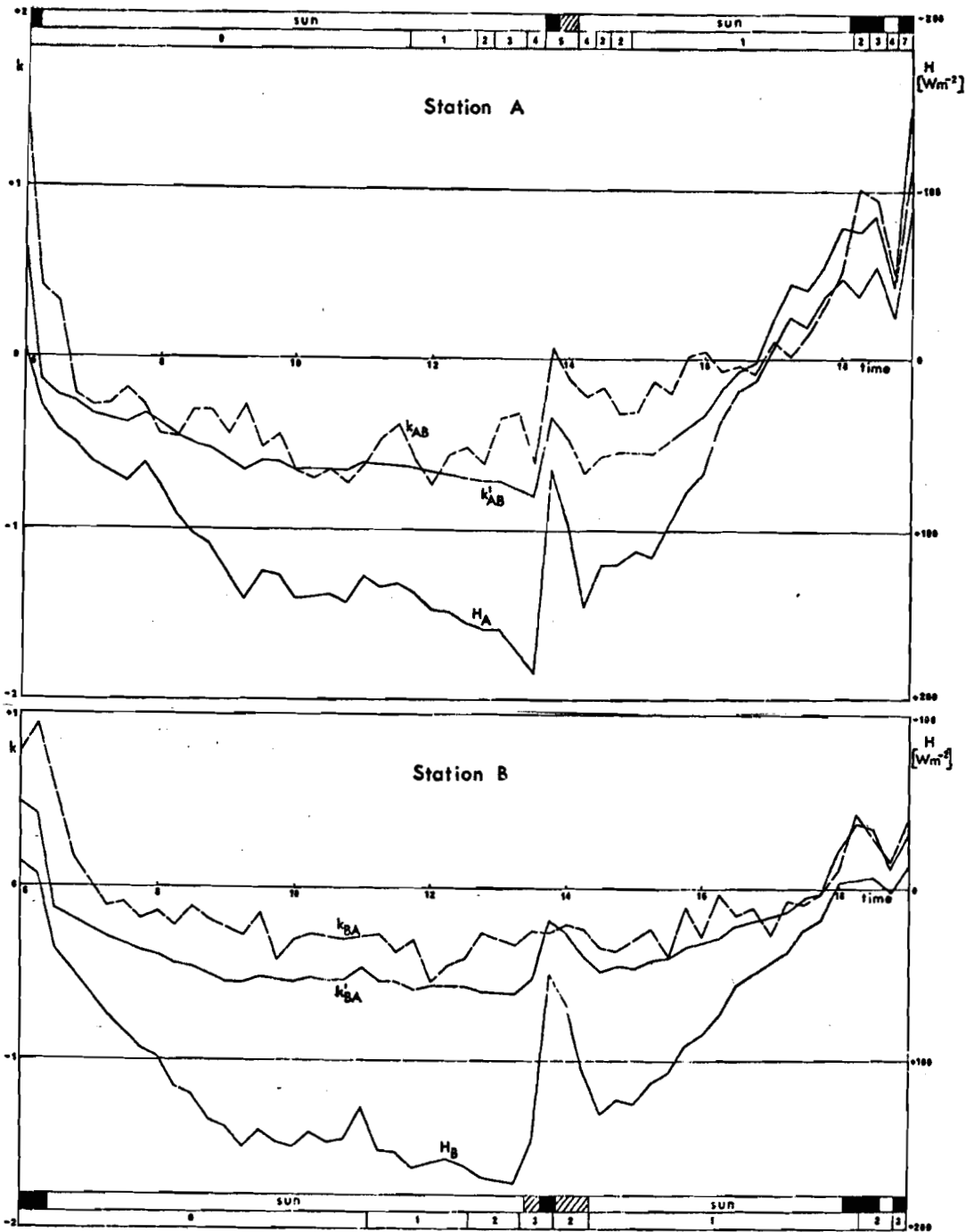


Fig. 2: Refraction coefficients from zenith distance observations (k), values of heat flux (H), and derived refraction coefficients (k'), cloudiness and sun/shadow, separated for station A and B, plotted against time.

4.2 Analysis

All calculations have been carried out separately for the directions AB and BA in order to study the behaviour of the individual refraction coefficients, and to facilitate understanding of the causes of the difference between reciprocal values of k .

Using the observations described previously, individual refraction coefficients k_{AB} and k_{BA} for every 15 minutes have been derived, and are shown in Fig.2. The standard deviation of an individual determination can be estimated as ± 0.13 , applying the law of propagation of variances to Eq.(4) and using the given numerical values.

Using the ground profile, equivalent heights have been calculated by the numerical integration of Eq.(12). This yields for $\beta = -1(-4/3)$, $h_{AB} = 3.67(3.51)$, and $h_{BA} = 4.56(4.39)$.

Values of heat flux, shown in Fig.2, have been calculated using the combination method described in section 3.2. The bulk aerodynamic coefficient η has been evaluated as 0.0045 for the estimated roughness length z_0 of 2 cm for both stations, [1]. Values for neutral and unstable conditions have been separated, and appropriate formulae are employed for the calculation of the parameter α , Eqs.(17, 18). Subsequently, the representative values of the refraction coefficients k'_{AB} and k'_{BA} shown in Fig.2, have been determined using the calculated equivalent heights. Assuming a 5% error in the heat flux determination, the standard deviation of k' can be estimated from Eqs. (17,13) as ± 0.03 , for average conditions of the experiment.

5. DISCUSSION

The height differences computed from simultaneous reciprocal zenith distance observations have been compared with the (true) value ΔH_{AB} obtained by spirit levelling. The standard error of a single height determination can be estimated as ± 2.7 mm, and the maximum error is found to be 6.6 mm. If the measurements are restricted to the working period 0900 to 1700 hours the standard error of a single height determination would have been ± 1.9 mm, and the maximum error 4.0 mm. These results again show the validity of trigonometrical levelling as a precise and accurate method for height difference determinations [5]. From an analysis of the variations of k with time and changing weather conditions the conclusion can be drawn that for changing weather conditions reciprocal zenith distances must be measured simultaneously, but for homogenous weather conditions (heavy overcast or clear sky) a time difference of up to one hour between the reciprocal measurements may be allowed, when observations are restricted to 0900 to 1700 hours.

Although temperature gradients have been evaluated from the mast measurements, and subsequently used for the calculation of refraction coefficients, these are not presented and discussed here. These values show very large fluctuations and are therefore considered as not representative, which is in accordance with previous experience.

The measured values of k determined by the geometrical method show high numerical values with a range of +1.5 to -0.8, which are in agreement with those values of k determined on a mountain slope in a previous investigation [6]. The short term fluctuations of k can partly be explained as a result of random observation errors of the zenith distances, and partly by the changing sun/shadow conditions at the terminals.

An inspection of the graphs (Fig.2) of the refraction coefficients determined by the two independent methods, zenith distance observations and heat flux approach, show high parallelism between them. This becomes especially stunning when the observation stations were in shadow, just before 1400 hours. Both methods also showed similar results when the setting sun was hidden by a cloud bank for $\frac{1}{2}$ hour, appeared for the 1845 hour observations, and finally set at 1855 hours. At both stations the reappearing sun radiation is perfectly illustrated by the increase of the heat flux value and the derived k' values, as well as by those k values which are derived from zenith distance observations. This short term variation would not have been modelled sufficiently if empirical formulae rather than the direct measurement of (R-G) had been used.

Assuming the refraction coefficients k' derived from heat flux measurements as error free, the linear regression with the observed k values can be calculated for all 106 pairs as:

$$k = +0.11 + 0.87 k' \quad (20)$$

In addition, the correlation coefficient has been estimated at 0.88. The relatively small intercept value of the regression line shows the importance of calculating the correct equivalent heights for the line of sight. However, in Eq. (20) both the intercept and the slope of the regression line are significant values on a 5% significance level. This difference from the hypothetical regression ($k = k'$) appears to arise through the presence of model errors; for example, the assumption of H and u_* being invariant with changing height [10]. Fortunately, for the difference of reciprocal refraction coefficients this fact will have little bearing.

The experimental results of this investigation have clearly shown that the derivation of refraction coefficients from heat flux measurements is an accurate and practical method. This method is therefore well suited for further research into the nature of the differences between reciprocal refraction coefficients, and their prediction. From this investigation it can be concluded that for longer lines of sight with asymmetric profiles, the equivalent heights for each terminal will become increasingly important. Furthermore it has been shown that the sun/shadow conditions at the observation station play an important role in the modelling of refraction coefficients. This effect becomes immediately apparent when (R-G) is measured by sensors, rather than modelled by empirical formulae.

The present paper has also shown that it is a practical possibility to determine heat flux values from reciprocal zenith distance observations, when the roles of refraction coefficient and heat flux are reversed. The advantage of this optical method is twofold; it does not require the physical presence of instruments in the measurement area, and it yields the integral value of the heat flux over the whole line of measurement. Evaluation of the effects of water vapour pressure gradients on light path curvature, and refinements to the profile relationships used in this method are presently under investigation.

6. ACKNOWLEDGEMENT

This project was supported by a Special Project Grant of the Faculty of Engineering, University of NSW, Australia.

The author wishes to thank the staff members of the School of Surveying, University of NSW for their assistance with the field work. Furthermore the author is grateful to Prof. P.V. Angus-Leppan for reviewing the manuscript, and to Mr. C.S. Fraser for his assistance with the field work and computations for the project.

7. REFERENCES

- [1] ANGUS-LEPPAN, P.V. (1971): Meteorological Physics Applied to the Calculation of Refraction Corrections. *Commonwealth Survey Officers Conference*, Paper No. B5, 9pp.
- [2] ANGUS-LEPPAN, P.V. & WEBB, E.K. (1971): Turbulent Heat Transfer and Atmospheric Refraction. *General Assembly IUGG, Moscow, Travaux IAG - Sec.1*, 15pp.
- [3] BROCKS, K. (1948): Über den täglichen und jährlichen Gang der Höhenabhängigkeit der Temperatur in den unteren 300 Metern der Atmosphäre und ihren Zusammenhang mit der Konvektion. *Berichte des Deutschen Wetterdienstes in der US-Zone*, 5, 1-30.
- [4] BRUNNER, F.K. (1973): Lotabweichungseinfluss bei der trigonometrischen Höhenmessung mit steilen Visuren. *Österr. ZfV*, 61, 126-134.
- [5] BRUNNER, F.K. (1975a): Trigonometric Levelling with Measured Slope Distances. *Proc. 18th Austral. Surv. Congr.* (Perth 1975), 79-94.
- [6] BRUNNER, F.K. (1975b): Coefficients of Refraction on a Mountain Slope. *Unisurv G22*, Univ. NSW, Sydney, 81-96.
- [7] BRUNNER, F.K. & ANGUS-LEPPAN, P.V. (1976): On the Significance of Meteorological Parameters for Terrestrial Refraction. *Unisurv G25*, Univ. NSW, Sydney., 95-108.
- [8] BRUNNER, F.K. & FRASER, C.S. (1977): An Atmospheric Turbulent Transfer Model for Edm Reduction. *Proc. Symp. EDM-REF* (Wageningen, 1977).
- [9] DEACON, E.L. (1969): Physical Processes Near the Surface of the Earth. *World Survey of Climatology*, 2 (General Climatology), 39-104.
- [10] LUMLEY, J.L. & PANOFSKY, H.A. (1964): *The Structure of Atmospheric Turbulence*. Interscience, New York, 239pp.
- [11] MORITZ, H. (1967): Application of the Conformal Theory of Refraction. *Österr.ZfV*, Sonderband 25, 323-334.
- [12] PRIESTLEY, C.H.B. (1959): *Turbulent Transfer in the Lower Atmosphere*. University of Chicago Press, 130pp.
- [13] SLATYER, R.O. & McILROY, I.C. (1961): *Practical Microclimatology*. CSIRO (UNESCO), Australia, 175pp.
- [14] WEBB, E.K. (1964): Daytime Thermal Fluctuations in the Lower Atmosphere. *Applied Optics*, 3, 1329-1336.
- [15] WEBB, E.K. (1969): The temperature structure of the lower atmosphere. *Proc. of REF-EDM Conference*, Univ. NSW, Sydney (1968), 1-9.
- [16] WEBB, E.K. (1975): Evaporation from Catchments. *Proc. Third Nat. Symp. on Hydrology, "Prediction in Catchment Hydrology"*, Canberra, 203-236.

Discussion (paper 21)

- Q. Over the kind of range, which you have been using, we used quite extensively the system in which we place a zoneplate in the middle of the range and a screen at the other; and we observed the image movements on that screen. We generally found that the searching with that kind of system is of a higher precision than with the theodolite. If you manage your three components on three stable pillars, I wonder whether that kind of system would give you more accurate measurements of the effective K.
- A. I must say that I thought about using other means than theodolites to measure the geometrical path of the refraction coefficient, but somehow, I could not attract funds for everything and so I had to go back to the old method of using the theodolite. Maybe the last application where you want it anywhere.
- There is somebody in America using a similar method as you just described to us and they had quite good results too, but they had to apply their tests on a salt lake because they were really scared about the topography. But also what I was worried about was at the time we investigated to use lasers, we found out that laser-beams are not really as stable as we want.
- Q. The system, which I described is not dependent on the stability point of the lasers. The laser simply acts as a point source and does not have to be stable.
- A. Well, I should like to hear more about that.
- Q. Can you give us an impression of the cost of the additional equipment of your heat-flux sensors and of your net radiometer.
- A. The net-radiation instrument costs about 450,- dollars (Australian) I'm sure the one we used is the best design available. The important part is, that if you would use it during night, during inversion, where you have dew coming down, then you would also need an outer shield, so that dew is not thrown on to the windshield of the sensor and this is a little bit of a head-ache, but we overcame

this problem then finally too. So, 450 dollars for the net-radiometer. The heat-flux plate costs you about 90 dollars. I found that was an increase of 20 dollars, when I decided to buy the net-radiometer at an other producer. He increased by 20 dollars then. 90 dollars each heat-flux plate, so you would have to reckon about 600 dollars, because you have to put three in series to get a reasonable result. Otherwise you have just a spot-measurement and don't get anywhere.

The heat-flux into the ground is the easiest path to the model and I think there is no trouble at all, because it is just one conduction equation which you have to solve.

But it is also a very small amount. So you would have to reckon there for both stations about 600 dollars for 6 heat-flux plates and a windspeed meter, a good anemometer is, quite expensive. You have to include a mechanical counter of about 350 dollars, maybe today already 360.

Q. Of course you in Australia are famous, you said that. And this is completely true, because already Bergstrand relied upon the meteorological conditions in Australia, when he should correct for his measurements in Sweden. Of course you are in a favourable position, because you can make all this measurements very easily, the conditions are very good. I know that Angus has dealt with such a topography as you have been dealing with, both over water-surfaces and over ice. Of course the heat-flux approach, is not so easy over water, but it is very important that we know the micro-meteorological conditions near the water-surfaces, because vertical angle-measurements will become very important when we shall make connections just from one island to another island.

Why I'm talking about that is that we are planning to go from the Swedish island to a Finnish island making vertical angle-measurements, correct them for refraction and make a levelling in this way. This is the only way we can do it and now I ask you, have you any experience in spite of the fact that you have been talking about the heatflux. It is just the question, where should I put my theodolite, my measuring instrument, shall I put it

over land at an elevation as high as you practically can, say 20 meters or something like that. That is, shall I go up at the island, put my theodolite there and the other island the same or shall I go very near the surface of the water, where the turbulence is most dangerous ?

Is that at 10 m or is it very near the surface of the water ? Have you any experience of that, because we are planning such a measurement now this fall, and of course if I use the multi-wave method, in any case, I like to have stable conditions from the point of view of turbulence. Have you an experience of watersurfaces ?

A. Well, you ask me a few questions and I have to say I have a few good news and a few bad news for you, but you should put this theodolite as high as possible at the surface.

Q. Even from island to island ?

A. I think so, that is confirmed by the good results prof. Hradilek gets with his measurements, because he uses a tower and then he gets, one refraction-coëfficiënt per station.

The higher the surface the better you are off. The other thing, which I have to say, I tend to disagree with you, when you say that all water is more difficult for the heat-flux approach, because, I don't think this is true: It is easier on the water and this is the good news. And it is easier on the water, because water is a homogeneous surface and has an almost homogeneous body and the evaporation is saturated at this surface and is equal to the potential one. If you have an ordinary salt-surface, the evaporation and the salt-saturation with water changes from place to place. That is quite obvious. So on the water you have a better situation for evaluation of the heat-flux.

Q. But you must measure the heat-flux .

A. Yes,

- Q. You need a lot of boats, simultaneous measurements with the other measurements. How do you measure the heat-flux over the water-surface? Well, your device, you have to distribute them in some way and you have to do it about the same time as your angle-measurements.
- A. Well, I will admit that I haven't thought about using it over water, but I think one would have to shield the out-going radiation from the surface. This can easily be done. Shield it completely and measure only the incoming radiation which will be the same over water and over the surfaces and combine it then with other equations, but I'm sorry I can't give you a complete impression.
- Q. Your heat-flux approach is very interesting in practical cases, because I can tell you that Mr. Kakuri has had practical experience from measurements from Finland to Öland. He told me, to put your theodolite as near at the surface of the water as possible, because there is the most stable condition. Real turbulence begins some meters up.
- Q. In the tropics you find the air temperature changes very rapidly in the morning, and around the midday it reaches a constant. It is accepted down there that, if you do observations for trigonometrical heighting you get the best values around midday.
- I would expect you have a graph to show more or less a constant value of the flux refraction-coefficient. This is in accordance to the accepted procedure of carrying out an observation for trigonometrical heighting around midday. It is often seen that the refraction-coefficient is constant around that time, the midday. However probably from the observations, that you carried out, what would you suggest as the best time for carrying out this trigonometrical heighting, because you suggest between 9 and 17.00 hrs.
- But we only accept around midday for any observation of trigonometrical heighting.

A. I would be very careful to suggest anything from one experiment for a practical method, where you only want to have one constant. I would be very cautious to do that. So, if you look at the graph, you just mentioned, then you indeed see that the refraction coefficient between about 10 o'clock with the exception of the sun-shadow condition, till about 4 o'clock in the afternoon is a reasonable constant. Of course it is negative because it was about only three meter above the ground. And what you said about observation during the noon period, well that is a standard procedure not only in the tropics but also especially in central-europe., they use the zenith distance observations around noon.

A REFRACTION MODEL FOR ELECTROOPTICAL RANGE FINDING IN THE MOUNTAINS

W. Mendel, Graz, Austria

1. Preliminary notes

Distance measuring by means of light or microwaves is gaining increasing importance. By using modern construction elements (integrated circuits etc.) the required apparatus is becoming smaller and smaller (and more and more reduced in weight) and its handling is quite unproblematic; no previous electronic knowledge is necessary to operate these measuring instruments. Expensive procedures are required, however, for the meteorological and geometrical reduction of the results of measurement obtained, particularly in the case of long distances. Meteorological reduction is the reduction of measurement results (transit time, rough distance and the like) to the length of the path curve.

The basic equation for meteorological reduction in a homogeneous medium is:

$$\begin{aligned} s &= v \cdot t \\ s &= \text{distance length} \\ v &= \text{velocity of signal} \\ t &= \text{transit time of signal} \end{aligned} \tag{1.1a}$$

Therefore, the following relation holds for v:

$$\begin{aligned} v &= \frac{c}{n} \\ c &= \text{light velocity} \\ n &= \text{group refractive index of air} \end{aligned}$$

Since in the medium "air" the group refractive index changes along the signal path the path curve length s must be calculated by integration:

$$s = \int_0^s ds = c \int_0^t \frac{1}{n_{gr}} dt \tag{1.1b}$$

Unfortunately it is not yet possible to determine the refractive index of air directly by simple means; it must be calculated from meteorological measurements by means of empirical formulas.

The refractive index of air mainly depends on the following parameters:

- 1) Wave length of light
- 2) Temperature
- 3) Atmospheric pressure
- 4) Partial steam pressure
- 5) Composition of the atmosphere (O_2 , O_3 , N, Argon, CO_2 , He, etc.)

The parameters 2-4 are highly variable and must therefore be measured. The wave length of light used is indicated by the manufacturer of the range finder. For parameter 5 assumptions will be sufficient but a CO_2 content of 0.03%, on which the following formulas are based, will most probably be too low. According to Barell and Sears the following equation holds for the actual group refractive index of air (see /5/, §38):

$$(n_{gr} - 1) 10^6 = 0,35853 \left[A + \frac{3B}{\lambda^2} + \frac{5C}{\lambda^4} \right] \frac{p}{T} - 15,02 \frac{e}{T} \quad (1.2)$$

A, B, C = constants

p = atmospheric pressure

T = temperature ($^{\circ}K$)

e = partial steam pressure

Among the three parameters of this equation, the temperature T and the atmospheric pressure p can be measured directly, the partial steam pressure e, however, only indirectly by measuring auxiliary quantities. Hygrometers and psychrometers have given good practical results.

The differential formula of Eq. (1.2) can be used to estimate the influence of incorrect initial values. The following equation holds for a mean wave length of 0.5μ , a temperature of $10^{\circ}C$, an atmospheric pressure of 760 torr and a partial steam pressure of 5 torr:

$$10^6 dn = 0,4 dp - 1,0 dt - 0,05 de \quad (1.3)$$

The influence of the atmospheric pressure dp is unproblematic, it nearly has a strictly regular effect, and so it is possible

The refractive index of air mainly depends on the following parameters:

- 1) Wave length of light
- 2) Temperature
- 3) Atmospheric pressure
- 4) Partial steam pressure
- 5) Composition of the atmosphere (O₂, O₃, N, Argon, CO₂, He, etc.)

The parameters 2-4 are highly variable and must therefore be measured. The wave length of light used is indicated by the manufacturer of the range finder. For parameter 5 assumptions will be sufficient but a CO₂ content of 0.03%, on which the following formulas are based, will most probably be too low. According to Barell and Sears the following equation holds for the actual group refractive index of air (see /5/, §38):

$$(n_{gr} - 1) 10^6 = 0,35853 \left[A + \frac{3B}{\lambda^2} + \frac{5C}{\lambda^4} \right] \frac{p}{T} - 15,02 \frac{e}{T} \quad (1.2)$$

A, B, C = constants

p = atmospheric pressure

T = temperature (°K)

e = partial steam pressure

Among the three parameters of this equation, the temperature T and the atmospheric pressure p can be measured directly, the partial steam pressure e, however, only indirectly by measuring auxiliary quantities. Hygrometers and psychrometers have given good practical results.

The differential formula of Eq. (1.2) can be used to estimate the influence of incorrect initial values. The following equation holds for a mean wave length of 0.5 μ, a temperature of 10°C, an atmospheric pressure of 760 torr and a partial steam pressure of 5 torr:

$$10^6 dn = 0,4 dp - 1,0 dt - 0,05 de \quad (1.3)$$

The influence of the atmospheric pressure dp is unproblematic, it nearly has a strictly regular effect, and so it is possible

to calculate, from end point measurements, a representative mean value for the path curves. Also the influence of the partial steam pressure p_{de} is very small and can be neglected when measuring with light electric (photoelectric) apparatus. The influence of temperature is most difficult to ascertain, and it is not permissible to determine, by finding mean values for end point temperatures, a representative value for the whole signal path. The daily temperature variation of air layers near the ground is abt. $10-15^{\circ}\text{C}$ in the summer months, that in the free atmosphere (500 m above ground) abt. 3.7°C at most (according to Sühning). Thus, higher temperatures are measured by day and lower ones at night in air layers near the ground than in the free atmosphere. Therefore, the mean representative temperature of the signal path can only be determined with the aid of models for the temperature field.

2. Development of the temperature model

2.1 Solar radiation

Solar radiation reaching the upper boundary of the atmosphere only varies abt. 1% depending on the distance from the sun and is therefore nearly constant. The energy that reaches the earth's surface, however, varies with the sun's zenith distance and is besides dependent on the absorption, the dispersion and the reflection in the clouds and in the atmosphere itself.

The variation of intensity along a light beam is given by the differential relation (see /6/, /7/):

$$dJ = -cJdm \quad (2.1)$$

J = intensity

c = absorption coefficient

dm = mass element

If J_0 is the intensity outside the atmosphere the following holds for the entire light path:

$$J = J_0 e^{-cm} \quad (2.2)$$

The entire radiation comprises the direct sun radiation and the diffused radiation from clouds and atmosphere. Empirical tests (Haurwitz and Brocks) yielded the absorption coefficient $c = 0.09$ for clear sky. The mass m was assumed with $1/\cos z_{\odot}$, i.e. the atmosphere was considered as a homogeneous layer, the mass of the air column to the zenith representing the unit mass. For the radiation R_e onto a plane surface the following holds (see /4/, /11/, /12/):

$$R_e = (a_0 - nb) \frac{1}{m} e^{-0.09m} \quad (2.3)$$

$$a_0 = 115 \text{ m} \quad \text{w/cm}^2$$

n = degree of covering

b = constant for type of cloudiness

m = air mass = $1/\cos z_{\odot}$

It follows for an inclined surface:

$$R = (a_0 - nb) \cos \alpha e^{-0.09m} \quad (2.3a)$$

α = angle of incidence of the sun

<u>Types of clouds</u>	<u>Symbols</u>	<u>Altitudes</u>	<u>b</u> <u>(m w/cm²)</u>
Cirrus	Ci	above 6,000 m	17
Cirrostratus	Cs		28
Alto cumulus	Ac	2,000-6,000 m	58
Altostratus	As		67
Stratocumulus	SC		78
Stratus	St	abt. 2,000 m	92
Nimbostratus	Ns		95
Fog			95

Table 1 (see /11/, /12/)

2.2 Thermal equilibrium on the earth's surface

The thermal influence R in Eq. (2.3) is the entire energy reaching the ground by way of short- and longwave radiation. It scatters manifoldly according to the following equation (see /3/, /5/):

$$R + I_u = \rho R + I_a + H + S \quad (2.4)$$

- ρ reflection factor
- I_u downward longwave radiation
- I_a upward longwave radiation
- H upward turbulent heat flow (affecting the temperature gradient near the ground)
- S heat flow to the earth's interior

In it ρR is the energy reflected from the earth's surface. The reflection factor ρ mainly depends on the condition of the surface (structure, moisture, vegetation) and, in some cases, on the angle of incidence.

Reflection factors

<u>Surfaces</u>		<u>Surfaces</u>	
Fresh snow	0,80-0,90	Water $z > 60^\circ$	0,05
Old snow	0,35-0,65	Stubble fields	0,16
Wet sand	0,9	Reaped fields	0,12-0,35
Dry sand	0,20-0,30	Wet fields	0,05-0,14
Green grass	0,16-0,27	Fir-pine woods	0,10-0,14
Dry grass	0,17	Leafy woods	0,16-0,37
Water $z = 85^\circ$	0,30-0,85	Corn fields	0,10-0,25

Table 2 (see /11/, /12/)

2.3 Upward longwave radiation

The Stefan-Boltzmann law for the entire emission M reads (see /3/, /6/, /7/):

$$M = \epsilon \sigma T^4 \quad (2.5)$$

ϵ = emission factor for black-body radiators $\epsilon = 1$

$\sigma = 5,67 \cdot 10^{-12} \text{ W cm}^{-2} \text{ }^\circ\text{K}^{-4}$ Stefan-Boltzmann constant

T = temperature on the surface in $^\circ\text{K}$

<u>Surfaces</u>	<u>Emission factors</u>
Snow cover	0,995
Grass	0,984
Water	0,96
Lime, gravel	0,92
Sand	0,90
Clouds	0,9-1,0
Polished metals	0,02

Table 3 (see /6/)

According to Table 3 the earth is almost a black-body radiator. The mean emission factor for the earth's surface is 0.06. Thus, the longwave radiation for a clear sky is

$$I_0 = 1,73, T^4 \cdot 10^{-9} \quad (2.6)$$

In a clouded sky only part of that energy becomes effective. Then, the following holds for the longwave radiation with clouded sky (see /11/, /12/):

$$I_n = 1,73 \left(1 - \frac{b}{\sigma_0} n\right) T^4 \cdot 10^{-9} = (1,73 - 0,015 b n) T^4 \cdot 10^{-9} \quad (2.7)$$

- b see Table 1 (constant for type of cloudiness)
n degree of cloudiness

2.4 Heat flow to the earth's interior

The temperature distribution on the earth's surface can be represented by a Fourier expansion (see /8/):

$$T_{0,t} = T_m + \sum_{i=1}^n t_i \cos(it + d_i) \quad (2.8)$$

- $T_{0,t}$ temperature on the earth's surface at the time t
 T_m mean day temperature
t clock time

The heat is transferred to the earth's interior only by heat conduction. Here, in all strictness, the equation of thermal conductivity holds:

$$\frac{\partial T}{\partial t} = K^2 \Delta t \quad (2.9)$$

with the boundary condition:

$$T_{0,t} = T_m + \sum_{i=1}^n A_i \cos(it + d_i)$$

The solution gives:

$$T_{z,t} = T_m + \sum_{i=1}^n A_i e^{-az} \cos(it + d_i - az) \quad (2.10)$$

$K = k_s/c$ = temperature conduction coefficient

k_s = heat conduction coefficient

c = specific heat

$$a = \sqrt{\frac{\pi}{24K}}$$

The heat flow S to the earth's interior is thus given by the temperature gradient and the heat conduction coefficient k_s :

$$S = -k_s \frac{\partial T}{\partial z} \quad (2.11)$$

2.5 Turbulent heat exchange

The heat exchange upward through the air is chiefly effected by turbulent heat exchange processes. The turbulent air exchange processes transport the heat much faster than the molecular heat conduction. There is a close relationship between atmospheric stability and turbulence.

For this reason, the potential temperature θ is defined as the temperature an air particle would assume if brought with no energy to the level of 1000 mb air pressure. An atmosphere with constant potential temperature (i.e. $\frac{\partial \theta}{\partial z} = 0$) has an adiabatic temperature gradient (neutral conditions), and the following holds (see /6/, /7/):

$$\frac{\partial \theta}{\partial z} = \frac{\partial T}{\partial z} + 0,01 \text{ } ^\circ\text{C m}^{-1} \quad (2.12)$$

If $\frac{\partial \theta}{\partial z}$ is positive, stable conditions will prevail. Under unstable conditions $\frac{\partial \theta}{\partial z}$ is negative, and any disturbance (e.g. turbulent winds) will produce lifting forces (back coupling, wind becomes stronger!).

For unstable weather conditions the atmosphere is divided into three zones a, b, c which are different by the so-called Obukov length L. Fig.1 shows the dependence of L on the wind velocity and the roughness of the ground.

a. Over-adiabatic underlayer

It reaches up to a height of $z < 0.03 L$, i.e. up to a max. of 2 m; in the mountains it reaches a max. of 0.5 m and can be neglected as the measuring instruments are generally arranged higher and the light path through this zone is in every case very short. The following is found for this zone (see /10/, /11/):

$$\frac{\partial \theta}{\partial z} = \frac{H}{c_p \sqrt{\rho} \gamma k} \quad (2.13)$$

H = heat flow

c_p = specific heat of air at constant pressure

ρ = density of air

γ = horizontal tensions (not recordable)

k = Karmon's constant = 0.4

b. Unstable intermediate layer

This zone reaches from $z = 0.03$ to $z = L$.

For this zone, Webb found the potential temperature gradient (see /10/, /11/, /12/):

$$\frac{\partial \theta}{\partial z} = \left[\frac{H^2 T}{1,2 \rho^2 c_p^2 g} \right]^{\frac{1}{3}} z^{\frac{4}{3}} \quad (2.14)$$

H = heat flow

T = air temperature

c_p = specific heat of air at constant pressure

g = gravitational acceleration

ρ = density of air

c. Free atmosphere

This zone reaches from the height $z = L$ to the fictitious upper border of the atmosphere $h = 11$ km. In this range, free convection will prevail where lifting forces are the principal reason for turbulence. Here, in the range $L < z < 10L$, the potential temperature gradient will go linearly from the value found in formula 2.14 toward 0 and will remain so as far as the lower border of the clouds.

3. Application of the model

Eq. (2.4) is the basic equation for the thermal equilibrium on the earth's surface. If the required parameters are known the turbulent heat flow upwards can be calculated for any point. Assuming that at a ground distance $z > 10L$ the isotherms are running at constant altitudes we can calculate - by iteration from the formulas given in section 2 - the temperature for every ground point and, thus, also for every point of the path curve.

For the heat flow to the earth's interior we require a Fourier analysis of the daily temperature distribution. If, however, we have not observed the temperatures throughout the day we can take - without committing too great inaccuracies of computation - the mean coefficients for the daily temperature distribution from meteorological almanacs or manuals (e.g. Lehrbuch der Meteorologie, by E.F.Schmid, Leopold-Voss-Verlag, 1890).

This temperature model is only useful for range finding in the mountains since in this case the lines of sight mostly run at great heights above ground, and therefore the influence of errors in the iterative back-calculation of ground temperatures is of little importance. Another weakness of the model is the neglect of horizontal temperature gradients. The terminal error of computation is only divided up linearly from the initial to the end point.

Example

For the Zinken-Gleinalpe side in the Styrian test network the end point values given in Annex 1 were measured or estimated. A radiation energy of 35.92 mW/cm^2 is obtained for both points from Eq. (2.3) and the values $a_0 = 115 \text{ mW/cm}^2$ and $b = 58 \text{ mW/cm}^2$ in Table 1. The effective longwave radiation L , the reflected shortwave radiation $g.R$ and the heat flow to the earth's interior s are deducted from that value to obtain the upward heat flow H which is decisive for the temperature gradient near the ground. Therefrom, the temperature distribution over the two end points can be computed with the aid of Eq. (2.14). Assuming an equal temperature of $T = -5^\circ\text{C}$ at 5,000 m altitude the temperature can be calculated for every point on the path curve by means of iteration from Eq. (2.14). The mean temperature calculated from this temperature model is 2°C lower than the mean value of the two end point values. This means a distance correction of 52 mm for the 26 km long Gleinalpe-Zinken side.

REMARK

Writing this paper I used the literature indicated in the references from /1/ to /11/. After presenting it I received the paper indicated with /12/. The partial identity of formulas, tables and the figure has the reason in the independent use of the same sources.

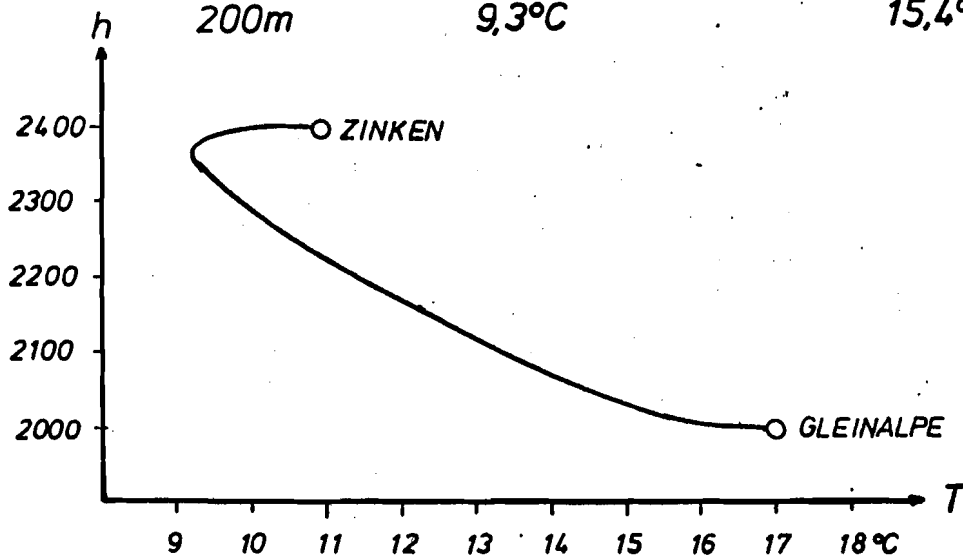
Given values:

	Zinken	Gleinalpe
H	2400m	2000m
p	750mb	790mb
T	284°K	290°K
z	60°	60°
t	13h	13h
A	5°C	7°C
n	0,5	0,5
Clouds	Alto cumulus	Alto cumulus

Computed values:

Gl. 2.3	Re	35,92mW/cm ²	35,92mW/cm ²
Gl. 2.7	I	8,42mW/cm ²	9,16mW/cm ²
Tab. 2	qR	7,18mW/cm ²	10,80mW/cm ²
Gl. 2.11	S	2,41mW/cm ²	2,11mW/cm ²
Gl. 2.4	H	17,91mW/cm ²	13,85mW/cm ²

Gl. 2.14	h	T	T
	1m	11,0°C	17,0°C
	2m	10,3°C	16,8°C
	5m	10,2°C	16,6°C
	10m	10,0°C	16,6°C
	20m	9,7°C	16,4°C
	50m	9,6°C	16,1°C
	100m	9,4°C	15,5°C
	200m	9,3°C	15,4°C



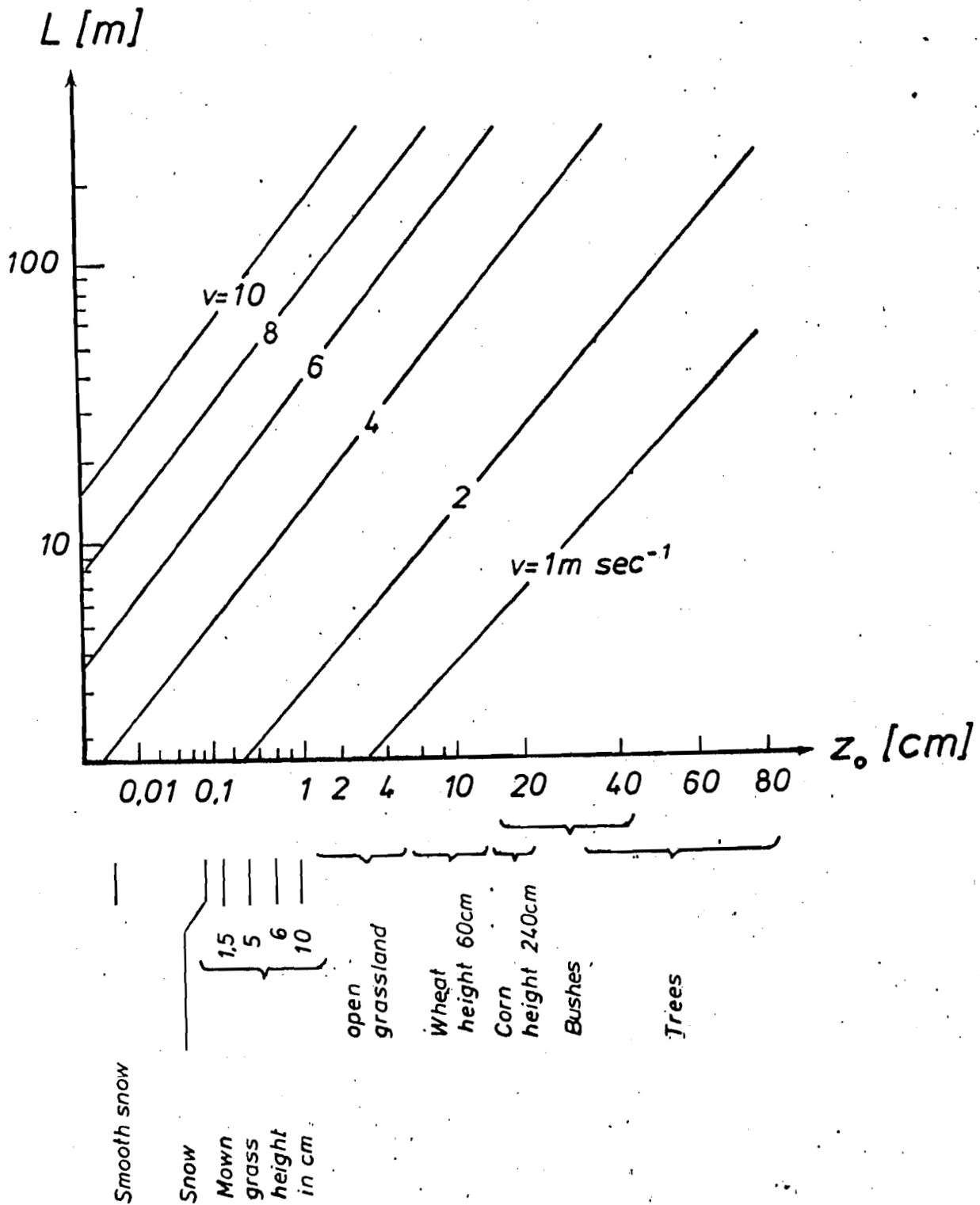


Fig. 1 (see /11/, /12/)

R E F E R E N C E S

- /1/ BROCKS, K. (1948): Über den täglichen und jährlichen Gang der Höhenabhängigkeit der Temperatur in den unteren 300 Metern der Atmosphäre und ihren Zusammenhang mit der Konvektion. Berichte des Deutschen Wetterdienstes in der US-Zone, 5.
- /2/ FLEAGLE, R. BUSINGER, J. (1963): Atmospheric Physics. Academic Press, New York and London.
- /3/ FORTAK, H. (1971): Meteorologie. Carl Habel Verlagsbuchhandlung Berlin und Darmstadt.
- /4/ HAURWITZ, B. (1945): Insolation in relation to cloudiness and cloud density. Journal of Meteorology Vol. 2.
- /5/ JORDAN, EGGERT, KNEISSEL (1966): Handbuch der Vermessungskunde, Band 6. Metzlersche Verlagsbuchhandlung, Stuttgart.
- /6/ MÖLLER, F. (1973): Physik der Atmosphäre. Bibliographisches Institut Mannheim.
- /7/ RAETHJEN, P. (1970): Dynamische Modell-Meteorologie. Hamburger Geophysikalische Einzelschriften, Heft 13. Meteorologisches Institut der Universität Hamburg.
- /8/ SCHWADERER, W. (1969): Der Straßenbau in physikalisch-meßtechnischer Betrachtung. Otto Graf Institut, Stuttgart.
- /9/ SÜHRING, R. (1937): Leitfaden der Meteorologie. Hirzel Verlag, Leipzig.
- /10/ WEBB, E. K. (1968): The temperature structure of the lower atmosphere. Proceedings of RED-EDM Conference, Univ. NSW Sydney.
- /11/ WEBB, E. K. (1971): Turbulent heat transfer and refraction. CSIRO Division of Meteorological Physics. Australia.
- /12/ ANGUS LEPPAN, P. V. (1971): Meteorological Physics Applied to the Calculation of Refraction Corrections. Commonwealth Survey Officers Conference, Paper No. B5.

Discussion (Paper 22)

- Q. I would like to ask about the graph, What is the reason for this ?
- A. The estimation depends on the temperature with the terrain elevation, that is to say on the profile. If there is little distance to the ground we have higher temperatures.
- Q. What do you think about the general application of your model ?
Do you think it can be used in flat regions or in mountains ?
- A. Sometimes it is difficult to describe the roundness of the topographical surface exactly, and one cannot measure the temperature along the total profile.
- Q. I would like to put, I would call it a junk question, to the reader of this paper and also to the president of this session here, namely we have here brought up some, let's call it, physical model of what is going to happen or what is happening in the atmosphere, when we are (? ed) promulgating (? ed.) information in it. In dr. Kahmens paper we heard about how one could statistically take hand of a large amount of information and how one tried to get, let's say an improvement of the answer. I have the feeling that the more you know about this physical reality behind a heap of information, before you do the statistical analysis on it, the better. So, I would like to ask, would it not be possible to apply some of the mechanism, described in this paper and also in Brunners paper to improve the statistical analysis as dr. Kahmen has made, it may be a serious question I'm just guessing, but I don't know who is going to answer this.
- A1) I think it will be possible and I intend to try it. My calculations are going on and in future I will use some more parameters to test these models.
- A2) I like to offer an answer to this question. Yesterday dr. Kahmen and myself had a discussion about his finding of peaks in his analysis. And maybe you will be able to see in my lecture this afternoon that we can explain several peaks, which dr. Kahmen found, looking at the boundary layer meteorology and the seasonal and diurnal variations.

A COINCIDENCE METHOD FOR REFRACTION ELIMINATING ANGLE MEASUREMENT

Tammo Glissmann, Technische Universität Hannover, Federal Republic of Germany

Summary

Some instruments are developed for the elimination of angular refraction by means of the dispersion method. With these instruments the measurement of dispersion angles has to be done simultaneously with the measurement of the refracted directions, thus two instruments are required.

The author proposes a measurement principle, based on the two-wavelength dispersion method, which produces the refraction-free direction in a direct way with only one (theodolite-like) instrument. The optical system of this instrument is composed by two coaxial systems. Their focallengths differ slightly, the difference depends indirectly on the dispersion coefficient. The focalplanes on the image side coincide. The refraction-free direction is established, when the two different-coloured images of the light source at the remote end of the optical path coincide. Coincidence is induced by the means of a positionsensing photodiode in connection with an electronic correlator. The dispersiometrically deterministic portion of direction scintillation is employed for increasing system accuracy.

INTRODUCTION

Angular refraction is the most limiting factor in terrestrial direction measurement. The influence on horizontal directions is less than $1.6 - 3.1 \mu\text{rad}$ under normal atmospheric conditions and may exceed $16 \mu\text{rad}$ under unfavourable conditions. With vertical directions the influence is larger and is approximately related to distance: $10 \mu\text{rad}/\text{km}$ under normal conditions and up to $50 \mu\text{rad}/\text{km}$ under unfavourable conditions.

There are various approaches to minimize angular refraction effects. One is the measurement of dispersion angles. Different kinds of dispersometers are described by BREIN 1968, PRILEPIN 1974, TENGSTROM 1974 and 1975, WILLIAMS 1974, GLISSMANN 1976.

Dispersion angle and refracted direction are measured by two separate instruments: dispersometer and theodolite. Observation techniques are or may be different with these two instruments; with respect to high precision ($< 1.6 \mu\text{rad}$) it may be very difficult to combine the results of both instruments. Therefore the search for an instrumental approach combining refraction elimination and angle measurement is thought to be of interest. This paper outlines a proposal for such an instrument.

BASIC PRINCIPLES

For the two-wavelength dispersion method the following first order approximation is valid:

$$\alpha_1 = \delta \cdot K, \quad (1)$$

α_1 = refraction angle for the (long) wavelength λ_1 ,

δ = dispersion angle, difference between refraction angle α_s (for the short wavelength λ_s) and α_1 ,

K = dispersion coefficient.

The numerical value of K depends on the selection of the wavelengths λ_s and λ_1 , for example $\lambda_s = 366 \text{ nm}$, $\lambda_1 = 578 \text{ nm} \rightarrow K = 36,8$ (GLISSMANN 1976).

With $\delta = \alpha_s - \alpha_1$ equation (1) may be written as follows

$$\frac{\alpha_1}{\alpha_s} = \frac{K}{K+1} \quad (2)$$

The refraction angles of different colours are related to each other by a constant factor. Under the condition of sufficient coincidence of the different coloured ray traces we assume that relation (2) is nearly invariant with respect to time. In other words, the statistical behaviour of the two-coloured direction scintillation is assumed to be more or less dispersiometrically deterministic.

The basic idea for the instrument proposed is quite simple. It is not necessary to measure the dispersion angle and multiply it by the dispersion coefficient K . The receiving optics however include K optically. The system operates with two different coloured images. Coincidence of these images is only then possible when the optical axis of the system coincides with the refraction-free direction.

How does such an optical system look like?

The system consists of two partial systems which

- are coaxial (have identical optical axes),
- are wavelength specific,
- have a common focalplane on the image side,
- have different focallengths f_1 and f_s .

Refraction-free direction and direction of the optical axis coincide under the following condition:

$$\alpha_1 \cdot f_1 = \alpha_s \cdot f_s \quad (3)$$

With equation (2) and (3) we get the focallength ratio for the two partial systems:

$$\frac{f_s}{f_1} = \frac{K}{K+1} \quad (4)$$

Using the above wavelengths the numerical value of this ratio is 0.9735; the equivalent difference in focallength is 2.65% of f_1 .

To illustrate the meaning of equation (3) we assume γ to be a deviation between optical axis and refraction-free direction. Then the different coloured images do not coincide:

$$(\alpha_1 - \gamma) \cdot f_1 \neq (\alpha_s - \gamma) \cdot f_s \quad (5)$$

and the lateral distance g of both image centers in the focalplane equals:

$$g = (\alpha_1 - \gamma) \cdot f_1 - (\alpha_s - \gamma) \cdot f_s = -\gamma \cdot \frac{f_1}{K+1} \quad (6)$$

Following equation (6) the image center distance g does not depend on (dispersiometrically deterministic) variations in α_1 and α_s . The problem is now to minimize g during image wandering due to direction scintillation. E.g. f_1 is 3 m and the desired accuracy in direction is about $\pm 1.6 \mu\text{rad}$ the coincidence accuracy necessary must be $\pm 0.125 \mu\text{m}$. It is evident that this can not be reached neither by visual observation nor by photographic registration. The only means for detecting near zero differences is a position sensing photodiode.

SUGGESTION FOR AN INSTRUMENTAL REALIZATION

The three essential parts of an instrument based upon the above described conception are

- receiving optics
- electro optical coincidence detector
- two-wavelength light source.

The angle measuring part of the system needs not be discussed here because it is identical to the angle measuring part of a theodolite. To eliminate residual instrumental errors, e.g. misalignment of the optical axes of the partial systems, asymmetry of figure of the optical elements ect., the measurement is proposed to be done a second time after reversing and rotating the system by 180° , as it is usually done with theodolites.

Receiving optics

Fig. 1 shows a possible arrangement for the two partial systems needed. The two Cassegrain reflecting telescopes consists of two different prime mirrors S_{11} and S_{1s} (focal-lengths f_{11} and f_{1s}) and a common secondary mirror S_2 . The focalplanes on the image side coincide. With an arrangement like this, ratio (4) is valid for the focallengths of the prime mirrors:

$$\frac{f_{1s}}{f_{11}} = \frac{K}{K + 1} \quad (7)$$

The mirrors are to be coated for spectral selection of wavelengths:

S_{11} for λ_1 , S_{1s} for λ_s and S_2 for λ_s and λ_1 .

The detector

The position sensing photodetector is situated at the focal-plane of the optical system. The position of a light spot falling on to the active area of the detector is signaled by the amount of current flowing through the grounded electrodes on the rear side of the detector. Different types of detectors are commercially available. Experiences made with the dual axis SC 10 (UDT, California, USA) prove that position repeatability of some 0.1 μm is obtainable under condition of a position fixed light beam (GLISSMANN 1976). Until now there are no experiences for coincidence accuracy for equidistant wandering light spots. The identification of the position differences of different coloured light spots demands some specific identification marks. This may be the modulation of the light source at the remote end of the optical path. The light has to be modulated

- at a constant frequency F_1
- at a colour alternating frequency F_2 .

F_1 has to be an integer multiple of F_2 .

The electronics (Fig. 2) produce a signal representing the wandering positions of the colour alternating light spots. Fig. 3a shows this signal, which appears after converting the electrode currents into voltages, filtering, forming the sum and the difference of these voltages, rectifying the sum and dividing the difference by the rectified sum. The output of the divider is phasesensitively rectified and filtered for the selection of the frequency F_2 (Fig. 3b). The rectified sum, which must have a not vanishing amplitude in F_2 , is also filtered (Fig. 3c). The latter renders possible cross-

correlation of the periodical (F_2) position signal and a signal of the same frequency. The not vanishing amplitude in the signal of the sum is given via different intensities of the two colours. Crosscorrelation with a zero time lag is done by a multiplier, the filtered output of which indicates zero in the case of coincidence. Crosscorrelation is of great advantage if a signal (the position difference) buried in extraneous noise (stochastic part of direction scintillation) is to be detected, even if the phase true frequency replica of the signal - represented by colour alternating intensities - is noisy too (intensity scintillation) (Fig. 3d).

The light source

Fig. 4 shows a possible design of the light source. A high pressure mercury lamp L is located at the focus of a Newtonian system. Near the lamp L is a modulating filter disc F attached. F is rotated by a frequency stabilized motor the rotational frequency of which is F_M . The filter disc is equipped with colour selective glass filters, the total number of which is m. The glass filters for each colour are arranged in p groups. Around the circle m/p filters for λ_s are followed by m/p filters for λ_1 . The modulation frequency F_1 than equals $F_M \cdot m$, the colour alternating frequency F_2 equals $F_M \cdot p/2$.

ACCURACY LIMITS IMPOSED BY METEOROLOGICAL CONDITIONS

The influence of water vapour gradients $\frac{dp_w}{dz}$ perpendicular to the line of sight can not be entirely eliminated by the two-wavelength dispersion method.

Defining a partial refraction angle α' for dry air and a partial refraction angle ϵ for moist air, the resulting refraction angle α is the composite of both components:

$$\alpha = \alpha' + \epsilon. \quad (8)$$

Following the OWENS 1967 formula for the refractive index of air the dispersion coefficient L for ϵ is $L = 25.6$ for the above wavelengths. Now in the state of image coincidence we find

$$(\alpha'_1 + \epsilon_1 + \phi)f_1 = (\alpha'_s + \epsilon_s + \phi)f_s, \quad (9)$$

where ϕ signifies the resulting error in direction determination caused by water vapour gradients. Substituting α'_s and ϵ by

$$\alpha'_s = \alpha'_1 \cdot \frac{K+1}{K} \text{ and } \epsilon_s = \epsilon_1 \cdot \frac{L+1}{L} \text{ and keeping in mind the}$$

ratio (4) we find

$$\phi = \epsilon_1 \cdot \frac{K - L}{K}. \quad (10)$$

The resulting error is about 44% of ϵ_1 .

$\frac{dP_w}{dz}$	ϕ	meteorological condition
0.005 mbar/m	0.2 μ rad/km	typical
0.1 mbar/m	4.7 μ rad/km	unfavourable

(DE MUNCK 1974, GLISSMANN 1976)

Since the distribution of $\frac{dP_w}{dz}$ along the line of sight is more or less symmetrically (for horizontal directions), simultaneous measurements from both sides reduce this effect upon ϕ .

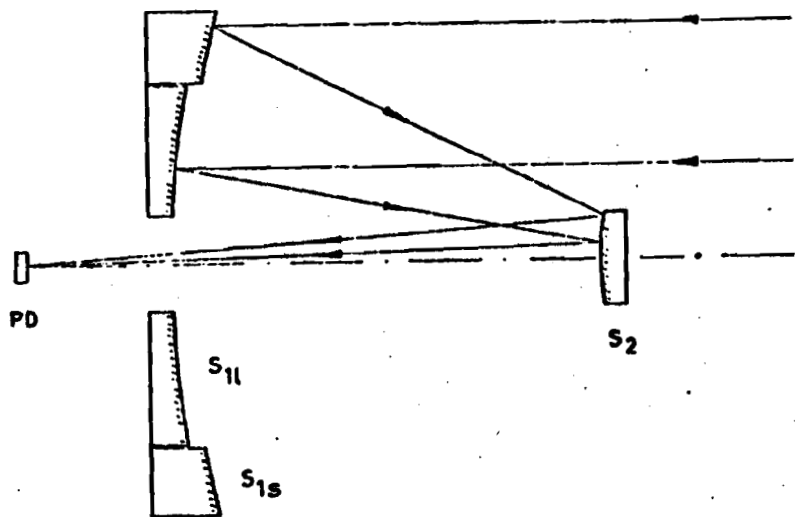


Fig. 1

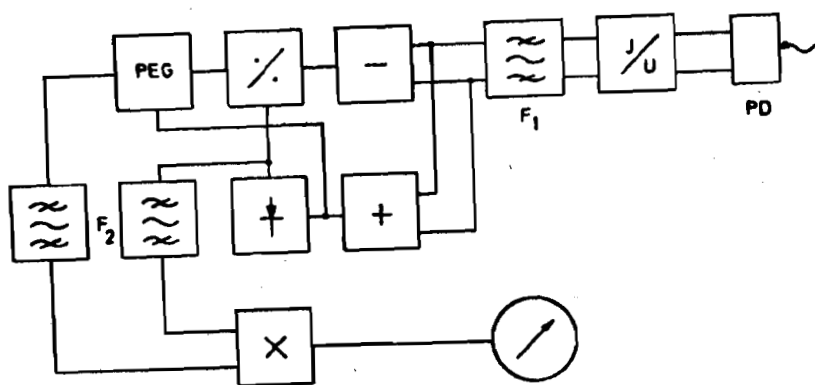


Fig. 2

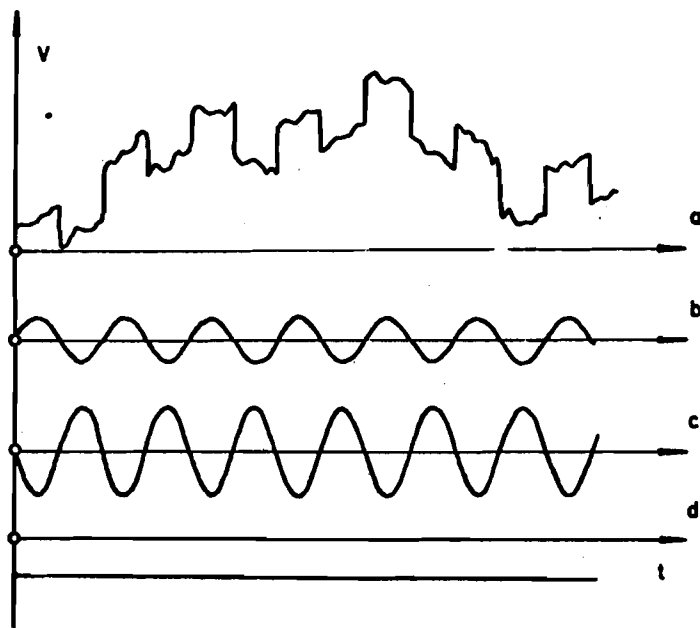


Fig. 3

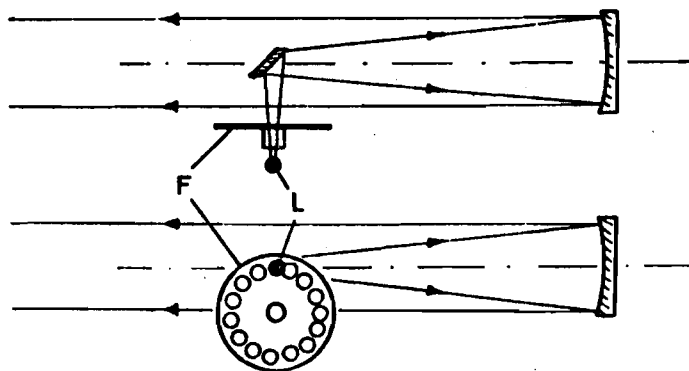


Fig. 4

References

- [1] BREIN, R. Die Bestimmung der atmosphärischen Refraktion aus der Dispersion des Lichtes; DGK, Reihe B, Heft 165, 1968
- [2] GLISSMANN, T. Zur Bestimmung des Refraktionswinkels über die Dispersion des Lichtes mittels positionsempfindlicher Photodioden; wiss.Arb. d. Lehrstühle f. Geod., Photogr. u. Kartogr. a.d. TU Hannover, Nr. 62, 1976, Dissertation
- [3] DE MUNCK, J.C. Limits of the use of dispersion in determining terrestrial refraction angle; Proceedings of the International Symposium on terrestrial Electromagnetic Distance measurements and Atmospheric Effects on Angular Measurements; Stockholm 1974, Vol. 5
- [4] OWENS, J.C. Optical Refractive Index of Air; Dependence on Pressure, Temperature and Composition, Applied Optics, vol. 6, No. 1, 1967
- [5] PRILEPIN, M.T. Elimination of Angular Refraction by Means of Multiple wavelength Method; Proceedings of the International Symposium on terrestrial Electromagnetic Distance measurements and Atmospheric Effects on Angular Measurements; Stockholm, 1974, Vol. 5
- [6] TENGSTRÖM, E. Report on the Results of IDM-experiments at Uppsala 1970, at the Finish base of Niinisalo 1971 and the further experiments with the He-Ne- and He-Cd-lasers, Proceedings of the International Symposium on terrestrial Electromagnetic Distance measurements and Atmospheric Effects on Angular Measurements; Stockholm 1974, Vol. 5
- [7] TENGSTRÖM, E. Report of IAG Special Study group No. 1.23 through the period 1971-1975 on Studies of Atmospheric Refraction; IUUG General Assembly, Grenoble, 1975

- [8] WILLIAMS, D.C. A Dispersiometer for the Measurement of Angular Refraction;
Proceedings of the International Symposium on terrestrial Electromagnetic Distance measurements and Atmospheric Effects on Angular Measurements; Stockholm 1974, Vol. 5

Discussion (paper 23)

- Q. Is it not necessary to synchronize the modulation at the remote point with the scanning at the instrument ?
- A. Well, I think not. We tried to stabilize the motor frequency to a very high extent so that the photographs you saw at the electronics are well in the middle of the frequency we need.
- Q. We wonder when it is the red filter and when it is the blue filter.
- A. That is the question and therefore you have to do something. I did it; in my paper I wrote that the intensities, the power of blue and green here must be different. Then you get a signal which is of the same frequency as the position signal, which should be a minimum. Perhaps there are other ways to reach this, this is only one and this is also only one sort of light-source; we are going to range 2 lasers as Mr. Williams is doing, modulating lasers.

Comments by Dr. Williams.

At the National Physical Laboratory, we have been thinking in fact within very similar lines to what by Dr. Glissman has been described, but the optical system, which we are proposing to realise the idea, is somewhat different.

Can I say just briefly what we are trying to do. In a normal dispersometer if the refraction changes, the separation between red and blue changes and that is what we measure. If the tilt of the instrument changes, the separation between the red and the blue remains constant and the measurement is insensitive to tilt. We are proposing a complementary system in which dispersion is built in into the instrument, so that as the instrument tilts, the separation between the red and the blue alters and we use the separation between the red and the blue to sense the tilt of the instrument and to point it into a particular direction.

But we are designing internal optics, so that changes in refraction are automatically compensated if the pointing of the instrument remains constant but the refraction changes and the red and the blue both move, but the images in red and blue stay together. Dr. Glissmann has proposed doing this by using 2 concentric telescopes effectively, with different focal lengths for the red and the blue. What we are proposing in the simplest versions, is shown in the first picture. In the upper picture I represented the reflecting telescope, by an achromatic lense in order to try to keep the diagram simple, but this would in fact be replaced by a telescope and it would be a completely achromatic lense forming images in the

identical positions for red and blue. What you can do is to insert just before the image plane a single positive lense which then focuses the blue image a little further in than the red and the effect of that I try to show, is to make the effective focal length of the telescope a little bit shorter for the blue than for the red. And you can make this modification to an ordinary dispersometer, either to ours or to Glissman's.

You simply put in this lense and you have produced the kind of instrument, which we are proposing. There is a slight difficulty in this case, in that the red and the blue images are literally separated. I think you could probably overcome that, although we haven't done the detailed calculations by making this separated pair of lenses of some kind. The other point is, that at NPL we did not originally conceive this idea for using the kind of application which Glissman has talked about.

We are thinking about it more recently incorporating it in a theodolite type instrument, just as is suggested. But our original idea was for testing our own dispersometer. We did not want a system, which moved the image, so, that when we inserted the lense we had to change the focus of the telescope. So we infact constructed a doublette lense, consisting of diverging and converging components, cemented together. But unlike the usual kind of doublette, it has an infinite focal length - the converging and diverging components have equal but opposite focal lengths.

But because they are not different glasses, it does produce lateral dispersion. We can now insert this into the dispersometer and try the idea. We have in fact tried it and we have showed it does basically work, but it did not compensate completely, it compensated till 5 procent or so. I think I know now why and I think I have to make it work properly, but we are really more interested in our basic dispersometer well work first, but with this kind of modification we can invert any dispersometer of this type to work in this way and to integrate the angle-measurement and dispersion-measurement. Thank you.

Chairman: Thank you very much. That was a real contribution.

It's just to show that there are 2 ways to solve the problem and of course it will probably be so in the future that we have an instrument, which eliminates the refraction.

So, if the work on the precursor have not reached that state, we can just forget about the refraction.

Q. I have one question. Do you have published this or written down ?

A. No, we haven't yet, in fact to be honest with you in the laboratory they asked me not to describe it unless Dr. Glissmanns ideas were very similar.

While Dr. Glissmanns were very similar I had in fact to describe it.

Q. So, if Dr. Glissmann had not presented his idea, you should not have said anything either.

A. It has been suggested by one of my seniors that this would be in fact difficult to realise in practice because of the fact that to build an instrument of this kind into a theodolite, and make it adequately stable would be quite difficult.

Comment

I think that it's the same in almost all parts of geodetic field instruments.

There will be at last so many types and solutions for the instruments, as soon as we know that we are making no systematical errors in the derivation of the quantity we need, from the quantity we measure. So, still, it is very important to prove that any simple dispersion measurement, which is correctly made with high accuracy gives us the refraction correctly.

APPLYING THE MOVEMENT SMOOTHNESS OF A VEHICLE TO DETERMINE THE POSITION OF TRANSPONDERS

J.C. de Munck, H.M. deHeus en W. Tuitman

Summary

For the determination of the positions of a number of points, distance measurements from a smoothly moving vehicle to these points are often used. If the time intervals between these measurements are short, the movement of the vehicle may be used to strengthen the adjustment or even make the adjustment possible.

In this paper the course of the vehicle is expressed in Chebyshev series for solving the unknown co-ordinates.

1. Introduction

Distance measurements are more and more performed by moving vehicles e.g. satellites, aeroplanes and ships. Some movements are more smooth than others. The movement of the stars e.g. can be predicted very well and is a very smooth one; for satellites, aeroplanes and ships the movements are successively less smooth. Still there is some correlation between the successive positions.

There are several techniques using the smoothness of the vehicle, e.g. the line crossing technique. In this case the vehicle is supposed to move along a straight course and the minimum of the sum of the two distances is considered to be the wanted distance. In this paper a more general situation is described.

2. Formulation of the problem

The relative positions and the heights of three or more points in space must be calculated from a great number of distance measurements between each of the three points and a smoothly moving vehicle of which the height is always known. See *Figure 1*. Here the relative positions of three or more acoustical transponders on the bottom of the sea are determined by distance measurements from a ship. Another example is the positioning of microwave transponders from an aeroplane.

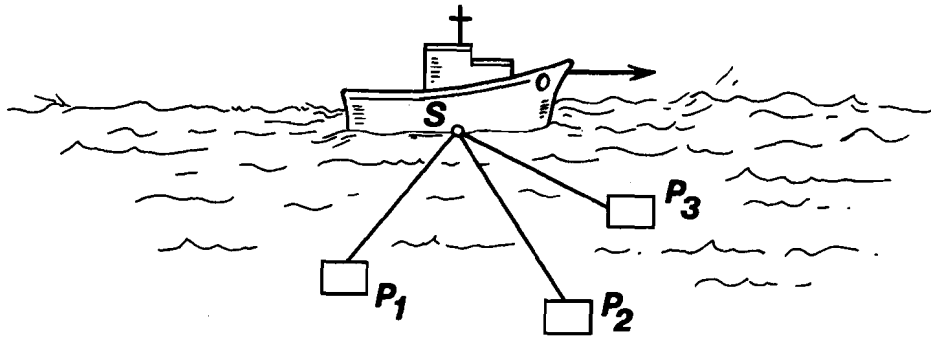


Figure 1
Distance measurements to three transponders

Using a ship the height may be found from the reduction of the sea level, and in the case of an aeroplane from the barometer readings. The level surfaces are assumed to be plane and the heights of the vehicle positions are supposed to be exactly known.

3. *The co-ordinate system*

The vehicle is supposed to sail along a flat smooth course which does not deviate much from a straight, horizontal line. Thus the whole geometry of transponder- and ship position is not well fixed: a rotation around this line is possible. Hence the X-Y-plane to be chosen, will not be exactly horizontal, but will be a plane through the first and the last ship position at a preassumed distance D from one of the transponders. D is then of course chosen in such a way that it equals an estimate of the depth of the transponder; the transponder should lay far from the vertical plane through the ship positions. So the X-Y-plane is not exactly horizontal (*Figure 2*) but the gravity-oriented co-ordinates of the transponders can be found by carrying out the same type of measurements with the vehicle sailing another course.

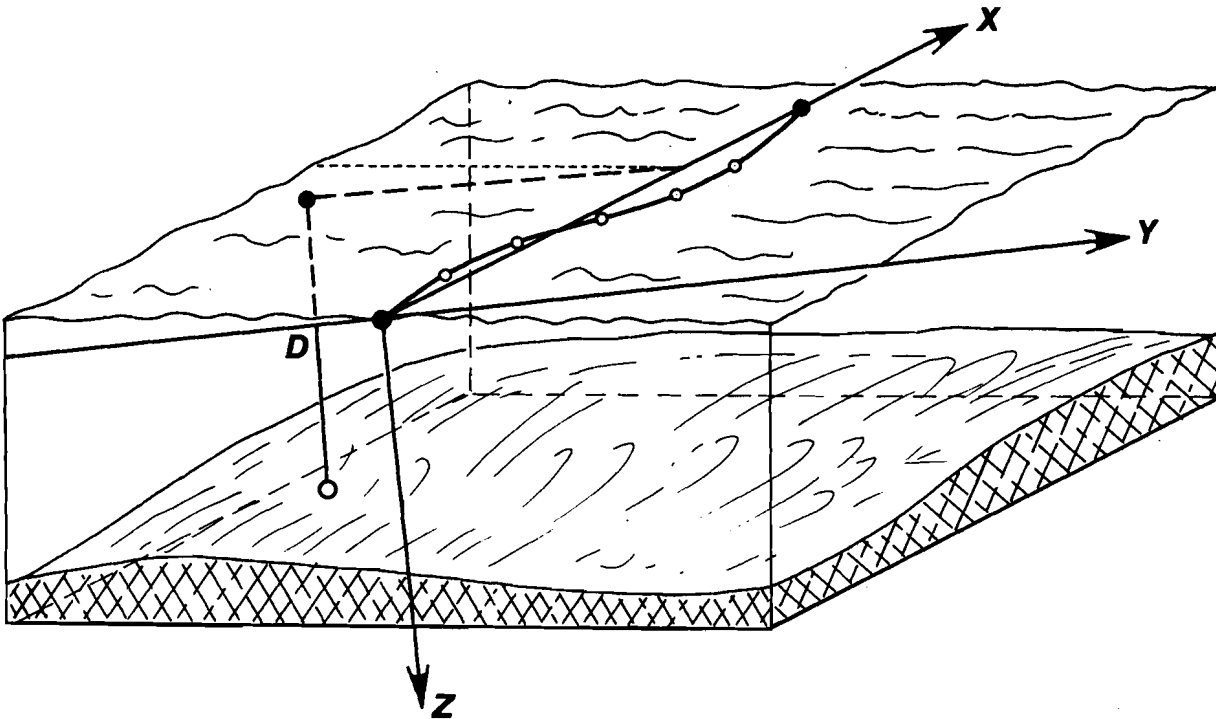


Figure 2

The choice of the co-ordinate system

The origin is the first ship position.

The Y-axis goes through the last ship position.

The Z-co-ordinate of one of the transducers equals D

4. The geometry

The measured distances l_{iq} between the transponder positions $\{X_i; Y_i; Z_i\}$ (with $i = 1, 2, \dots, I$) and the vehicle positions $\{X_q; Y_q; Z_q\}$ (with $q = 1, 2, 3, \dots, Q$) can easily be expressed in these co-ordinates:

$$(l_{iq})^2 = (X_i - X_q)^2 + (Y_i - Y_q)^2 + (Z_i - Z_q)^2 \quad (1)$$

If the deviations of the vehicle from the X-axis are small and if the Z-co-ordinate D has been chosen fairly well, the Z-co-ordinates of the vehicle may be neglected:

$$Z_q \rightarrow 0$$

If reasonable provisional values are available equation (1) may be linearized by taking differences from these provisional values, such as:

$$\Delta l_{iq} = l_{iq} - (l_{iq})_0, \quad \Delta X_i = X_i - (X_i)_0, \quad \text{etc.}$$

One finds:

$$\begin{aligned} (l_{iq})_0 \Delta l_{iq} = & (X_i - X_q)_0 (\Delta X_i - \Delta X_q) + \\ & + (Y_i - Y_q)_0 (\Delta Y_i - \Delta Y_q) + (Z_i)_0 \Delta Z_i \end{aligned}$$

If the proportional precision of the measured distances is constant (see section 6) it is useful to consider $(\Delta l_{iq}) / (l_{iq})_0 \approx \Delta \ln l_{iq}$ as observations. Then the above equation may be written as:

$$\Delta \ln l_{iq} = \frac{(X_i - X_q)_0 (\Delta X_i - \Delta X_q) + (Y_i - Y_q)_0 (\Delta Y_i - \Delta Y_q) + (Z_i)_0 \Delta Z_i}{(l_{iq})_0^2} \quad (2)$$

The choice of the co-ordinate system gives the conditions:

$$(X_q)_{q=0} = (Y_q)_{q=0} = (Y_q)_{q=Q} = 0 \quad (3a)$$

$$\text{and } (Z_i)_{i=3} = 0 \quad (3b)$$

if the Z-co-ordinate of the transponder $i=3$ has been assumed. Further we have the trivial conditions:

$$(\Delta X_q)_{q=0} = (\Delta Y_q)_{q=0} = (\Delta Y_q)_{q=Q} = 0 \quad (4)$$

Of course the provisional values have to be chosen in such a way that they fulfill the condition (1), (3a) and (3b). If a sufficient number of measurements is performed the difference quantities - and from them the co-ordinates of the vehicle positions (if wanted) and the co-ordinates of the transponders - can be calculated by adjustment, assuming a stochastic model.

5. The smoothness of the movement

In many cases the course of the vehicle will be so smooth that the measuring positions are fixed quite well by a relatively small number of parameters, which may be found by expressing the positions of the vehicle in one or more polynomials such as power-series or Fourier series. One can also use spline function or assume a correlation between the positions which may be a decreasing function of the distance between the points.

At the Delft Geodetic Institute we have chosen the polynomials, not because they lead necessarily to the best solution but because we found it the most straight-forward one. We did not choose the Fourier series because there is no reason for a periodicity. The Chebyshev polynomials were preferred because they fit fairly well over a limited section of the ship's course.

Because longitudinal and transversal deviations of an uniform linear motion may be quite different in character, we expanded the X- and the Y-co-ordinates of the ship positions each in a polynomial:

$$\left. \begin{aligned} X(\tau) &= \sum_{n=0}^N a_n T_n(\tau) \\ Y(\tau) &= \sum_{m=0}^M b_m T_m(\tau) \end{aligned} \right\} \quad (5)$$

where:

τ is a linear transform of the time t , so that $\tau = -1$ for the first vehicle position ($q=1$) and $\tau = +1$ for the last position ($q=Q$):

$$\tau = 2 \frac{t - t_i}{t_Q - t_i} - \frac{t_Q + t_i}{t_A - t_i} \quad (6)$$

$T_k(\tau)$, with $k = n$ or m , are Chebyshev polynomials with the argument τ and of the degree k , defined as:

$$T_k(\tau) = \cos(k \arccos \tau) \quad (\text{see also table 1})$$

a_n and b_m are the coefficients, considered as unknowns in the problem.

The measurements are only performed on discrete moments given by t_q or by τ_q .

<i>The lowest degree Chebyshev polynomials</i>	
$T_0(\tau)$	$= 1$
$T_1(\tau)$	$= \tau$
$T_2(\tau)$	$= 2\tau^2 - 1$
$T_3(\tau)$	$= 4\tau^3 - 3\tau$
$T_4(\tau)$	$= 8\tau^4 - 8\tau^2 + 1$

Table 1

Because of the choice of the co-ordinate system and because of the choice of τ , there are three relations between the coefficients a_n and b_n . They follow from (3a).

$$(X_q)_{q=0} = \sum_{n=0}^N a_n T_n(-1) = 0$$

$$(Y_q)_{q=0} = \sum_{m=0}^M b_m T_m(-1) = 0$$

$$(Y_q)_{q=Q} = \sum_{m=0}^M b_m T_m(+1) = 0$$

Now from the definition of the Chebyshev polynomial it follows that

$$T_k(-1) = (-1)^k$$

and $T_k(+1) = 1$

So one finds the relations:

$$\sum_{n=0}^N (-1)^n a_n = 0, \quad \sum_{m=0}^M (-1)^m b_m = 0 \quad \text{and} \quad \sum_{m=0}^M b_m = 0$$

or:

$$\left. \begin{aligned} a_0 &= a_1 - a_2 + a_3 - a_4 + \dots + a_N \\ b_0 &= -(b_2 + b_4 + b_6 + \dots + b_{m \leq M}) \\ b_1 &= -(b_3 + b_5 + b_7 + \dots + b_{m \leq M}) \end{aligned} \right\} \quad (7)$$

In case the functions $X(\tau)$ and $Y(\tau)$ are almost linear, the coefficients a_2, a_3, \dots, a_N and b_2, b_3, \dots, b_M are very small. So according to (7):

$$a_0 \approx a_1, \quad b_0 \approx 0, \quad b_1 \approx 0.$$

If the provisional value for a_1 is chosen: $(a_1)_0$ then the provisional value for a_0 can be assumed to be equal to $(a_1)_0$. The provisional values for all other coefficients are taken 0, so that with (5) for discrete moments τ_q :

$$\left. \begin{aligned} (X_q)_0 &= (a_1)_0 + (a_1)_0 \tau_q \\ (Y_q)_0 &= 0 \end{aligned} \right\} \quad (8)$$

The differentials of the vehicle co-ordinates are found by subtracting (8) from (5) for the moments τ_q :

$$\begin{aligned} \Delta X_q &= X_q - (X_q)_0 = \Delta a_0 + \Delta a_1 \tau_q + \sum_{n=2}^N a_n T_n(\tau_q) \\ \Delta Y_q &= Y_q - (Y_q)_0 = b_0 + b_1 \tau_q + \sum_{m=2}^M b_m T_m(\tau_q) \end{aligned}$$

with $\Delta a_0 = a_0 - (a_1)_0$, $\Delta a_1 = a_1 - (a_1)_0$ and with (7) these equations may be written as:

$$\left. \begin{aligned} \Delta X_q &= (1 + \tau_q) \Delta a_1 - \sum_{n=2}^N \{ (-1)^{n-1} T_n(\tau_q) \} \cdot a_n \\ \Delta Y_q &= \sum_{m=2}^M \left\{ -\frac{1 + (-1)^m}{2} - \frac{1 - (-1)^m}{2} \tau_q + T_m(\tau_q) \right\} \cdot b_m \end{aligned} \right\} \quad (9)$$

Substitution of these forms for ΔX_q and ΔY_q in (2) and using (3b) and (4) gives a number of relations between the unknown differentials of the co-ordinates of the transponders, the unknown coeffi-

icients of the Chebyshev polynomials and the differentials of the measured distances. In vector form these relations may be written as:

$$E\Delta U = \Delta O \quad (10)$$

where ΔU and ΔO are column vectors and E is a matrix;

ΔU is a column vector with the components $\Delta X_i, \Delta Y_i, \Delta Z_i, \Delta a_1, a_n, b_m$, where $i = 1, 2, \dots, I$, except for the components ΔZ_i of which the value corresponding with the assumed depth D (for instance ΔZ_3) must be omitted, and where $n = 1, 2, 3, \dots, N$ and $m = 2, 3, 4, \dots, M$.

ΔO is a column vector with the components $\Delta \ln l_{iq}$, where $i = 1, 2, \dots, I$ and $q = 1, 2, \dots, Q$.

E is a matrix with $(3I-2+N+M)$ columns and $3Q$ rows. The non-vanishing elements are functions of the provisional co-ordinates $(X_i)_0, (Y_i)_0, (Z_i)_0$ and $(X_q)_0 = (a_1)_0 + (a_1)_0 \tau_q$. See appendix.

6. The adjustment

If the stochastic model is known, the differential values ΔU of the unknowns may be found by adjustment. For this stochastic model we simply assume that all "observations" $\ln l_{iq}$ have equal standard deviations τ and that there is no correlation between the observations.

The adjustment gives:

$$\Delta U = [E^T P^{-1} E]^{-1} E^T P^{-1} \Delta O \quad (11)$$

where $[E^T P^{-1} E]^{-1}$ is the covariance matrix of the unknowns, and P is the covariance matrix of the observations, in our case:

$$P = \begin{vmatrix} \sigma^2 & 0 & 0 & \text{-----} \\ 0 & \sigma^2 & 0 & \text{-----} \\ 0 & 0 & \sigma^2 & \text{-----} \\ \vdots & \vdots & \vdots & \diagdown \\ \vdots & \vdots & \vdots & \end{vmatrix} = \sigma^2 I \quad \begin{array}{l} \text{if } I \text{ is a unit matrix} \\ \text{of } 3Q \times 3Q \text{ elements.} \end{array}$$

For this simple matrix $P = \sigma^2 I$ one finds:

$$\Delta U = [E^T E]^{-1} E^T \Delta O \quad (12)$$

7. Extensions of the problem

A.

As mentioned in section 3. a better determination of the transponder co-ordinates is possible if the measurements are done along more than one straight path of the vehicle. Also in this case the adjustment of the whole problem is possible in one step. However, the choice of the co-ordinate system is then more complicated than for one straight path. Further the matrix of the coefficients of the unknowns (comparable with E) becomes very large. Since the matrix has many zero's special methods can be used, see e.g. [Kok, 1977]. However, the adjustment may better be done in two

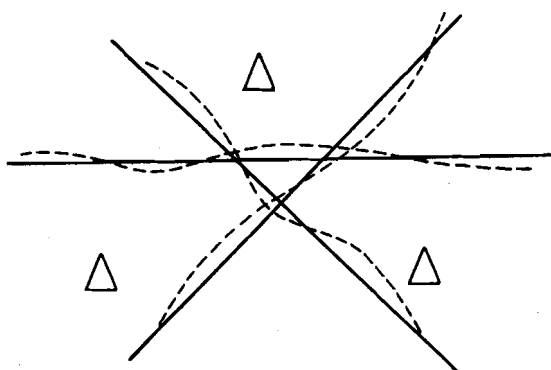


Figure 3

Fixing 3 transponders using 3 straight-line paths.

steps. In the first step a series of measurement over each of the straight lines is adjusted as described in section 6. In the second step the different co-ordinate systems are transformed into one system. This is possible by an adjustment because all the co-ordinates of the transponders are known in each of the co-ordinate systems.

B.

Another extension is a combination of two systems of position fixing, the so-called "integrated navigation". The co-ordinates of the vehicle found in one system may then be expressed in the observations of the other system.

C.

It is not necessary to carry out measurements from each ship position q to all of the transponders. Often the measurements are done alternatively to each of the transponders. With the use of the polynomials enough redundancy may remain to perform the calculations in the manner described in the sections 2. - 6.

D.

If more than three transponders are used the three-dimensional positions may be found without knowledge of the height of the vehicle. An additional series of polynomials can then be used for the vertical co-ordinates of the vehicle.

References

- J.J. Kok - "An Algorithm for the Reduction of Sparse Symmetric Matrices, for Use in Least-squares Adjustment Programmes". To be presented at the I.A.G. International Symposium on Optimization of Design and Computation of Control Networks, in Sopron, Hungary, July 1977.

Appendix

In this appendix the design matrix E is given for three transponders (I = 3) and for Chebyshev series of the third degree (N=M=3), assuming the Z-co-ordinate Z_3 .

The elements e_f^g of the matrix are found with the following rules:

$$\begin{aligned} g &= 3q + i - 3, & f &= 1, 2, 3, \dots, 13 \\ i &= 1, 2, 3 \\ q &= 1, 2, 3, \dots, Q \end{aligned}$$

for i = 1:

$$e_1^g = \left(\frac{X_1 - X_q}{1^2_{iq}} \right)_0 = A_{iq} \quad e_2^g = \left(\frac{Y_1}{1^2_{iq}} \right)_0 = B_{iq} \quad e_3^g = \left(\frac{Z_1}{1^2_{iq}} \right)_0 = C_{iq}$$

for i = 2:

$$e_4^g = \left(\frac{X_1 - X_q}{1^2_{iq}} \right)_0 = A_{iq} \quad e_5^g = \left(\frac{Y_1}{1^2_{iq}} \right)_0 = B_{iq} \quad e_6^g = \left(\frac{Z_1}{1^2_{iq}} \right)_0 = C_{iq}$$

for i = 3:

$$e_7^g = \left(\frac{X_1 - X_q}{1^2_{iq}} \right)_0 = A_{iq} \quad e_8^g = \left(\frac{Y_1}{1^2_{iq}} \right)_0 = B_{iq}$$

for i = 1, 2, 3:

$$\begin{aligned} e_9^g &= - (1 + \tau_q) A_{iq} & e_{10}^g &= -2 (\tau_q^2 - 1) A_{iq} & e_{11}^g &= - (4\tau_q^3 - 3\tau_q + 1) A_{iq} \\ e_{12}^g &= -2 (\tau_q^2 - 1) B_{iq} & e_{13}^g &= -4 (\tau_q^3 - \tau_q) B_{iq} \end{aligned}$$

Remark: The elements in the upper and lower righthand rectangles all become zero.

$E =$

ΔX_1	ΔY_1	ΔZ_1	ΔX_2	ΔY_2	ΔZ_2	ΔX_3	ΔY_3	Δa_1	a_2	a_3	b_2	b_3	i	q
e_1^1	e_2^1	e_3^1	0	0	0	0	0	e_9^1	e_{10}^1	e_{11}^1	e_{12}^1	e_{13}^1	1	1
0	0	0	e_4^2	e_5^2	e_6^2	0	0	e_9^2	e_{10}^2	e_{11}^2	e_{12}^2	e_{13}^2	2	1
0	0	0	0	0	0	e_7^3	e_8^3	e_9^3	e_{10}^3	e_{11}^3	e_{12}^3	e_{13}^3	3	1
e_1^4	e_2^4	e_3^4	0	0	0	0	0	e_9^4	e_{10}^4	e_{11}^4	e_{12}^4	e_{13}^4	1	2
0	0	0	e_4^5	e_5^5	e_6^5	0	0	e_9^5	e_{10}^5	e_{11}^5	e_{12}^5	e_{13}^5	2	2
0	0	0	0	0	0	e_7^6	e_8^6	e_9^6	e_{10}^6	e_{11}^6	e_{12}^6	e_{13}^6	3	2
0	0	0	0	0	0	0	0	0	0	0	0	0	1	0-1
0	0	0	e_4^{3Q-4}	e_5^{3Q-4}	e_6^{3Q-4}	0	0	e_9^{3Q-4}	e_{10}^{3Q-4}	e_{11}^{3Q-4}	e_{12}^{3Q-4}	e_{13}^{3Q-4}	2	Q-1
0	0	0	0	0	0	e_7^{3Q-3}	e_8^{3Q-3}	e_9^{3Q-3}	e_{10}^{3Q-3}	e_{11}^{3Q-3}	e_{12}^{3Q-3}	e_{13}^{3Q-3}	3	Q-1
e_1^{3Q-2}	e_2^{3Q-2}	e_3^{3Q-2}	0	0	0	0	0	e_9^{3Q-2}	e_{10}^{3Q-2}	e_{11}^{3Q-2}	e_{12}^{3Q-2}	e_{13}^{3Q-2}	1	Q
0	0	0	e_4^{3Q-1}	e_5^{3Q-1}	e_6^{3Q-1}	0	0	e_9^{3Q-1}	e_{10}^{3Q-1}	e_{11}^{3Q-1}	e_{12}^{3Q-1}	e_{13}^{3Q-1}	2	Q
0	0	0	0	0	0	e_7^{3Q}	e_8^{3Q}	e_9^{3Q}	e_{10}^{3Q}	e_{11}^{3Q}	e_{12}^{3Q}	e_{13}^{3Q}	3	Q

Discussion (paper 24)

Q. For which task do you use transponders in Holland

A. For finding pipelines and boreholes, and survey the topography of the sea bottom, where a platform is to be placed.

Q. In which regions of Holland do you use it

A. In the North Sea. But electro magnetic transponders are also used from aircraft, and not especially in Holland but in other countries too.

Q. I think they are mostly used to find relative positions not absolute positions.

A. If the method is integrated into another system one can find absolute positions.

Q. I would like to ask whether you do the summations in the Chebyshev polynomials by the Clinshaw method.

You know there is a special method if you are summing a polynomial, where the coefficients have a recursion between them, there is a very elegant method for summation indicated by Clinshaw. It is a small algorithm which makes the summation easy both from a mathematical and a numerical point of view. To a certain extent it resembles the Horner scheme.

A. I don't know the method.

Q. In that case the restriction to the 3th or 4th degree for convenience is quite irrelevant.

And I have done some fitting of polynomials, where I didn't decide in the beginning to which degree I wanted to go. For instance to find a transformation between 2 coordinate systems. There you can start with a very low degree and find how the variants come out and then you can increase the degree until the variants coming out of the adjustment remain constant. It means, then you are at noise-level.

- A. Actually, mr. Tuitman, who did these calculations has just something in that direction. Maybe it's the same.
- Q. You see the danger of fitting with polynomials of a very high degree is, that it eventually fits only in the points. But if you have a reasonable redundancy then you can play quite safely and you can see that the noise in general will stop and you can stop your increase of degrees, when you use Clinshaw summations, then you don't have to worry about the degree from the programme point of view. It is immaterial whether to use the degree of 3 or 25 for that matter.
- Q. May I ask: Do you need equally spaced data for this or any data ?
- A. Of course, This is one of the snags of Chybeshev polynomials; In general you would like equally spaced data. But you could possibly use also other kind of orthogonal polynomials All orthogonal polynomials with a recursion structure could be used.
- Q. I missed in your explanation the relation between the dimension of the standard ellipses in meters and the standard deviation in the beginning which was expressed in percentages or rather as a proportion 10^{-3}
- A. In the figure we have assumed an equilateral triangle with sides of 100 m.
- Q. Did you do any investigations as to the optimum course the vessel should follow in order to get the best determination of the coordinates of your transponder. Because that is one of the problems we always face in practice, we normally sail at random some 8 figures through the area. We have to work with discrete measurements of course, when you cannot work with continuous measurements and we never know whether we are doing things right. I would like an optimum trace to follow with the vessel, still limited to a reasonable number of points.
- A. No, we did not. We assumed a straight line only to begin with because this is the simplest. One could use crossing lines or a number of parallel lines, but we did not look for the best method to sail

AN ATMOSPHERIC TURBULENT TRANSFER MODEL FOR EDM REDUCTION

F.K. Brunner and C.S. Fraser, Department of Geodesy, The University of New South Wales, Kensington, Sydney, Australia.

ABSTRACT

Atmospheric effects remain the limiting factor for the precision of single wave length edm, and hence a new atmospheric model for the reduction of edm has been developed. The prediction of meteorological parameters along an edm line, from ground based measurements, is only practically possible during periods of free convection. The atmosphere is generally found to be homogeneous between 1000 and 1500 hrs for moderate weather conditions. Such periods have long been favoured for trigonometric levelling and are considered, in the present paper, to be also the optimum for edm.

Within the turbulent regime, during thermal instability, three height regions with different potential temperature gradients have been distinguished. For a typical edm line with elevated endpoints, the wave path will lie predominately in the upper region, in which adiabatic conditions prevail. Adiabatic conditions are best described by the conservative parameters of potential temperature and specific humidity.

In ordinary edm practice, meteorological measurements at the terminals of an edm line are carried out at instrument height. These measurements, however, are only representative for the unstable surface layer and need to be transformed to the boundary between this layer and the adjoining adiabatic layer. This transformation requires the determination of the representative potential temperature gradient and the height of the atmospheric surface layer, for which the appropriate laws governing atmospheric turbulent transfer processes are employed. In these calculations the sensible heat flux, which can be determined from the energy balance equation, plays a fundamental role. The application of this approach involves the determination of additional meteorological parameters to those normally measured for edm reduction; these are: net radiation, heat flux into the ground, evaporation and wind speed. These parameters can be measured directly or, with the exception of wind speed, estimated from empirical formulae.

The atmospheric turbulent transfer model developed is applicable to both light and microwave edm and appropriate reduction formulae are derived. Field measurements involving edm observations, as well as heat flux determinations, have been carried out in order to test this new model. The results, which are reported elsewhere, support the use of the turbulent transfer model as a viable reduction technique for edm.

1. INTRODUCTION

1.1 Preamble

For single wavelength edm, using laser light or microwave instruments, the determination of the mean (integral) refractive index over the propagation path is crucial. Methods of determination have been the topic of numerous papers in the last decade. However, the problem is nowadays even more relevant as the instrumental and ground swing errors have undergone a drastic reduction in magnitude as a result of new instrumental developments.

The arithmetic mean of the refractive indices, derived from meteorological observations at the terminals of the edm line, is generally not equal to the integral refractive index. It has been found [11] that this error is largely dependent on the profile of the line and the time of the edm observation. There are currently several diverging opinions regarding the selection of the most suitable time of observation for edm. However, the general conditions favoured appear to be the morning and afternoon transition periods when a near-isothermal vertical distribution may be expected.

The time period of 1000 to 1500 hrs has long been favoured as the optimum period of observation for trigonometric levelling, though rarely for edm. During this period, the atmosphere above the lowest few metres of the boundary layer is generally in an adiabatic state as a result of thermal mixing from turbulent transfer processes. During dry adiabatic processes, the prevailing temperature gradient is the adiabatic gradient (-0.00977 Km^{-1}). Using the well-known formula for the vertical refraction of lightwaves, the refraction coefficient k_L corresponding to the adiabatic temperature gradient can be calculated. For average meteorological conditions ($p = 950 \text{ mb}$, $T = 283 \text{ K}$, $e = 7.6 \text{ mb}$ at relative humidity of 60%) a value for k_L of 0.146 is calculated. This value is very close to the empirical mean value of $k_L = 0.13$, which is generally accepted as the standard value in geodesy. This empirical mean value for k_L has been derived from reciprocal zenith distance observations in hilly to mountainous areas, with the times of observation being between 1000 and 1500 hrs. The excellent results from trigonometric levelling during this time period of adiabatic conditions encourage an investigation of the application of adiabatic models for atmospheric edm reduction.

Because the vertical and horizontal distribution within the adiabatic layer is essentially homogenous, extending from about 20-50 m to heights of a few hundred metres above the ground, a modelling of this layer is relatively simple when the conservative atmospheric parameters of potential temperature and specific humidity are employed. Bearing in mind the practicability of the model to be developed, meteorological measurements are confined to the endpoints only. However, the meteorological measurements at the terminals are generally taken at the instrument level which invariably falls in the unstable atmospheric surface layer. Thus, the measurements need to be transformed to the lower boundary of the adiabatic layer, the layer in which the predominant portion of the propagation path falls. For this transformation the appropriate laws governing turbulent transfer processes will be applied. A turbulent transfer model will be developed and new formulae for the reduction of both light and microwave edm will be derived. The suggestion for such a model must be attributed to ANGUS-LEPPAN[1].

Field measurements involving edm and heat flux determinations have been carried out in order to test the new model. The results, which are reported elsewhere [6], support the use of the turbulent transfer model as a viable reduction technique for edm.

1.2 Conservative Meteorological Parameters

An adiabatic process is one in which heat does not enter or leave the system; these processes play a fundamental role in meteorology. Potential temperature θ and specific humidity q are invariant with height during adiabatic processes and are therefore referred to as conservative parameters. The specific humidity q is defined as the ratio of the mass of water vapour to the total mass of air, and can be calculated with sufficient accuracy from the formula:

$$q = 0.622e/p \quad (1)$$

where p is the atmospheric pressure.

e is the partial pressure of water vapour.

(Throughout this paper, pressure is taken in mb, but all other quantities are expressed in SI units)

The potential temperature θ of an air mass is defined as the temperature it would assume if it were brought adiabatically to the standard pressure of 1000 mb. The expression relating absolute temperature T and potential temperature θ is given as:

$$\theta = T \left(\frac{1000}{p} \right)^{0.286} \quad (2)$$

The vertical gradient of potential temperature ($d\theta/dh$) can be used to determine the thermal stability of the atmosphere. Three main states of ($d\theta/dh$) may be distinguished: stable, neutral and unstable stratification.

1.3 Thermal Stability and its Effects on Edm

Stable conditions, characterised by positive ($d\theta/dh$), tend to exercise a stabilising influence on air motion such that turbulence is suppressed. Stable conditions are generally found on clear nights when temperature inversions form as a result of ground cooling. For medium to long edm lines, observations during inversions have been found to produce systematically shorter distances of lesser precision than the corresponding determinations in unstable conditions. The poor results obtained during inversion conditions can be mainly explained by two factors: humidity anomalies along the propagation path, and the fact that for a typical edm line of elevated endpoints, much of the wave path may be above the shallow intense inversion layer. Above the inversion, neutral to near-stable conditions are generally found and endpoint meteorological measurements cannot be safely extrapolated to greater heights because of the discontinuity between the inversion and upper layers.

Neutral, or adiabatic conditions, characterised by zero ($d\theta/dh$), generally persist in the atmospheric surface layer for only short periods. A zero potential temperature gradient is usually found during the transition periods which, in ideal conditions, fall a short time

after sunrise and a short time before sunset. The neutral stratification within the transition periods is a short term phenomenon, rarely exceeding periods of more than a few tens of minutes, and usually confined to the lowest few tens of metres of the atmosphere. Hence, the proposal to confine edm observations to the times of transition is generally impractical.

Adiabatic conditions may also prevail in certain special circumstances, the most typical of these is when the cloud cover is very thick and there is a moderate or high wind. In addition, near-neutral conditions are encountered in the upper region of the turbulent regime, above the unstable layer, and this adiabatic layer plays a fundamental role in the development of the proposed model.

Unstable conditions, characterised by negative $(d\theta/dh)$, occur when the earth's surface is strongly heated by incoming short-wave solar radiation. Any disturbance of the air mass under these conditions is accentuated by buoyancy forces, so turbulence increases. In the lowest few metres of the atmospheric boundary layer, strongly negative temperature gradients can occur, their magnitude being dependent on the upward sensible heat flux.

Attempts to evaluate the effects of the temperature distribution close to the ground on edm reduction have included the use of meteorological measurements from masts. However, in general the mast heights have been arbitrarily chosen (10 m is the common height) and investigations have met with limited success, partly because variations in the height scale of the turbulent regime have not been considered.

2. MICROMETEOROLOGICAL BACKGROUND

2.1 Turbulent Transfer of Sensible Heat and Obukhov Length

Turbulent transfer of sensible heat H (heat flux) forms one component of the energy balance equation [7], [9] which can be given in the form:

$$H = (R - G) - \lambda E \quad (3)$$

where R is the net radiation.
 G is the heat flux into the ground.
 λE is the latent heat flux of evaporation or condensation,
with λ being the latent heat of the change of phase.

Values for $(R - G)$ can be measured directly using commercially available net radiometers and heat flux plates, or indirectly estimated from empirical formulae [2] using qualitative observations of prevailing weather conditions, i.e. cloud type, surface material, vegetation, soil type and moisture. The principles of measurement of evaporation E have been extensively discussed in literature [12], [16], and of the many methods employed, the so-called 'combination method' appears to be the most suitable for the evaluation of Eq.(3). The major advantage of the combination method is that it is defined in terms of standard meteorological measurements only; i.e., wet- and dry-bulb temperatures, and wind speed.

In similarity considerations of atmospheric turbulence a scale length, termed the Obukhov length, L has proved very valuable [10], [13].

L is defined by the equation:

$$L = -u_*^3 c_p \rho \theta (K g H)^{-1} \quad (4)$$

where u_* is the friction velocity.
 c_p is the specific heat at constant pressure.
 ρ is the density of air.
 K is the von Karman's constant, with value 0.4.
 g is the acceleration due to gravity.

The friction velocity u_* is a reference velocity, which characterises the particular turbulent regime. The magnitude of u_* is dependent on the winds shearing stress and on air density. For the evaluation of u_* [10], [12], [14], the well-known logarithmic wind profile relationship is generally used. This evaluation requires the measurement of the horizontal wind speed at only one height.

In unstable conditions the Obukhov length L is negative, in stable conditions positive, and in near-neutral conditions L becomes indefinitely large. Small values of L occur when large heat flux and weak wind cause strong thermal effects, a typical example being the noon period on a hot clear summer's day. For the use of the Obukhov length in the present context, it is important to note that the height scale of atmospheric turbulence expands and contracts in accordance with the magnitude of L [7],[13]. It is therefore an advantage to introduce the ratio h/L as a convenient stability and height parameter, where h is the height above the ground.

The evaluation of H and L from actual field measurements, in conjunction with the proposed model for edn reduction, has been discussed in detail by the authors, BRUNNER and FRASER in [6].

2.2 The Unstable Potential Temperature Profile

The unstable, and the adjacent adiabatic layer in the lower atmosphere have been discussed qualitatively by BROCKS [3]. Within the unstable turbulent regime, WEBB[13] has identified three regions of different physical behaviour, with associated different potential temperature gradients. The typical form of the potential temperature gradient prevailing in unstable conditions is shown in Fig. 1. The boundaries of the three regions are defined in terms of the Obukhov length L . The physical nature of the regions can be discussed in terms of convective processes [13] and a brief account of the types of convection - natural, free, forced - will now be given in conjunction with the discussion of the profile $(d\theta/dh)$ which predominates in each region.

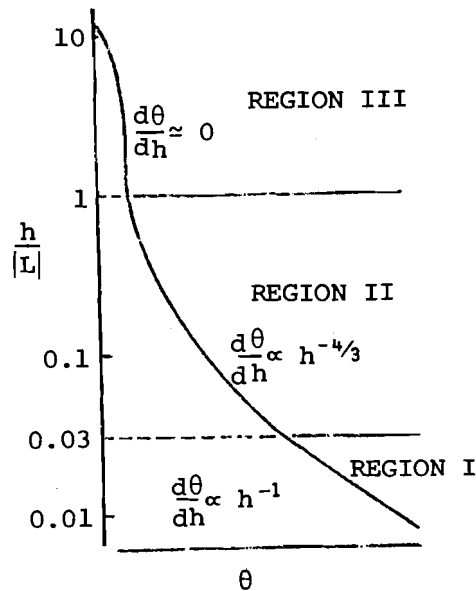


Fig. 1: A typical profile of mean potential temperature θ with logarithmic scale $h/|L|$, in unstable conditions [14].

Forced convection occurs with the passage of wind over a rough surface. The resulting wind-generated turbulence is the primary mode of heat transfer in region I, and the atmospheric conditions are always near-neutral. The prevailing potential temperature gradient within this region is in accordance with the well-known logarithmic profile. The upper height limit of region I can be estimated as $h = 0.03|L|$, see Fig. 1. The profiles of temperature within region I have limited applications in geodesy, as most geodetic measurements are generally above this region. Exceptions are found in conditions of weak instability when the wind is strong or the skies are heavily overcast.

Free convection is caused by density or buoyancy differences within moving air, and this type of convection governs the heat transfer in region II. Here the turbulent heat flux H is the main factor in determining the gradient $(d\theta/dh)$. Region II extends in height between the limits $0.03|L| < h < |L|$, see Fig. 1. The prevailing potential temperature gradient within this region is described by the so-called $(-4/3)$ law, [10]. Introducing for convenience a term α :

$$\alpha = \left[\frac{H^2 \theta}{(c_p \rho)^2 g} \right]^{1/3} \quad (5)$$

which can be considered independent of height and windspeed, the potential temperature gradient can be expressed with sufficient accuracy by:

$$(d\theta/dh) = -\alpha h^{-4/3} \quad (6)$$

Eq.(6) defines the vertical potential temperature gradient within region II, the region where most meteorological measurements are made for the purposes of determining refractive index and the coefficient of refraction. On clear days with moderate winds, over a grassland surface, region II generally extends from heights less than a metre up to a few tens of metres [15].

Quasi-free convection governs the transfer process in region III [13], [14] ; the convection is not wholly free because the existence of region III depends on the presence of thermal upcurrents from region II.

Within the range $|L| < h < 10|L|$, the air mass, with the exception of the thermal plumes, is gently descending and is essentially neutral in stability. In this region it appears that the effect of wind-induced turbulence has become so feeble that the buoyant elements rise in thermal plumes which suffer no appreciable diffusion with the surrounding air. Because of the adiabatic conditions which prevail, the mean potential temperature gradient within region III can be considered to be near-zero, see Fig. 1.

3. DEVELOPMENT OF THE TURBULENT TRANSFER MODEL

3.1 Atmospheric Model for Unstable Conditions

Fig. 2 gives a simplified schematic representation of the structure of the thermal regions II and III as they might appear over a typical edm line in unstable conditions. Profiles of potential temperature θ and relative humidity f are shown at both terminals, and a typical trace of the Obukhov scale length L is also given.

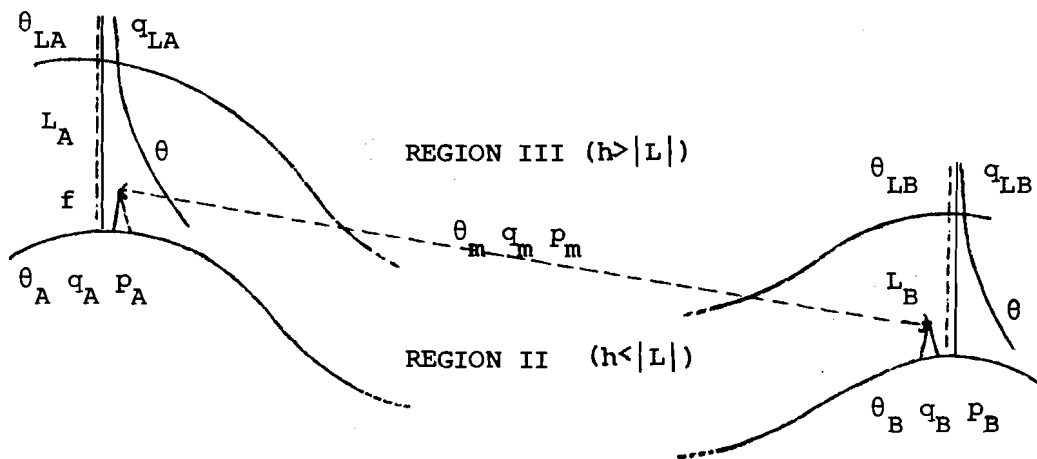


Fig.2: Schematic representation of the Turbulent Transfer Model for an edm line.

Within region II, for typical sunny conditions around noon, strongly negative potential temperature gradients ($d\theta/dh$) are encountered, corresponding to the large upward heat flux H . The increased turbulence resulting from the transfer by free convection causes increased mixing between the heat and water vapour carried by the turbulent eddies, and that present in the surrounding air. As the extent of turbulent mixing increases, the atmosphere becomes more homogenous and the previously strong potential temperature gradients are reduced to near-zero as adiabatic processes become apparent in the well mixed air.

If similar turbulent processes are assumed to act over the length of an edm path, then for the typical edm line profile with elevated endpoints, the wave propagation will be through the essentially quiescent air of region III. However, meteorological measurements for edm are usually carried out with aspirated psychrometers at or near the instrument height (typically around 1.5 m), which will be well within region II. To obtain the potential temperature at the upper boundary of region II, which will be representative and constant for the whole adiabatic region III, an integration of the potential temperature gradient over the appropriate height interval is required. Designating the parameters at the station A by a subscript A, the potential temperature θ_{LA} at the Obukhov scale height L_A is given by:

$$\theta_{LA} = \theta_A + \int_{h_A}^{L_A} \left(\frac{\partial\theta}{\partial h}\right) dh \quad (7)$$

where h_A is the height at which the potential temperature θ_A is obtained. Substitution of Eq. (6) for $(\partial\theta/\partial h)$ gives the practical equation:

$$\theta_{LA} = \theta_A + 3\alpha_A (L_A^{-1/3} - h_A^{-1/3}) \quad (8)$$

Relative humidity f is defined as the ratio of the partial pressure of water vapour e to the saturation water vapour pressure e_s at the dry-bulb temperature. For unstable conditions, the gradient of f with height, (df/dh) , has been shown to be near-zero throughout the turbulent regime [4]. Thus the relative humidity f_A , determined at the psychrometer height h_A , will also be appropriate at the lower boundary of region III. The specific humidity, q_{LA} , at the Obukhov scale height can therefore be calculated from the equation:

$$q_{LA} = f_A \cdot q_{S(LA)} \quad (9)$$

where $q_{S(LA)}$ is the saturation specific humidity for the dry bulb temperature at height L_A , calculated from θ_{LA} .

It has been shown that in region III of the unstable regime the conditions approach near-neutral and the conservative parameters θ and q may be considered invariant with height. Thus in estimating the mean potential temperature θ_m and mean specific humidity q_m which characterise the mean conditions for the ray path, only horizontal temperature and humidity gradients need be considered. In the formulation of the atmospheric turbulent transfer model, advection processes are not examined and horizontal gradients are assumed to be linear. Hence for the situation depicted in Fig.2, θ_m and q_m are given by:

$$\theta_m = \frac{1}{2}(\theta_{LA} + \theta_{LB}) \quad (10)$$

$$q_m = \frac{1}{2}(q_{LA} + q_{LB}) \quad (11)$$

where the subscript LB denotes the appropriate values at the terminal B.

3.2 Edm Reduction Formulae

3.2.1 General derivations

Electromagnetic distance measurements (light and microwave) between two terminals A and B give the optical path length σ , but for geodetic purposes the geometric (chord) distance S is needed. The optical path length σ of a wave propagation through an inhomogeneous medium is described by a first order partial differential equation, the so-called eikonal equation. The original solution of the eikonal equation of geometrical optics by MORITZ [8] has been reviewed and the following revised formula for edm reduction has been derived [5]:

$$\Delta S = \sigma - S = 10^{-6} \int_0^S N dx - \frac{1}{2} \cos^2 \beta \cdot 10^{-12} \int_0^S \frac{\left(\int_0^x \frac{dN}{dh} \xi d\xi \right)^2}{x^2} dx \quad (12)$$

where N is the refractivity of air, $N = (n-1)10^6$.
 (dN/dh) is the vertical gradient of refractivity.
 β is the inclination of the chord AB.
 x and ξ are the integration variables along the chord.

The advantage of Eq. (12) over other edm reduction formulae is that the integrations are carried out along the known chord and not along the unknown wave path. Hence, it is necessary to know either the value of the refractivity N and its gradient at all points along the chord, or the respective meteorological data which are necessary for the evaluation of N and (dN/dh) .

Ignoring the short portions of the path length at the terminals, which lie in the unstable surface layer (region II), the chord AB will be predominantly in the temperature and humidity quiescent air of region III, see Fig.2. For the situation depicted, the potential temperature θ_m and specific humidity q_m may be considered constant along the chord, their respective vertical gradients being zero in the adiabatic layer. Hence, only pressure will be a function of height between the terminal values p_A and p_B ; for convenience, the mean pressure p_m is introduced:

$$p_m = \frac{1}{2}(p_A + p_B) \quad (13)$$

For constant (dN/dh) along the chord, Eq. (12) can be evaluated as:

$$\Delta S = \sigma - S = 10^{-6} \int_0^S N dx - \frac{S^3}{24} [10^{-6} \cos \beta (dN/dh)]^2 \quad (14)$$

which is a valid assumption for almost any case considering the magnitude of the second term of Eq. (14).

3.2.2 Lightwave Edm

Using the formula of Barrell and Sears the refractivity of lightwave propagation can be given in terms of conservative parameters as:

$$N_L = (1.944 N_{GO} - 130 q) p^{0.714} \theta^{-1} \quad (15)$$

where N_{GO} is the group refractivity. The vertical gradient of refractivity (dN_L/dh) may then be expressed for dry adiabatic conditions with sufficient accuracy as:

$$(dN_L/dh) = -100.2 p^{0.428} \theta^{-2} \quad (16)$$

Substituting Eqs. (15) and (16) into Eq. (14) and using the mean values θ_m and q_m which are representative for the edm line yields:

$$\Delta S = (1.944 N_{GO} - 130 q_m) \theta_m^{-1} 10^{-6} \int_0^S p^{0.714} dx \quad (17)$$

$$- \frac{S^3}{24} \cos^2 \beta 10^{-12} (dN_L/dh)^2$$

The integral of the pressure in Eq. (17) can be solved either rigorously, leading to the distribution function of the normal distribution, or by a numerical integration method. However, it seems to be more convenient to use the following expression:

$$\int_0^S p^{0.714} dx = s [p_m^{0.714} + C] \quad (18)$$

where C is a correction term which can be assumed with sufficient accuracy to be zero for all edm lines shorter than 40 km. Details of this integration and formulae for the correction term C for longer edm lines have been given by BRUNNER and FRASER in [6].

3.2.3 Microwave Edm

Using the formula of Essen and Froome the refractivity of microwave propagation can be given in terms of conservative parameters as:

$$N_M = (559.87 - 150q) p^{0.714} \theta^{-1} + 3109 \cdot 10^4 q p^{0.428} \theta^{-2} \quad (19)$$

and the vertical gradient (dN_M/dh) for dry adiabatic conditions as:

$$(dN_M/dh) = -98.7 p^{0.428} \theta^{-2} - 3282 \cdot 10^3 q p^{0.142} \theta^{-3} \quad (20)$$

Substitution of these equations into the correction formula, Eq. (14), and using the mean values θ_m , q_m and p_m yields, with sufficient accuracy, the final form:

$$\Delta S = (559.87 - 150q_m) \theta_m^{-1} 10^{-6} \int p^{0.714} dx + 31.09 S q_m p_m^{0.428} \theta_m^{-2} - \frac{S^3}{24} \cos^2 \beta 10^{-12} (dN_M/dh)^2 \quad (21)$$

This equation will only be applicable for dry adiabatic conditions along the chord, as saturated adiabatic processes have not been considered here.

4. REFERENCES

- [1] ANGUS-LEPPAN, P.V.(1971): Meteorological Physics Applied to the Calculation of Refraction Corrections. *Commonwealth Survey Officers Conference*, Paper No. B5, 9pp.
- [2] ANGUS-LEPPAN, P.V. & WEBB, E.K.(1971): Turbulent Heat Transfer and Atmospheric Refraction. *General Assembly IUGG, Moscow, Travaux IAG - Sec.1*, 15pp.
- [3] BROCKS, K.(1948): Über den täglichen und jährlichen Gang der Höhenabhängigkeit der Temperatur in den unteren 300 Metern der Atmosphäre und ihren Zusammenhang mit der Konvektion. *Berichte des Deutschen Wetterdienstes in der US-Zone*, 5, 1-30.
- [4] BRUNNER, F.K.(1977): On the Refraction Coefficient of Microwaves. *In press*.
- [5] BRUNNER, F.K. & ANGUS-LEPPAN, P.V.(1976): On the Significance of Meteorological Parameters for Terrestrial Refraction. *UNISURV G25*, Univ. NSW, Sydney., 95-108.
- [6] BRUNNER, F.K. & FRASER, C.S.(1977): Application of the Atmospheric Turbulent Transfer Model for the Reduction of Edm. *In press*.
- [7] DEACON, E.L.(1969): Physical Processes Near the Surface of the Earth. *World Survey of Climatology*, 2 (General Climatology), 39-104.
- [8] MORITZ, H.(1967): Application of the Conformal Theory of Refraction. *Österr.ZfV*, Sonderband 25, 323-334.
- [9] MUNN, R.E.(1966): *Descriptive Micrometeorology*. Advances in Geophysics, *Supp. 1*, Academic Press, 245pp.
- [10] PRIESTLEY, C.H.B.(1959): *Turbulent Transfer in the Lower Atmosphere*. University of Chicago Press, 130pp.
- [11] RINNER, K.(1976): Bericht Über Laser - und Mikrowellen Messungen im Testnetz Steiermark. *Mitt.Geodät.Inst.Techn.Univ. Graz*. Folge 22, 106pp.
- [12] SLATYER, R.O. & McILROY, I.C.(1961): *Practical Microclimatology*. CSIRO (UNESCO), Australia, 175pp.

- [13] WEBB, E.K.(1964): Daytime Thermal Fluctuations in the Lower Atmosphere. *Applied Optics*, 3, 1329-1336.
- [14] WEBB, E.K.(1965): Aerial Microclimate. *Meteorological Monographs*, 6(28), 27-58.
- [15] WEBB, E.K.(1969): The temperature structure of the lower atmosphere. *Proc. of RED-EDM Conference*, Univ. NSW, Sydney(1968), 1-9.
- [16] WEBB, E.K.(1975): Evaporation from Catchments. *Proc. Third Nat. Symp. on Hydrology, "Prediction in Catchment Hydrology"*, Canberra, 203-236.

Discussion (paper 25)

Q. You have shown us a very interesting slide with a three dimensional image of the behaviour of the atmosphere with a cold airstream coming downward and the separated streams of hot air going upward.

What I would like to ask you: what is the diameter of such a atmospheric adiabatic element and what is the diameter of the hot-air walls of this element ?

A. I would think about 5 years ago I would have asked the same question, but that is a typical question of geodesists. Other scientists never ask questions like this, because most of the things that they do are speculative. You are happy if you get some idea what is going on. It is difficult to get some measurements. I tell how they do it. They use gliders. I think a fact in that the rising air and the sinking air do not exchange heat with the surrounding air, and therefore only pressure adjustment is happening. The parcels of air move up and down with a change of temperature only, but there are no changes of the specific humidity and the potential temperature because they are adiabatic processes, that is all there is. There are no other forces involved.

Of course there is some wind there but you can consider the wind only as mixing. This area here is in a real mixed state. And therefore because it is well mixed, and it is a representative temperature profile, it will show you always this condition. But you must have a turbulent surface-layer to get these conditions. I have forgotten to mention one thing: the model will work also if you have heavily overcast skies, because then this turbulent surface-layer will not generate and therefore this constant profile will go down right to the surface. So, I'm sorry I can't tell you any diameters or anything like this, but people are working on it. So, this is the knowledge of meteorologists at present.

Q. An additional remark: In physics of fluids, such structures are well known, and also the diameter of such structures, and these are functions of the viscosity. For me it is only of general interest to know the diameter of this, to get a better suggestion of the atmosphere. It is not a question to have a suggestion for correction.

A. Sorry. I can't help you.

Q. May the theory you have, also be used to understand forward scatter. For instance very long distances can be measured on a frequency of 400 MHz which is probably a matter of forward scatter. Do you know something about it.

A. A theory like this could open many other areas, and throw up many questions. I cannot answer you.

METEOROLOGICAL CORRECTION OF LASER AND MICROWAVE DISTANCES

K. Rinner, Graz, Austria

In the test network "Steiermark" (Styria) several 24-hour distance measurements were carried out in the years 1967 to 1975 with measuring intervals of abt. 30 minutes for various distances with various profiles by means of laser and microwaves. With the meteorological data measured in the end points (atmospheric pressure p , temperature t , steam pressure e) and the measured values of the instruments (geodimeter 8 and tellurometer MRA 3), non-reduced and meteorologically reduced distances G and R were determined, and Fourier functions were interpolated and graphically represented for G , R and the data p , t , e .

As a result, typical relations between these curves were obtained for laser and microwave measurements. Examples therefor are given in Figs. 1 and 2. The following results have been derived therefrom in /1/:

- (1) Though a constant portion of the meteorological influence is taken into account by the customary meteorological reduction (according to Owens, from end point values) the variable portion will be overcorrected. Since between the mean temperature values t_m and the reduced measured values R a significant correlation can be observed it seems possible to correct individual measurements from temperature measurements of one day cycle. The mathematical formulation of the correlation as a function of parameters of the measuring profile and of general meteorological data should be studied.
- (2) The usual reduction of microwaves (according to Essen) is less efficient so that the variable portions of the meteorological influence will be undercorrected. Less significant correlations seem to exist between the reduced distance R and the mean values e_m and t_m (partial water pressure and

temperature). Therefore it should be difficult to formulate a correlation function and to determine the corresponding parameters.

- (3) The mean values of microwave measurements over several years (1967 - 1969) are of high intrinsic accuracy of abt. ± 1 mm/km comparable to that of laser measurements. They are, however, shorter than laser sides and are distinguished from them, in the Styrian test network, by a significant scale factor of $(+ 4.1 \pm 0.4)$ mm/km. Since the cause for this pseudosystematic difference lies in the insufficient consideration of the partial steam pressure an attempt is made to eliminate it by calculating position constants. A respective theory is given in /1/ and /2/, a phenomenological explanation in /3/.

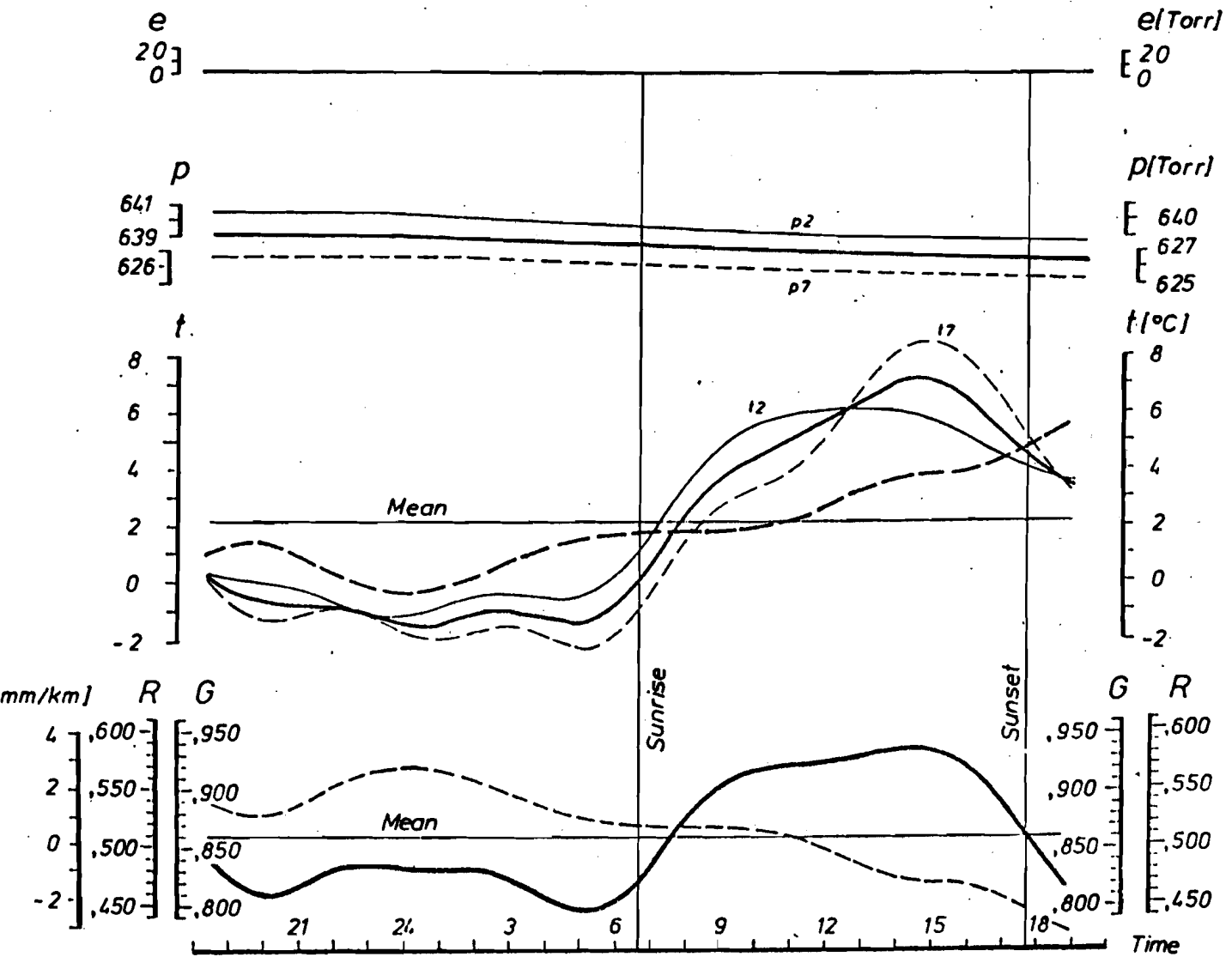
Since the above results may lead to a simple correction of laser and microwave distances raising theoretically interesting problems they are again communicated here and submitted to discussion.

Literature:

- /1/ RINNER K.: Bericht über Laser- und Mikrowellen-Messungen im Testnetz Steiermark, Mitteilungen der geodätischen Institute der TU Graz, Folge 22, 1976
- /2/ RINNER K.: Bericht über die 1971 ausgeführten Laser- und Mikrowellenmessungen, Mitteilungen der geodätischen Institute der TH in Graz, Folge 13, 1973
- /3/ BREITENBAUER K.: Phänomenologische Deutung der Rinner'schen Ortskonstanten, Verm. Photogr., Kulturtechnik, 000/IV/75, p. 231-233, 1975

Distance: 2-7 (Schöckl-Rennfeld) Date: 28.2./1.3.75									
Heights				Time	Centered mean dist.		Mean of met. Datas		
Pt	Hi		ΔHi		GL	RL	tm	pm	em
2	1.445,31	B	+1,50	T	24.302,838	24.304,557	5,2	632,4	3,2
7	1.628,79	B	+1,50	N	24.302,875	24.304,470	-0,4	633,4	2,6
				T+N	24.302,859	24.304,508	2,1	632,9	3,0

Lasergeodimeter 8



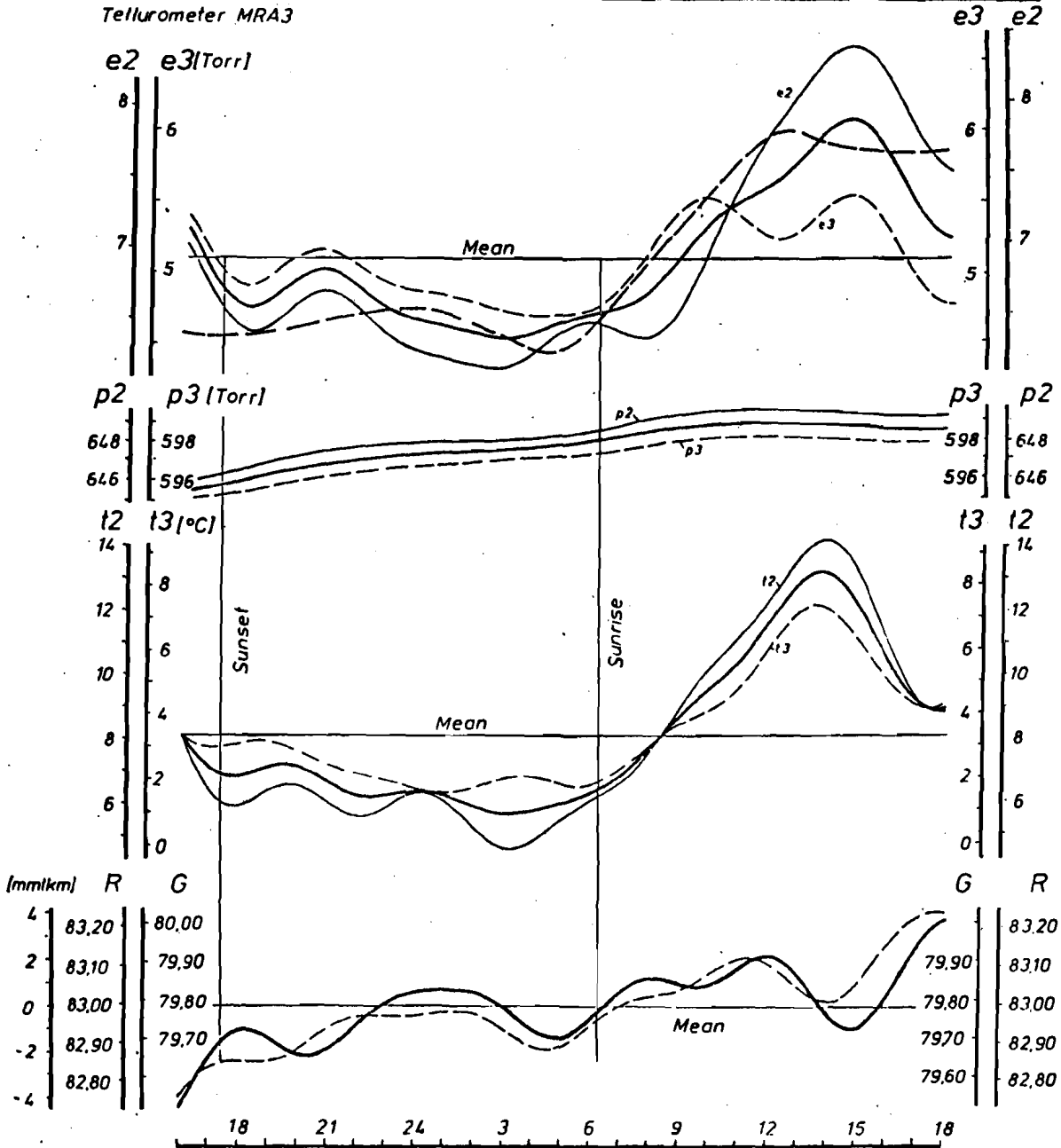
- | | | | | |
|-------------|--|-------|----|-------------------------------|
| Hi | Height of i [m] | ----- | ei | Water vapor pressure in i |
| ΔHi | Height above ground of the thermometer | ===== | em | Water vapor pressure mean |
| B | Met. datas at ground | ----- | eg | Water vapor pressure computed |
| T | Day | ===== | ti | Temperature in i |
| N | Night | ----- | tm | Temperature mean |
| ----- | G measured value | ===== | tg | Temperature computed |
| ===== | R met. red. slope distance | ----- | pi | barometric pressure in i |
| | | ===== | pm | barometric pressure mean |

Distance: 2-3 (Schockl-Koralpe)

Date: 9./10.10.1968

Heights				Time	Centered mean dist.		Mean of met. Datas		
Pt	Hi	B	ΔHi		GM	RM	tm	pm	em
2	1445.31	B	+ 1.50	T	59 179.848	59 183.031	7.1	623.5	6.3
3	2140.68	B	+ 1.50	N	59 179.712	59 182.956	3.9	621.8	5.4
				T+N	59 179.788	59 182.998	5.7	622.6	6.0

Tellurometer MRA3



- | | | | | |
|-------------|--|-------|----|-------------------------------|
| Hi | Height of i [m] | ----- | ei | Water vapor pressure in i |
| ΔHi | Height above ground of the thermometer | ----- | em | Water vapor pressure mean |
| B | Met. datas at ground | ----- | eg | Water vapor pressure computed |
| T | Day | ----- | ti | Temperature in i |
| N | Night | ----- | tm | Temperature mean |
| ----- | G measured value | ----- | tg | Temperature computed |
| ----- | R met red slope distance | ----- | pi | barometric pressure in i |
| | | ----- | pm | barometric pressure mean |

Discussion (paper 26)

- Q. I'm delighted to see that one of your geodimeterlines was nearly 60 km. long.
I thought 60 km. was something that only our Scandinavian colleagues could achieve with the laser- geodimeter.
But you managed that also ?
- A. We measured even longer distances, about 93 km. We did do that 4 times in 2 years. The test net is in the mountains and in autumn there is a very clear atmosphere.
- Q. You told us, there is a systematical difference between laser and microwaves of about 4 mm/km.
And you said this is a difference caused by steam pressure but you know there is a systematic difference from temperature influence too.
You have different signs on micro-waves and on light-waves.
Don't you think there is an influence on this 4 ppm from temperature ?
- A. I think the greatest portion of this difference should come from the differences in the determination of the water vapour pressure.

AN EXPERIMENT WITH A HIGH PRECISION METHOD OF ALIGNMENT

P. Richardus and R.H. Masée

SUMMARY

It is generally known that the alignment of three points at a maximum distance of say 30 meters as applied to industrial purposes frequently constitutes a problem in respect of the precision required.

One of the most precise methods of alignment is described by Van Heel (1950) employing a beam of coherent light, and a zone plate between two fixed points represented respectively by the centre of a circular diaphragm and the intersection point of crosswires. It owes its high precision to the fact that it does not apply an optical lens system, thus obviating the influence of the non-symmetric aberrations of such a system, and the detrimental influence of the need of focussing at various distances. The precision of each setting is therefore independent of distance. The method is, however, just as well liable to the influence of refraction.

An experiment has been conducted in the laboratory investigating the possibilities of improving the precision of alignment in a vertical sense by trying to eliminate – at least partly – the influence of the vertical refraction. This improvement is thought to be obtained by the application of a liquid level surface (water) as a reference surface, the alignment in a horizontal direction still being performed with the conventional Van Heel's arrangement.

The results are very encouraging. It appeared that by the instrumentation and the method described in this paper, one may measure the vertical distance of two fixed (terminal) points of the alignment in respect of this surface with micrometers; calculate the position of intermediate points by interpolation and set the micrometers accordingly. The internal standard deviation of alignment is estimated at approximately 3–5 μm (single setting). The total length of the line in the experiment was 13½ meter, with 4 intermediate points at equal distances. An extension to 30 meters is possible maintaining the same precision.

1 Introduction

The requirement of the highest possible precision of a three point alignment at relatively short distances is particularly stringent in respect of industrial and other technical purposes. Refraction and the many mechanical inaccuracies of the optical instruments have a considerably detrimental influence on the precision particularly of the pointing at short distances. The standard deviation (sq. root of the variance: s.d.) of pointing (horizontal as well as vertical) may be expressed (in sex. sec. of arc) by the formula (Richardus 1963, 1968)

$$\sigma_p = 1.48 \sqrt{\left(\frac{C}{M}\right)^2 + 0.064^2 d^4} \quad (1)$$

where C is the "vernier acuity" of the observer; M the magnification of the optical system and d the distance to the target in meters.

One may allow for laboratory circumstances by taking $\frac{2}{3}\sigma_p$. This formula is based on a very large number of observations by Washer and Williams (1946); Washer (1947) and Anon. (1968). It is noteworthy that very few references to this problem are found in the literature to this date.

Characteristic for the optical systems is that the influence of diffracted light is eliminated as much as possible.

A very high precision method of alignment has been

* Paper presented at the VII International Course of Technical Measurements of High Precision and The Symposium F.I.G. Commissions 5 and 6, Darmstadt, W.-Germany, 29th September–8th October 1976.

published by Van Heel (1950), employing diffracted light only. A coherent wavefront in the form of a narrow pencil proceeding through or from a circular diaphragm is caught by a zone plate. The interference patterns formed at any arbitrary distance from this plate will consist of concentric coloured rings with a clear centre. In the case of a monochromatic wavefront the pattern shows light and dark rings. An index (circles or crosswires etched on glass) can be set on this interference pattern with a micrometer.

This will effect the alignment of the centres of the first diaphragm, the centre of the zone plate and the index. It is noted instantly in comparison with the conventional use of telescopes, that focussing has been eliminated as a source of errors. Van Heel claims a precision of pointing (under laboratory circumstances) of 0,01 mm (standard deviation) for distances of 0.5 to 30 metres. This linear measure is *independent* of the distance. A second advantage of this method is, that a diffraction pattern is formed at *any* arbitrary place passed the zone plate, where the index can be set without loss of precision. This eliminates the error-theoretical difficulty that becomes apparent in continuing a line by extrapolation.

For these reasons a similar set up was selected for the experiment. A 1.5 mW LS-32/E.N.L. HeNe gas laser system provided a coherent pencil of optical red (632.8 nm) light, the diameter being 2 mm at the exit aperture. The zone plate produces a pattern of red and black rings on which could be pointed with an index of three concentric rings etched on glass. It is possible to use the centre of the beam for the alignment, or the centre of the circular aperture of the optical system with which the convergence of the beam can be adjusted. As could be expected, however (see a.o. Geilen 1971), the directional stability of the beam was by no means sufficient to maintain the required high precision of alignment especially during the three hours after first triggering the laser. Deviations could amount to 0.2 mm at a distance of a few meters. This difficulty was avoided by locating an independent circular diaphragm at a few centimeters in front of the laser. This diaphragm (diameter 0.1 mm) then

acts as an independent source of coherent light and produces a high quality pattern as long as it remains situated within the laser beam. The line could now be held fixed perfectly between the centre of this diaphragm and the index.

After the arrangement of the alignment in the laboratory with an initial total length of approximately 30 meters, the internal precision of pointing was checked. The zone plate, being attached to a micrometer reading directly to 0.01 mm and an estimation of 2 μm , could be moved by remote electrical control from the observer's place (at the index). The observations were subdivided into groups of 10 settings in order to avoid long term influence of refraction.

The position of the diffraction pattern reacted sharply to short term turbulence, caused mainly by walking along the line; therefore one should wait observing until the unrest in the atmosphere settles down. It then appeared that the internal precision of pointing (s.d.) was 6.5 μm . This agrees with the findings of Van Heel, the difference being caused by the use of a more precise micrometer and the fact that the laser did not exist at the time of Van Heel's experiment.

The influence of refraction cannot be eliminated, at least not the horizontal refraction. The question arose whether the alignment could be improved in a vertical direction by the use of a liquid level surface as a reference surface.

A number of points should be considered when using a liquid surface in this way:

1. The surface is in fact an equipotential surface, which can be taken as spherical over the short distances involved.

The corrections Δh to the horizontal direction at a point of the surface can be calculated with the formula (see Fig. 1)

$$\Delta h = \frac{a^2}{2R} \quad (2)$$

where a is the distance from the tangent point and R the radius of the earth (6378 km).

2. It is a known fact in hydrostatic levelling, that the tidal forces cause the liquid to follow a

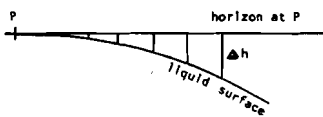


Fig. 1.

periodic movement. The difference of level between two points may be given by the formula:

$$\Delta l = k \cdot a_{km} \sin 2Z \cos(\alpha - A) \quad (3)$$

where k is a constant equal to 0.032 and 0.068 for the influence of the sun and the moon respectively; Z is the zenith angle; α and A the azimuth of the alignment and the sun/moon respectively (Jensen 1950, Waalewijn 1964). The amplitude reaches an absolute maximum when $Z = 45^\circ$ and $\cos(\alpha - A) = 1$ for both the sun and the moon *at the same time* (i.e. $1.5 \mu\text{m}$). It was considered that the necessary time of observation was that short in comparison with the time between two such amplitudes, that the influence could be neglected as disappearing in the "noise" of the measurements.

3. To establish the liquid reference surface, a PVC pipe of a length of approximately 13 meter was filled with distilled water. Windows in the pipe every 2.6 meters made it possible to reach the surface. Since the measurements involve conducting an electrical current through the liquid, some chemicals were added in order to increase the conductivity. Special care must then be taken that the specific density is the same everywhere in the solution. Differences in the specific density may have a noticeable local influence on the level of the surface in the pipe.
4. The height of points above the surface is being measured at different times and not simultaneously at the same instant. Therefore the influence of evaporation; of the fluctuations of the temperature of the air and of the liquid internally; and of the air pressure should be assessed. By the measurement of the various parameters and the knowledge of the coefficients of expansion, elasticity, compressibility of water, etc., it would be possible to calculate the movements of the liquid surface with the applicable formulae (Waalewijn 1964, Sneddon 1974, 1975). The

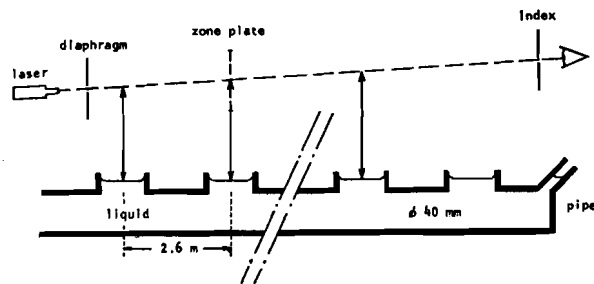


Fig. 2.

check measurements made in the experiment, however, were nowhere in agreement with the results of the calculations, most probably because the constants given in these formulae were not applicable. The formulae indicate a proportionality of the change in volume to the differences in pressure and temperature. The internal temperature differences in the liquid are much more critical than the external ones. Within the relatively short time of observations these differences will be considered proportional to time also.

The alignment set up is shown schematically in the figure 2.

Problems on cohesion and adhesion, capillary action in the liquid system are assumed to be solved in the instrumentation as described in the next section. It should be mentioned that in many respects use is made of the experiences as laid down by Oostenrijk (1968) in his paper on the "Nivelmatic", a multi precision hydrostatic levelling instrument for the precise placing and checking of large machine beddings, surface plates etc. in heavy industry.

2 Instrumentation (design and specifications by Masée)

The height of a point is measured with two micrometers (1), (2) as shown in the figure 3; one moving upward with the zoneplate (3) attached, and the other moving downward initially with a needle attached to touch the liquid surface. The movements of both micrometers are electronically controlled with servomotors and switches from the observer's place. The downward movement is measured automatically with a counter that stops when the needle touches the surface. The pointing of the

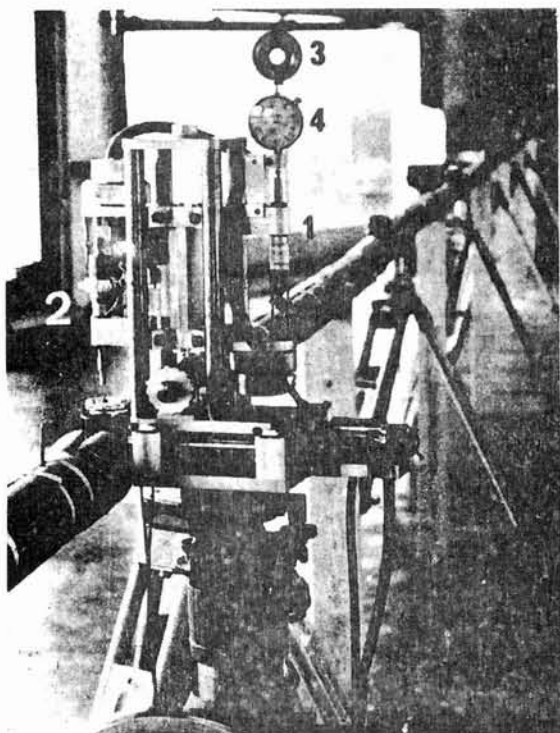


Fig. 3.

interference pattern is done by the observer by remote control; the micrometer (2) of the zoneplate is read on a clock (4). The total arrangement is fixed within a frame of four pillars standing on a sledge allowing a small horizontal movement (also by remote control) for easier pointing. The total instrument is placed on a triback on a heavy mobile industrial tripod. The height of the instrument is approximately 50 cm.

The windows in the pipe have a diameter of 42 mm thus allowing for a flat liquid surface in the centre. The arrangement of the needle did not appear satisfactory because of adhesion and corrosion problems. After much experimenting the following design gave the best results. The needle was replaced by a cap with a flat bottom and a float (of a carburettor) was placed in the window (Fig. 4). It consisted of a barrel (diam. 21 mm) with a vertical bar in the centre of which a platinum wire of 0.2 mm length. Underneath three horizontal bars placed under an angle of 120° made the float automatically maintaining a central position (Fig. 5). Such a float was placed in each window. It was then necessary for the alignment to standardise them for the reduction of differences in height of the platinum wire above the liquid level. It was found that the precision of measuring the downward movement of the micrometer until the cap touched the platinum wire could not

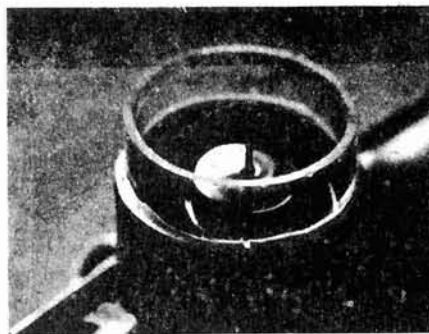


Fig. 4.

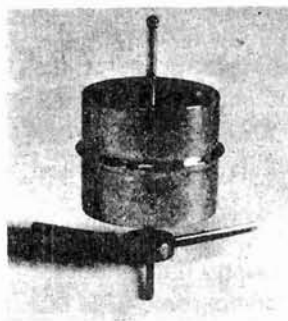


Fig. 5.

only be kept steady, but was also the highest of all possibilities tried. The s.d. derived from the counter readings was $2.1 \mu\text{m}$.

3 The observations; precision

During the measurements, airpressure and air-temperature (wet and dry) and the internal temperature of the liquid at every window (by built-in thermocouples) were registered. The evaporation was checked by separate regular readings at one of the floats (the other windows remaining covered) during a number of extended periods when airpressure and temperatures were stable. The amount of evaporation was approximately $0.03 \mu\text{m}$ per minute.

The order of observation decided upon was the following. It was not possible in the present arrangement to fix the two terminal points independently and measure the height above the liquid level (the ideal situation as it should be effected in the industry). The position of the zoneplate in the "laser" line was determined instead above the terminal floats nos. 1 and 6 by the mean of 4 series of 10 settings. These two points were then assumed to be fixed with a s.d. of $1.1 \mu\text{m}$.

It was decided that the influence of the evaporation for the 10 minutes necessary to take these measurements and the shifting of the tripod in be-

tween, could be ignored. Then the tripod was moved consecutively to the floats 5, 4, 3 and 2, and the respective micrometer readings registered together with those of the corresponding settings of the interference pattern in the laser line. The sequence was concluded by readings at the terminal no. 1 again. After a proportional reduction for the differences between the readings at this terminal the intermediate readings may be compared with the settings of the micrometer as calculated by interpolation. The differences Δ would show at least the order of magnitude of the influence of the vertical refraction. The intermediate readings were the mean of two series of 10 settings each. The s.d. can be estimated as 1.6 μm (inclusive the s.d. of the standardization) so that the s.d. of a difference Δ would amount to 1.9 μm .

Four examples are given below, the first one showing the method of calculation, the last one showing the largest difference Δ ever obtained. (Rounded off to μm).

float	1	2	3	4	5	6
1st example						
readings	7985					9054
	7972	8196	8426	8637	8824	
interp. for time*	13	10	8	5	3	0
reduced read.	7985	8206	8434	8642	8827	9054
earth curv. (-)	0	1	2	5	8	13
correct. read.	7985	8205	8432	8637	8819	9041
calcul. interp.	7985	8196	8407	8619	8830	9041
differences $\Delta\mu\text{m}$	0	+9	+25	+18	-11	0
2nd example						
differences $\Delta\mu\text{m}$	0	+15	-4	+15	+7	0
3rd example						
differences $\Delta\mu\text{m}$	0	+16	+18	+26	-6	0
4th example						
differences $\Delta\mu\text{m}$	0	+35	+14	+48	+19	0

* infl. of evapor., temp. etc.

4 Conclusion

From the results it may be inferred that the vertical long term refraction has a more considerable influence on an alignment than would be expected at first sight. It seems possible to eliminate the larger

part of this influence by the inclusion of a liquid level surface as a reference. One can measure the vertical distance of two fixed terminal points of the alignment in respect of this surface, calculate the position of intermediate points by interpolation and set the micrometer accordingly. The instrumentation required is complex, but may be justified for specific purposes. The instrumentation described is only experimental and can of course be perfected for use in practice.

Acknowledgements

The high precision instruments were built in the workshop of the Department by Messrs. D. A. de Wit and D. Joghems with exceptional skill. The electronics was designed and built on specification by the Technical and Physical Engineering Services at Wageningen.

References

- Anon., 1948. Precision of telescope pointing. *J. Coast and Geodetic Survey* no. 1.
- Geilen, Q., 1971. Untersuchungen zur Richtungstabilität von HeNe-Lasern mit Hilfe von Elektronischen Messlatten. *Veröff. Geodät. Inst. T.H. Aachen* no. 19.
- Van Heel, A. C. S., 1950. High precision measurements with simple equipment. *J. Opt. Soc. Am.* Vol. 40, nr. 12, p. 809-816.
- Jensen, H., 1950. Formulas for the astronomical correction to precise levelling. *Bull. Geodésique* no. 17, p. 267-277.
- Oostenrijk, G., 1968. Het nieuwe meerpoints precisie waterpas „De Nivelmatic”. *Tijdschr. Kadaster Landmeetkunde* (84) no. 4, p. 212-238.
- Richardus, P., 1963. The application of diffractive light in Surveying. *Ph.D. dissertation.*
- Richardus, P., 1968. Richten en Inrichten. *Tijdschr. Kadaster en Landmeetkunde* (84) no. 6, p. 415-427.
- Sneddon, J., 1974. Temperature effects in hydrostatic levelling. *Survey Review* no. 174 p. 361-374.
- Sneddon, J., 1975. Hydrostatic methods of precise levelling. *Ph.D. dissertation, The University of New South Wales.*
- Waalewijn, A., 1964. Hydrostatic levelling in the Netherlands. *Survey Review* no. 131, p. 212-221; no. 132, p. 267-276.
- Washer, F. E. and Williams, H. B., 1946. Precision of telescope pointing for outdoor targets. *J. Opt. Soc. Am.* 36.
- Washer, F. E., 1947. Effect of magnification on the precision of outdoor telescope pointing. *J. Research (U.S.). Bureau of Standards* 39.

MEETING OF SSG 1.42

The meeting was held for the purpose of inspiring members, present, to contribute in various areas of the SSG 1.42 - research.

The Chairman opened the meeting, by indicating some lines of research, which should be followed by the members.

These lines were:

- 1) Absolute tests in using δ -measurements for determining refraction.
 - a) Error of κ in the dry air term $\kappa\delta$, due to ev. variations in the relative contents of dry air constituents.
 - b) Humidity correction Q in [1] has been derived, assuming, that waterdamp behaves like an ideal gas, that is, Laplace equation is valid for Q . Is this correct? The elimination of the Q -term, is it possible?
 - c) Concerning the H -term of humidity. Can it be neglected?
 - d) Ev. errors in the absolute test formula, presented as eq. (9) in my own contribution here [1].
- 2) Research into the development of instruments, giving directly refraction-free angles and distances. This goal is reflected in the suggested resolution 1, which he hoped should pass.
- 3) A general solution of the problem of parallactic refraction is urgently needed, taking local atmosphere into account.
- 4) Shimmer problems must be considered, especially in satellite direction observations.
- 5) To improve the accuracy of the direction observations of passive satellites, the s.c. Kakkuri time recorder [2], will play an essential role in the future, not least because it seems to enable the determination of shimmer effects. It will probably also increase the accuracy of

star observations for Polar Motion studies with long-focus zenith telescopes. SSG 1.42 is certainly concerned!

- 6) To avoid refraction effects at all, the fore-runner problem must be solved. If these fore-runners could be observed, no refraction problems would exist. What is the state of recent research?
- 7) The statistical analysis of obtained terrestrial refraction by means of the two wave method should be done by spectral analysis. The important work [3] by Kahmen on series of refraction angle and n-observations could serve as guideline. The chairman mentioned also Livieratos' interesting approach for statistically studying terrestrial refraction in mountainous areas from exposures of laser lightsources against the starry background. ^[5] The statistical treatment of refraction and meteorological data should be dealt with during a special workshop on Friday 27 May, entitled "Correlation analysis and systematical errors". It was here already stressed, that when sampling data for such a statistical analysis, various topographical and climatological conditions should be paid due attention to.
- 8) In general, the analysis of errors in the results of geodetic measurements should be performed with modern statistical methods (confidence- and test analysis). The role of correlation- and spectral analysis should be emphasized.
- 9) For range- and range-rate observations, investigations of ionospheric and tropospheric corrections should be continued and intensified.
- 10) Studies of astronomical refraction must be intensified. New tables and better local models should be elaborated in cooperation with WGAR (Working Group on Astronomical Refraction in Comm. 8 of IAU). Special attention should be paid to the problem of determining the zenith refraction.
- 11) Levelling refraction should be investigated more carefully.

Statistical analysis of levelling data should be continued in a way, which already had been followed by Ole Remmer in his important studies (e.g. "Levelling Errors in Statu Nascendi").[4]

- 12) The chairman announced an international symposium to be held in Uppsala in August 1978 with the title "Refractional Influences in Astrometry and Geodesy". A symposium with same title was originally prepared to be held in Belgrade May 1978 with prof. Teleki as convenor (chairman of WGAR), but political reasons made it impossible. Attempts are now made for arranging this symposium in Uppsala, in cooperation between IAU and IAG (through WGAR and 1.42). It is planned to carry out refraction measurements during this symposium along the 20 km testbase near the Geodetic Institute of Uppsala University, by means of instruments and methods, developed by various investigation groups within 1.42. (Moscow-group, Teddington-group, Hannover-group and Uppsala-group).
- 13) The chairman touched the question about necessary consequences for future 3D geodesy and geodynamics, arising from the fact, that refraction-free angles and distances are soon possible to obtain during actual field measurements. The desirability of having handy instruments, commercially available, which directly give refraction-free data, is reflected in the proposed resolution no 2, which hopefully will pass. The importance of carefully studying the influence of atmospheric turbulence on multi-wave refraction determinations was also emphasized.

The discussion, which followed, was animated, and inspiring.

As we had no tape-recorder during this meeting, I'll try to sketch the main lines only of the discussion, relying on my notes and my memory.

As regards the point 1), I did not get a clear answer at 1a). Nobody knew, if local air composition could essentially change the C-constant in Barrel and Sears' formula. So this question is still open.

With respect to 1b), it was felt - from the discussion - , that multi-wave methods must be unsuccessful. The only possibility of calculating a reliable Q-term was to use meteorological data of some kind (Glissmann, Bradsell, Williams, Brunner).

What concerns the H-term 1c), no answer could be given. The whole theory of humidity effects on the refraction formula should be further investigated! (de Munck).

1d) gave no response for the moment!

What concerns 2), it should be mentioned that Glissmann had a solution, which was supported by Williams. Further details of the Glissmann solution will be brought to the 1.42 members attention very soon, or at least in the proceedings of the symposium.

As regards point 3), Parm indicated, that Kakkuri in Finland is about to publish an important paper about the solution of this problem, especially of value for the observations at low altitudes in stellar triangulation.

The chairman pointed out, that on point 4), the Kakkuri "Time-micrometer", the theory and application of which is already published, will be able to solve the problem. For further information, please, contact Kakkuri directly!

Point 6) deals with a question, which is very old. I (the chairman) asked for recent news as regards the possibility of observing the fore-runners. No immediate response was given to this question, but information about the theoretical work on the subject was delivered by Brunner and Williams. The concept of refraction-free signals was, in fact, treated by Sommerfeld long time ago. Williams promised to send a copy of Sommerfeld's original article on the subject to the chairman of 1.42 as soon as possible, to be distributed to all members of the group.

As to point 5), no special discussion followed. The chairman reported, that a cooperation between the Geodetic Institute in Uppsala and the Astronomical Observatory there has already been started for carrying out experiments into solving the problem of increasing the direction accuracy when observing satellites photographically by means of long focus cameras.

7),8) The statistical analysis of all geodetic data, obtained from signals in our atmosphere was discussed. Hopefully future

methods of treating these data will be settled after the discussions at the workshop on Friday. Parm declared, that the accuracy of the 800 km baseline in Finland will be re-computed, using modern statistical analysis. [6]

9) It was emphasized, that the refractional corrections in range related methods should be investigated still more carefully than til now. Suggestions were given by Hopfield and others.

10), 11) No contributions from the people present. However these two items are of utmost importance for the work of 1.42, and it is hoped, that we shall soon have more contributions to their solutions, both theoretically and practically.

13) Mr Poder pointed out, that with refraction-free directions and distances in 3D work, the concept of geoidal heights and deflections are unnecessary and should be avoided in the treatment of the results, which serve mainly geometrical and geodynamical purposes. The chairman answered to Poder's remark, that he was interested also in the mapping of Marussi's intrinsic coordinates over the investigated area, being essential for the modern treatment of general dynamical geodesy (fixed BV-problem), and therefore formally needs the concepts of potential, geoidal heights (height anomalies) and deflections.

Taken from my memory

Erik Tengström

References

- [1] Tengström, E.: "Some absolute tests of the results of IDM-measurements in the field, with a description of formulas used in the tests", presented at the Int. Symp. on Electromagnetic Distance Measurement and the Influence of Atmospheric Refraction, Wageningen, the Netherlands, May 1977.
- [2] Kakkuri, J. and Kalliomäki, K.: "Photoelectric Time Micro-meter", Publ. of the Finnish Geodetic Inst., no. 74, 1972.
- [3] Kahmen, H.: "Einige Betrachtungen über das Stochastische Verhalten der Refraktionswinkel und der Brechungsindizes, die Laser- und Mikrowellen-entfernungsmessungen betreffen", presented at the Int. Symp. on Electromagnetic Distance Measurement and the Influence of Atmospheric Refraction, Wageningen, the Netherlands, May 1977.
- [4] Remmer, O.: "Levelling errors in statu nascendi", Meddelelse no. 51, Geodaetisk Institut, København 1975.
- [5] Livieratos, E.: "On the Refraction Problem of Ground Target Photography with Stellar Background as applied in the 3-D Terrestrial Triangulation by using Pure Satellite Triangulation Methods", estratto dal Bollettino di Geodesia e Scienze Affini, Anno XXXV, N.4, 1976.
- [6] Parm, T.: "High precision traverse of Finland", Publ. of the Finnish Geodetic Inst., no. 79, 1976.
- Kakkuri, J. and Kalliomäki, K.: "An automatically operated weather station", Reports of the Finnish Geodetic Inst., 76:4, Helsinki 1976.

List of some recent papers, dealing with problems of atmospheric effects on wave propagation.

D.C. Cooper and J. Blogh: "The Use of an Electro-Magnetic Acoustic Probe to Detect Air Turbulence", Dept. of Electronic and Electrical Engineering, The University of Birmingham, 23 pages.

S.F. Clifford, G.R. Ochs and T-i. Wang: "Optical wind sensing by observing the scintillations of a random scene", reprinted from Applied Optics, vol. 14, p. 2844-2850, December 1975.

T-i. Wang, S.F. Clifford and G.R. Ochs: "Wind and Refractive-Turbulence Sensing using Crossed Laser Beams", reprinted from Applied Optics, vol. 13, p. 2602-2607, November 1974.

The theory of optical propagation through atmospheric turbulence demonstrates the sensitivity of such quantities as log-amplitude variance and covariance to strength of refractive turbulence and transverse wind. We exploit this sensitivity by using a crossed-path technique to derive path profiles of these quantities. The results are insensitive to changes in the spatial spectrum of the refractive-index variations. The path resolution is easily varied by changing the receiver and transmitter separations and is ultimately limited by signal-to-noise considerations. The experimental results for horizontal paths, described here, will ultimately be used to indicate the feasibility of profiling on vertical paths with passive sources.

G.R. Ochs, S.F. Clifford and T-i. Wang: "Laser wind sensing: the effects of saturation of scintillation", reprinted from Applied Optics, vol. 15, p. 403-408, February 1976.

We have developed a physically based extension of the first-order

perturbation theory of optical scintillation that accounts for the observed variance and covariance of the amplitude fluctuations in strong integrated turbulence. We use this model to analyse the experimentally observed changes in the operation of our laser wind sensor. The theory suggests a transmitter-receiver configuration that can nearly eliminate the performance-degrading effects of strong turbulence. Based on this analysis, we have developed a saturation-resistant optical wind sensor that maintains its calibration and wind-weighting function throughout the observed range of integrated-turbulence values.

M.S. Frankel and A.M. Peterson: "Remote temperature profiling in the lower troposphere", *Radio Science*, vol. 11, no 3, p. 157-166, March 1976,

Remote probing of atmospheric phenomena has become an area of intense research during the past decade. One result of this research is a technique for remote measurement of temperature profiles in the lower troposphere, which was developed and is being tested at Stanford University. This technique is based on the concept of Doppler-tracking an acoustic pulse by an electromagnetic radar; hence the name radio-scoustic sounding system (RASS). With this system, real-time temperature profiles from near ground level to 1 to 3 km have been obtained. These data compare in accuracy with those obtained from radiosondes...

MINUTES OF THE WORKSHOP MEETING

Present: Prof. K. Rinner - President of Section I of IAG (in the chair)
Prof. E. Tengström - President of SSG I:42 of IAG

Backer, A.	Mendel, W.
Bradsell, Dr. R.H.	Milewski, Dr. J.
Brückner, R.	de Munck, Prof. J.C.
Brunner, Dr. F.K.	Overgaard, T.L.
Ducloux, J.	Parm, Prof T.V.J.
Ehbets, H.	Poder, Prof. K.
Engen, O.	Prils, H.
Gatome, J.H.	Proctor, D.W.
van Gein, W.A.	Richards, M.R.
Hopfield, H.S.	Richardus, Dr. P.
Hradilek, Prof. L.	Stenström, J.
Kahmen, Dr. H.	Tuitman, W.
Kouba, J.	van Wely, G.A.
Louis, M.	Williams, D.C.

Prof. Rinner opened the meeting and explained briefly why "Spectral Analysis of Effects of Atmospheric Refraction" had been chosen as the topic for this special workshop meeting. He pointed out that the atmospheric effects on geodetic measurements are generally of a nonstationary random character. Hence, modern statistical tools should be applied to study explanations for those effects, for they are not fully explained by conventional statistical techniques. He then invited Dr. Kahmen to give an introduction into spectral analysis and its relationship to geodetic refraction problems.

Dr. Kahmen pointed out at the beginning of his short lecture that the very small rms errors obtained for the measurements in test nets were of similar order as those of dual or triple wavelength edm equipment. The question therefore arises if the expensive equipment is really necessary for such measurements. A similar situation could be found for vertical angles. He used statistical tools to investigate the correlation function of the atmospheric effects in order to attempt an explanation of the above mentioned results. Significant periods of the fluctuations of the meteorological parameters (temperature, temperature gradient) are the annual and diurnal period. Short term fluctuation were not considered in his studies.

Considering some results of "Spectral Analysis of Geodetic Observations", he stated that the rms errors of geodetic observations depend greatly on the time period over which these measurements are spread, and this finding should be used for the studies of separating the inner (precision) from the external accuracy (accuracy) of geodetic measurements.

Prof. de Munck pointed out that there also exist errors which do not vary with time and hence will not show up in such investigations.

Prof. Rinner referred to the high accuracy of which geodetic measurements are capable. This is mainly due to the excellent instruments and the advanced observing techniques. It would therefore now be appropriate to concentrate on the atmospheric processes in order to develop better models of the atmosphere for the determination of the refraction effects.

In this context he recommended as text, the book by V.I. Tatarskii (1961). In "Wave propagation in a turbulent medium", Dover Publications.

Mr. Kouba stated that in his opinion statistical methods should only be used, when modelling of the atmosphere could not be carried out.

Prof. Tengström agreed with this statement, and mentioned that modelling should be used to study the different atmospheric effects on astronomical observations during different nights. The answer to such problems could come from an analysis of the peaks in the appropriate spectral analysis.

Dr. Kahmen explained that he has tried to find the spectra of geodetic measurements from the atmospheric data, and not from geodetic data. His task had been to find the correlation function of geodetic measurements which could subsequently be used in the formulation of the adjustment of all geodetic data spread over many years in the form of a collocation procedure.

Prof. Rinner asked for the explanation of the pseudo-systematic error (about 4 ppm) between light and microwave edm (he mentioned that Prof. K. Bretterbauer had given a phenomenological explanation).

Dr. Kahmen stated, that the meteorological process must be considered as a random process which is superimposed by a trend. The trend-model may give an explanation of the pseudo-systematic error.

Prof. Poder agreed with the statement that systematic errors should not be eliminated by statistical methods. For the analysis of such effects, meteorological parameters should be used.

Prof. Tengström asked Mr. Kouba if the American Doppler data had been analysed by a method of similar concepts.

Mr. Kouba answered that the analysis had been carried out along similar lines, and he stressed the importance of such an analysis as a most useful tool. It is important to remove the correlation between the observations by models, and hence also in future, the development of such models will be necessary.

Prof. Tengström asked Dr. Kahmen for details about the determination of the correlation function.

Dr. Kahmen replied that for the practical analysis the long-periodic and short-periodic fluctuations were split up by filtering into individual sections, which were then analysed. He found that it would be sufficient to approximate the correlation function of long periodic processes by a cosine function, whose amplitude slowly decreases. The fluctuations of the short-periodic fluctuations may be described by a delta-function.

Dr. Brunner pointed out that the analysis of such meteorological data usually had the advantage of equal spacing. However, the analysis of geodetic data which are generally not equally spaced, would need prefiltering of the original data set.

Prof. Poder stated that in his opinion, not all the refraction problems will be solved by statistical methods and asked for balancing the different approaches.

Prof. Rinner requested Prof. Tengström to give a brief review of the book by Tatarskii, because several colleagues might not be familiar with it.

Prof. Tengström then gave us his review about the book: V.I. Tatarskii (1961) "Wave propagation in a turbulent medium" Dover Publications. He stressed the fact that the book gives an excellent introduction to nonstationary random processes with special consideration of the atmospheric processes.

The treatment of these processes leads to the development of atmospheric structure functions in order to describe the wave propagation in a turbulent medium.

Prof. Rinner summarised the workshop meeting and concluded that there is a need for a better (more realistic) atmospheric model for the treatment of atmospheric effects on geodetic measurements. He recommended that the necessary contacts with meteorologists should be established.

In the second part of the workshop the question of laser safety was brought up by P. Richardus.

The Symposium had been informed that the International Technical Commission proposed restrictions which would virtually prevent geodesists and landsurveyors using class 3A lasers (up to 5 mw). It was decided that a resolution be passed to the International Association of Geodesy suggesting to establish contact to ensure a reasonable code of practice for providing adequate safety.
(see resolution 4)

RESOLUTIONS

1. This symposium supports and encourages investigation into the use of the multi-wavelength principle as applied to the elimination of refractive influences in Geodesy.

It recognises the great need for instruments that are able to give directly refraction free angles and distances and urges that all efforts should be made to develop such instruments.

2. The symposium

- recognising that studies of wave propagation in a turbulent medium become increasingly important, recommends that the scope of these studies should be such as to include already available research results from other branches of science.

3. The symposium

- recognising the need for further investigations of the spectra of geodetic measurements in conjunction with results from boundary layer meteorology, encourages the search for quantitatively complementary methods to determine the effects of electromagnetic wave propagation in Geodesy.

4. The symposium

- noting with concern the form taken by preliminary and developing use guidelines for lasers, feeling that unnecessary restrictions are being imposed while in some respects not providing adequate safety recommends that the A.I.G. establishes the appropriate contacts to ensure the development of a safe and reasonable code of practice.

5. The symposium

- thanks The Netherlands Geodetic Commission, the International Agricultural Centre, Wageningen, and particularly the Department of Surveying and Photogrammetry of the Agricultural University, Wageningen, for the excellent arrangements for this meeting.

International Symposium on
Electromagnetic Distance Measurement
and the Influence of Atmospheric Refraction

List of Participants

AUSTRIA

- R. Bruckmüller - T.U. Wien, Institut für Landesvermessung,
A-1040 Vienna
- W. Mendel T.U. Graz, Institut für Landesvermessung,
A-8010 Graz
- K. Rinner - Institut für Landesvermessung und Photo-
grammetrie,
T.U. Graz,
Rechbauerstrasse 12,
8010 Graz
- W. Roessler - Institut für Höhere Geodäsie T.U.,
A-1040 Vienna

AUSTRALIA

- F.K. Brunner - Lecturer,
Department of Geodesy, University of
New South Wales,
P.O. Box 1, Kensington 2033

BELGIUM

- H. Prils - Nationaal Geografisch Instituut,
De Smetstraat 90,
Gent

CANADA

- J. Kouba - E.M.R. Surveys and Mapping,
Geodetic Survey,
615 Booth Street, Ottawa

CZECHOSLOVAKIA

L. Hradilek

- Charles University Prague
Albertov 6,
Prague 2

DENMARK

T.L. Overgaard

- Geodetic Institute,
7 Rigsdagsgarden,
DK 1218 Copenhagen

K. Poder

- Geodetic Institute,
Gamlehavn Allé 22,
DK 2920 Charlottenlund

FINLAND

T.V.J. Parm

- Helsinki University of Technology,
Department of Surveying,
SF-02150 Otaniemi-Helsinki

FRANCE

J. Ducloux

- Institut Geographique National,
2 Avenue Pasteur,
94160 Saint-Mandé

M. Louis

- Institut Geographique National,
2 Avenue Pasteur,
94160 Saint-Mandé

GERMANY (Federal Republic)

A. Bantellas

- Geodätisches Institut, Universität
Karlsruhe (TH),
D-75 Karlsruhe

GERMANY (Federal Republic) (cont'd)

- R. Brückner - Hauptstrasse 53,
D-3000 Hannover
- D. Ehlert - Institut für Angewandte Geodäsie,
Weinbergstrasse 9,
D-623 Frankfurt-Sindlingen
- T. Glissmann - Sonderforschungsbereich 149,
Nienburgerstrasse 1,
3000 Hannover
- A. Grewe - Max-Planck Institut für Radioastronomia,
Auf dem Hügel 69,
Bonn
- W. Harth - Max-Planck Institut für Radioastronomia,
Auf dem Hügel 69,
Bonn
- H. Kahmen - Geodätisches Institut,
Universität Karlsruhe (TH),
D-75 Karlsruhe, Postfach 6380
- F. Löschner - Geodätisches Institut,
Lehrstuhl 1 der RWTH,
Templergraben 55,
51 Aachen
- W. Maurer - Lehrstuhl für Geodäsie,
TH Munchen,
Arcisstrasse 21,
D-8000 Munchen 2
- Mrs. B. Meier-Hirmer - Geodätisches Institut,
Universität Karlsruhe (TH),
Postfach 6380,
D-75 Karlsruhe

GERMANY (Federal Republic) (cont'd)

- G. Soltau - Vermessungsdirektor
Institut für Angewandte Geodäsie,
Weinbergstrasse 9,
D-623 Frankfurt-Sindlingen
- J. Stenström - c/o AGA Optronik GmbH,
Industriestrasse 4,
D-6236 Eschborn
- B.U. Witte - Geodätisches Institut der Universität
Bonn,
Nussallee 17,
5300 Bonn 1
- H. Zetsche - Geodätisches Institut der Universität
Bonn,
Nussallee 17,
5300 Bonn 1

KENYA

J.M. Gatome

- Survey of Kenia,
P.O. Box 30046,
Nairobi

THE NETHERLANDS

A. Backer

- Technische Hogeschool Delft,
Leidekkersdreef 22,
Apeldoorn

J.D. Bregman

- Netherlands Foundation for Radio
Astronomy,
Oude Hoogeveensedijk 4,
Dwingeloo

W.N. Brouw

- Netherlands Foundation for Radio
Astronomy,
Oude Hoogeveensedijk 4,
Dwingeloo

D.C. de Bruyn

- Rijkswaterstaat,
Meetkundige Dienst,
Lindelaan 8,
Pijnacker

W.A. van Gein

- Hydrografic Dept, R. NL. Navy,
Badhuisweg 171,
Den Haag

D. Grosman

- HTS afdeling Landmeetkunde,
Utrecht,
De Wetstraat 9,
Arnhem

N. Hoschtitzky

- Internationaal Instituut voor Lucht-
kartering en Aardkunde ITC,
Enschede.

J.J. Krol

- Ingenieursbureau Passe Partout,
Abel Tasmanlaan 60,
Gouda

A. Kruidhof

- Generaal Foulkesweg 87 A
Wageningen

- J.C. de Munck - Julianalaan 125,
Delft
- P. Plantinga - Kadaster,
Abbema 13,
Grouw
- P. Richardus - Vakgroep Landmeetkunde LH,
Hesselink van Suchtelenweg 6,
Wageningen
- K. van der Schaaf - Nederlandse Vereniging voor Geodesie,
Glindhorst 15,
Ede
- P.G. Sluiter - Shell Internationale Petroleum Maat-
schappij,
Willem Pijperlaan 16,
Leidschendam
- S. Stellingwerff Beintema - Radio-Holland,
Burg. Bultenlaan 5,
Voorhout
- W. Tuitman - Hydrografic Dept. Royal Neth. Navy,
Kaersemaekerstraat 7,
Zierikzee
- J.S. Versteeg - Bendienlaan 46,
Nieuwegein
- J.H.M. v.d. Wal - Rijkswaterstaat,
Meetkundige Dienst,
Holierhoek 14,
Schipluiden
- I.M. Wassenaar - HTS - Landmeetkunde Utrecht,
Vleermuislaan 15,
Wageningen
- G.A. van Wely - Vakgroep Landmeetkunde LH,
Hesselink van Suchtelenweg 6,
Wageningen
- F.W. Zeeman - Postbus 581,
Apeldoorn
- N. Zondag - O'Harris,
Herengracht 22,
Amsterdam

NORWAY

O. Engen

- P.O. Box 8153,
Oslo 1

POLAND

J. Milewski

- The Higher School of Engineering,
Department of Geodesy,
WSI Zaklad Geodezji ul. Raclawicka 16/17,
75-620 Koszalin

SWEDEN

E. Tengström

- Statens Landmåteriverk,
Lantmåterigaten 2,
801 12 Gävle

- Geodetic Institute,
Uppsala University,
Hällby, Uppsala

SWITZERLAND

H. Ehbets

- c/o Wild Heerbrugg AG,
CH-9435 Heerbrugg

UNITED KINGDOM

R.H. Bradsell

- National Physical Laboratory,
Teddington, Middlesex

A.H. Dodson

- Department Civil Engineering,
Nottingham University,
Nottingham

D.W. Proctor

- Directorate of Overseas Surveys,
Kingston Road
Tolworth, Surbiton Surrey KT5 9NS

M.R. Richards

- Ordnance Survey,
Romsey Road,
Southampton 509 4DH

UNITED KINGDOM (cont'd)

D.C. Williams

- Division of Mechanical and Optical Metrology,
National Physical Laboratory,
Teddington, Middlesex, TW11 0LW

UNITED STATES OF AMERICA

Mrs. H.S. Hopfield

- Johns Hopkins University, Applied Physics Laboratory,
Johns Hopkins Road,
Laurel Maryland 20810

G.R. Huggett

- Applied Physics Laboratory,
1013 N.E. 40th,
Seattle Wa. 98105

B. Lesley

- National Geodetic Survey,
Corbin, Virginia

